



Corso di laurea in Ingegneria Energetica e Nucleare

Tesi magistrale

**Dynamic simulation and energy efficiency scenarios
of
the District Heating Network of Fiumicino Airport**

Anno accademico 2017-2018

Relatore: Prof. Vittorio Verda

Relatore esterno: Ing. Fabio Zanghirella

Candidato: Daniele Lops

Matricola: 240173

Tesi ENEA ref. nr. 2424, titolo originale “Analisi delle prestazioni e degli scenari di efficientamento energetico di una rete di riscaldamento di un’infrastruttura aeroportuale mediante metodi di calcolo dinamici”.

Acknowledgment

I would like to take a few lines to thank all the people who helped me over the period of my academic formation.

I would especially like to thank my family for the love, support, and constant encouragement I have received over the years.

I would like to thank my tutor, the ENEA researcher Fabio Zanghirella for guiding me over the period I worked on my thesis.

I would like to thank my colleagues, Federica Azzarri and Marta Trinchieri for teaching me lots of Matlab skills and for helping me in the data analysis of the Airport of Roma Fiumicino.

Last but not least, I would like to thank Ella Watson for helping me in the linguistic correction of my thesis.

Table of Contents

Introduction.....	8
List of Abbreviations.....	10
Chapter 1: District Heating.....	11
1.1 Brief overview of DH.....	11
1.2 Heat distribution.....	12
1.3 Main components of a district heating system.....	13
1.3.1 Thermal Power station.....	13
1.4 Italian situation.....	18
1.4.1 DH Italian regulation.....	19
1.4.2 CHP Italian normative.....	20
1.5 Absorption Chillers.....	21
Chapter 2: The District Heating Network for the Airport of Roma Fiumicino.....	23
2.1 Brief description.....	23
2.2 Thermal Power Station.....	26
2.3 Pumping Station.....	27
2.4 User substations.....	28
2.5 Analysis of data.....	31
2.5.1 February 2018.....	31
Chapter 3: General description of the simulation Platform: ENSim.....	39
3.1 Brief overview of the simulation model.....	39
3.2 The Input excel File.....	40
3.3 Matlab and Simulink Inputs.....	41
3.4 Software IHENA: Intelligent Heat Energy Network Analysis.....	45
3.5 Overcoming of the previous model.....	48
3.7 Management of The Mass Flow rate inside the Thermal Power Station.....	55
3.8 Fictitious Network Storage tank.....	57
3.9 Return Collectors Block.....	59
3.10 CHP: Cogeneration Combined Heat and Power Units.....	60
3.11 Network Dissipater.....	66
3.12 Hot Storage Tank (HST).....	67
3.13 Network Modelling.....	70

Chapter 4: Validation of the heat distribution losses: The Equivalent Network.....	73
4.1 Brief overview on the meaning of ‘Equivalent Network’	73
4.2 Estimated heat distribution losses analysis.....	75
4.3 Validation of the simulated Heat Distribution Losses	80
4.4 Simulation Results of the Equivalent Network.....	82
4.4.1 December 2017	84
4.4.2 February 2018.....	85
4.4.3 March 2018.....	86
4.4.4 April 2018	87
Chapter 5: Simulation results of the Validation Scenario	88
5.1 Brief introduction to the simulation of the Working Network.....	88
5.1 Simulation Results of the Working Network	90
Chapter 6: Working Network at Time 0.....	105
6.1 Brief introduction to the simulation of the Working Network at Time 0.....	105
6.2 Simulation Results of the Working Network at Time 0	106
6.3 Brief Introduction to the energy efficiency scenarios	113
Chapter 7: Scenario 1: Two Temperatures Network.....	114
7.1 Brief introduction to scenario ‘Two Temperatures Network’	114
7.2 Simulation Results of scenario ‘Two Temperatures Network’	120
Chapter 8: Scenario 2: Two Temperatures Network with Dissipated Heat Recovery by the Installation of Absorption Chillers	132
8.1 Brief Introduction to scenario ‘Two Temperatures Network with Dissipated Heat Recovery’	132
8.2 The modelling of the Absorption Chiller	136
8.3 Calibration analysis and simulation results	137
8.3.1 Calibration analysis of the Absorption chillers loads.....	138
8.3.2 Simulation results of scenario ‘Two Temperatures Network with Dissipated Heat Recovery by the Installation of Absorption Chillers’	142
Chapter 9: Scenario 3: Network DN 350 only, at low Temperature.....	149
9.1 Brief introduction to scenario ‘Network DN 350 only, at low Temperature’	149
9.2 Simulation results of scenario ‘Network DN 350 only, at low temperature’	152
Chapter 10: Scenario 4: Network DN 350 only, at low Temperature, with Dissipated Heat Recovery by the Installation of Absorption Chillers	161
10.1 Brief introduction to scenario ‘Network DN 350 only, at low Temperature, with Dissipated Heat Recovery by the Installation of Absorption Chillers scenario’	161
10.2 Calibration analysis of the Absorption chillers loads.....	164

10.3 Simulation results of scenario ‘Network DN 350 only, with dissipated heat recovery by the installation of Absorption Chillers’	169
Chapter 11: Energy Efficiency Indexes	177
11.1 Brief overview of European Regulation.....	177
11.2 Simulations results analysis.....	182
11.2.1 Primary Energy Factor ($f_{p,DH}$):.....	183
11.2.2 Plant primary energy factor PEF_{plant}	184
11.2.3 District Heating Global Efficiency η_{DH} :.....	185
11.2.4 Primary Energy Efficiency (PEE):.....	186
Conclusions.....	188
List of Figures.....	191
List of Tables	195
Bibliography.....	198

Introduction

Energy efficiency is a very common expression nowadays because climate change forces human kind to use natural sources more efficiently in order to preserve them for the next generation. There are several types of energy efficiencies and this thesis intends to show what kind of efficiency scenarios could be planned for a district heating infrastructure. The European Union, by the standard 2012/27/UE, and the Italian government, by the standard SEN 2017, recognize in efficient district heating and cooling a way to reduce air pollution and to promote a process of decarbonisation, in particular when district heating networks are fed by waste heat or cogeneration at high performance.

This thesis was written as part of the Italian research plan called 'Ricerca di Sistema Elettrico', that is led by the Italian National Agency for the Sustainable Technologies. 'Ricerca di Sistema Elettrico' has the aim to reduce the user cost of the grid electricity and to enhance the quality and the reliability of the power displacement in Italy.

The district heating network studied is the one that serves the airport of Roma Fiumicino. It is made by two loops in flow and two loops in return, with secondary branches feeding the users, for an overall length of almost 33 kilometres. The loops work like a single hydraulic circuit. The users are heat exchangers and double stage absorption chillers. Inside the network superheated water flows. The reference supply temperature is 130 °C, whereas the reference return temperature is 80 °C. Inside the Power Station there are three Combined Heat and Power units with a nominal thermal power of 8 MWth each.

The purpose of this thesis is:

- to model a district heating system in Simulink platform;
- to simulate the district heating system;
- to validate the model comparing the simulation results with the monitored data;
- to simulate four efficiency scenarios;
- to compare the efficiency scenarios with the reference one by energy efficiency indexes.

In the first chapter we will describe the state of the art district heating, with reference to the international situation and to the Italian situation. In the second chapter we will analyse the monitoring data collected inside the power station and inside the user monitoring chambers.

In the third chapter we will face the modelling of the network. The starting point of the modelling is the simulation platform of ENSim developed by ENEA, to which we will join a matlab function, called IHENA (Intelligent Heat Energy Network Analysis) developed by the University of Bologna. It solves the district heating network at each time step of simulation hydraulically and thermally.

In the fourth chapter we will validate the heat distribution losses along the network comparing the simulation results of an 'Equivalent Network' with the estimated heat losses for the months of December 2017, February, March and April 2018.

In the fifth chapter we will run the model in the working conditions derived from the data analysis. We will validate the model by the comparison between the simulation results and the monitoring data collected for the month of February 2018. In the sixth chapter we will run the validated model in the working conditions the managers of the airport claimed are the real ones. After validating the model, from chapter seven to chapter ten, we will simulate four efficiency scenarios to reduce the energy consumption and the environmental impact of the actual district heating network of Roma Fiumicino.

The first efficiency scenario is about managing one of the two loops at a low temperature (90°C), actually both working at a flow temperature of 130 °C. The second efficiency scenario will show it is possible to reduce the heat dissipated by the network dissipater of the loop at low temperature by the installation of two absorption chillers.

In the third efficiency scenario we will run only the loop at low temperature, closing the other one completely, and we will shift on the working loop also the load previously connected to the loop at high temperature. In the fourth and last efficiency scenario we will only run the loop at low temperature and we will install two new absorption chillers, to reduce the heat dissipated by the network dissipater.

In the last chapter we will compare the simulated scenarios by some energy efficiency indexes to evaluate which one uses the primary energy consumed better.

List of Abbreviations

ADR Aeroporti di Roma;

CHP Combined Heat and Power unit;

DH District Heating;

DN 200 Loop of the network with nominal pipes diameter of 200 millimetres;

DN 350 Loop of the network with nominal pipes diameter of 350 millimetres;

G Flow Rate;

HST Hot Storage Tank;

MFR Mass Flow Rate;

PG Heat Exchange User Substation

PRMSE Percentage Root Mean Square Error

P.S. Power Station;

P_{th} Thermal Power;

Q Heat Power;

RMSE Root Mean Square Error

Chapter 1: District Heating

1.1 Brief overview of DH

Reducing emissions in the energy sector is of fundamental importance for climate change mitigation. District heating (DH) may have an essential role in the decarbonisation of the international energy system and respect to other technologies, DH might be an instrument to achieve reductions of carbon emissions and use of primary energy with higher efficiency. District heating is a technology for distributing centrally produced heat for space heating and sanitary hot-water generation for residential and commercial buildings. Heat is distributed to the consumers by a network of pipes using water as main transport medium. The market for district heating is primarily based on residential buildings in cities. There is no development of district heating for isolated houses because of distribution costs and heat distribution losses. There are significant regional variations in the usage of district heating systems. In countries with cold climates the district heating technology in urban areas has been used from the last century. However, in southern European countries, where mild climates prevail, this technology is still not common. Despite the milder weather, which implies shorter usage periods, governments support combined heat and power(CHP) plants and district heating by subsidies for investments, fuels, preferential feed-in tariffs and connection rights. The high-energy efficiency in district heating projects, often combined with the use of renewable fuels, makes the technologies attractive in order to reduce emissions of greenhouse gases and enhance air quality. From the beginning of this century, the Commission of the European Communities proposed standards on the promotion of combined heat and power, because cogeneration of electricity and heat makes possible a more efficient utilization of fuel than electricity production or heat generation alone. District heating is the way to make use of the produced heat in cogeneration that would be otherwise wasted in the environment, this is the main reason why the usage of district heating systems is increasing all over the world. Many different heat sources can be used to supply district heating networks with hot water. The most common fuels for district heating are natural gas and coal, but oil and renewables are also commonly used. Waste heat from industrial processes can also be reused, as well as heat from waste incineration, geothermal heat and solar heat. The heat supplied into district heating networks is characterized by four different heat supply methods in the world, fossil fuels, renewables (geothermal, biomass), recycled heat renewable (waste), recycled heat from CHP and industries. With respect to heat supply methods, the European Union has higher proportions of both recycled heat and renewable heat compared to the world situation with proportions of recycled heat and renewable heat ¹.

¹ A. Hast, S. Syri, V. Lekavicius, A. Galinis. *District heating in cities as a part of low-carbon energy system* [11].

1.2 Heat distribution

There are three generations of heat distribution, these are: steam, high temperature water, low temperature water. Steam was the heat carrier in the first generation, while water has been the heat carrier in the following generations. The most part of first generation systems have been converted to water systems or they have been closed, since steam is nowadays considered an inefficient heat carrier because of heat losses and maintenance costs. However, steam is still used as a heat carrier in the Manhattan system in New York and in Paris. The second generation of district heating technology was introduced in the 1920s. This generation of technology was considered the best available until the 1970s, when Scandinavian countries shifted the second generation into a third generation, introducing more insulated prefabricated pipes joined with lower distribution temperatures.

All these three generations were based on the use of fossil fuels and the connected building had high heat demands. A fourth generation will be characterized by less fossil carbon dioxide emissions. The new energy systems will have other supply and use conditions with more renewable energy sources, less thermal power plants, and customer buildings with lower heat demands. A major feature of the fourth generation is that heat will be distributed with lower temperatures than applied in the third generation². The total length of distribution pipelines can be estimated to about 600 000 km in the world and about 200 000 km in the European Union. There are various applied temperature levels, insulation materials, and heat densities; the heat distribution losses are commonly between 5 and 25%. In Europe, most customers are connected by substations to primary distribution networks supplying heat with the same supply temperature to all customers³. Nowadays the functioning systems compute the distributed heat by the product of mass flow and the temperature difference between the supply and return pipes. The corresponding overall control system is based on four different and independent control systems we will see in the next section. The heat demand and flow control systems are located in each customer heating system and substation, while the heat supplier is responsible for the centralised differential pressure and supply temperature control systems.

²S. Werner. *International review of district heating and cooling* [12].

³J. O. Sola, X. Gabarrell, J. Rieradevall. *Environmental impacts of the infrastructure for district heating in urban neighbourhoods* [10].

1.3 Main components of a district heating system

The main components of a district heating system are:

- Thermal Power station;
- Distribution Network;
- Pumping Station;
- Heat exchange substations.

1.3.1 Thermal Power station

This is the place where the heat production happens. The heat produced must be equal to the energy necessary to feed the loads plus the heat distribution losses along the network. The thermal power stations can be basic ones when they produce only the heat necessary to supply the load, principally they use boilers where the heat propagated by the combustion of a fuel is exchanged with a thermic vector fluid. More complex thermal power stations can combine heat and power (CHP) when they are characterized by machines that can produce at the same time heat and electric power; the last ones are the most efficient. Nowadays, district heating systems are commonly fed by power stations with CHP units whereas boilers are used as back-up systems for peaks loads.

1.3.1.1 CHP: Combined heat and Power

Cogeneration or combined heat and power (CHP) is the usage of a heat engine or power station to generate electricity and useful heat at the same time; CHP units recover thermal energy for heating otherwise wasted. A district heating network is a heat supply system based on centralized production and on distribution to the end user through an energy vector consisting of a fluid in temperature⁴. The idea of combining cogeneration systems with district heating arises from combining the advantages of the two technologies (flexibility and heat recovery) to obtain a more efficient energy system, with a total cost reduction and an improvement in terms of environmental impact. The combined production of electricity and heat allows to improve the overall efficiency of energy systems compared to the case of separate electricity production in thermoelectric plants and heat in conventional thermal power station. This technology is particularly convenient when electric requirements join thermal requirements, in particular in the industrial sector, and, this is the case, in airport stations.

⁴ A. Franco, F. Bellina. *Methods for optimized design and management of CHP systems for district heating networks (DHN)* [9].

An important parameter for CHP units is the cogeneration ratio, defined as the ratio between the thermal and the electric power generated in nominal conditions.

$$\lambda = \frac{Q_{th}}{P_{el}}$$

From this parameter depend the positive and the negative aspects of the CHP itself, and the advantages and the disadvantages to feed a certain system with this technology.

Technology	λ	Positive characteristics	Negative characteristics
Medium to high size			
Steam turbine (ST)	0.5-10	Modulability, quite low costs	Quite low electrical efficiency, not good for intermittent operations
Gas turbine (GT)	0.5-2.5	High temperature recovery, high flexibility	Low operational flexibility, medim to low efficiency values
Combined cycle (CC)	0.5-3	High electric efficiency, possibility of modulation	Reduced starts-and-stops, high specific costs
Medium to low size			
Internal combustion engines (ICE)	1-5	Flexibility, quite good efficiency at partial load	Direct link between electricity and thermal energy
ORC plants (ORC)	0.5-10	Adaptability at Renewable Energy Sources	Use of a different operating fluid
Fuel cells (FC)	0.5-2	Very low power	Technology not commercially developed
Microturbines (μ TG)	0.5-2.5	High quality technology	Reduced flexibility, quite low efficiency values, high costs

Figure 1.1: Cogeneration Ratio λ , [9].

1.3.2 Distribution Network

The distribution network is made by pipelines that connect the thermal power station to the loads in flow and in return and distribute the hot fluid to the users. The pipes can be disposed in different configuration:

Tree configuration:

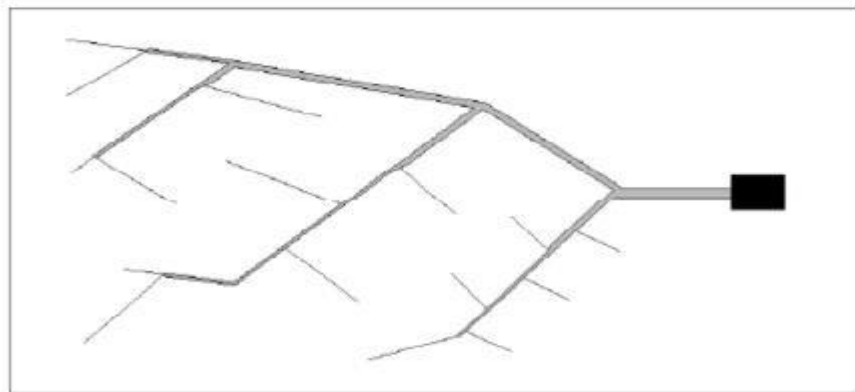


Figure 1.2: DH Network Tree configuration

It is made by a main pipeline with a major diameter, to connect the thermal power station to the bigger users, and secondary branches with a smaller diameter to the less energy demanding users.

Loop configuration:

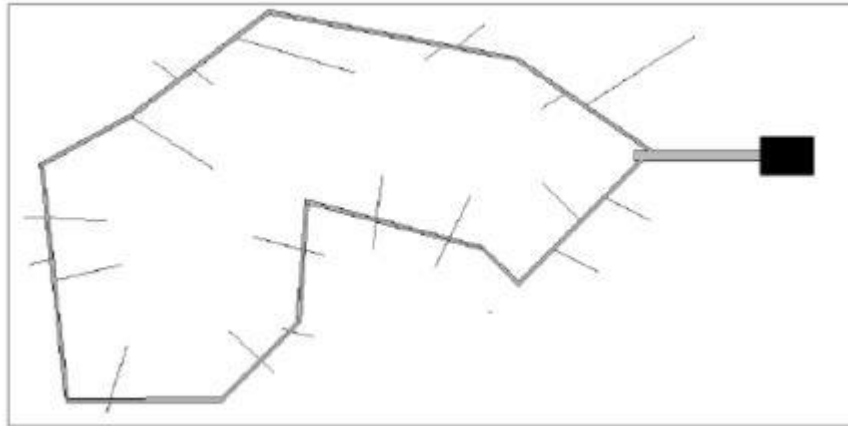


Figure 1.3: DH Network Loop configuration

It is made by a closed circuit of pipes. This is the most flexible system and it is the easiest to expand.

Mesh network configuration:

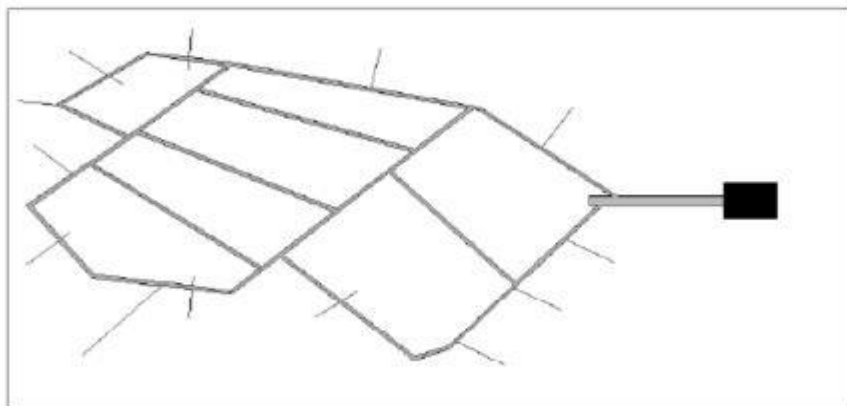


Figure 1.4: DH Mesh Network configuration

It is made by several closed loops connected to each other; it is the most expensive one but it is the best to manage in terms of control and distribution of the heat produced in the thermal power station. It is the most reliable typology, since in the case of a failure in a pipe, it is possible to close the valves upstream and downstream and to continue to feed the users, except for the ones immediately closed to the damaged pipe⁵.

The pipes of the network are made typically using stainless steel; then they present a layer of insulation, like polyurethane foam, that has a conductivity close to 0.040 W/mK, and an external coating of polyethylene.



Figure 1.5: Pipe of a DH network

1.3.3 Pumping Station

A district heating system must be balanced from the hydraulic point view, in consequence must show the same hydraulic resistance in each branch of the network. The working pressure has to consider the difference in elevation between the power station and the higher user, while the pressure drop that the pumps must compensate depends on the total length of the network. The pumping station has the main goal to guarantee the correct operation of the system from the hydraulic point of view. The electro pumps are the main components inside the pumping station, then we have filters, the water quality system, the expansion vessel, the automatic pressure control system and the tank for water integration. The water flowing inside the distribution network has a speed in the range 1-3 m/s. High speed causes high pressure drop along the network, whereas low speed district heating systems need bigger diameters, it means higher investment cost. That is why during the design phase it is necessary to find a compromise between this last variables: water speed and diameters geometry.

⁵ A. Sciacovelli, V. Verda, R. Borchiellini. Numerical design of thermal systems, 2nd edition [32].

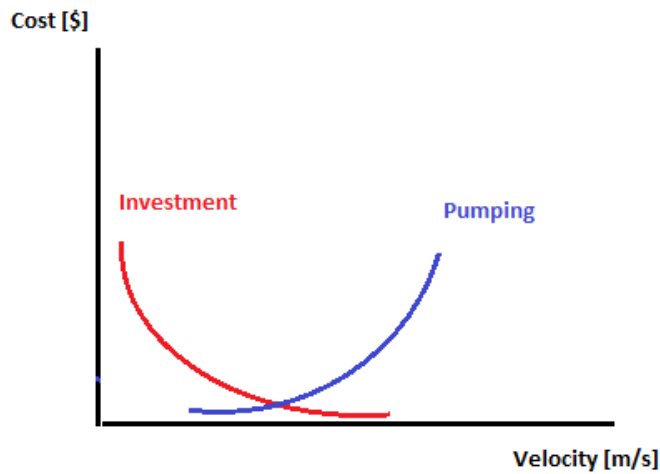


Figure 1.6: Investment and pumping trend for a DH network⁵ [32]

The optimum working point is the intersection between the two curves in Figure 1.6.

1.3.4 Heat exchange substations

The distribution system could be direct or indirect. In the direct distribution system, typically used in northern European countries, there is no difference between the primary network circuit and the secondary user circuit. It causes major problems in flow rate balancing and in the hot fluid distribution, but it is simpler from the point of view of the connection to the network, since it does not need a heat exchanger as interface between the network and the user. In the indirect distribution system, a heat exchanger is located in each supplied building and it is the interface between the network and the user. Here the supplied water exchanges heat with the vector fluid flowing in the secondary circuit, the user one. In this second case, the external thermal condition determines the flow temperature on the user circuit, while the mass flow rate on the network circuit is managed in order to have the set point temperature on the user circuit.

1.4 Italian situation

In Italy the first district heating networks were built in the 1970s. Now this technology is present only in the north of the country, with some exceptions in the centre.

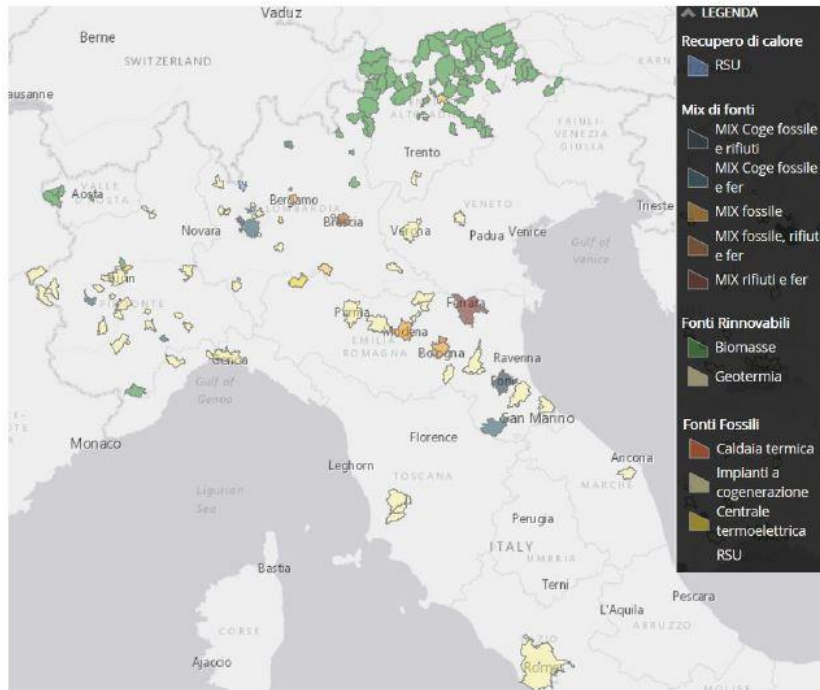


Figure 1.7: Italian DH systems with reference to the primary energy, [31].

The mite climate has obstructed a more rapid development of this technology in Italy; nevertheless, the number of DH networks is increasing in the last decades.

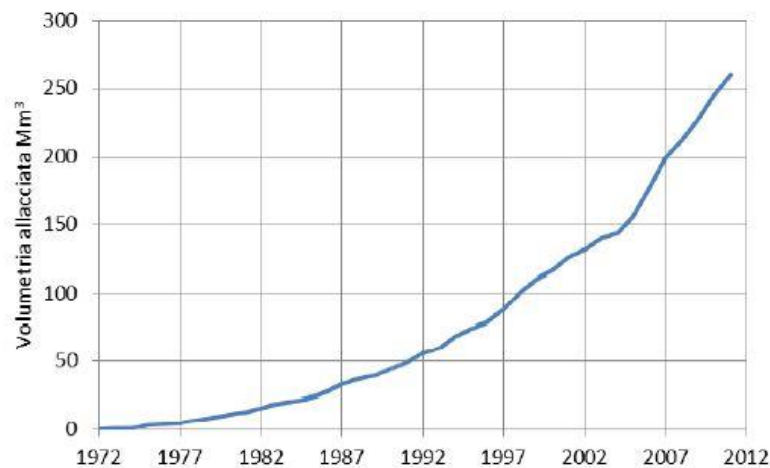


Figure 1.8: Building Cubic meters connected to DH in Italy from 1972 to 2012: [18].

In 2014 the number of DH networks was 209, in 179 cities, supplying the 10 % of the Italian thermal energy demand for the residential sector, with high potential⁶.

1.4.1 DH Italian regulation

Nowadays a regulation frame dedicated only to district heating does not exist in Italy. For many years DH was associated to the CHP technology and only with '*Decreto Legislativo 29 dicembre 2006, n. 311 "Disposizioni correttive ed integrative al decreto legislativo 19 agosto"*' the Italian regulation recognized the benefits for the environment of the district heating technology itself, saying that all the new buildings closed to a pre-existent DH network (less than 1 km) have to be connected to this infrastructure. The Italian regulation is still weak about DH, since a mild climate prevails here and this technology is completely absent in the south of the country. The first Italian standard that defined district heating was '*D. Lgs. 28/2011*'; here we can read the first definition of DH in Italian regulation: 'District heating and cooling is the distribution of thermal energy, for heating or cooling, by means of vapour, water or refrigerant fluid, flowing inside pipes to residential or industrial buildings for sanitary or industrial purpose'. With '*Decreto Legislativo 4 luglio 2014, n. 102*' the Italian regulation defines what is an efficient DH system; in particular, a DH system is efficient when it uses:

-50% of energy from renewable sources;

-50% of energy from waste heat;

-75% of energy from cogenerated heat;

-50% of energy from a mix of the previous points.

The main goal of this standard is the decarbonisation and the reduction of energy consumption of Italian buildings based on energy efficiency, the shift to renewable energy and the synergies between the heating and electricity systems by means of efficient district heating systems. Specifically, the standard mentioned above, recognises the key part that district heating, based on waste heat recovery, cogeneration and integration of renewable energy, might play in the decarbonisation process of the heating space sector.

⁶Annuario Airu 2015. *Il teleriscaldamento urbano* [18].

1.4.2 CHP Italian normative

Italy has obtained important benefits from an effective and structured incentive plan concerning the cogeneration sector. The first time the Italian standard defined the term CHP was in 1999 in '*Decreto Legislativo n.79*' (16/03/1999), here we can read that '*Cogeneration is the combined heat and power production in the same system to reduce the primary energy consumption compared to systems that produce heat and power separately*'. The main goal of this standard was the electric sector liberalization in Italy, because since the 60s the electric market was a monopoly of the government. To promote energy efficiency in the cogeneration sector, the European Union published the directive 2004/8/CE. In Italy, this was transposed in 2007 with '*Decreto Legislativo n.20 of 8/02/2007*'. It defined an efficient cogeneration system as the one that produces heat to satisfy a real load and not just to produce electricity in order to sell it to the grid. The standard mentioned defined a way to compute the primary energy saving of a cogeneration system: PES.

$$PES = 1 - \frac{1}{\frac{\eta_{th,CHP}}{\eta_{th,s}} + \frac{\eta_{el,CHP}}{\eta_{el,s}}}$$

$\eta_{th,CHP}$: thermal efficiency of the CHP system, it is the ratio of the useful heat produced and the fuel energy consumed;

$\eta_{th,s}$: reference thermal efficiency for separated heat production;

$\eta_{el,CHP}$: electric efficiency of the CHP system, it is the ratio of the electricity produced and the fuel energy consumed ;

$\eta_{el,s}$: reference thermal efficiency for separated electricity production;

The same standard introduced the concept of high efficiency cogeneration (CAR), based on the saving of primary energy obtained by the system. The requirements are different according to the size of the CHP plant.

-PES>0.1 for unit bigger than 1 MWeI;

-PES>0 for unit smaller than 1 MWeI;

1.5 Absorption Chillers

Refrigeration is a process of extracting heat from a low temperature medium and transferring it to a high temperature heat sink. Refrigeration maintains the temperature of the heat source below that of its environment while transferring the extracted heat to a heat sink. Absorption chillers use heat to drive the refrigeration cycle, they produce chilled water while consuming just a small amount of electricity to run the pumps on the unit. Absorption chillers generally use steam or hot water to drive a lithium bromide refrigeration cycle but can also use other heat sources⁷.

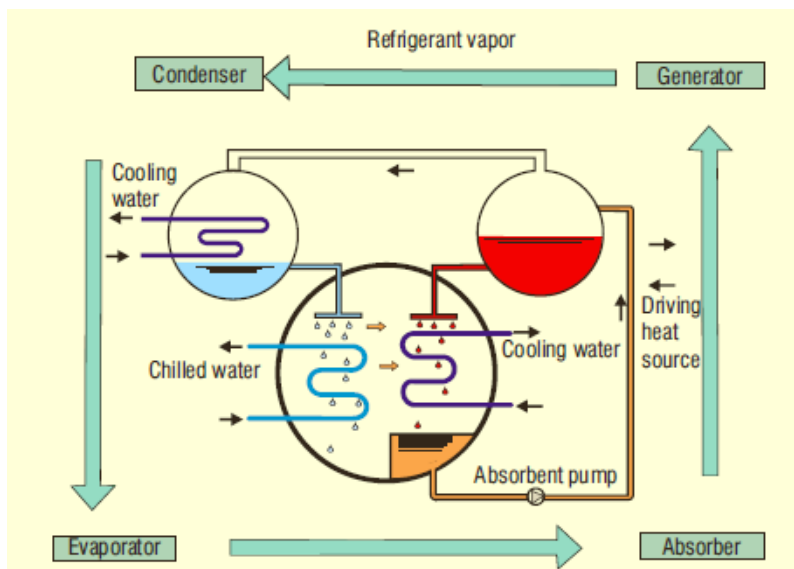


Figure 1.9: Cooling cycle ⁷ [28].

Absorption systems use heat energy to produce the cooling effect. The refrigerant, water, absorbs heat at low temperature and at low pressure during evaporation and releases heat at high temperature and high pressure during condensation. The refrigerant goes through a series of cycling processes. These are evaporation absorption, pressurization, vaporization condensation, throttling and expansion. In particular, the absorbent, in general a LiBr solution, absorbs the vaporized refrigerant in the absorber. The diluted solution, water-LiBr, is heated up at a higher pressure. This leads to the vaporization of the water and the LiBr solution comes back to its original concentration. The cycle keeps repeating to give the cooling effect desired. There are two main classes of Absorption Chillers nowadays used in industrial and civil application:

- Single-effect absorption chiller uses low pressure steam or low grade hot water to drive the absorption cycle. This absorption chiller is particularly useful for energy conserving applications such as heat recovery or process applications where a low cost heat source is available, common COP=0.7.

⁷Trane Commercial Global Product System, (<http://www.trane.com>). Accessed on August 20 2018, [28].

-Two-Stage Absorption Chillers provide chilled water for cooling using high temperature hot water, common COP>1. To increase the efficiency of the cycle, the hot water first passes through a high pressure generator and then through a low pressure generator.

Chapter 2: The District Heating Network for the Airport of Roma Fiumicino

2.1 Brief description

The district heating network for the Airport of Roma Fiumicino is the main topic of this thesis; it distributes heat to the biggest Airport station in Italy. It has an indirect distribution system with hydraulic separation between the primary circuit and the secondary circuit. Since user loads have been modelled just as load profiles, in this thesis we are going to focus our attention only on the primary circuit.

The DH Network studied is made by two different loops with nominal diameters 200 mm (DN 200) and 350 mm (DN 350), each one equipped of a return circuit, for an overall length of almost 33 kilometres, considering flow and return. That is why as we can see in Figure 2 1 there are four main pipes connected to the flow and return collectors. The flow collectors are connected to each other by a bypass valve, as well as the return collectors.

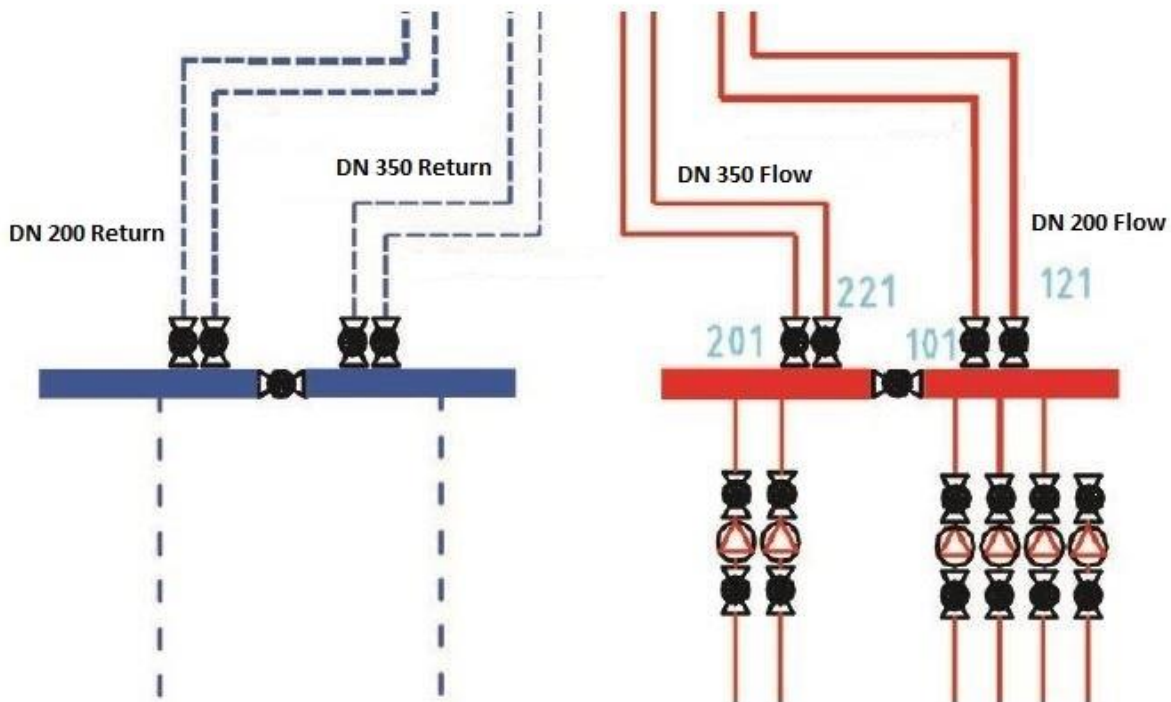


Figure 2 1: Hydraulic network representation, [29]

There are 19 monitoring chambers:

Chamber	1	2	3	7	9	9.1	11	12	13	14
Chamber	15	D	E	2A	17	19	20	22	24	/

Table 2 1: Monitoring chambers

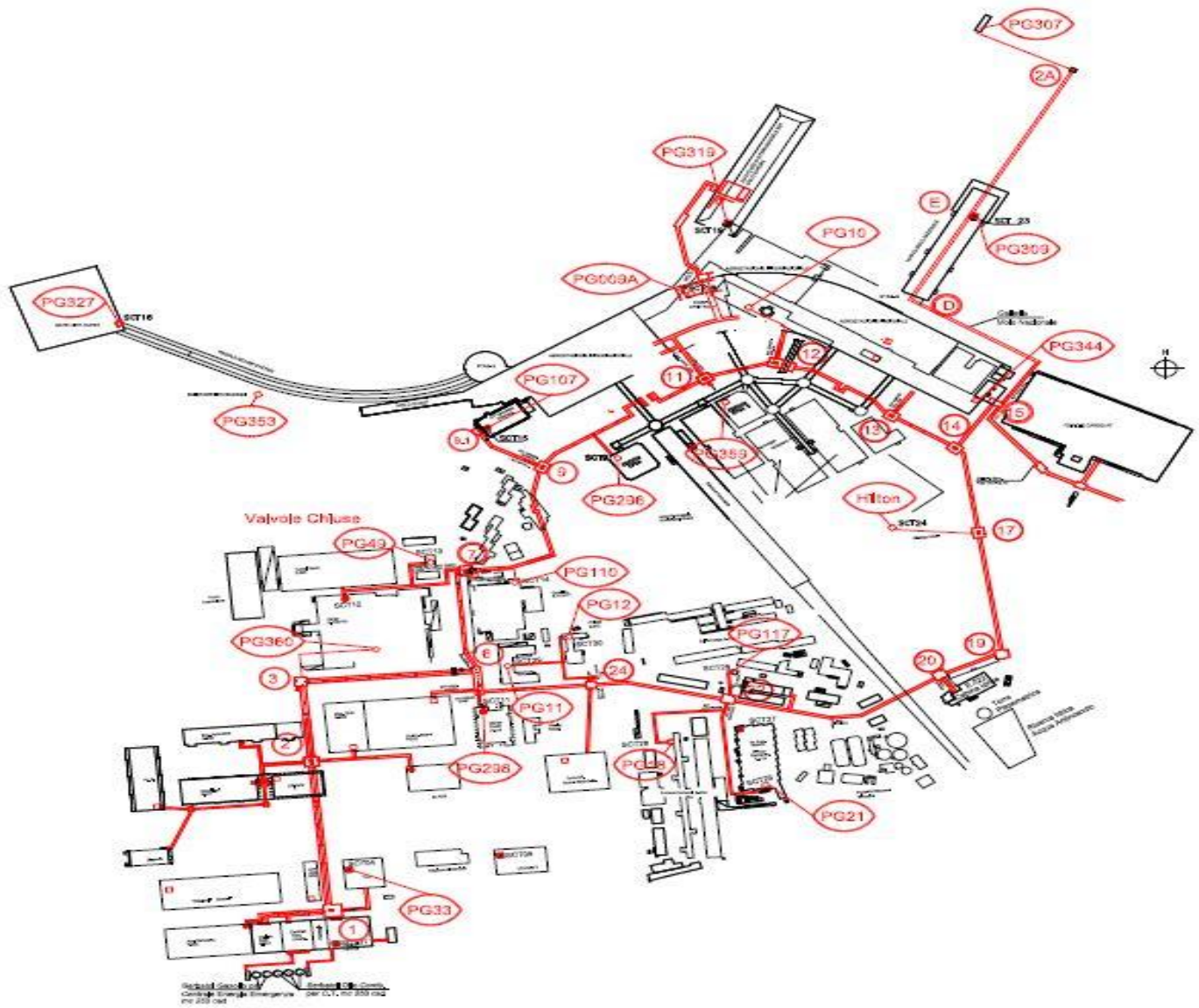


Figure 2 2: Map with the identification number of the load chambers and user substations, [29]

For chamber 2, 15, D, 2A, 19, 20 we do not have data. The pipes of the distribution network run inside tunnels built below the streets at a yearly constant temperature of almost 28 °C. Inside the pipes superheated water flows.

As a previous technical analysis underlined, 'Relazione Tecnica della Rete Acqua Surriscaldata', Ciriè 2011, the design values of the DH network of Roma Fiumicino are:

- 60 °C, nominal temperature drops on users, on the primary circuit (150 °C – 90 °C);
- 80 MWt, maximum thermal load;
- 85 MWt, maximum heat generation through 6 units for heat production;
- 4 pumping systems with inverters of 350 m³/h, 4 pumping systems with inverters of 175 m³/h;
- 15.2 bar, maximum working pressure.

Nowadays the working conditions are:

- 50 °C, nominal temperature drops on users, on the primary circuit (130 °C – 80 °C);
- 18 MWt from CHP, thermal power exploited;
- 8.8 bar in flow, 7.4 bar in return, working pressure.
- 0.5 m/s, maximum velocity of the water in the pipes.
- 4 pumping systems with inverters of 350 m³/h + 2 pumps of 175 m³/h on DN 350;
- 2 pumping systems with inverters of 175 m³/h on DN 200;

The technical report, mentioned before, underlined that the DH network of the airport of Roma Fiumicino was strongly oversized, thinking about future extensions.

2.2 Thermal Power Station

Inside the thermal power station there are 3 Rolls-Royce co-generators, with intern combustion motors fed by methane. They have a thermal nominal power of 7,987 MWth and an electric nominal power of 8,566 MWe, an electric efficiency of 47% and a global efficiency of 78.8%. Co-generators can cover 100% of the yearly thermal load and more than the 90% of the electric demand.

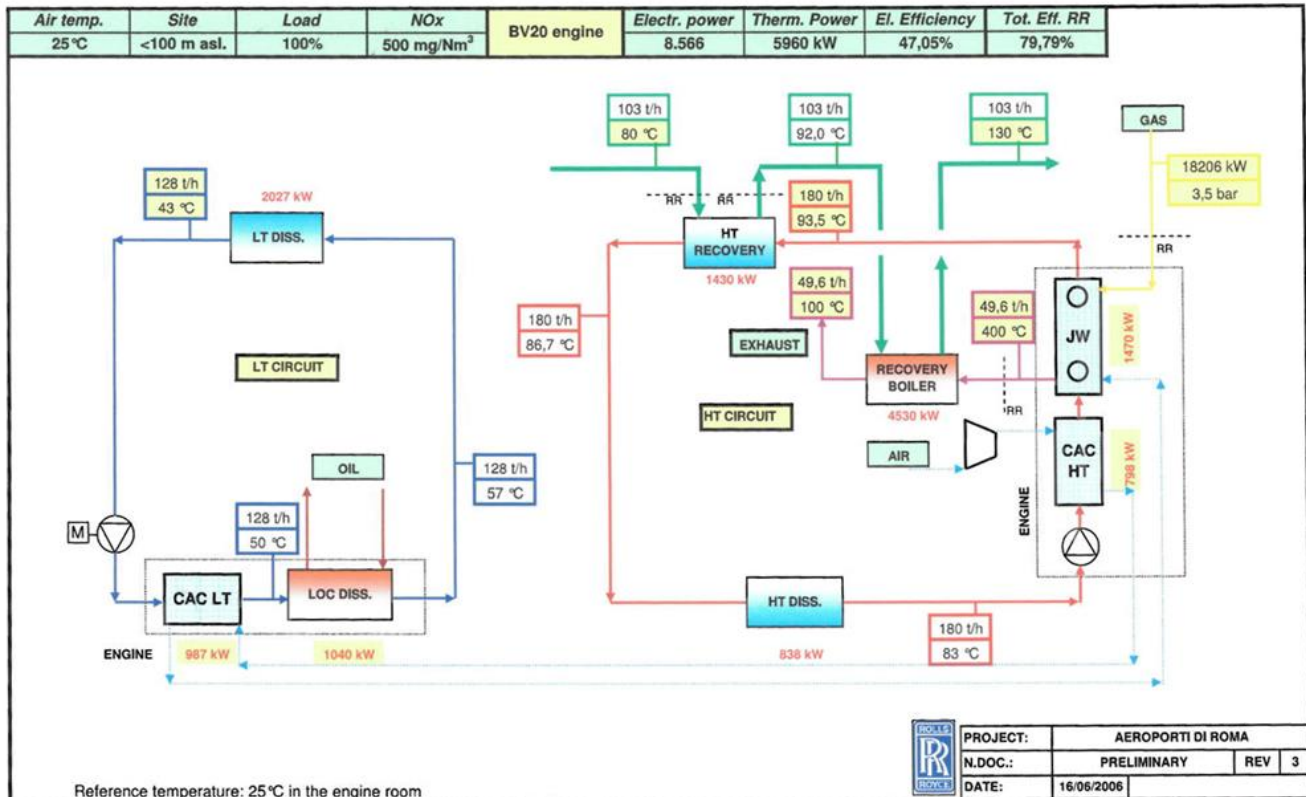


Figure 2 3: Operation scheme of CHP units

Today it is not possible to exploit all the thermal potentiality of the co-generators because the return temperature in the power station is too high in the actual configuration, above 60 °C, to recover thermal power from the low temperature circuit of the motor. As we can see from the scheme in Figure 2 3, the cooling water of the lubricant oil needs to exchange with a fluid below 57 °C, otherwise it dissipates in air. The CHP are managed according to economic reasons, since they are ON at full load when the grid electricity is expensive and managers prefer auto producing the electricity, whereas they are not at full load when the grid electricity is cheaper and managers prefer buying electricity from the grid.

Besides CHP, inside the power station there are 5 backup boilers, 3 with a nominal thermal power of 8 MWth, and 2 with a nominal thermal power of 2.5 MWth.

As we said, the CHP units cover 100% of the thermal demand and in consequent the backup boilers are OFF for the most of the year. In parallel with the CHP there are 4 Hot storage tanks of 250 cubic meters working in series each other, at almost 140 °C. During the day when the heat produced by CHP is more than the load, the excess heat is used to recharge the tanks, whereas when the heat produced by CHP is not enough to satisfy the load, the hot storage tanks supply the thermal power needed. The hot storage tanks have not only a thermal function but also a hydraulic one, since they place flow rate into the network even if they are not at the proper temperature when the CHP cannot supply all the load.

2.3 Pumping Station

Nowadays, since the flow and the return collectors of the two loops (DN 350 and DN 200) are connected by bypass valves, the loops work as a single hydraulic circuit, where the pressure inside the pipes of the flow circuit is about 8.8 bar, whereas the pipes of the return circuit present water at almost 7.4 bar. To guarantee the circulation of the mass flow rate there are 4 pumps of 350 m³/h plus 2 pumps of 175 m³/h on the DN 350, whereas there are 2 pumps of 175 m³/h on the DN 200. The management logic of the pumping system is to switch ON the pumps one by one. In general, they switch ON one pump of 350 m³/h first to guarantee the pressure difference of 1.4 bar between flow and return, if one pump is not enough they switch ON a second pump, and so on. We have to point out that the DH network of Roma Fiumicino is strongly oversized for the actual load, that is why just one pump of 350 m³/h is enough for the circulation of the mass flow rate. For the same reason, the velocity of the fluid inside pipes is really low, about 0.5 m/s.

2.4 User substations

In the DH network of Roma Fiumicino there are 13 working monitoring chambers, inside which 20 active user substations (PG) are monitored, each one can contain one or two users fed by both DN 350 and DN 200 or only by one loop, for an overall number of 29 users, each one characterized by an identification number, as it is indicated in Table 2 2

Substation	Chamber	ID User node	DN
<i>PG 33</i>	1	54	350 & 200
<i>PG 360</i>	3	22	350 & 200
<i>PG 118</i>	7	23	350 & 200
<i>PG 107</i>	9.1	125	200
<i>PG 107</i>	9.1	225	350
<i>PG 327,</i>	9.1	128	200
<i>PG 327</i>	9.1	228	350
<i>Molo E</i>	9.1	27	350 & 200
<i>PG 296</i>	9	1129	200
<i>PG 296</i>	9	1229	350
<i>PG 009</i>	11	133	200
<i>PG 009</i>	11	233	350
<i>PG 319</i>	11	134	200
<i>PG 319</i>	11	234	350
<i>PG 359</i>	11	1359	200
<i>PG 359</i>	11	2359	350
<i>PG 010</i>	12	35	350 & 200
<i>PG 344</i>	13	137	200
<i>PG 344</i>	13	237	350
<i>T1</i>	14	155	350 & 200
<i>PG 307</i>	E	141	200
<i>PG 307</i>	E	241	350
<i>PG 309</i>	E	142	200
<i>PG 309</i>	E	242	350
<i>PG Hilton</i>	17	43	350 & 200
<i>PG 21</i>	22	47	350 & 200
<i>PG 117</i>	22	49	350 & 200
<i>PG 11</i>	24	51	350 & 200
<i>PG 298</i>	6	53	350 & 200

Table 2 2: Users identification data

Inside the user substations there are double stage absorption chillers or heat exchangers, each one is considered as a user, that separate the primary circuit from the secondary circuit. Inside the monitoring chamber there are control systems that monitor:

- The energy getting inside the substations;
- The mass flow rate inside the derived branches;
- The flow and return temperature to the users;
- The thermal power exchanged on the primary circuit inside the substations for each user;
- The opening value of the valves;

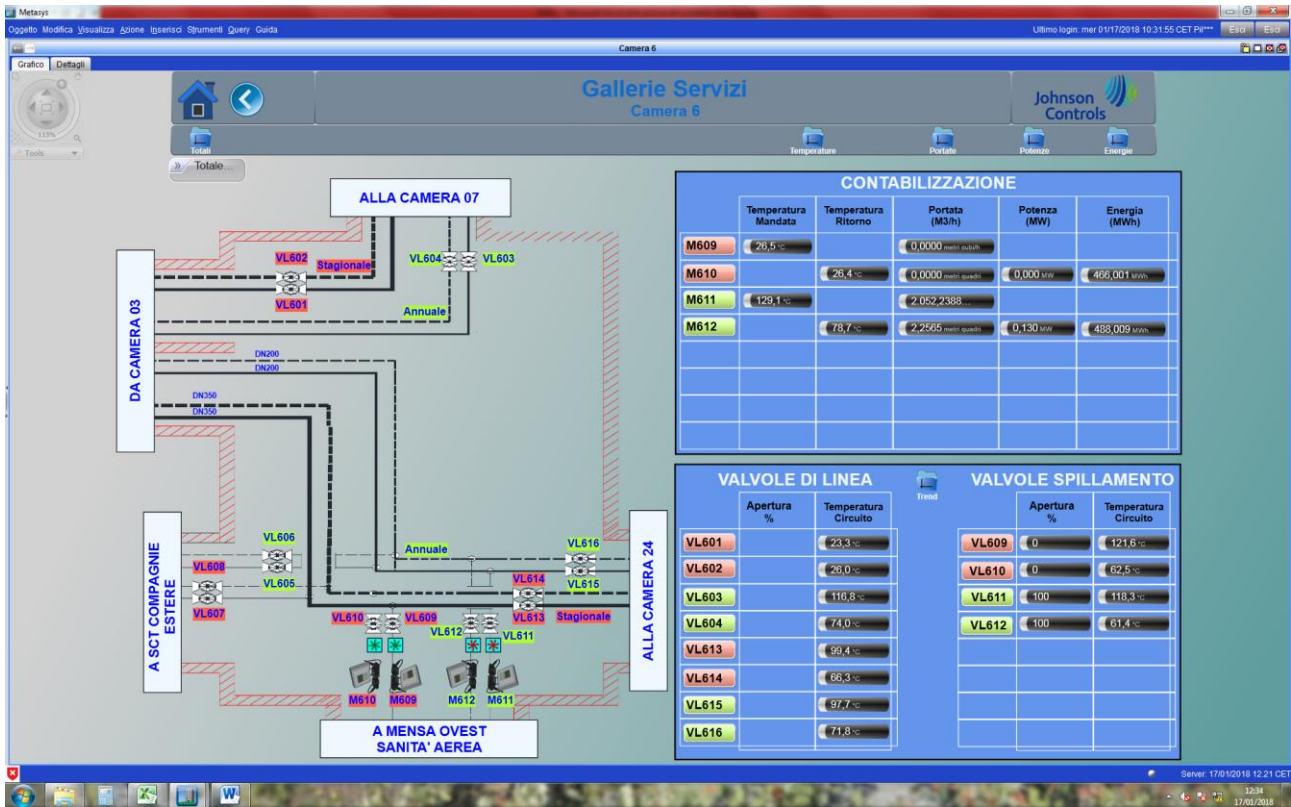


Figure 2 4: Inspection chamber 6

Today the most part of the user loads are heat exchangers, but almost 20 % of the winter load is due to the absorption cooling machines. There are 5 double stage absorption chillers: two are connected to Molo E but they are not working, one is in substation identified by PG 107, user 125, and two are in terminal 1, user 155, between chamber 14 and chamber 15. The absorption chillers are bound to temperature constraints: they need a flow temperature of 130 °C and a return temperature not below 68 °C, whereas the other loads do not have these constraints. As we said, there are 20 user substations inside which may be more than one user with its own thermal load profile. From the data at our disposal we found 29 load profiles. The frequency of monitoring of each thermal load is 20 minutes, and this is why we fixed the time step of simulation to 1200 seconds.

Two load profiles have been obtained by difference (Molo E, user 27, and cooling machine of Terminal 1, user 155), subtracting to all the load of the respective chamber (respectively chamber 9.1 and chamber 14) the loads of the other users connected to the same chamber (PG 107 and PG 328 for chamber 9.1, and PG 307 and PG 309). For the month of February, we have data about the temperature drops on the primary side of the users' heat exchangers and the mass flow rates required.

ADR, Aeroporti di Roma, told us that the user substations work at a fixed temperature drop on the primary circuit, but as we can see from Figure 2 5, the temperature drop is not constant during the period monitored and it seems that there is neither a constant mass flow rate management on the user substations. The substation PG 319 was chosen because it presents all the values of temperature drops and of mass flow rate on the primary circuit, for the whole month of February with neither one missing data.

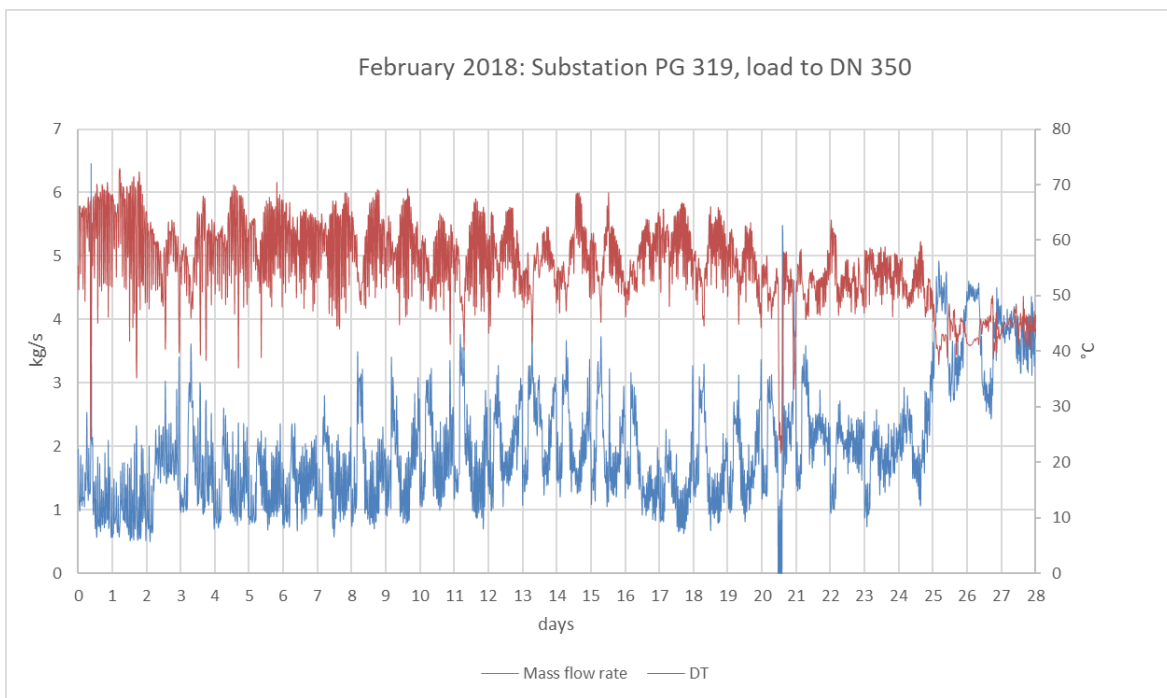


Figure 2 5: Temperature drop and Mass flow rate for substation PG 319, February 2018

2.5 Analysis of data

The following graphs and images have been made from the data given by ADR and are the same as those with which the results of the simulations will be compared.

2.5.1 February 2018

First of all, we are going to analyse the heat production behaviour of the Power Station.

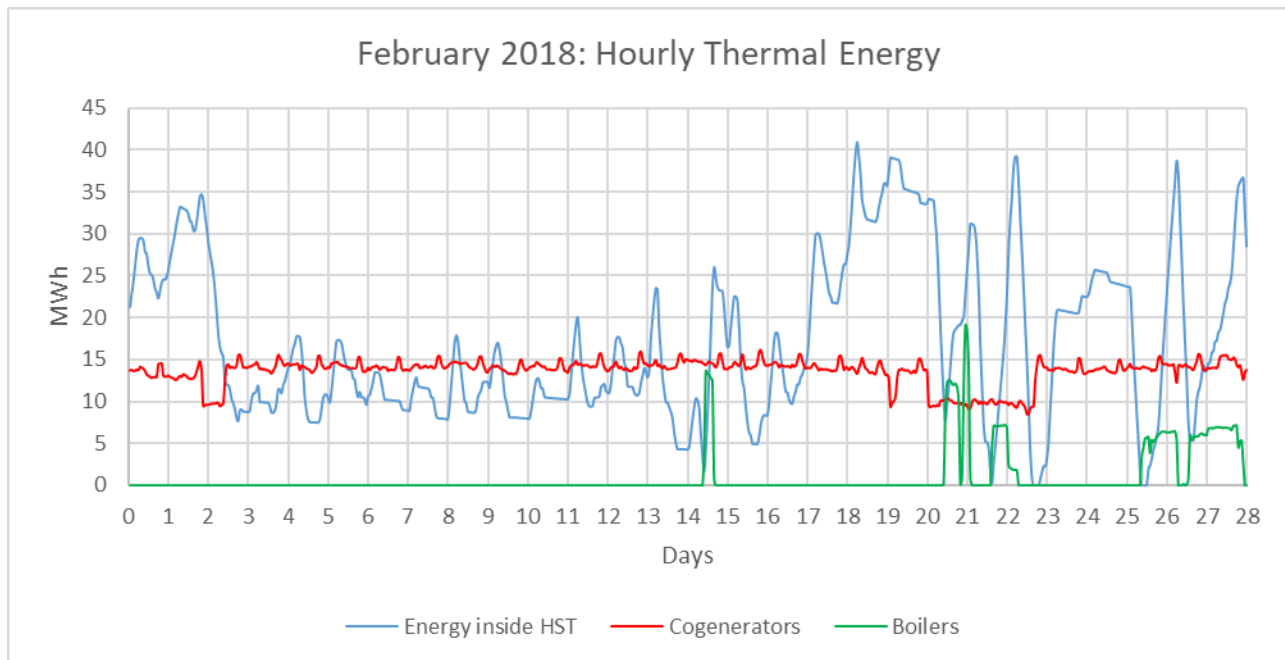


Figure 2 6: Hourly Thermal Energy in Power Station, February 2018

		Cogenerators	Boilers
<i>Energy produced</i>	<i>MWh</i>	9,170	657
<i>Average th. Power</i>	<i>MW</i>	14	1

Table 2 3: Thermal production in Power Station, February 2018

		Tanks
<i>Maximum th. Energy inside</i>	<i>MWh</i>	41
<i>Minimum th. Energy Inside</i>	<i>MWh</i>	0
<i>Average th. Energy inside</i>	<i>MWh</i>	17

Table 2 4: Energy inside the HST

As we can see, in February the boilers were almost OFF, whereas the storage tanks were strongly present in the last week of the month, from the 20th to the 28th, with quickly charging and discharging phases, during the period of the snowstorm that passed through Italy in those days. The cogenerators thermal power production was almost constant during the month, around 14 MWth, with a slight decrease between the 20th and the 23rd day, when the third CHP unit was OFF and the boilers were switched ON to replace it.

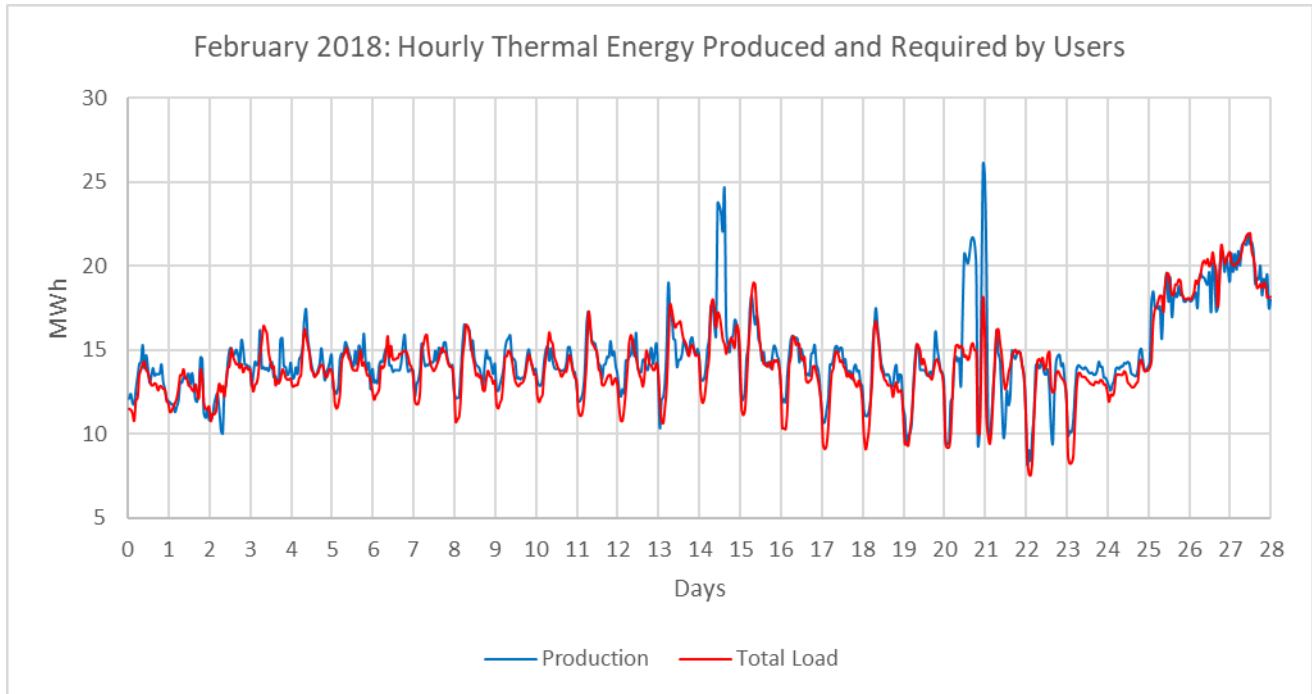


Figure 2 7: Accumulated thermal production and Load, February 2018

	Total	maximum	minimum	average
	<i>MWh</i>	<i>MW</i>	<i>MW</i>	<i>MW</i>
Load	9,518	22	8	14
Production	9,826	26	8	15

Table 2 5: Comparison production and load, February 2018

The load had daily cycles with peaks at the beginning of each day; in particular, the last four days required the higher load.

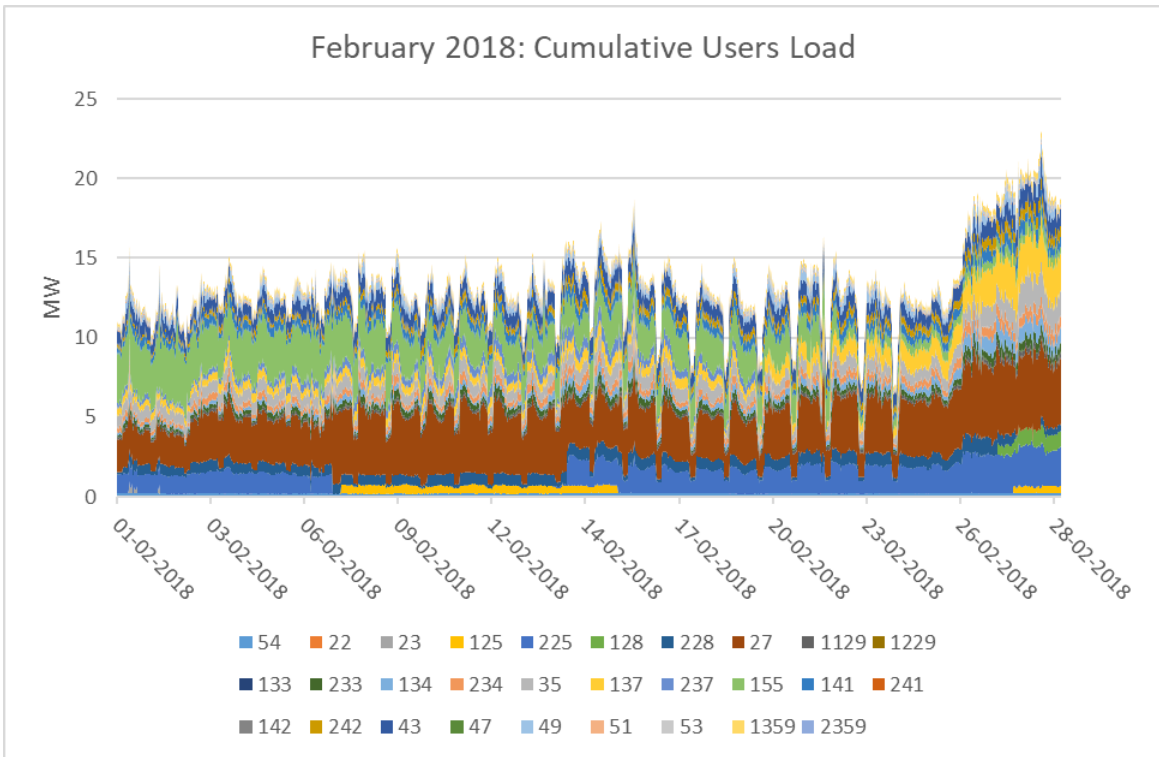


Figure 2 8: Cumulative Users Load, February 2018

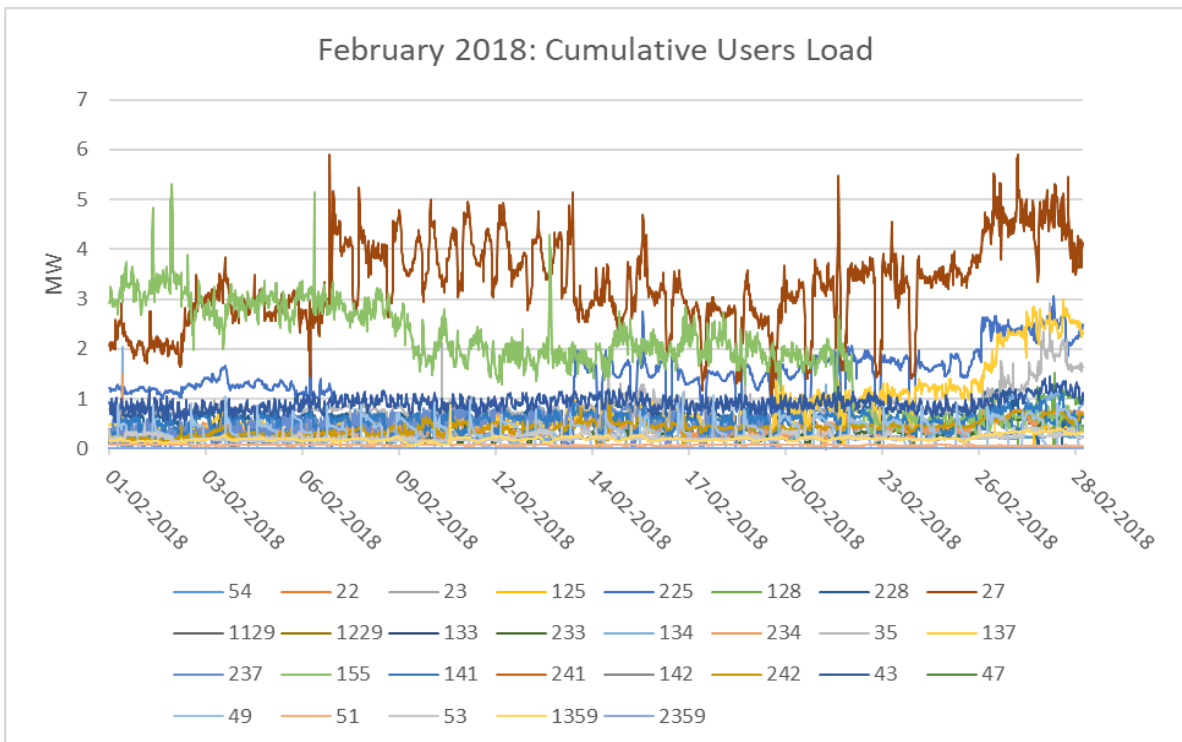


Figure 2 9: Users Loads, February 2018

Chamber	1	3	7	9.1	9.1	9.1
Node	54	22	23	125	225	128
Maximum [MW]	0.3	0.0	0.0	0.7	3.1	1.5
Minimum [MW]	0.1	0.0	0.0	0.0	0.0	0.0
Average [MW]	0.2	0.0	0.0	0.2	1.2	0.1

Chamber	9.1	9.1	9	9	11	11
Node	228	27	1129	1229	33	33
Maximum [MW]	1.2	5.9	0.4	0.0	0.0	0.9
Minimum [MW]	0.0	0.9	0.1	0.0	0.0	0.1
Average [MW]	0.6	3.3	0.2	0.0	0.0	0.3

Chamber	11	11	12	13	13	14
Node	134	234	35	137	237	155
Maximum [MW]	2.1	0.3	2.9	3.0	1.0	5.3
Minimum [MW]	0.0	0.1	0.0	0.1	0.0	0.3
Average [MW]	0.4	0.2	0.8	0.8	0.3	1.9

Chamber	E	E	E	E	17	22
Node	141	241	142	242	43	47
Maximum [MW]	1.1	0.0	0.1	1.0	1.5	0.0
Minimum [MW]	0.1	0.0	0.0	0.0	0.5	0.0
Average [MW]	0.5	0.0	0.0	0.4	0.9	0.0

Chamber	22	24	6	11	11
Node	49	51	53	1359	2359
Maximum [MW]	1.1	0.3	0.6	0.9	0.0
Minimum [MW]	0.0	0.0	0.1	0.0	0.0
Average [MW]	0.3	0.1	0.2	0.2	0.0

Table 2 6: Users Loads, February 2018

In February the most energy demanding users were user 155 (requiring 14 % of the load), and Molo E, user 27 (requiring 24 % of the load). In particular, the user 155 (representing two absorption chillers) was switched OFF on the 22nd of February and to replace it the absorption chiller in PG 107 increased its load till the end of the month. Furthermore, we have to point out that the user 225 increased its load significantly in the last two weeks, whereas all the other user loads were almost constant during the month.

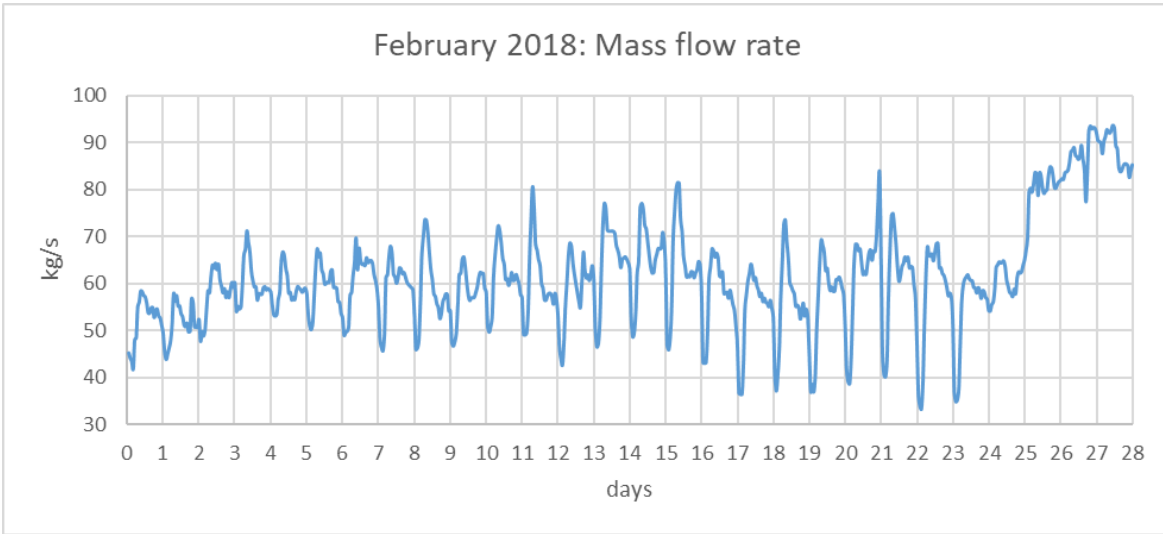


Figure 2 10: Mass flow rate, February 2018

The mass flow rate, as the load, had daily cycles and increased during the last four days of the month.

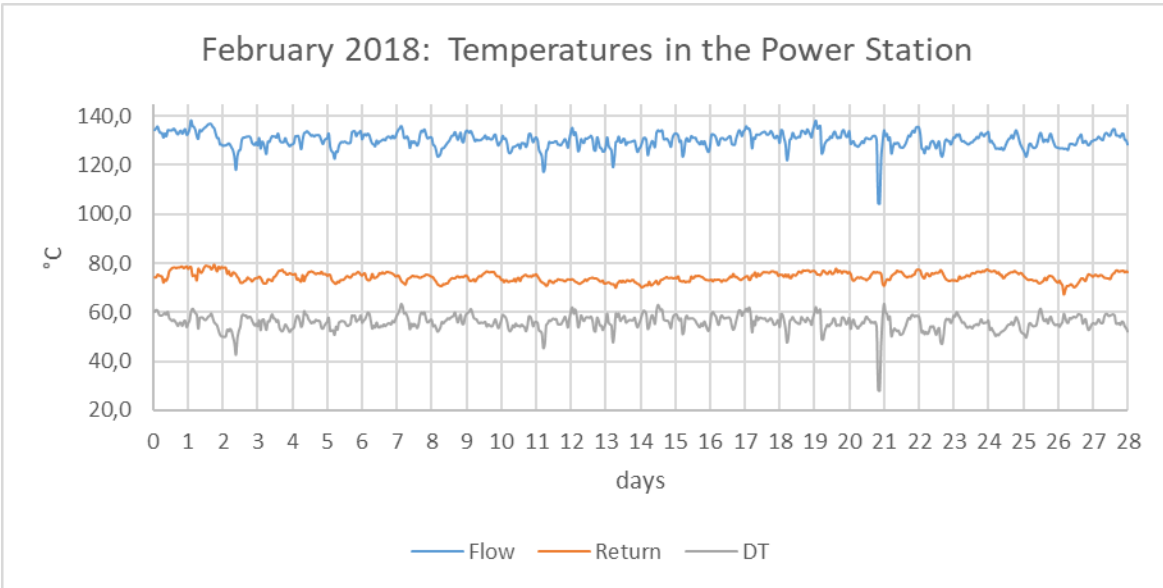


Figure 2 11: Temperature profiles, February 2018

	T Flow	T Return	DT
	°C	°C	°C
Average	130	74	56

Table 2 7: Temperature comparison in the Power Station, February 2018

The flow and return temperatures were almost constant during the month, with regular profiles, except for the end of the 20th day when they had a brief drop down.

In the following figures, we will see the hourly electric production of the CHP units.

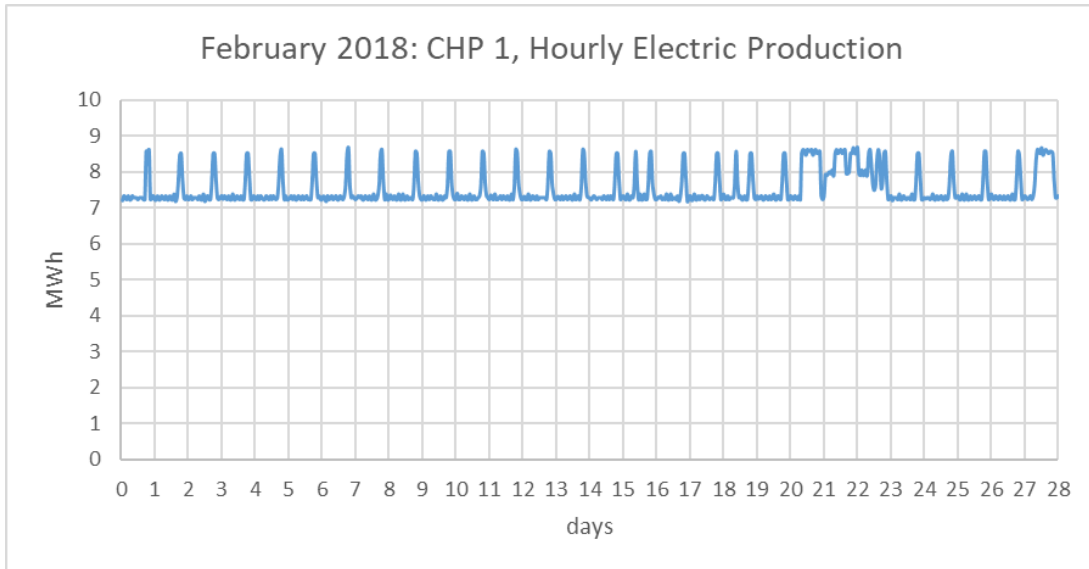


Figure 2 12: Electric production of the CHP 1, February 2018

		CHP 1
<i>Electric Energy produced</i>	<i>MWh</i>	5,046
<i>Average Power</i>	<i>MW</i>	7.5

Table 2 8: Electric production CHP1, February 2018

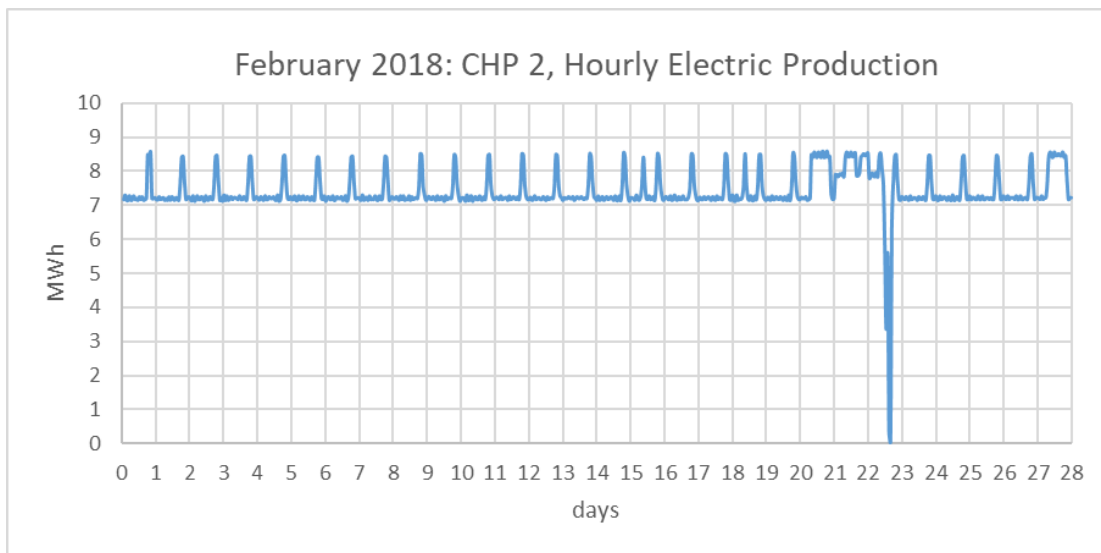


Figure 2 13: Electric production of the CHP 2, February 2018

		CHP 2
<i>Electric Energy produced</i>	<i>MWh</i>	4,973
<i>Average Power</i>	<i>MW</i>	7.4

Table 2 9: Electric production CHP2, February 2018

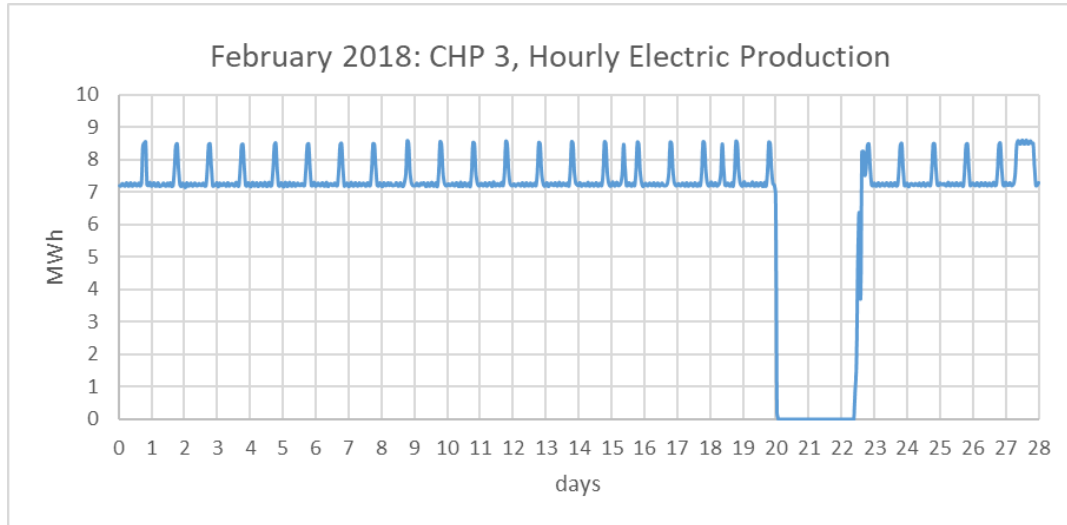


Figure 2 14: Electric production of the CHP 3, February 2018

		CHP 3
<i>Electric Energy produced</i>	<i>MWh</i>	4,548
<i>Average Power</i>	<i>MW</i>	6.8

Table 2 10: Electric production CHP3, February 2018

As we can see, only the third CHP was OFF for a significant period in February, between the 20th and the 23rd, the same days during which the boilers were ON to replace it.

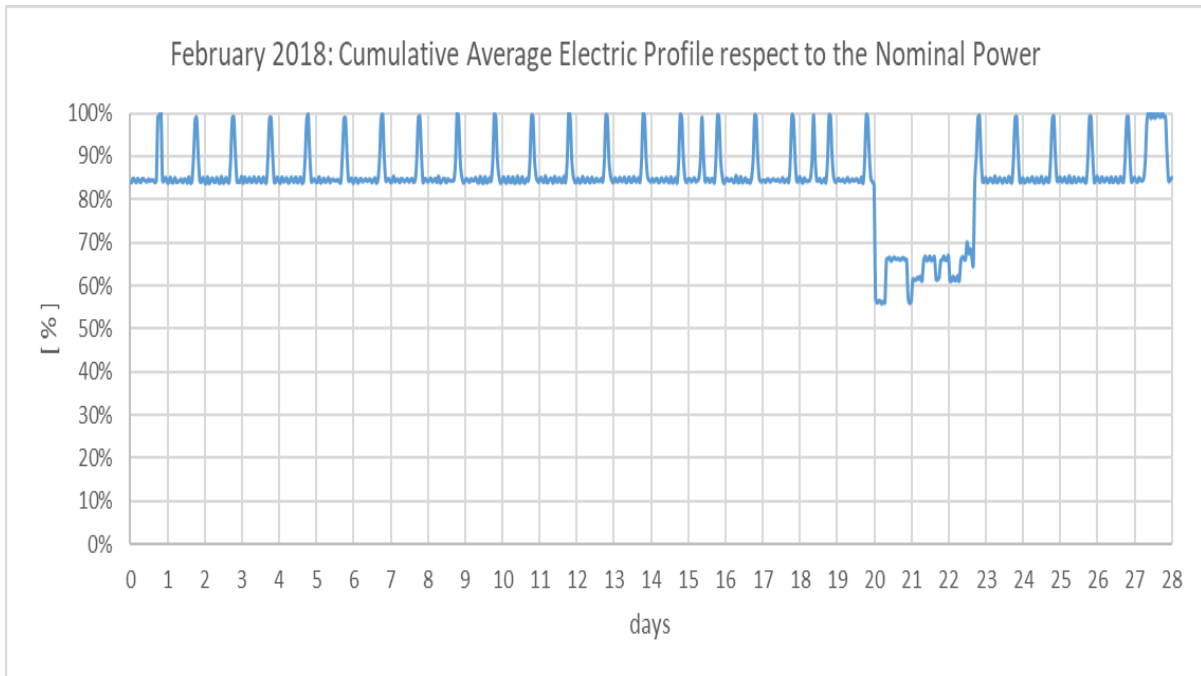


Figure 2 15: Cumulative Average Electric Profile respect to the Nominal Power, February 2018

Miximum	%	100
Minimum	%	56
Average	%	84

Table 2 11: Cumulative Average Electric Profile, February 2018

As we can see in Figure 2 15, in February the CHP units worked on average at 84 % of their electric nominal power, with daily peaks of 100%, except for the period from the 19th to the 23rd day when the third CHP was OFF.

Chapter 3: General description of the simulation Platform: ENSim

3.1 Brief overview of the simulation model

The simulation model is software ENSim, developed in Simulink platform. The simulation model is made of different blocks representing each component of the district heating network. Inside each block a number of equations are modelled and these are solved at each step of simulation. The time step of simulation has been fixed at 1200 seconds, because the user substations collect the load data each 1200 seconds. A short step in comparison to the length of the periods analysed (one month) during simulation makes ENSim a software for dynamic simulation, since it can simulate the dynamic behaviour of a system during long periods in terms of thermal powers, temperatures and mass flow rates. To start the simulation, it is necessary to firstly run a Matlab script called 'Start all' that calls others scripts that download on the workspace the variables needed for the simulation.

The first script to be called is 'Parmod' that defines the time step of simulation, the volume, the reference temperature and the thermal transmittance of the Hot Storage Tank;

Parmod calls other scripts:

- 'Definizione tratti';

- 'Definizione Carichi';

- 'InputCHP';

- 'Definizione Temperature'.

The last script that 'Start all' launches, is called 'MAIN_PROGRAM_DEF', here is implemented software IHENA [16], that solves hydraulically and thermally the network at the first iteration. When 'MAIN_PROGRAM_DEF' quits the simulation of the Simulink model starts.

But let us see in detail the purpose of each input.

3.2 The Input excel File

The Input excel File is called by the script 'Definizione Tratti'; it has to be compiled by the user and it creates the topology of the network.

First of all, it is necessary to define:

- Number of nodes;
- Number of pipes;
- Number of sources;
- Reference ambient temperature;
- Maximum number of mass flow rate algorithm iterations;

Afterwards it is necessary to define all nodes;

For nodes, it is mandatory to define the ID, it means the identification number, the spatial coordinates and the typology:

- 0 for sources;
- 1 for mixing nodes;
- 2 for user nodes;

Sources nodes need the initial flow temperature and pressure, the expansion vessel pressure. and the efficiency of pumping station more. Mixing nodes do not need other inputs.

User nodes need the default thermal load; it is computed as the average load of the user in the period of study. User nodes need the typology of algorithm to compute the mass flow rate at each time step, 1 for constant mass flow rate, 2 for constant DT. For user nodes, it is also necessary to define the nominal temperature drop between flow and return, the default load, the default mass flow rate, the last two ones have to be defined only if present.

Afterwards it is necessary to define all branches;

For branches is mandatory to define the ID, the inlet node and the outlet node, moreover they need:

- Intern diameter of pipes;
- Thickness and conductivity of the tube;
- Thickness and conductivity of the insulation;
- Thickness and conductivity of the coating;
- Friction inside the tube
- ID of the pipe;
- Coefficient of concentrated load losses.

3.3 Matlab and Simulink Inputs

As we said, to run the simulation it is necessary to launch a script called 'Start all'; this script runs other scripts that define the variables that the model needs to read in the workspace during the simulation.

The first script launched by 'Start all' is 'Parmod'; inside this script there are some sections and each one defines variables for a specific part of software IHENA or a specific Simulink block.

The first section is about 'Common parameters', which are defined:

– $cp_h = 4.186 \left[\frac{kJ}{kgK} \right]$, specific heat of water;

– $T_{amb} = 28 [^{\circ}C]$, temperature of the tunnels where the pipes are posed, and it is supposed to be equal to the external surface temperature of the pipes themselves.;

– $step = 1200$ seconds, step of simulation;

The second section is about 'Network parameters', which are defined:

– $F_{cor} = 0.7$; it is a parameter that multiplies the conductivity of each pipe in the computation of the thermal decay along each duct; this value has been chosen, as we will see, after a work of thermal losses calibration between the measured data and simulation results.

–'Definizione tratti', it is the script that reads the Input excel file where is designed the network from the geometric point of view, with its nodes and branches. This script calls a Matlab function called 'Resis_tub' that computes the thermal resistance of each pipe, cylindrical geometry, by the values of the diameters and conductivities of each layer of the pipe. It then saves this information for each pipe inside variables used during the simulation to compute the temperature decay along the network.

$$Res_{tube} = \frac{\log\left(\frac{r_{est\ tube}}{r_{int\ tube}}\right)}{2*\pi*k_{tube}} \left[\frac{^{\circ}C*m}{W} \right] \text{ thermal resistance of the tube (3.1);}$$

$r_{est\ tube}$: external radius of the tube [m];

$r_{int\ tube}$: internal radius of the tube [m];

k_{tube} : thermal conductivity of the tube $\left[\frac{W}{m^{\circ}C} \right]$;

$$Res_{ins} = \frac{\log\left(\frac{r_{est\ ins}}{r_{int\ ins}}\right)}{2*\pi*k_{ins}} \left[\frac{^{\circ}C*m}{W}\right] \text{ thermal resistance of the insulation (3.2);}$$

$r_{est\ ins}$: external radius of the insulation [m];

$r_{int\ ins}$: internal radius of the insulation [m];

k_{ins} : thermal conductivity of the insulation $\left[\frac{W}{m^{\circ}C}\right]$;

$$Res_{coat} = \frac{\log\left(\frac{r_{est\ coat}}{r_{int\ coat}}\right)}{2*\pi*k_{coat}} \left[\frac{^{\circ}C*m}{W}\right] \text{ thermal resistance of the coating; (3.3)}$$

$r_{est\ coat}$: external radius of the coating [m];

$r_{int\ coat}$: internal radius of the coating [m];

k_{coat} : thermal conductivity of the coating $\left[\frac{W}{m^{\circ}C}\right]$;

$$R_{tot} = Res_{tube} + Res_{ins} + Res_{coat} \left[\frac{^{\circ}C*m}{W}\right] \text{ thermal resistance of the pipe; (3.4)}$$

$$K_{cond} = \frac{1}{A*R_{tot}} \left[\frac{W}{m^2^{\circ}C}\right] ; \text{ thermal conductivity of the pipe}$$

$$A = 2 * \pi * (r_{est\ pipe}) [m];$$

$$-cp_{ft} = 4,186 \left[\frac{J}{kgK}\right], \text{ specific heat of water;}$$

The third section is about 'Hot Storage Tank parameters', it defines:

$$-V_{acc\ tot} = 1,000 [m^3], \text{ volume of the tank;}$$

$$-Diam_{acc\ fisico} = \left(\frac{4*Volume}{3*\pi}\right)^{\frac{1}{3}} [m], \text{ diameter of the tank;}$$

$-KACC = 0.2 \left[\frac{W}{m^2K} \right]$, conductivity of the tank;

The third section is about 'User loads parameters', where the script 'Definizione carichi' is launched.

This script creates the variables which contain the values of the loads in kW of each user node for each step of simulation. Each load profile is associated to its own user node by the ID number. Moreover, this script defines the time variables of simulation:

$-passi_{dati}$: steps of simulation;

$-secondi_{dati}$: seconds of simulation;

$-minuti_{dati}$: minutes of simulation;

$-ore_{dati}$: hours of simulation;

$-giorni_{dati}$: days of simulation;

The fourth section is about 'Thermal Power Station parameters', it defines:

$Trif_{accumulo}$: reference temperature for the hot storage tank;

T_{tank0} : Temperature of the hot storage tank at the first step of simulation;

The fifth section is about 'CHP input parameters', where the script 'INPUT_CHP' is launched. This script creates the variable containing the electric profile, and the mass flow rate profile of each CHP. Inside it all the parameters the model of the CHP needs for the simulation are defined, these parameters are constant values taken from the data sheets of the machine:

$m_{dot,hCHP,LT} = 35.56 \left[\frac{kg}{s} \right]$, Mass flow rate of cooling water of the lubricant oil;

$m_{dot,hmCHP} = 50 \left[\frac{kg}{s} \right]$, Mass flow rate of cooling water of the motor;

$G_{max,un,CHP}$

$= 28.61 \left[\frac{kg}{s} \right]$, Maximum mass flow rate of water, user side, that can flow inside the CHP;

$\eta_{el,nomCHP} = 0.4705$, electric efficiency;

$P_{el,maxCHP} = 8,566 [kW]$, Nominal electric power;

$P_{th,maxCHP} = 7,897 [kW]$, Nominal thermal power;

$Hi_{CH4} = 35,600 \left[\frac{kJ}{Sm^3} \right]$, Low Heating Value of Methane;

$densità_{CHP} = 0.71692 \left[\frac{kg}{Sm^3} \right]$, density of Methane;

$alfa_{CHP}$ = assumed to 17.2, stoichiometric constant for combustion;

$perdite_{CHP}$ = assumed to 14%, heat losses due to irradiation of exhaust gases;

eta_{alt} = assumed to 0.95, alternator efficiency;

cp_f = assumed to $1.2 \left[\frac{kJ}{kgK} \right]$, specific heat of exhaust gases;

$eff_{sc,af}$ = 0.75, efficiency of the heat exchanger user water/exhaust gases;

$eff_{sc,aa}$ = 0.75, efficiency of the heat exchanger user water/motor cooling water;

$eff_{sc,LT}$ = 0.75, efficiency of the heat exchanger user water/oil cooling water;

$profilo_{GTC_{elettrico}}$: hourly electric profile, it is different for each CHP, and it is the real electric profile measured in the studied period;

$potenza_{th_{CHP}}$: hourly thermal profile, it is different for each CHP. It is necessary to compare the thermal power produced in the simulation and the real thermal power produced in the studied period;

$profilo_{CHP,portata}$: hourly mass flow rate profile, it is different for each CHP.

It is the real mass flow rate profile of water getting inside each CHP at each time step;

The sixth section is about 'Temperature input parameters', where the script 'Definizione_Temperature' is launched. This script creates the variables containing the value of temperature drops on each user node at each time step of simulation, this script works only in the simulation of validation.

In this last version of software ENSim, we give the model both the MFR profile of the CHP units, and the temperature drops profiles on the users as input. This management of the MFR inside the power station allows to reach a good correspondence between the simulated global mass flow rate flowing inside the network and the measured one.

3.4 Software IHENA: Intelligent Heat Energy Network Analysis

This software has been implemented by the University of Bologna⁸ and since the previous version of ENSim became the algorithm computing the mass flow rate flowing inside each pipe of the Network. From this new version of ENSim, this software, modelled as a Matlab function at each time step solves not only hydraulically but also thermally the network according to the loads required by the users. It computes the mass flow rate and the temperature decay for each pipe of the network. Software IHENA is implemented in the script 'MAIN_PROGRAM_DEF', it solves hydraulically and thermally the network at the first time step, and after the simulation starts, it is recalled at each time step of simulation by the matlab function 'MAIN_DEF_2'.

Software IHENA is based on Todini Pilati's algorithm⁹. This algorithm was chosen because of the quick convergence and the trusty resolution method. Every district heating system can be represented as a certain number of nodes (NN) and branches (NR). Nodes can be sources, it means point of heat production, mixing point, where the incoming mass flow rate is equal to the exiting, and users. For each branch r_{ij} of the grid, where i and j are the inlet and outlet nodes, we can write the energy balance:

$$\Delta H_{rj} - (H_i - H_j) = 0 ;(3.5)$$

where ΔH_{rj} represents the pressure drop along branch r_{ij} , and H_i and H_j is the energy content of the fluid in nodes i and j.

The pressure drop is the sum of distributed load losses and concentrated load losses.

Distributed load losses are computed by the Darcy-Weisbach equation:

$$\Delta H_{dis} = f \frac{L}{D} \rho \frac{v^2}{2} ;(3.6)$$

f: friction factor of Darcy;

L: length of the branch;

D: diameter of the branch.

Concentrated load losses are computed by the following expression:

$$\Delta H_c = \beta \rho \frac{v^2}{2} ;(3.7)$$

⁸ M. A. Ancona, F. Melino. *Analisi di soluzioni tecniche e gestionali che favoriscano l'implementazione di nuovi servizi energetici nelle reti termiche in presenza di sistemi di generazione distribuita*. Report RdS/PAR2013/053.

⁹ E. Todini. A gradient method for the analysis of pipe networks [14].

β : coefficient of concentrated load losses ;

For each node of the network the mass flow rate balance is defined:

$$\Sigma_{in} Q_{in} - \Sigma_{out} Q_{out} - \Sigma_u q_u = 0 \quad (3.8)$$

where:

$\Sigma_{in} Q_{in}$: sum of mass flow rates getting inside the node;

$\Sigma_{out} Q_{out}$: sum of mass flow rates getting out of the node;

$\Sigma_u q_u$: sum of the mass flow rates extracted, positive, or injected, negative, at the node.

In a network composed of NN nodes and NR branches there are NN equation of mass flow rate balance and NR equation of energy balance, that in matrix form can be written as:

$$F_p(Q, H) = A_{11}Q + A_{12}H = 0; \quad (3.9)$$

$$F_Q(Q, H) = A_{21}Q - q = 0; \quad (3.10)$$

We obtain a system of NR+NN equations that can be written as:

$$\begin{cases} F_p(Q, H) = A_{11}Q + A_{12}H = 0 \\ F_Q(Q, H) = A_{21}Q - q = 0 \end{cases} ;(3.11)$$

$A_{11}[NR \times NR]$ is a diagonal matrix where the elements of the main diagonal are:

$$A_{11}(j, j) = \frac{\partial F_{pj}}{\partial Q_j} = \frac{\partial \Delta H_j}{\partial Q_j} ;(3.12)$$

$A_{21}[NN \times NR]$ is the matrix where the lines are the nodes of the network and the columns are the branches; its elements are +1 when the mass flow rate gets inside the node, -1 when the mass flow rate exits the node, 0 when there is no relation between the node and the branch.

Then $A_{12}[NR \times NN]$ is the transposed matrix of A_{21} .

The NR+NN system is solved in IHENA in an iterative way by the Newton Raphson method generalized in a matrix form by Todini Pilati.

To start the iterative process, it is necessary to define NR attempts value for the mass flow rate, set to 1 kg/s, NN attempts value for the energy content of the fluid, set to 20 m, and the direction value of the mass flow rates, meaning the elements of matrix A_{21} .

For the generic iteration (m) the system to solve is:

$$\begin{cases} F_p(Q, H) = A_{11}Q^m + A_{12}H^m = 0 \\ F_Q(Q, H) = A_{21}Q^m - q = 0 \end{cases} ;(3.13)$$

Moving to Newton Raphson method it becomes:

$$\begin{cases} F_p(Q, H) = A_{11}\Delta Q^m + A_{12}\Delta H^m = -dE \\ F_Q(Q, H) = A_{21}\Delta Q^m = -dq \end{cases} ;(3.14)$$

dE and dq are the residuals for the energy balance and for the mass flow rate balance at the iteration (m-1). Considering the generic node i and the generic branch j , we can write:

$$-dq = -(\Sigma_{in} Q_{in} - \Sigma_{out} Q_{out} - \Sigma q_u) ;(3.15)$$

$$-dE = -\left[\Delta H_{r_{ij}} - (H_i - H_j)\right] ;(3.16)$$

The solution of the system is to determine ΔQ^m and ΔH^m .

At each iteration it is necessary to update the value of the mass flow rate for each branch and the energy content for each node:

$$H^m = H^{m-1} + \Delta H^m ;(3.17)$$

$$Q^m = Q^{m-1} + \Delta Q^m ;(3.18)$$

If the result of the mass flow rate in a branch is negative it means that the mass flow rate flows in the opposite direction inside the branch and consequently at each time step the matrix A_{21} has to be updated. The iterative process stops when the convergence fixed at $10e-9$ is reached for dq_i and dE_i . The same algorithm is used to solve the network hydraulically in the return configuration.

After having solved the network hydraulically, software IHENA starts to compute the temperature at each node of the network, using the parameters of length and of thermal conductivity of each pipe defined by the scripts described previously. The algorithm in flow starts from the source nodes, the flow collectors, and calculates the temperature distribution along the network till the user nodes. It uses the formula of the exponential temperature decay along each pipe (cylindrical geometry) at a fixed surface temperature and the mixing in the mixing nodes is supposed to be perfect. The same algorithm is applied in return; this time it starts from the user nodes and it reaches the sources, considered as the return collectors. The nodes in return have the same spatial coordinates of the nodes in flow. In the end, IHENA computes the heat distribution losses summing the heat losses in flow and in return along each pipe of the network. We are going to show the formula to compute the heat distribution losses only in flow, since in return it is the same.

$$Q_{th,losses,flow} = \sum_{i=1}^{NR} G_i * cp_h * (T_{n,i} - T_{n,o}); (3.19)$$

G : mass flow rate flowing inside the pipe $\left[\frac{kg}{s}\right]$;

$T_{n,i}$: Temperature of the inlet node of the pipe $[^{\circ}C]$;

$T_{n,o}$: Temperature of the outlet node of the pipe $[^{\circ}C]$;

3.5 Overcoming of the previous model

The previous version of the model was only run for the first twenty days of December 2017. It was based on a fixed hydraulic scheme of the network during all the simulation, created by two Simulink blocks, one in flow and one in return, hydraulically and thermally solving the network by a number of matlab functions equal to the pipes of the network. The flow rates flowing inside each pipe at each time step were computed by software IHENA. The fixed scheme of the network was designed solving the hydraulic problem at the first time step of simulation. In the dynamic hydraulic solution of the network computed by IHENA, when a user node is fed by two different loops and one loop supplies MFR in excess, the difference between the MFR supplied and the MFR required by the user exits the user node and it gets into the pipe of the second loop. This aspect was not considered in the previous version of the model. The first step of this work was:

-to replace the fixed scheme of the network with the dynamic one provided by software IHENA at each time step;

-to compute the temperature distribution along each segment of the network by software IHENA, deleting the Simulink blocks that, in the previous version, solved the network thermally and in which was the fixed hydraulic scheme of the network.

At that point, we decided to replace the lines of code inside software IHENA, computing the linear temperature decay inside each pipe (cylindrical geometry) considering convection and conduction, with the formula of the exponential temperature decay at fixed surface temperature considering only conduction, as it happened in the Simulink blocks of the previous model. The formula of the linear temperature decay is:

$$T_{out} = T_{in} - (T_{in} - T_{surface}) * \left(\frac{1}{Res * G * c}\right) [^{\circ}C] ; (3.20)$$

$$Res = Res_1 + Res_2 + Res_3 + Res_4 + Res_5; (3.21)$$

$$Res_1 = \frac{1}{2r_{int}\pi\alpha_1L} \left[\frac{^{\circ}C}{W}\right] ; (3.22)$$

$$Res_2 = \frac{\log_{10}\left(\frac{r_{est\ tube}}{r_{int\ tube}}\right)}{2*\pi*k_{tube}L} \left[\frac{^{\circ}C}{W}\right] ; (3.23)$$

$$Res_3 = \frac{\log_{10}\left(\frac{r_{est\ ins}}{r_{int\ ins}}\right)}{2*\pi*k_{ins}L} \left[\frac{^{\circ}C}{W}\right] ; (3.24)$$

$$Res_4 = \frac{\log_{10}\left(\frac{4*Zeta}{2*res_{iso}}\right)}{2*\pi*k_{earth}L} \left[\frac{^{\circ}C}{W}\right]; (3.25)$$

$$Res_5 = \frac{1}{2r_{iso}\pi\alpha_2L} \left[\frac{^{\circ}C}{W}\right]; (3.26)$$

α_1, α_2 : inner and outer convective coefficients $\left[\frac{W}{m^2^{\circ}C}\right]$;

k_{earth} : linear conductivity of earth $\left[\frac{W}{(m^{\circ}C)}\right]$;

$Zeta$: earth depth of pipes burying [m];

The exponential temperature decay for a fluid inside a pipe (cylindrical geometry) at a fixed surface temperature is computed as:

$$T_{out} = T_{surface} + (T_{in} - T_{surface}) * \exp\left(-\frac{\pi*D_{est}*K_{cond}*L*F_{cor}}{G*c}\right) [^{\circ}C] ; (3.27)^{10}$$

T_{out} : Temperature of the fluid exiting the pipe [$^{\circ}C$];

$T_{surface}$: Temperature of the external surfaces of the pipe [$^{\circ}C$];

T_{in} : Temperature of the fluid getting inside the pipe [$^{\circ}C$];

D_{est} : External diameter of the pipe [m];

$R_{tot} = Res_{tube} + Res_{ins} + Res_{coat}$ $\left[\frac{^{\circ}C*m}{W}\right]$ thermal resistance of the pipe;

$K_{cond} = \frac{1}{A*R_{tot}}$ $\left[\frac{W}{m^2^{\circ}C}\right]$; thermal conductivity of the pipe

$A = 2 * \pi * (r_{est\ pipe})$ [m];

L : Length of the pipe [m];

F_{cor} : Correction factor of the pipe conductivity [-];

G : Mass flow rate flowing inside the pipe $\left[\frac{kg}{s}\right]$;

¹⁰ F. Incropera, D. Dewit, T. Bergman, A. Lavine. *Introduction to heat transfer, 6th edition.*

c : Specific heat of water $\left[\frac{J}{Kg^{\circ}C}\right]$;

After having simulated the first twenty days of December 2017 using the new model, we obtained different results for the supply temperature compared to the simulation of the previous version of the model, for the same period, as we can see in Figure 3. 1 . First of all, we should say that at each time step software IHENA solves the hydraulic problem of the network differently, according to the loads of the users, and even if the previous version of the model exploited the same flow rates coming from IHENA, it used a fixed hydraulic scheme of the network to calculate the temperature distribution, meaning that the verses of the flow rates were always the same during the simulation.

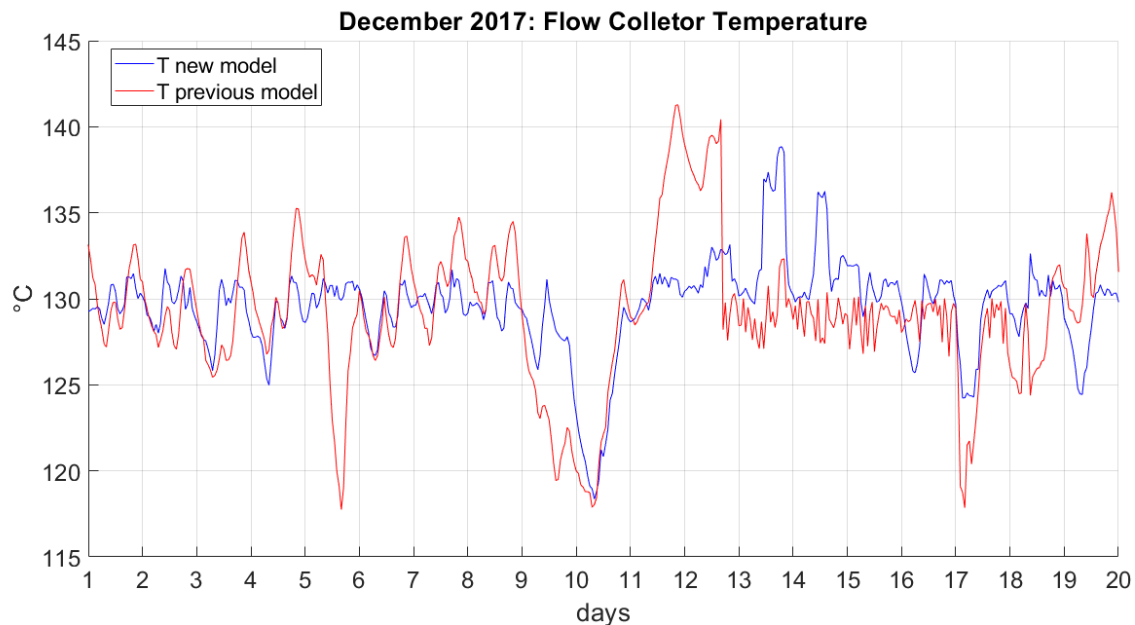


Figure 3. 1: Flow Collector Comparison, New model VS Previous model, December 2017

From Figure 3. 2 we can appreciate how many branches the fixed scheme of the network had the verse of MFR wrong per single time step in flow, with reference to the dynamic scheme produced by software IHENA, in the simulation of the first 20 days of December 2017.

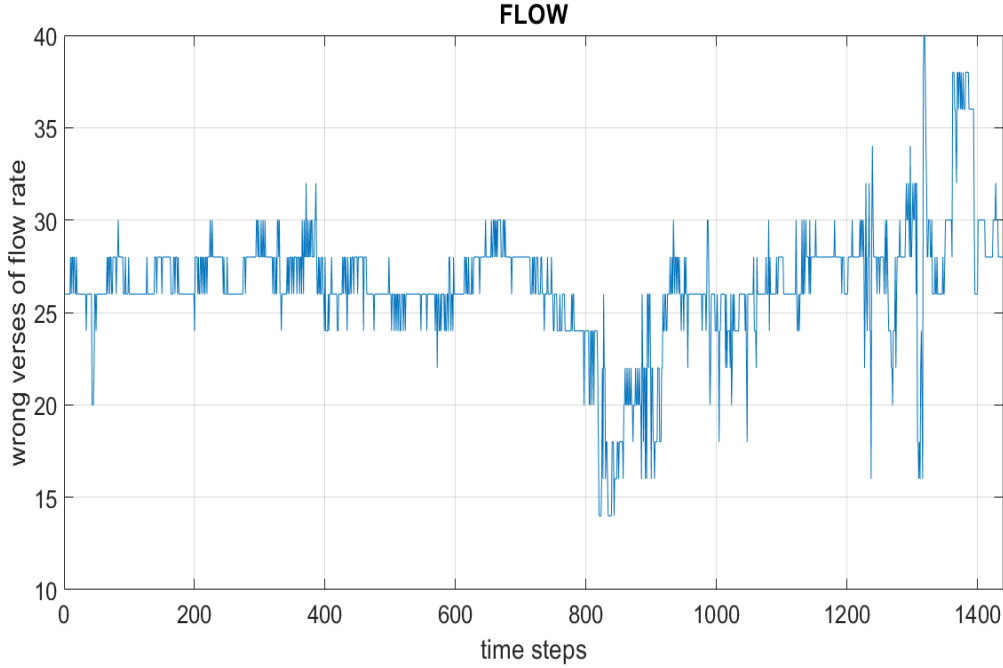


Figure 3. 2: Wrong verses in flow, December 2017

Another possible reason why the results of the simulation of December 2017 were different between the two versions of the model was due to the way the temperature exiting the user nodes was computed. In the Simulink Blocks of the previous version of the model, the temperature exiting the user node was computed as:

$$T_u = T_{in} - \frac{Q_{load}}{G_{getting\ inside\ user\ node} * cp} [^{\circ}C] \quad (3.28)$$

In software IHENA the temperature exiting the user node, even when the load on the user was null, was computed as:

$$T_u = T_{in} - \Delta T_{fix} [^{\circ}C] \quad ;(3.29)$$

We decided to replace in IHENA the previous formula, 3.29, with the following one, 3.30, to compute the temperature exiting the user node:

$$T_u = T_{in} - \frac{Q_{load}}{G_{asked\ by\ the\ user} * cp} [^{\circ}C] \quad ;(3.30)$$

Where $G_{asked\ by\ the\ user}$ at each time step is:

$$G_{asked\ by\ the\ user} = \frac{Q_{load}}{cp * \Delta T_{fix}} \left[\frac{kg}{s} \right] \quad ;(3.31)$$

$$G_{asked\ by\ the\ user} \neq G_{getting\ inside\ user\ node} ;(3.32)$$

$G_{asked\ by\ the\ user}$ is different from $G_{getting\ inside\ user\ node}$ because in the previous model the verses of the MFR flowing inside the network were fixed and this configuration forced the flow rates to get inside the user node, and consequently changed the computation of the temperature exiting the user node. In Figure 3. 3 we can see an image taken from the previous version of the model where a user node is fed in flow by the two rings. The two mass flow rates coming from the different loops are forced to get inside the user node because of the fixed scheme of the hydraulic network.

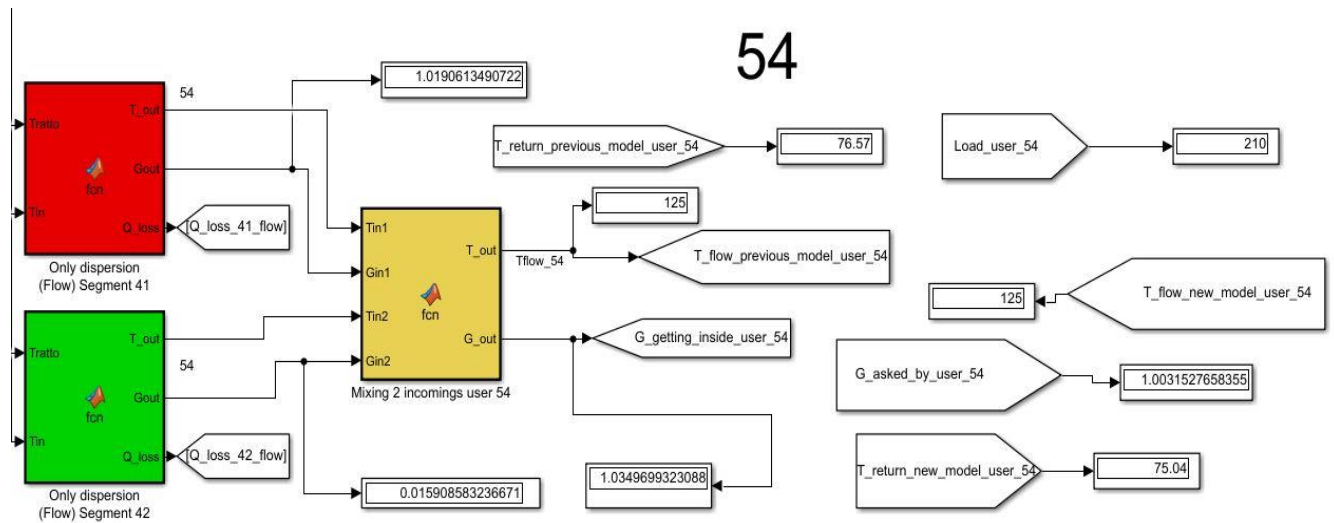


Figure 3. 3: Detail of the flow network from the previous model

The mass flow rate getting inside the user node was the sum of the MFR coming from the two different loops:

$$G_{getting\ inside\ user} = G_{DN\ 200} + G_{DN\ 350} = 1.019 + 0.016 = 1.035 \left[\frac{kg}{s} \right] ;(3.33)$$

But the flow rate asked by the user node was:

$$G_{asked\ by\ the\ user} = 1.003 \left[\frac{kg}{s} \right] ;(3.34)$$

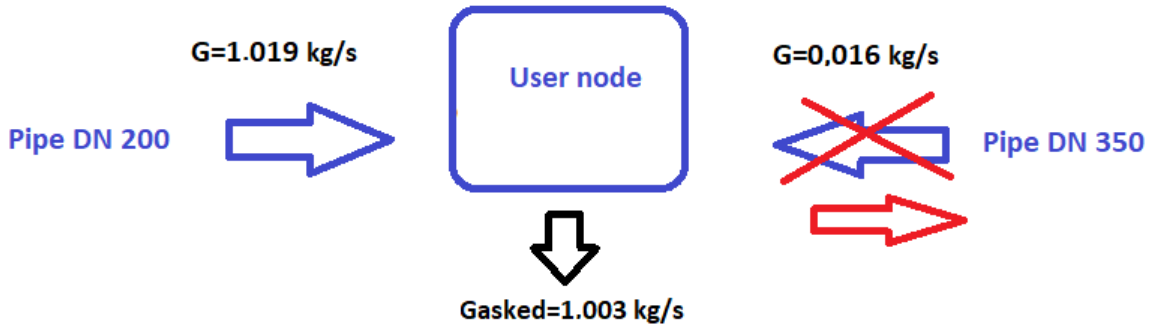


Figure 3. 4: Schematic representation of the MFR balance at the user node

It means that a part of the mass flow rate getting inside the user node from the loop supplying MFR in excess went to the other loop, after feeding the user:

$$G_{2^{nd}ring} = G_{1^{st}ring} - G_{asked\ by\ the\ user} = 0.016 \left[\frac{kg}{s} \right] ;(3.35)$$

For this reason, the previous version of the model solved the thermal distribution problem of the network wrong. In the previous model the temperature exiting the user was:

$$T_{exit\ user\ node} = 125 - \frac{210}{4.186 * 1.035} = 76.57 [^{\circ}C] ;(3.36)$$

Whereas in the new model the temperature exiting the user node is:

$$T_{exit\ user\ node\ new\ model} = 125 - \frac{210}{4.186 * 1.003} = 75.04 [^{\circ}C] ;(3.37)$$

The difference in the temperature exiting the user nodes changes:

- the heat losses on the return path;
- the hydrostatic head of the expansion vessel and consequently the hydraulic resolution of the network, as we can appreciate from the following formulas:

$$Exp.\ vessel\ hydrostatic\ head = \frac{100,000 \frac{Pa}{bar} * 7.8\ bar}{g * \rho_{water}(Tu', Pu')} [m] ;(3.38)$$

$$g: 9.81 \left[\frac{m}{s^2} \right];$$

$$\rho: 1,000 \left[\frac{kg}{m^3} \right]$$

$$Tu' = \frac{\Sigma(T_{exit\ user\ nodes})}{n.\ user\ nodes} [^{\circ}C] ;(3.39)$$

$$Pu' = \frac{\Sigma(P_{exit \ user \ nodes})}{n.user \ nodes} [bar] ;(3.40)$$

n.user nodes: number of user nodes;

This is why simulating the network of Roma Fiumicino with the previous version of the model, and with the new one, we obtained different results for the first twenty days of December 2017. In summation, compared to the previous version of the model, the new one solves the hydraulic problem of the network according to the loads at each time step, and the flow rates flowing inside the pipes can change their verse during the simulation. Inside Software IHENA we replaced the formula to compute the linear temperature decay along a pipe, with the formula of the exponential temperature decay. Moreover, for the computation of the temperature exiting a user node we substituted the formula 3.29 with the formula 3.30. The latter also takes into account the case a user node does not require load at the generic time step.

3.7 Management of The Mass Flow rate inside the Thermal Power Station

The mass flow rate circulating inside the power station is managed regulating the valves of the branches of the power station two by two. This means that the mass flow rate circulating inside branch 1 is the same in branch 6, and the same for branch 3 and 5, branch 2 and 8, branch 4 and 7. The Storage tank can be only charged or discharged, but not both at the same time step.

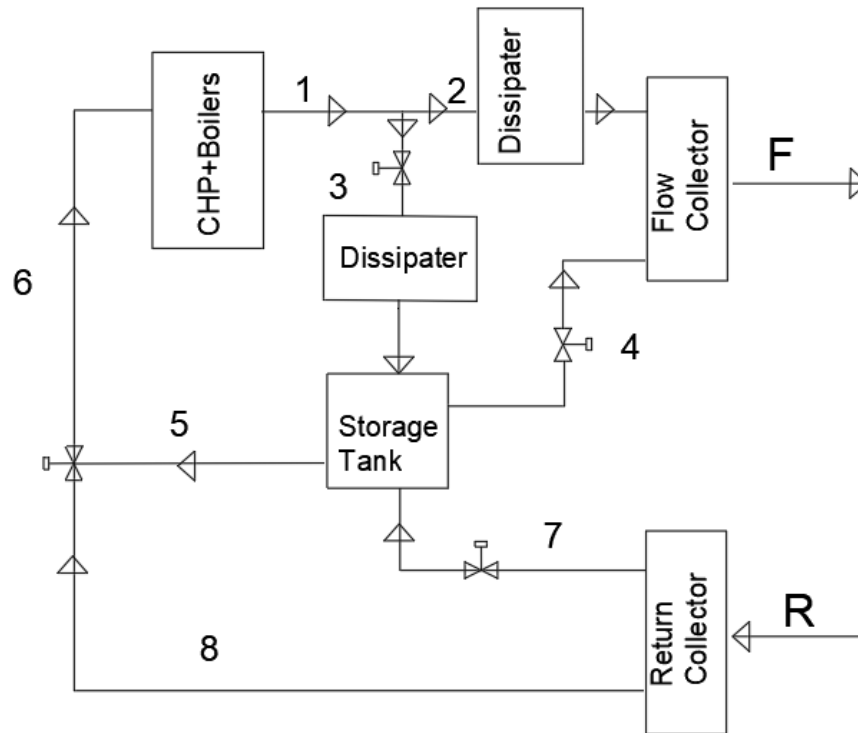


Figure 3. 5: Scheme of the Power Station

No flow rate losses are in the network, and the MFR in flow, G_F , is equal to the MFR in return, G_R .

The MFR flowing inside the network at each time step is computed as the sum of the MFR required by the users.

$$G_F = G_R = \sum G_{users}; \quad (3.41)$$

The mass flow rate getting inside the three CHP units is an input of the simulation, branch 6. The MFR rate getting inside each CHP is not a fixed value but it changes hourly for each CHP; it is the real hourly average value of MFR getting inside the CHP and it has been taken from the data of the power station provided to us by ADR.

$$G_6 = G_1 = \sum G_{CHP}; \quad (3.42)$$

The mass flow rate getting inside the storage tank from the power station, branches 3, is equal to the positive difference between the mass flow rate required by the CHP units, G_6 , and the return mass flow rate of the network, G_R .

$$G_3 = G_5 = |G_6 - G_R|; (3.43)$$

$$G_2 = G_8 = G_6 - G_3; (3.44)$$

The mass flow rate getting inside the tank from the Return Collector, branches 7, is equal to the positive difference between the network MFR and MFR required by the CHP units.

$$G_7 = G_4 = |G_R - G_6|; (3.45)$$

The hot storage tank is managed to guarantee the mass flow rate to the users, even if it is not at the proper temperature; so when it places mass flow rate into the network, branch 4, it is possible it could decrease the flow temperature.

3.8 Fictitious Network Storage tank

This is the component giving thermal inertia to the supply temperature of the network. It is constituted by a storage tank, with a volume equal to the global volume of the pipes; it is collocated at the beginning of the network, which are supposed to be the flow collectors of the thermal power station. The thermal inertia of the network is concentrated inside this fictitious storage tank and it is not distributed along the pipes of the grid. This approximation introduces a little error in the computation of the temperature along the grid but reduces the computational cost of the simulation. This component is modelled as a Matlab function solving the following equation at each time step:

$$\frac{dT}{dt} = \frac{Q_{load} - Q_{aux} - Q_{storage\ tank\ losses}}{c_p * \rho * V_{pipes}} ; (3.46)$$

– Q_{load} : global load of the network including the user load and the heat distribution losses in flow and in return [kW];

– Q_{aux} : thermal power placed into the network by the power station, so at net of the network dissipater [kW];

– $Q_{storage\ tank\ losses}$: heat losses of the hot storage tank inside the model of the thermal power station [kW];

– c_p : specific heat of water $\left[\frac{kJ}{kgK}\right]$;

– ρ : density of water $\left[\frac{kg}{m^3}\right]$;

– V_{pipes} : global volume of the network pipes [m³];

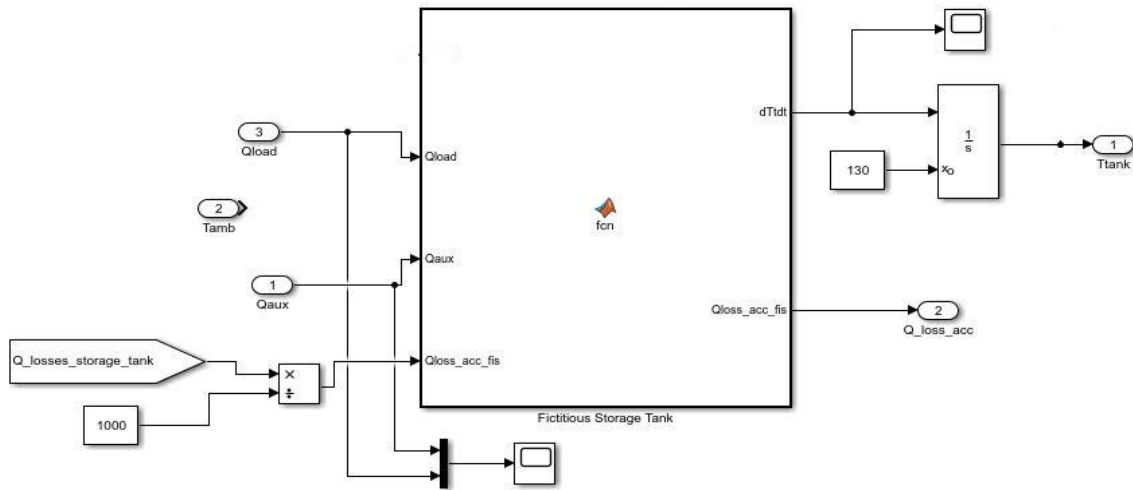


Figure 3. 6: Fictitious Storage Tank

After the Matlab function that models the fictitious HST, there is an integrator Simulink block that solves the differential equation and gives the temperature of the fictitious storage tank and consequently the supply temperature of the network. The integrator has an initial value (130°C), equal to the reference temperature of the storage tank at time zero, because the network is supposed to be at work at time zero.

3.9 Return Collectors Block

This block is useful to keep the two loops of the network separated when they work at different temperatures, or connected when they work at the same temperature. In particular, this block makes a mixing of the return mass flow rates at the return collectors when the two loops work at the same temperature, otherwise they are kept separated.

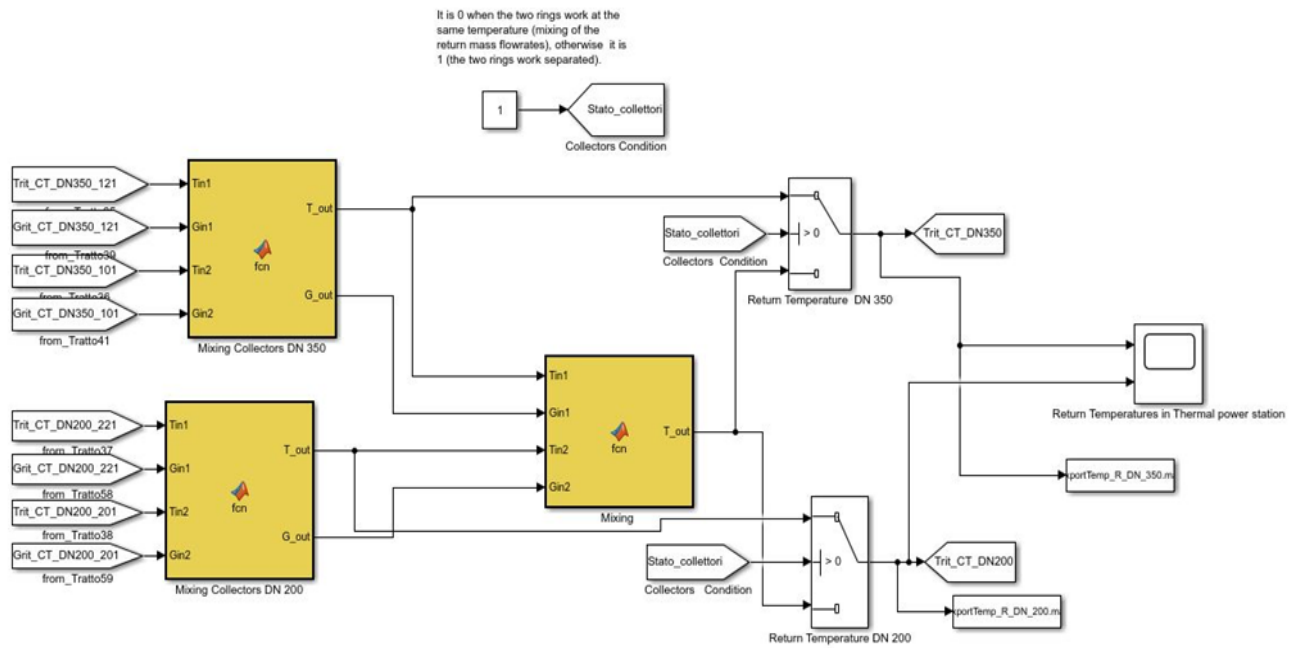


Figure 3. 7: Particular from the return collectors block

3.10 CHP: Cogeneration Combined Heat and Power Units

As we stated previously, there are three cogenerators inside the thermal power station that are identical to each other. The model of the cogenerator is a heritage of the previous version of software ENSim, to which has been added the model of the low temperature heat exchanger.

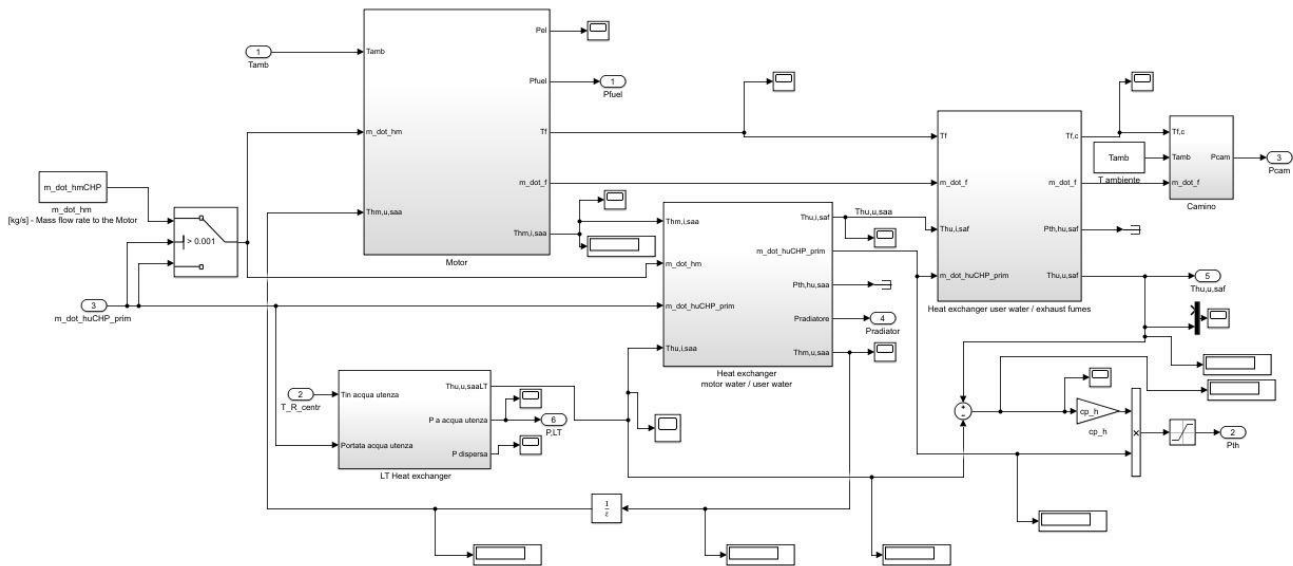


Figure 3. 8: CHP scheme

The cogenerator model is made by four main blocks: the motor, the low temperature heat exchanger, the motor-water/user-water heat exchanger and the user-water/exhaust fumes heat exchanger. The motor is ON when the electric profile given to the model as input is bigger than 0. The mass flow rate required by the CHP is an input of the model and it comes from the documentation of the period case of studying provided by Aeroporti di Roma. The temperature of the mass flow rate getting inside the CHP units is equal to the mixing temperature between the recirculating water going from the hot storage tank to the power station and the network return water:

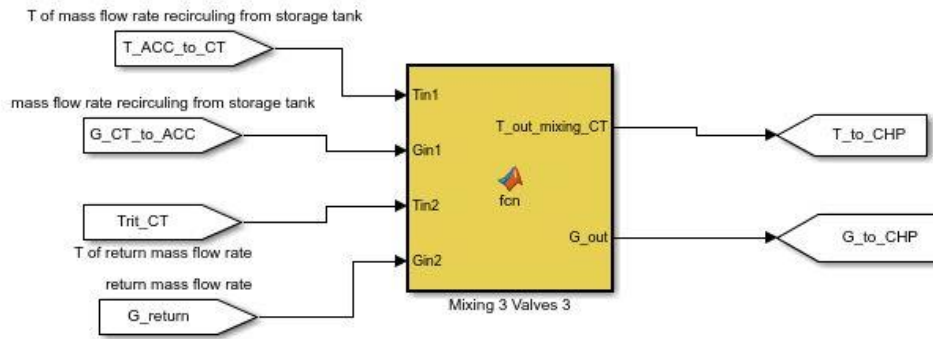


Figure 3. 9: Mixing 3 valves block

$$T_{to\ CHP} = \frac{T_{ACC\ to\ CT} * G_{CT\ to\ ACC} + T_{rit\ CT} * G_{return}}{G_{CT\ to\ ACC} + G_{return}} \text{ [}^{\circ}\text{C]} \quad ;(3.47)$$

$T_{to\ CHP}$: Return Temperature in the power station [$^{\circ}\text{C}$];

$T_{ACC\ to\ CT}$: Temperature of the recirculation mass flow rate going from the HST to the P.S. [$^{\circ}\text{C}$]

$T_{rit\ CT}$: Return collector temperature [$^{\circ}\text{C}$];

G_{return} : Global MFR flowing inside the network, it is the MFR required by the user $\left[\frac{kg}{s}\right]$;

$G_{ACC\ to\ CT}$: Recirculation mass flow rate going from the HST to the P.S. $\left[\frac{kg}{s}\right]$;

Inside the motor block there is an injection system that computes the fuel power consumed according to the electric profile provided to the CHP model as input. Afterwards, according to the fuel consumption, an electric map provides the electric power produced, and an exhaust fumes map provides the temperature of the exhaust gases; these two maps come from the data sheets of the CHP. The last part of the motor block computes the temperature of the cooling motor water exiting the motor itself, $T_{hm,i,saa}$.

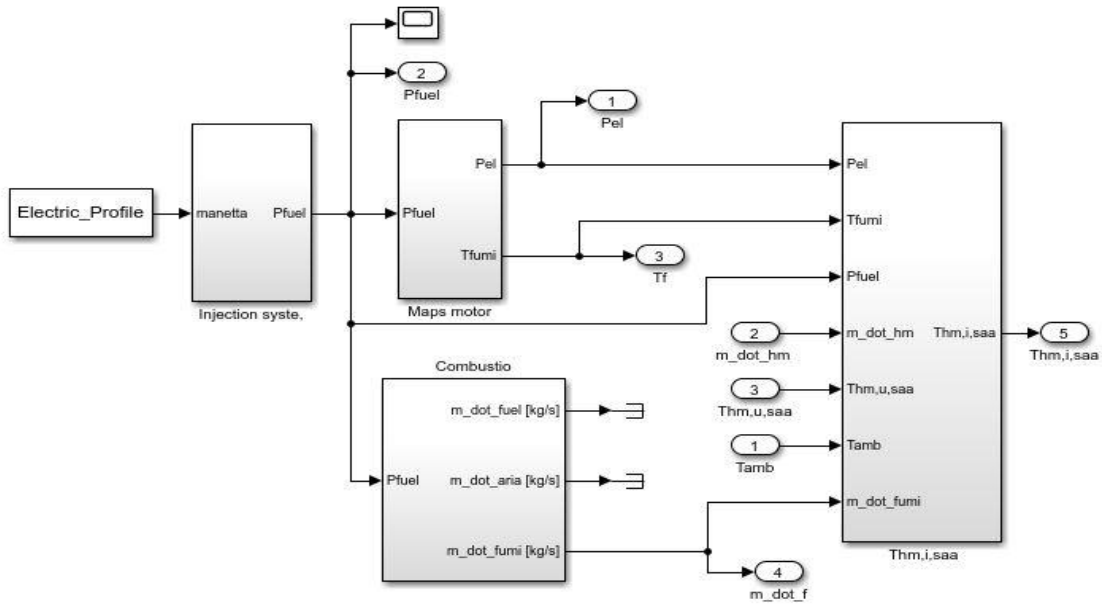


Figure 3. 10: Motor scheme

The second component of the CHP model is the Low temperature heat exchanger, where the heat transfer, between the cooling water of the lubricant oil of the motor and the return user water, happens. When the return user water is more than 57 °C, the cooling water heat is dissipated by a dissipater and not recovered. At each time step of simulation, the cooling water of the lubricant oil has to remove 2,083 kW of heat from the lubricant oil itself, making a temperature drop between 43 °C and 57 °C.

The temperature of the user water exiting the low temperature heat exchanger is equal to the entering value, no heat exchange, when it is above 57 °C, otherwise it is:

$$T_{hu,u,saaLT} = T_{h,in,userLT} + m_{dot,hCHP,LT} * \eta_{LT} * \frac{57 - T_{h,in,userLT}}{m_{dot,h,user}} [^{\circ}C] ;(3.48)$$

$T_{hu,u,saaLT}$: Temperature of the user water exiting the low temperature heat exchanger [°C];

$T_{h,in,userLT}$: Temperature of the user water getting inside the LT heat exchanger [°C];

$m_{dot,hCHP,LT}$: Mass flow rate of the cooling water of the lubricant oil $\left[\frac{kg}{s}\right]$;

$m_{dot,h,user}$: User mass flow rate $\left[\frac{kg}{s}\right]$;

η_{LT} : Efficiency of the LT heat exchanger;

The low temperature heat exchanger will be really important in the simulations at low temperature because the return user water will come back in the power station, $T_{to\ CHP}$, below 57 °C and we will recover up to 6 MW by the three CHP.

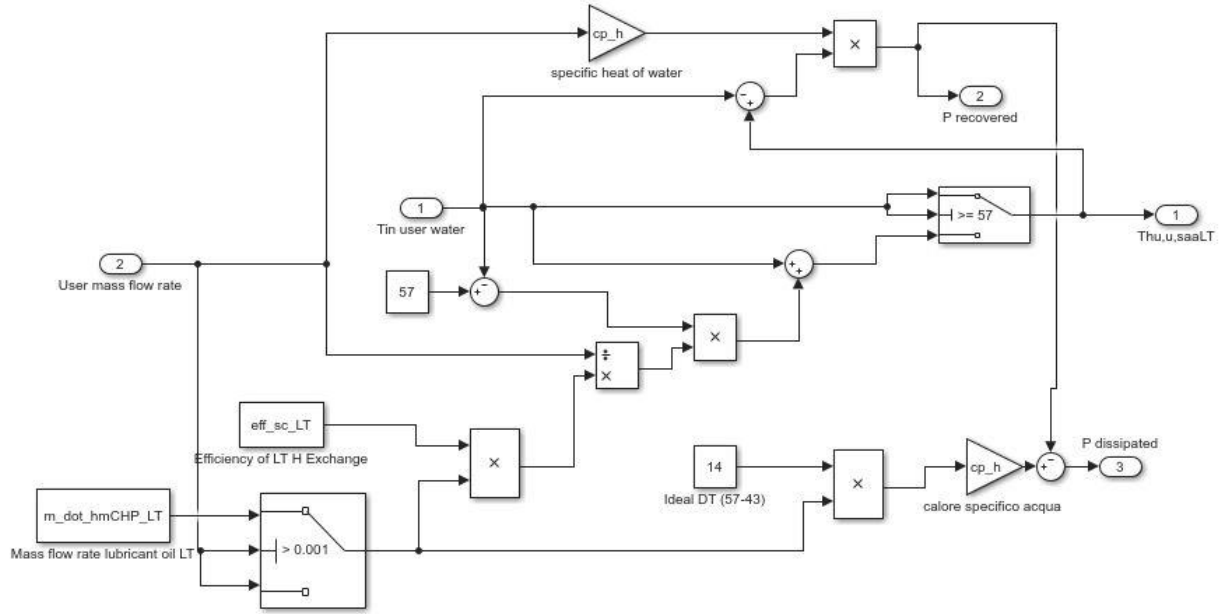


Figure 3. 11: Low temperature heat exchanger model

The third component of the CHP units is the high temperature heat exchanger, where the user water exchanges heat with the cooling motor water. The formulas to compute the exiting temperature of the user water exiting the user water/ motor water heat exchanger are:

$$P_{th,hu,saa} = (T_{hm,i,saa} - (T_{hm,i,saa} - (T_{hm,i,saa} - T_{h,in,u,saa}) * \eta_{saa})) * cp_h * m_{dot,h,CHP} \quad (3.49)$$

$$T_{hu,u,saa} = T_{h,in,u,saa} + \frac{P_{th,hu,saa}}{cp_h * m_{dot,h,user}} \quad [^{\circ}C] \quad ;(3.50)$$

$T_{hu,u,saa}$: Temperature of the user water exiting the user water /motor water heat exchanger [°C];

$T_{hm,i,saa}$: Temperature of the motor water getting inside the user water /motor water heat exchanger [$^{\circ}C$];

$P_{th,hu,saa}$: Thermal Power exchanged in the user water /motor water heat exchanger [kW]

$T_{h,in,u,saa}$: Temperature of the user water getting inside the user water /motor water heat exchanger [$^{\circ}C$];

$m_{\dot{h},CHP}$: Mass flow rate of the cooling motor water $\left[\frac{kg}{s}\right]$;

$m_{\dot{h},user}$: User mass flow rate $\left[\frac{kg}{s}\right]$;

η_{saa} : Efficiency of the user water /motor water heat exchanger;

The fourth component is the user water/ exhaust fumes heat exchanger. The formulas to compute the exiting temperature of the user water exiting the user water/ exhaust fumes heat exchanger are:

$$P_{th,hu,saf} = (T_f - (T_f - (T_f - T_{h,in,u,saf}) * \eta_{saf})) * cp_{fumes} * m_{\dot{h},fumes} \quad (3.51)$$

$$T_{hu,u,saf} = T_{h,in,u,saf} + \frac{P_{th,hu,saf}}{cp_h * m_{\dot{h},user}} \quad [^{\circ}C] \quad ;(3.52)$$

T_f = temperature of the exhaust fumes getting inside the user water /exhaust fumes heat exchanger [$^{\circ}C$]

$T_{hu,u,saf}$: Temperature of the user water exiting the user water /exhaust fumes heat exchanger [$^{\circ}C$];

$P_{th,hu,saf}$: Thermal Power exchanged in the user water /exhaust fumes heat exchanger [kW]

$T_{h,in,u,saf}$: Temperature of the user water getting inside the user water /exhaust fumes heat exchanger [$^{\circ}C$];

$m_{\dot{h},fumes}$: Mass flow rate of the exhaust fumes $\left[\frac{kg}{s}\right]$;

η_{saf} : Efficiency of the user water / exhaust fumes heat exchanger;

cp_{fumes} : specific heat of exhaust fumes $\left[\frac{kJ}{KgK}\right]$

Using the overall balance of the heat exchanged by the user water, it is possible to compute the thermal power supplied by each CHP. By the following scheme, Figure 3. 12, provided by Aeroporti di Roma, we took the values for the magnitudes of the CHP units mentioned before.

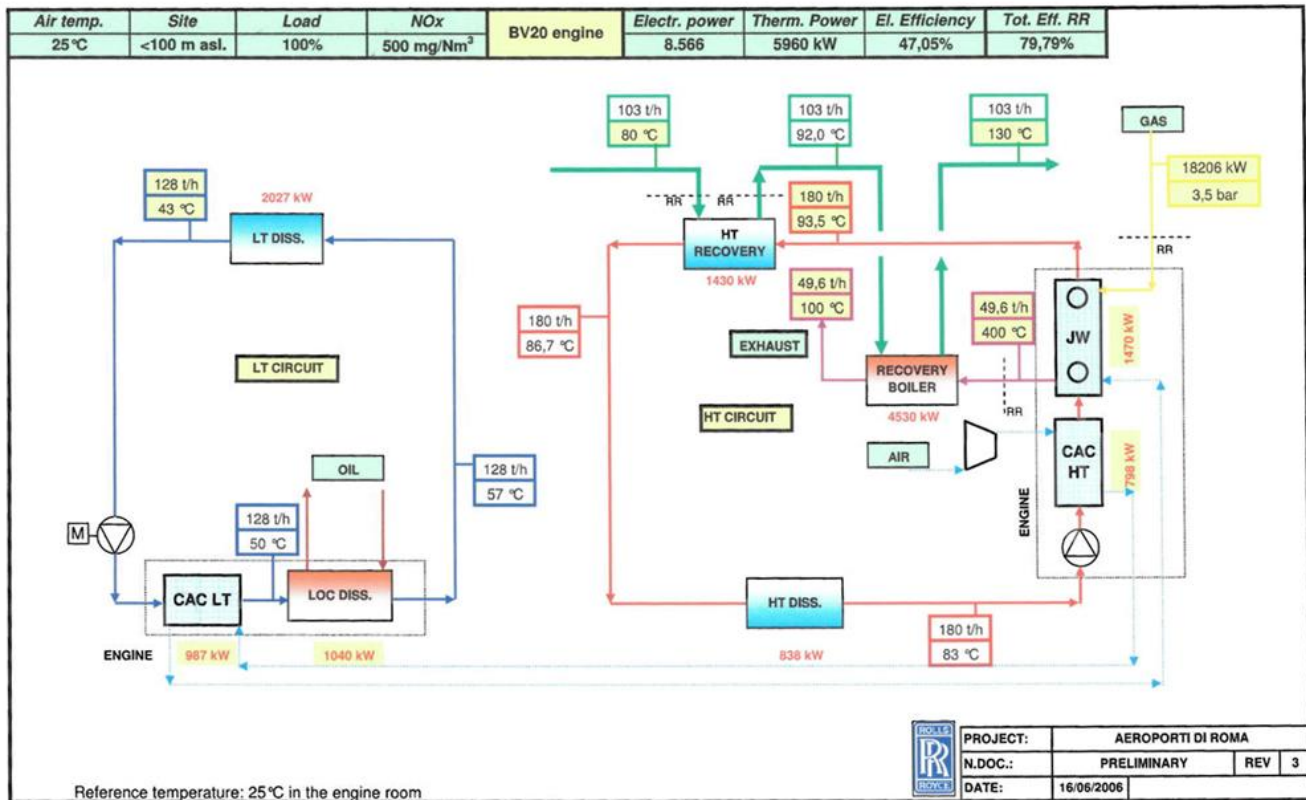


Figure 3. 12: CHP unit reference scheme

3.11 Network Dissipater

This is the component that controls the Flow Collector Temperature. Basically, it has been modelled as a PI (proportional, integrative) controller that receives the flow temperature of the network at the actual time step as input and compares it with its reference temperature. The reference temperature of the dissipater has been set to the maximum flow temperature acceptable in the network, 140 °C. It means that the dissipater dissipates all the heat produced inside the power station when the flow temperature is above 140°C. The reference temperature of the dissipater has been set ten degrees higher than the reference temperature of the network, because we want to limit the use of this component that would otherwise produce instability on the heat produced by the power station and consequently could even stop the simulation.

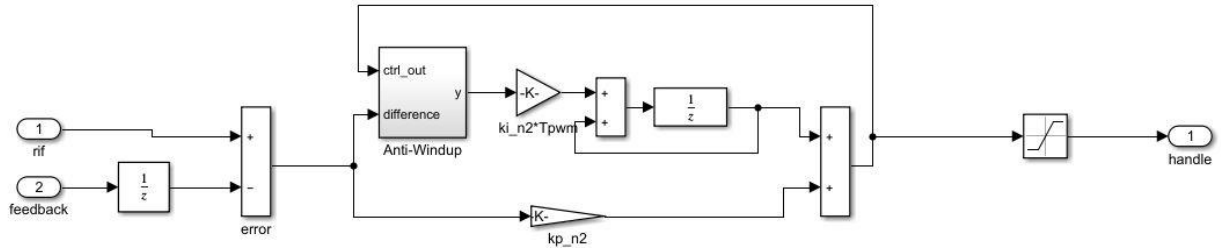


Figure 3. 13: Network dissipater model

The PI controller gives an output between 0 and 1 that is multiplied for the thermal power exiting the power station; the resulting heat power is placed into the network.

3.12 Hot Storage Tank (HST)

Even though inside the real thermal power station there are four Tanks of 250 cubic meters, we decided to use the model of a single thermal storage tank of 1000 cubic meters to avoid complicating the modelling and because it is a good approximation of the actual situation, since the four real tanks work in series of each other. The model of the Thermal Storage Tank has been developed by ENEA and it was added to ENSim in the previous version of the software. It was modelled as a stratified tank, with ten layers. At each time step it receives the thermal conductivity of the tank as input, the geometrical parameters, where the volume is 1000 cubic meters and the diameter is:

$$D = \left(\frac{4 * Volume}{3 * \pi} \right)^{\frac{1}{3}} ; (3.53)$$

Then the model receives the mass flow rate from the power plant as input, meaning the recirculation flow rate. Then it receives the mass flow rate going from the tank itself to the network, that as we said is different from zero if the recirculation mass flow rate is zero. It receives the return temperature of the network, and finally it receives the temperature of the recirculation mass flow rate coming from the power station. To prevent the tank overheating above its reference temperature, we modelled a heat dissipater that controls the thermal power getting inside the tank through the recirculation mass flow rate coming from the power station. It works mainly when the heat production in the power station is bigger than the users' loads, and the recirculation MFR is high.

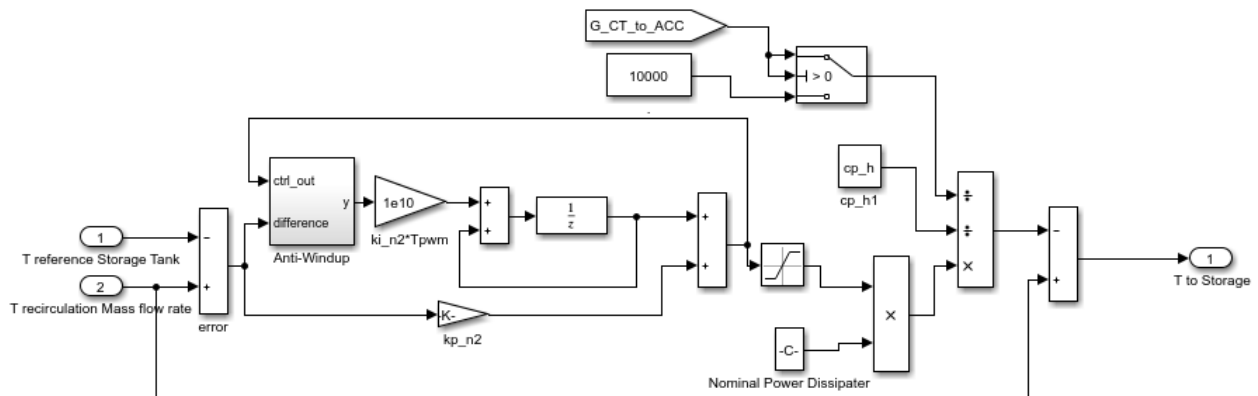


Figure 3. 14: Dissipater of the thermal storage tank

The nominal power of the storage dissipater has been set to 3 MW. This value is equal to the average thermal power the recirculation mass flow rate introduced inside the storage tank in previous test simulations. The temperature of the recirculation mass flow rate getting inside the HST is equal to:

$$T_{in} = T_{from P.S.} - \frac{P_{N.dissipater}}{G_{recirculation} * cp_w} * f ; (3.54)$$

T_{in} : Temperature of the recirculation MFR getting inside the HST [°C];

$T_{from P.S.}$: Temperature of the recirculation MFR coming from the P.S. [°C];

$P_{N.dissipater}$: Nominal Power of the dissipater [kW];

$G_{recirculation}$: Recirculating MFR $\left[\frac{kg}{s}\right]$;

cp_w : Specific heat of water $\left[\frac{kJ}{kg \text{ } ^\circ C}\right]$;

f : Handle value depending on how much the $T_{from P.S.}$ is closed to $T_{reference}$ of HST, between 0 and 1;

The thermal storage tank gives the temperature of each layer as output. The temperature of the highest layer is the highest one and it is equal to the temperature of the mass flow rate going from the tank to the network in discharging phases, and the temperature of the lowest layer is the lowest one and it is equal to the temperature of the recirculation mass flow rate going from the tank to the power station.

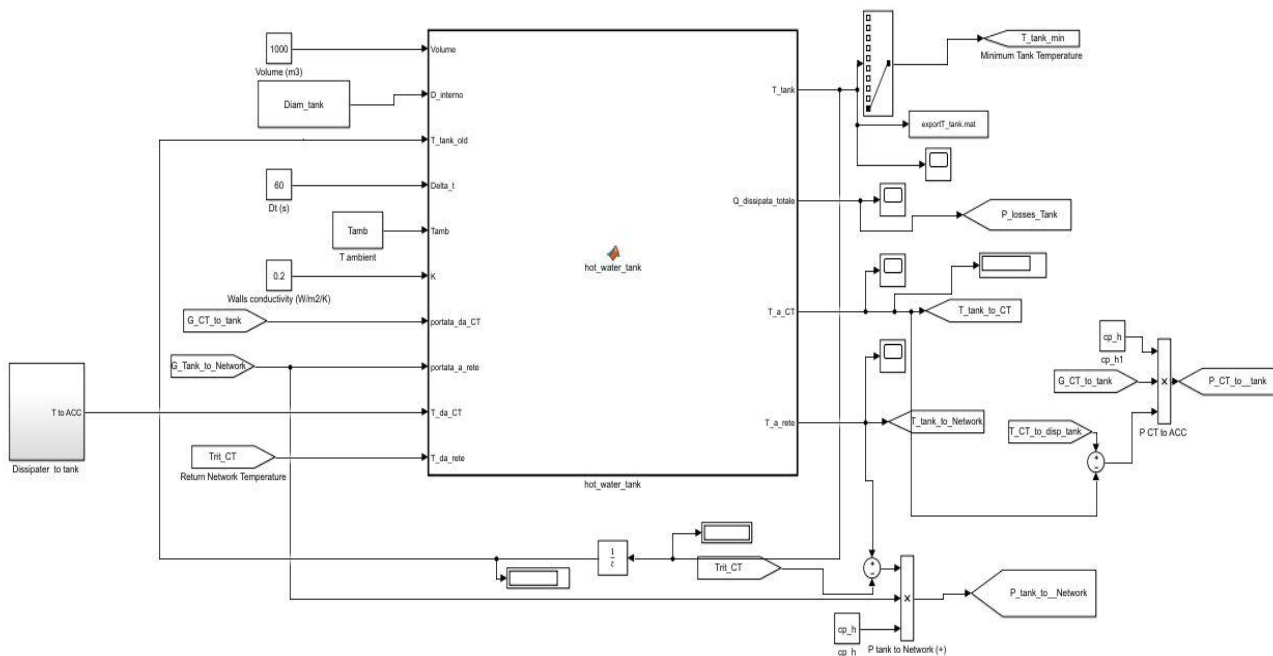


Figure 3. 15: Thermal storage tank model

The hot storage tank was modelled as a Matlab function. The water in the tank is considered subdivided into isothermal layers, characterized by the same volume and height of water.

The energy balance equation in transient regime is applied at each layer at each time step and it is formulated as:

$$\rho_w c_w V_w \frac{dT_w}{dt} = UA(T_{w,T} - T_{amb}) + c_w G_w (T_{in} - T_{out}) \quad [W]; (3.55)$$

G_w : Flow rate entering or exiting the layer, it is different from zero in the first and in the last layer $\left[\frac{kg}{s}\right]$;

T_{in}, T_{out} : inlet and outlet temperatures of the water at the boundaries of the tank $[^{\circ}C]$;

V_w : Volume of water inside the tank $[m^3]$;

ρ_w : water density $\left[\frac{kg}{m^3}\right]$;

c_w : specific heat of water $\left[\frac{j}{kgK}\right]$;

$T_{w,T}$: water temperature of the layer $[K]$;

T_{amb} : Ambient Temperature $[K]$;

For each time-step and for each layer, Eq. (3.55) is solved by using the implicit Euler method. Afterwards the empirical reversion-elimination algorithm is implemented to take into account the effects of natural convection between the water layers at different heights in the thermal stratification inside the tank. The result at each time step is that the layers are at different increasing temperature from the lowest layer to the highest. For each layer the heat losses are computed as:

$$Losses = U * A * (T_{layer} - T_{amb}) ; (3.56)$$

$$UA = K * (h_{layer} * \pi * D) \left[\frac{W}{K}\right];$$

$$K = 0.2 \text{ thermal conductivity of the tank } \left[\frac{W}{m^2K}\right];$$

$$h_{layer} = 4 * \frac{V_w}{\pi * D^2} \text{ height of the layer } [m];$$

D : diameter of the tank $[m]$;

3.13 Network Modelling

The real spatial coordinates of the network are not directly given to software IHENA that, as we said, solves it thermally and hydraulically. The real network was linearized to simplify the topology of the network, but we kept the real length between node and node. To linearize the network, the nodes positioned on the principal pipeline of the loops were located on the x-axis, whereas all the nodes of the secondary branches and the users' nodes were disposed on the y-axis with a fix x coordinate corresponding to the x coordinate of the derivation node from the main loop.

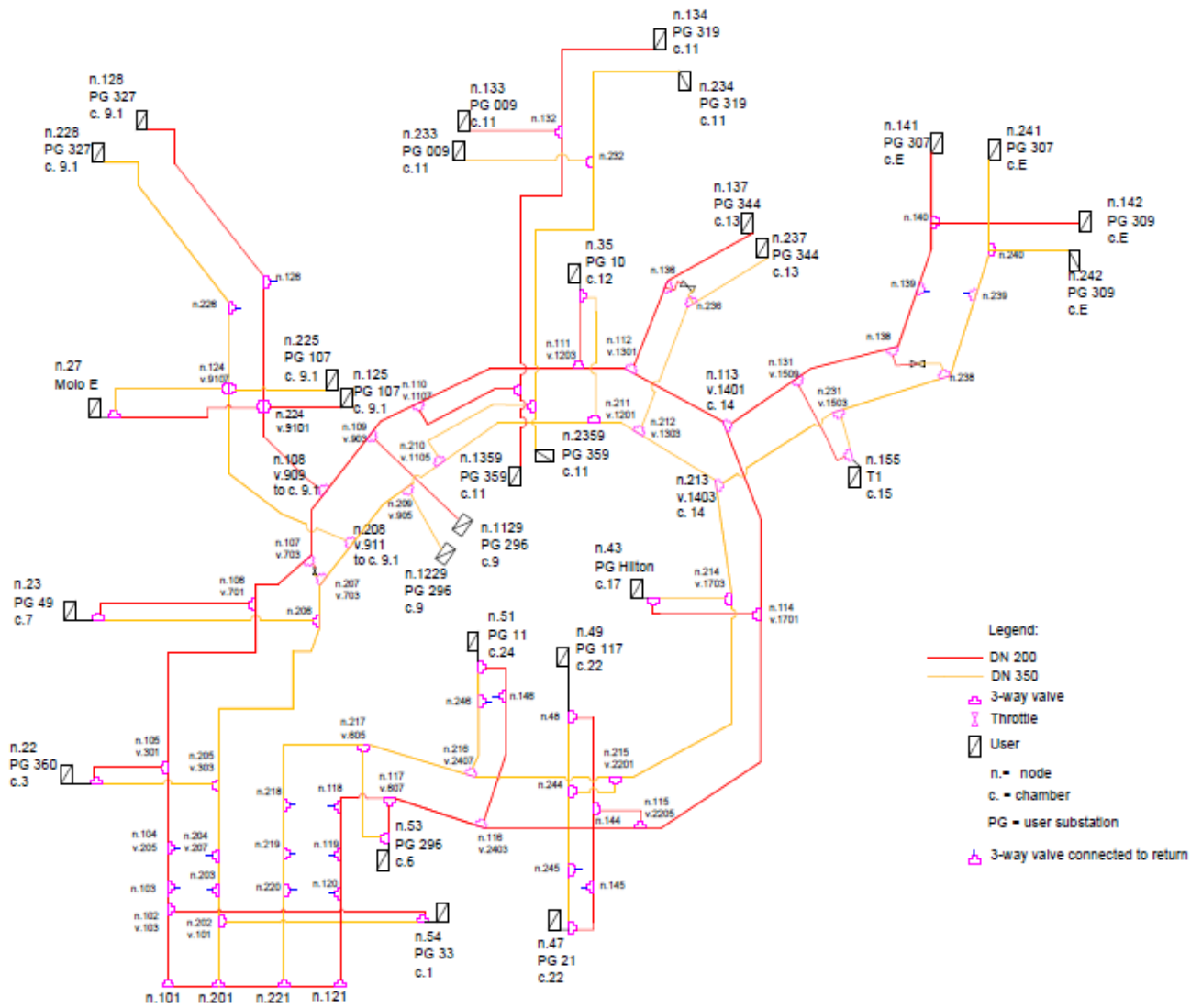


Figure 3. 16: Real Network: hydraulic scheme

The nodes were positioned on the flow collectors, on the users, on the three way-valves that connect the main rings with the derivation branches, on the three way-valves that connect the two loops by throttle valves, considered closed, and on the three way-valves that connect the flow and return circuit, considered closed. The name and the position of the valves come from the hydraulic scheme of the network that ADR gave us. Since we do not know which throttle valves are closed and which ones are opened, we considered them always closed to simplify the treatment and also because we cannot change the condition of a valve (ON or OFF) during a simulation; the same is true for the three way valves that connect the flow and return circuits. We also considered the closed valves as nodes of the linearized network that we give to the model as input, to make the modelled network as similar to the real one as possible. The overall length of the modelled network is 33,125 metres, considering the pipes in flow and in return.

The working network consists of 4 source nodes, 29 user nodes, 63 mixing nodes and 105 pipes.

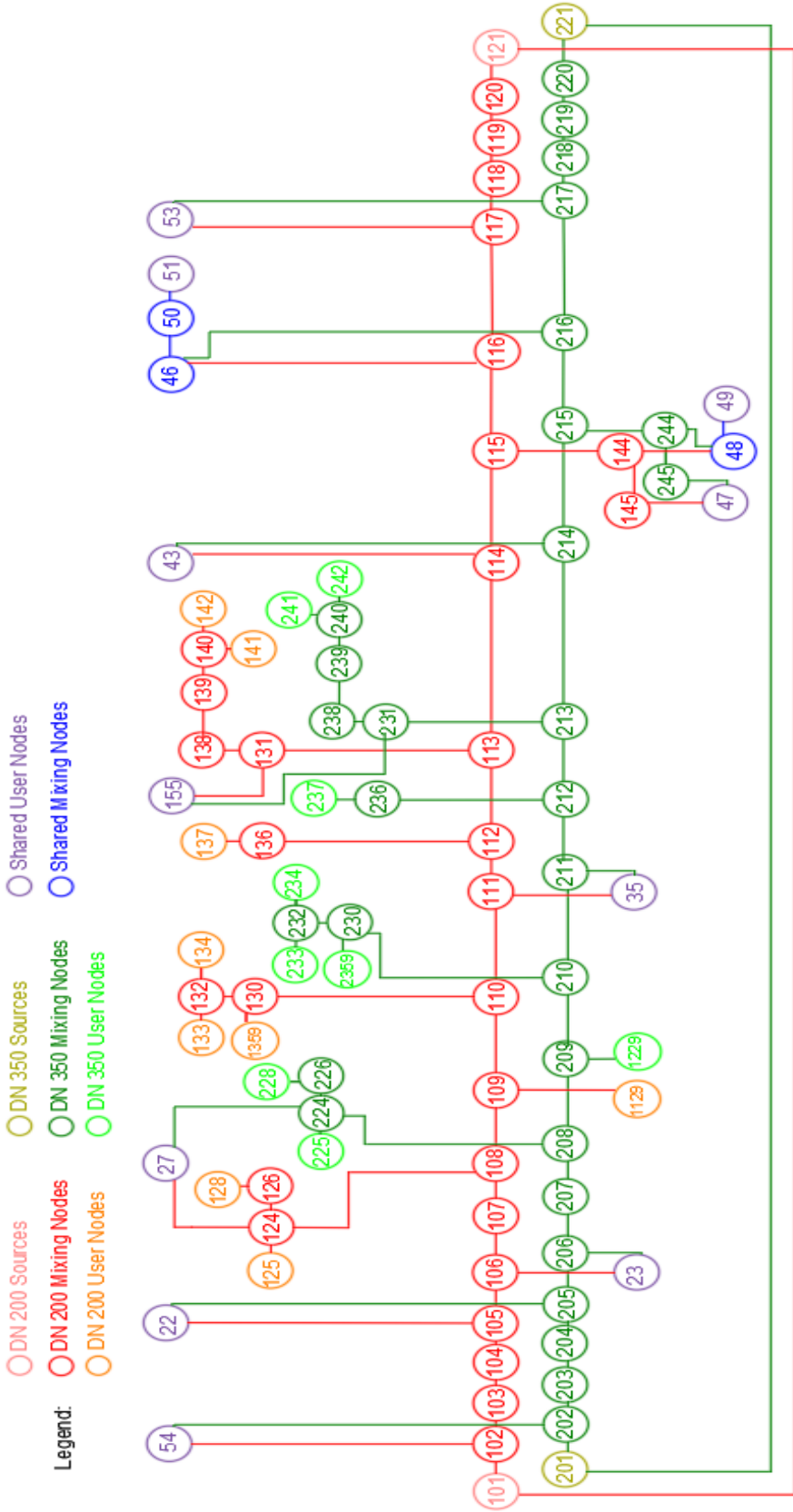


Figure 3. 17: Working Network, linearized representation

To overcome the overestimation of the loads we do not know, we built the equivalent network. Unlike the real one, it does not have the branches of chamber 9.1, it does not have all the branches to the users monitored in chamber 11 and it does not have all the branches to the users monitored in chamber 14. We decided to also cut the branches to the users of chamber 11 since the power meters inside the substations monitored in chamber 11 were off during the first 20 days of December, and we obtained the load profiles of their users by the energy meters of chamber 11.

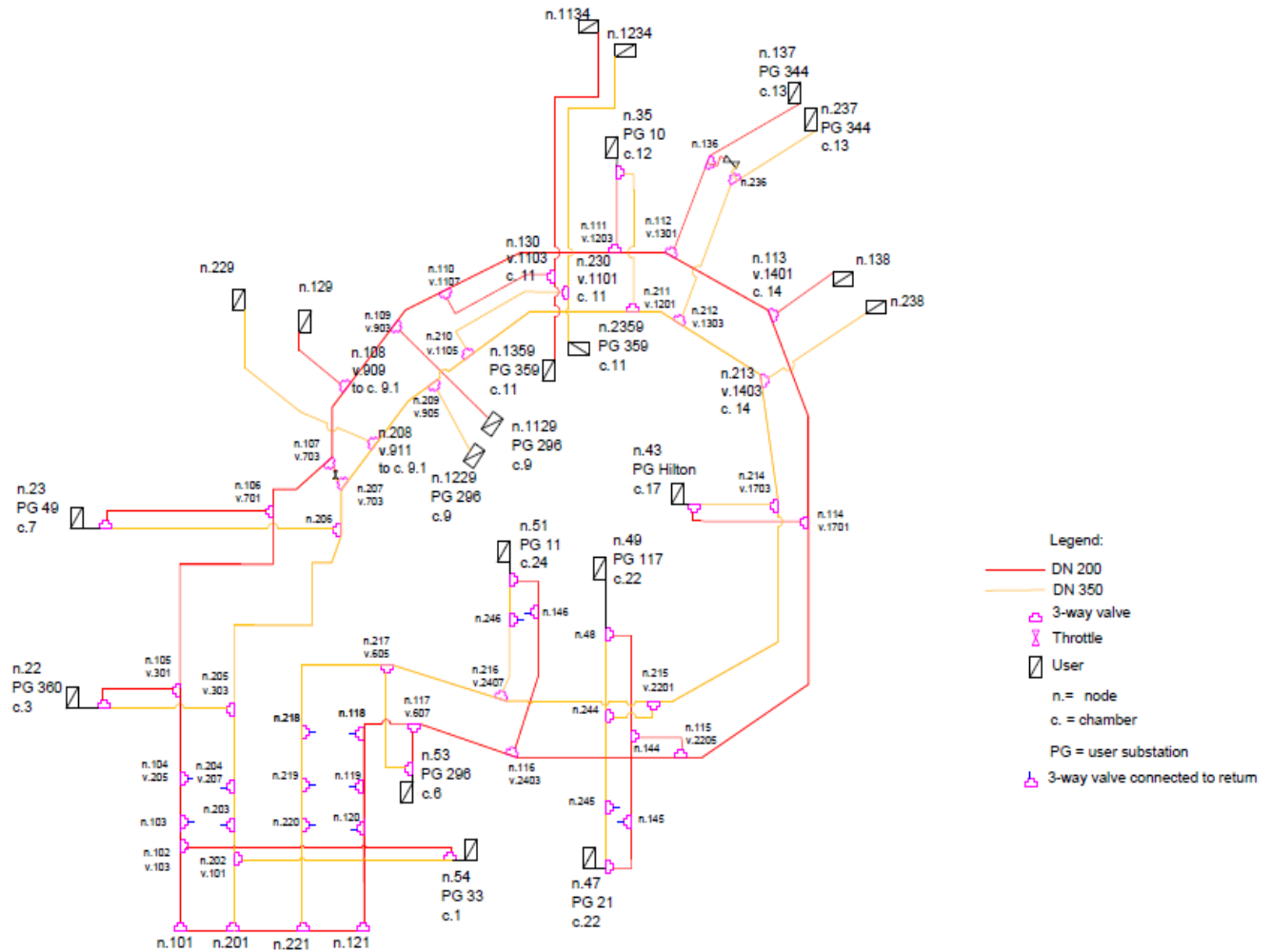


Figure 4. 2: Equivalent Network: hydraulic scheme

4.2 Estimated heat distribution losses analysis

The heat distribution losses along the network were computed for the four months for which we have data, December 2017, February, March, April 2018. The heat losses were computed as the difference between the global energy required by the network and the global energy required by the users. Both terms were obtained, period by period, by the data given by ADR. In Figure 4. 3 we can see the comparison between the energy required by the network, the energy generated in the power station and the energy required by the loads. The first two terms were collected hourly in the power station, whereas the energy required by the loads comes from the integration of the data coming from the power meters inside the user substations, collected each twenty minutes. The energy generated in the power station takes into account the thermal energy produced by the CHP units plus the energy produced by the boilers. The difference between the energy generated by the power station and the global energy required by the network is supposed to be due to the network dissipater that dissipates the excess heat produced. The difference between the energy required by the network and the energy required by the loads is supposed to be equal to the heat distribution losses.

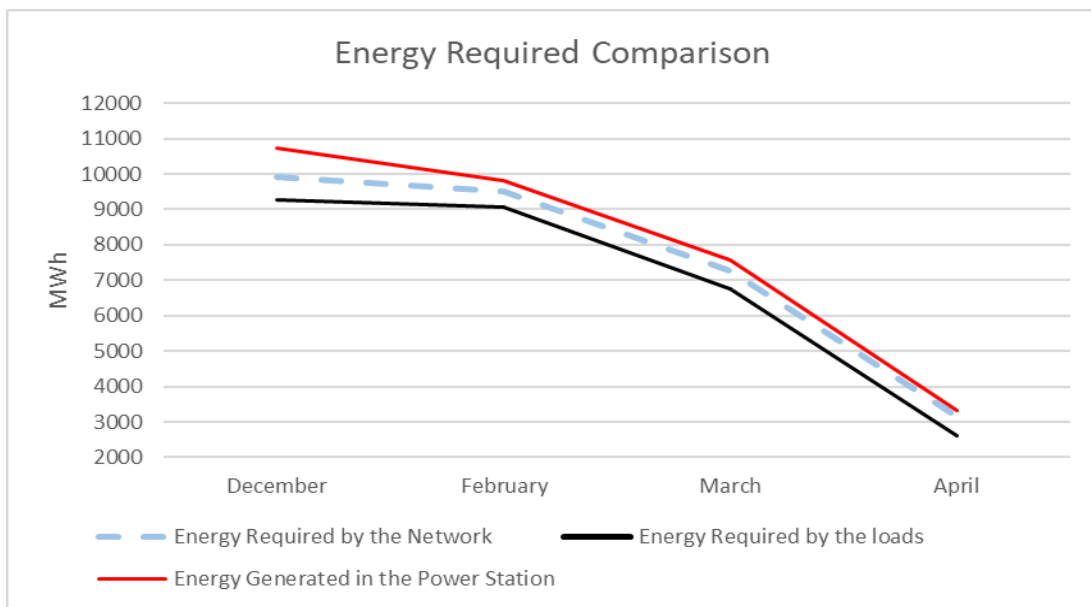


Figure 4. 3: Energy comparison

	Energy required by the Network	Energy required by the Loads, from Power meters	Energy generated in P.S.
<i>Month</i>	<i>MWh</i>	<i>MWh</i>	<i>MWh</i>
December	9,902	9,282	10,741
February	9,518	9,066	9,822
March	7,276	6,766	7,565
April	3,152	2,610	3,305

Table 4. 1: Energy comparison

The maximum thermal energy generated in the power station is in December, 10,741 MWh, and minimum in April, 3,305 MWh, with a difference of 7,436 MWh. The global load is maximum in December, 9,905 MWh, and minimum in April, with a difference of 6,750 MWh.

For the month of December, the global user load was obtained from the power meters, integrated with the data coming from the energy meters when the power meters were OFF. In the next figures we will see the heat distribution losses computed as the difference between the global energy required by the network and the energy required by the loads. This last term can be computed by the data coming from the energy meters and by the integration of the data coming from the power meters, both are inside the user substations. For this reason, we will indicate the heat distribution losses computed as the difference between the global energy required by the network and the energy required by the loads coming from the power meters as 'Heat losses from Power meters', whereas we will indicate the heat distribution losses computed as the difference between the global energy required by the network and the energy required by the loads coming from the energy meters as 'Heat losses from Energy meters'.

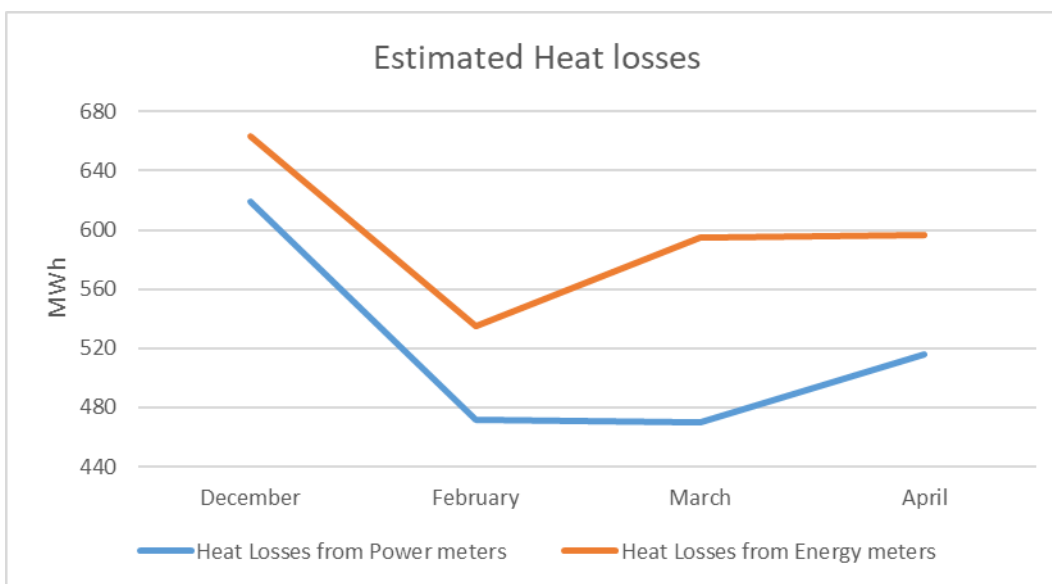


Figure 4. 4: Estimated heat distribution losses MWh

	Heat Losses from Power meters	Heat Losses from Energy meters
Month	MWh	MWh
December	619	663
February	472	535
March	470	595
April	516	597

Table 4. 2: Estimated heat distribution losses MWh

The heat losses are maximum in December, 619 MWh, and minimum in March, 470 MWh, 24 % less, with a difference of 149 MWh.

As we can see in Figure 4. 4, the user load computed by the energy meters and by the power meters are different, and consequently, the ‘Heat Losses from Energy meters’ are different from the ‘Heat Losses from Power meters’. Even if the data collected inside the user substations by the energy meters are hourly, whereas the power meters collect data every twenty minutes, it is not possible to explain a difference so big.

Considering the length of the equivalent network, 22,322 meters, in flow and in return, and the number of hours in each month, we can estimate the heat distribution losses as W/m, and as MWh/m:

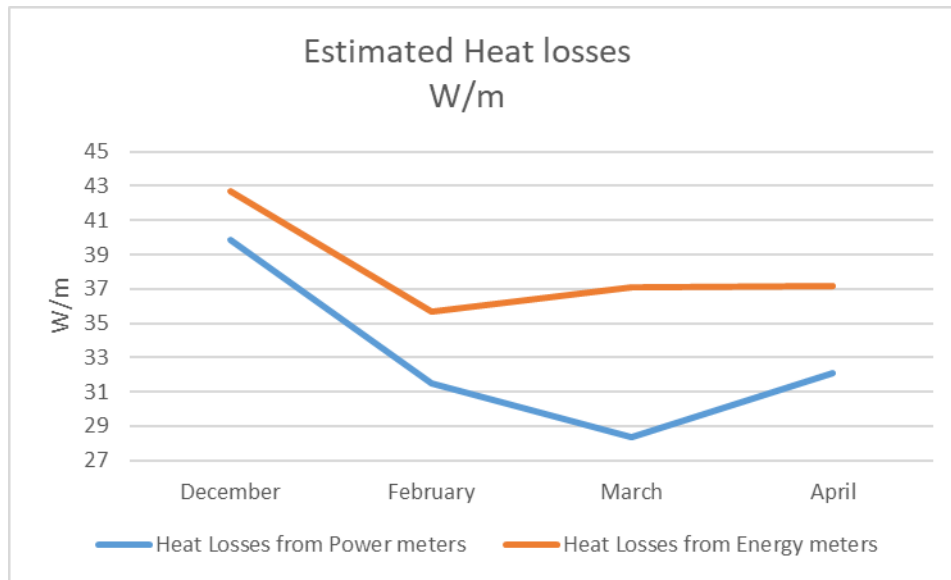


Figure 4. 5: Estimated heat distribution losses W/m

	Heat Losses from Energy meters	Heat Losses from Power meters
Month	W/m	W/m
December	42.7	40.0
February	35.7	31.5
March	37.1	28.3
April	37.2	32.1

Table 4. 3: Estimated heat distribution losses W/m

The heat losses, computed in W/m, are maximum in December, 40.0 W/m, and minimum in March, 28.3 W/m.

In Figure 4. 6 we will see the estimated distribution losses computed as MWh/m.

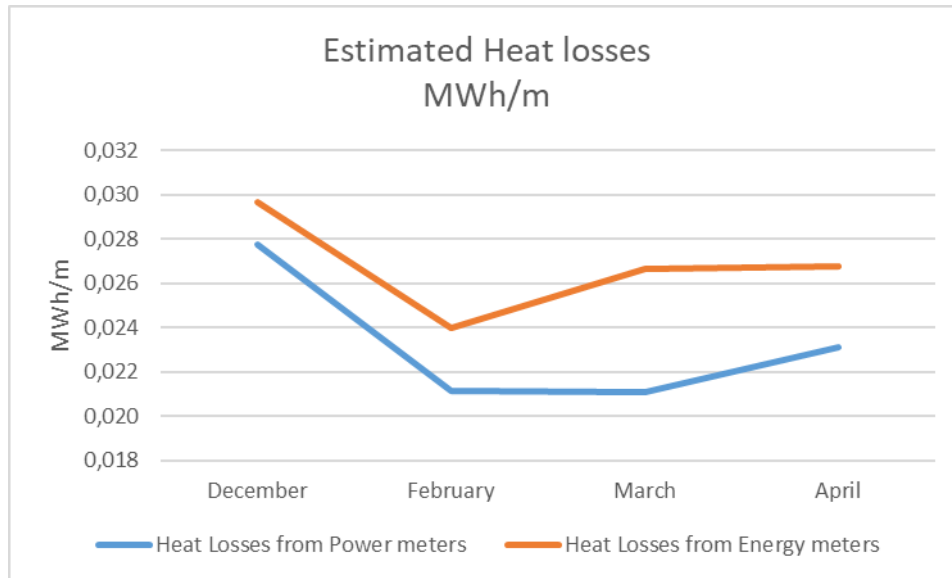


Figure 4. 6: Estimated heat distribution losses MWh/m

	Heat Losses from Energy meters	Heat Losses from Power meters
Month	MWh/m	MWh/m
December	0.030	0.028
February	0.024	0.021
March	0.027	0.021
April	0.027	0.023

Table 4. 4: Estimated heat distribution losses MWh/m

The heat losses, computed in MWh/m, are maximum in December, 0.028 MWh/m, and minimum in March and February, 0.021 MWh/m. The global user load measured by the energy meters is always less than the user load energy measured by the integration of the data coming from the power meters, consequently the 'Heat Losses from Energy meters' are higher than the 'Heat Losses from Power meters'. In Figure 4. 7 we can see the ratio between the 'Heat Losses from Energy meters' and the heat generated in the power station, and the ratio between the 'Heat Losses from Power meters' and the heat generated in the power station.

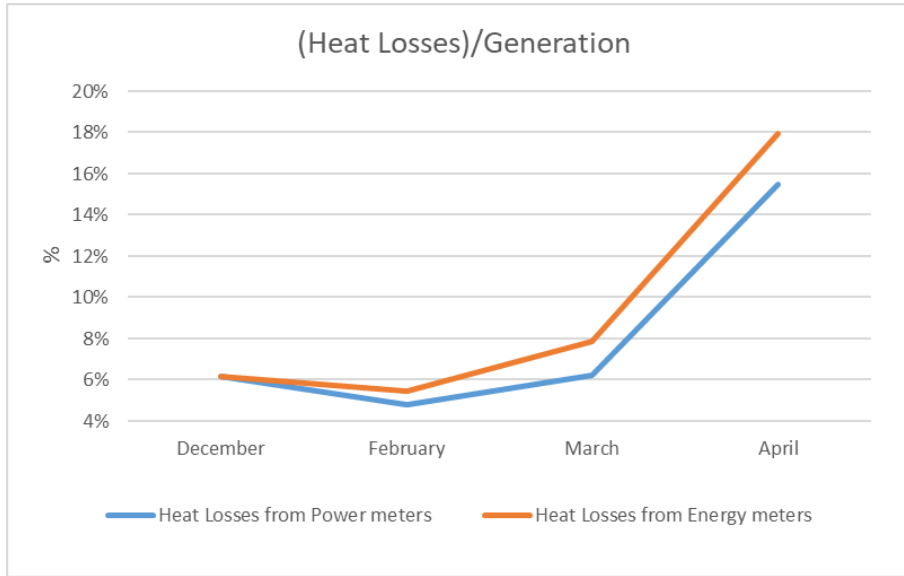


Figure 4. 7: Ratio (heat distribution Losses)/Generation

	(Heat Losses)/Generation, from Power meters	(Heat Losses)/Generation, from Energy meters
<i>Month</i>	%	%
December	6	6
February	5	5
March	6	8
April	16	18

Table 4. 5: Ratio (heat distribution Losses)/Generation

The results we can see in Figure 4. 7 mainly depend on the variation of the heat generated in the power station, since the biggest variation of the monthly heat distribution losses, 149 MWh, is only 2 % of the biggest variation of the monthly thermal energy generated in the P.S., 6,750 MWh. We can say that the monthly thermal losses stay quite constant compared to the monthly heat generated in the P.S. As we would expect, the ratio (Heat Losses)/Generation increases in the spring, April, since the monthly heat produced in P.S. decreases more than the heat distribution losses.

4.3 Validation of the simulated Heat Distribution Losses

At each time step the model computes the global heat distribution losses summing the heat losses of each pipe obtained as the product of the mass flow rate flowing in the duct, the temperature difference between the inlet node and the outlet node of the duct, and the specific heat of water. For this reason, it is of fundamental importance to understand which equation software IHENA solves to compute the temperature decay along each pipe. The formula exploits the log mean temperature difference for a fluid inside a pipe (cylindrical geometry) with fixed surface temperature:

$$T_{out} = T_{surface} + (T_{in} - T_{surface}) * \exp\left(-\frac{\pi * D_{est} * K_{cond} * L * F_{cor}}{G * c}\right) \text{ [}^\circ\text{C]}; \quad (4.1)$$

T_{out} : Temperature of the fluid exiting the pipe [$^\circ\text{C}$];

$T_{surface}$: Temperature of the external surfaces of the pipe [$^\circ\text{C}$];

T_{in} : Temperature of the fluid getting inside the pipe [$^\circ\text{C}$];

T_{out} : Temperature of the fluid exiting the pipe [$^\circ\text{C}$];

D_{est} : External diameter of the pipe [m];

K_{cond} : Conductivity of the pipe $\left[\frac{W}{m^2K}\right]$;

L : Length of the pipe [W];

G : Mass flow rate flowing inside the pipe $\left[\frac{kg}{s}\right]$;

c : Specific heat of the fluid $\left[\frac{J}{kgK}\right]$;

F_{cor} : Correction factor for the conductivity of the pipe;

The stratigraphy of the pipes has been taken by the literature available on this topic:

DN	D external [mm]	Tube Thickness [mm]	D internal [mm]	Insulation [mm]	Coating [mm]
350	356	6	344	50	1
300	324	6	313	50	1
250	273	5	263	50	1
200	219	5	210	50	1
150	168	4	160	50	1
125	140	4	133	50	1
100	114	3	108	50	1
80	89	3	83	50	1
65	76	3	70	50	1
50	60	3	55	50	1

Table 4. 6: Layers' thickness

	Tube	Insulation	Coating
Layers Conductivity	$\frac{W}{m^2K}$	$\frac{W}{m^2K}$	$\frac{W}{m^2K}$
Kcond	25	0.04	210

Table 4. 7: Layers' conductivity

The last term of the temperature decay equation, F_{cor} , is really important in our discussion, since it allows us to change the simulated heat distribution losses along the network. To find which F_{cor} apply to our model, we simulated four months for which we have data (December 2017, February, March, April 2018) in the equivalent network configuration, with different values of F_{cor} , till the heat losses simulated fitted the estimated ones.

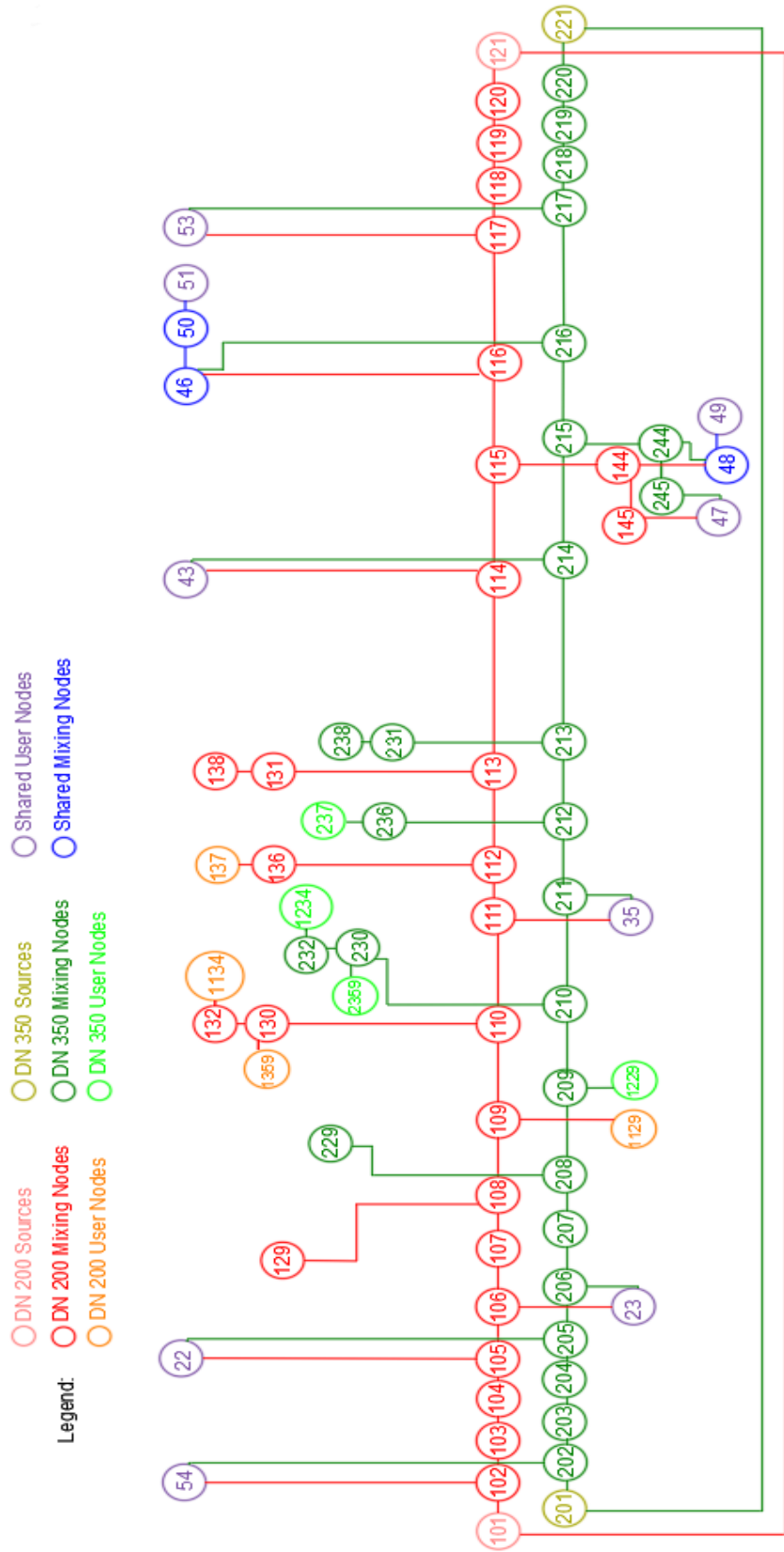


Figure 4. 9: Equivalent Network, linearized representation

The equivalent network consists of 4 source nodes, 21 user nodes, 51 mixing nodes and 83 pipes.

In the next section we will compare the estimated heat distribution losses and the simulated ones. We have divided the monitored months in three periods to compare the estimated and the simulated heat losses in each one. The simulated heat losses have been taken from the simulations of the equivalent network run with different Fcor. The Fcor is of fundamental importance in the computation of the temperature decay along the network, and consequently in the analysis of the heat distribution losses along the network.

4.4.1 December 2017

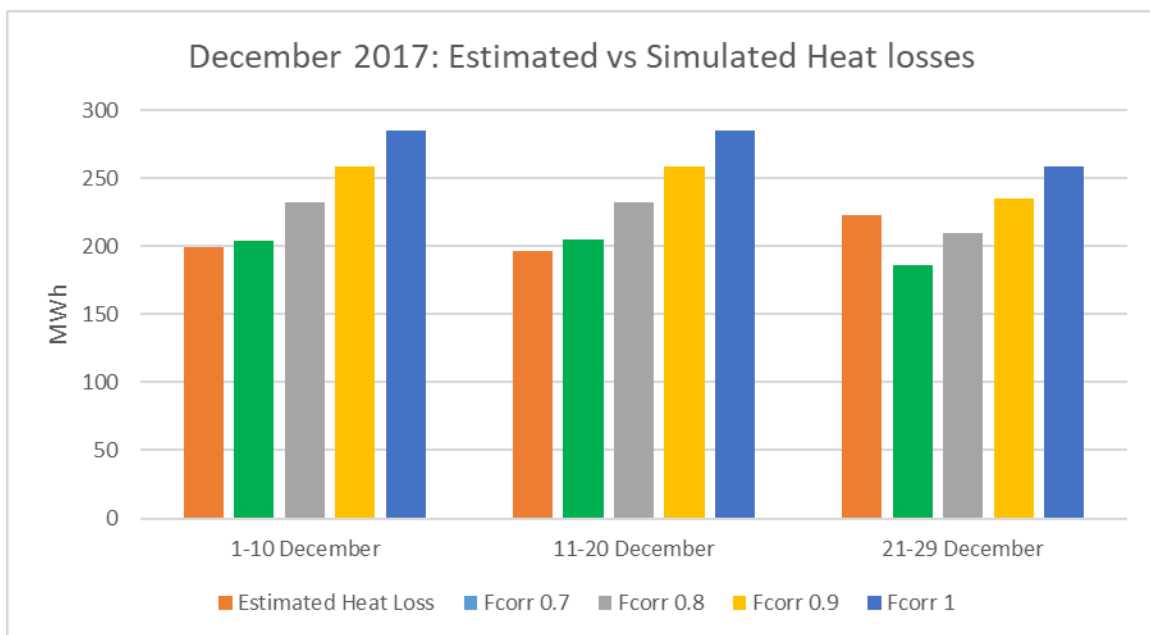


Figure 4. 10: Heat losses comparison: December 2017

	1-10 December	11-20 December	21-29 December
	MWh	MWh	MWh
Estimated Heat Losses	200	197	223
Fcor= 0.7	204	205	186
Fcor= 0.8	232	232	210
Fcor= 0.9	259	259	235
Fcorr= 1	285	285	259

Table 4. 8: Heat losses comparison: December 2017

As we can see in Figure 4. 10, the simulation with $F_{cor} = 0.7$, better fits the estimated heat distribution losses during the first two period of December, even if $F_{cor} = 0.9$ better represents the third one.

4.4.2 February 2018

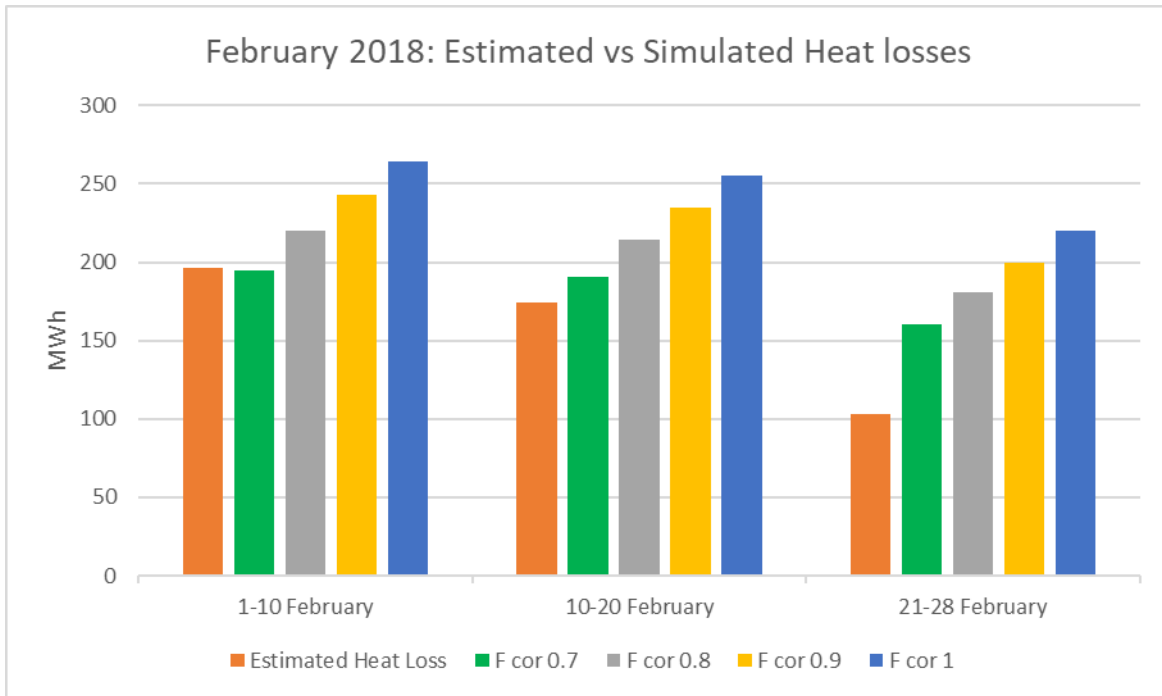


Figure 4. 11: Heat losses comparison: February 2018

The simulation with $F_{cor} = 0.7$ is the one which better approximates the estimated heat distribution losses in February.

	1-10 February	10-20 February	21-28 February
	<i>MWh</i>	<i>MWh</i>	<i>MWh</i>
Estimated Heat Losses	196	174	103
Fcor= 0.7	195	191	160
Fcor= 0.8	220	214	181
Fcor= 0.9	243	235	200
Fcorr= 1	264	255	220

Table 4. 9: Heat losses comparison: February 2018

4.4.3 March 2018

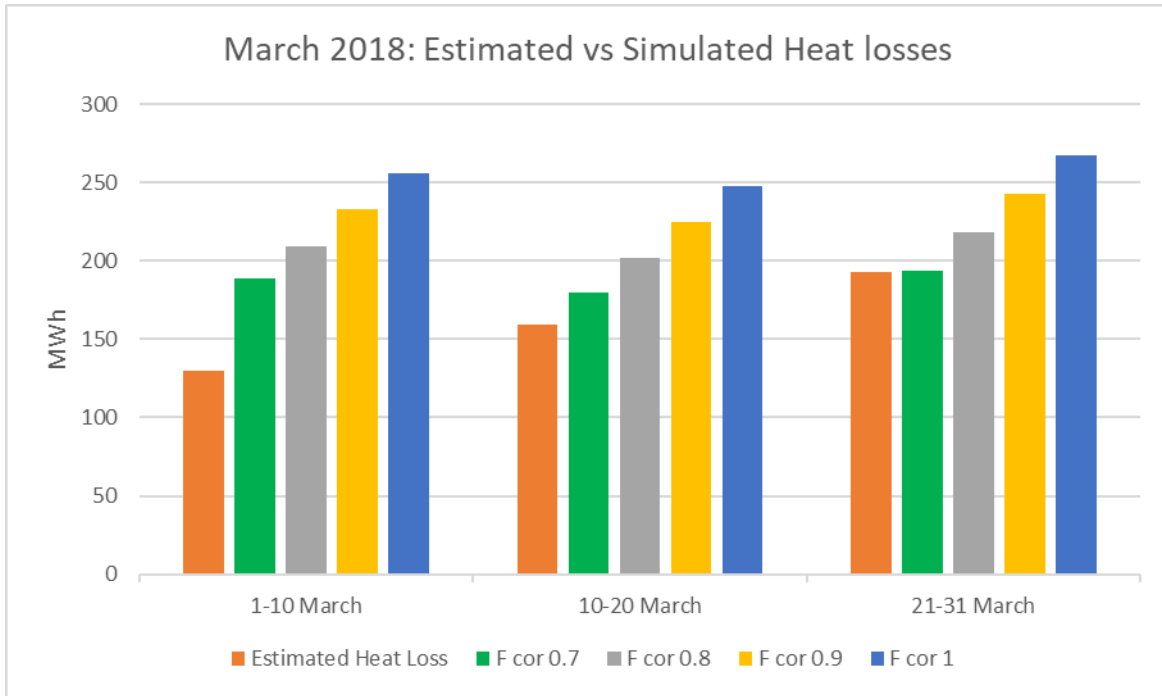


Figure 4. 12: Heat losses comparison: March 2018

Also for March the simulation with $F_{cor} = 0.7$ is the one which better approximates the estimated heat distribution losses

	1-10 March	10-20 March	21-31 March
	MWh	MWh	MWh
Estimated Heat Losses	130	160	193
Fcor= 0.7	189	180	194
Fcor= 0.8	209	202	218
Fcor= 0.9	233	225	243
Fcorr= 1	256	248	267

Table 4. 10: Heat losses comparison: March 2018

4.4.4 April 2018

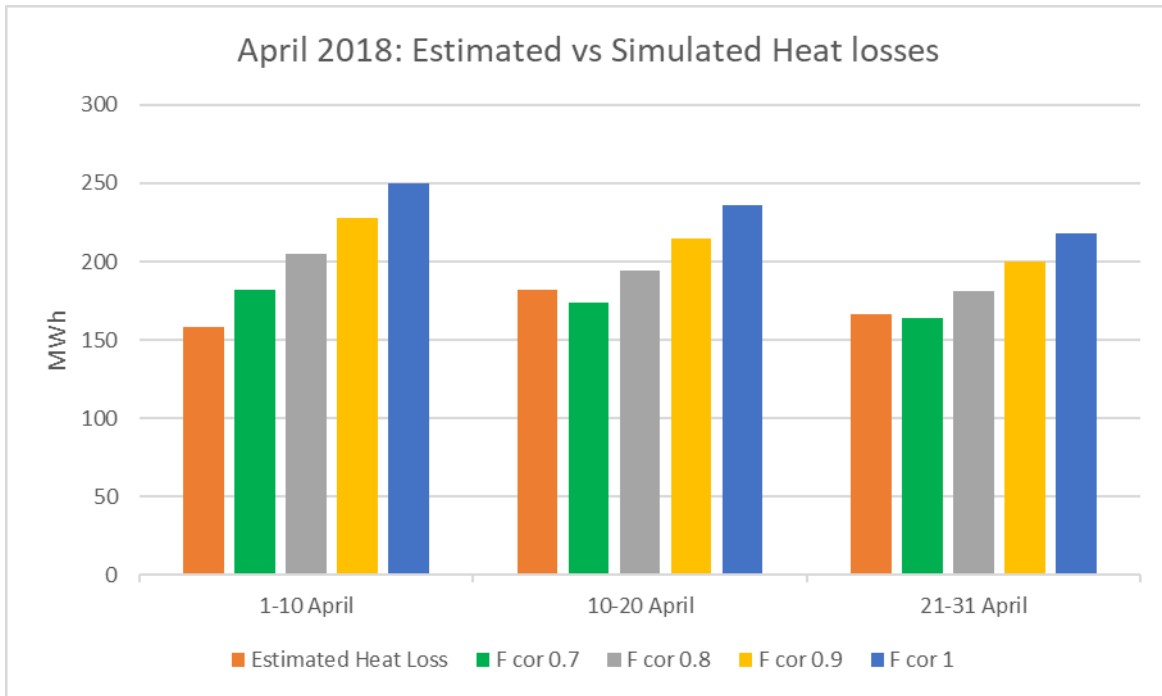


Figure 4. 13: Heat losses comparison: April 2018

As for the previous results the simulation with $F_{cor} = 0.7$ is the one which better approximates the estimated heat distribution losses in April.

	1-10 April	10-20 April	21-31 April
	MWh	MWh	MWh
Estimated Heat Losses	158	182	166
Fcor= 0.7	182	174	164
Fcor= 0.8	205	194	181
Fcor= 0.9	228	215	200
Fcor= 1	250	236	218

Table 4. 11: Heat losses comparison: April 2018

As we have seen in this comparison between the estimated and the simulated heat distribution losses, the $F_{cor} = 0.7$ is the factor that, multiplied for the thermal conductivity of each pipe in the formula of the temperature decay, formula 4.1, allows the simulated heat losses to fit the estimated ones, in each period we monitored the network of Roma Fiumicino. For this reason, all the following simulation results come from models where the F_{cor} is equal to 0.7.

Chapter 5: Simulation results of the Validation Scenario

5.1 Brief introduction to the simulation of the Working Network

In this chapter we are going to validate the model comparing the simulation results of the working network in the real working conditions, derived from the data analysis, with the monitored data for the month of February 2018. Even if we studied other months, December 2017, March and April 2018, we decided to validate the model for the month of February 2018 because it is the one for which we have all the temperature drops on the primary circuit of all the users, excluding user 155, 27, 53, 54. Giving the model the temperature drops on the user nodes at each time step, it is possible to have a high correspondence between the simulated global mass flow rate and the measured one.

The working network also includes the branches that we neglected in the discussion of the equivalent network: the branches to the users of chamber 9.1, the branches to the users of chamber 11 and the branches to the users of chamber 14. As we said previously, we obtained the load profile of user 27, Molo E in chamber 9.1, and the load profile of user 155, Terminal 1 between chamber 14 and chamber 15, by the difference between the global load of chamber 9.1-14 respectively and the other users inside.

$$Load_{user\ 27} = Load_{chamber\ 9.1} - Load_{user\ 128} - Load_{user\ 228} - Load_{user\ 125} - Load_{user\ 225}; \quad (5.1)$$

$$Load_{user\ 155} = Load_{chamber\ 14} - Load_{user\ 141} - Load_{user\ 241} - Load_{user\ 142} - Load_{user\ 242}; \quad (5.2)$$

This way to act causes an error in the calculation of the load profile of user 27 and of user 155, since in their load the heat losses of chamber 9.1 and 14 are included. To avoid the overestimation of the load profiles of user 27 and of user 155 we subtracted from their loads the heat losses in flow and in return of chamber 9.1 and chamber 14, respectively found for a test simulation where we did not subtract anything from the load profile of user 27 and of user 155.

$$Load'_{user\ 27} = Load_{user\ 27} - Heat\ Losses_{chamber\ 9.1}; \quad (5.3)$$

$$Load'_{user\ 155} = Load_{user\ 155} - Heat\ Losses_{chamber\ 14}; \quad (5.4)$$

The heat losses along the branches of the chambers mentioned do not change significantly when we subtract the heat losses of chamber 9.1 from the load profile of user 27 and the heat losses of chamber 14 from the load profile of user 155, since they are negligible compared to the load managed by the network in the respective chambers.

Inside the power station of the model we have three CHP units, a hot storage tank of 1,000 cubic meters, and a network dissipater that can dissipate all the thermal power produced inside the P.S. and not required by the load. The real thermal profile of the back-up boilers is given directly to the model as input, because we did not receive enough information to create a model of the boilers installed.

Power Station			
3 CHP units	<i>Nominal th. Power</i>	<i>[kW]</i>	3x7,987
3xBoilers	<i>Nominal th. Power</i>	<i>[kW]</i>	3x8,000
HST	<i>Volume</i>	<i>[m³]</i>	1,000

Table 5. 1: Power Station in working conditions

5.1 Simulation Results of the Working Network

In this section we are going to compare the simulation results of the model in the real working conditions with the measured data. For the month of February, at our disposal we have the temperature drops on the users' primary circuit that we give to the model at each time step as input.

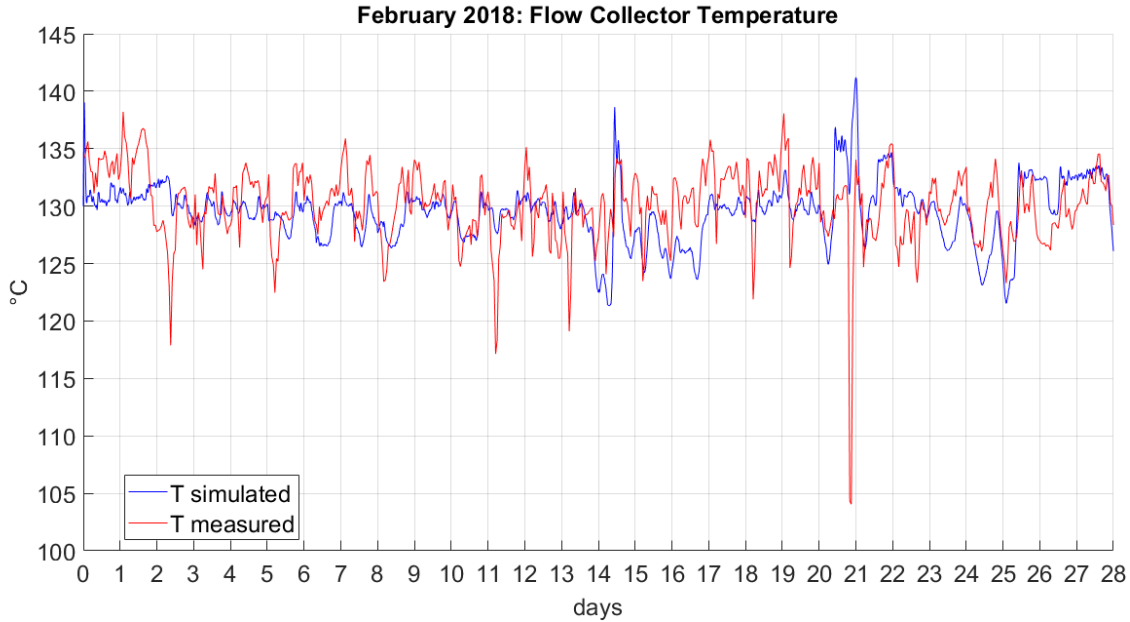


Figure 5. 1: Flow collector temperature comparison, February 2018, Validation

Simulated Average flow Temperature	[°C]	130.1
Measured Average flow Temperature	[°C]	130.5

Table 5. 2: Flow collector temperature comparison, February 2018, Validation

As we can see in Figure 5. 1, the simulated flow collector temperature follows the measured profile quite well even if it cannot reproduce the sudden drops that happen on the 2nd, the 5th, the 11th, 13th, 18th and 21st day.

In Figure 5. 2 and Figure 5. 3 we can see the percentage root mean square error and the root mean square error of the simulated flow collector temperature every 24 hours, with reference to the measured flow collector temperature, computed as:

$$RMSE = \sqrt{\frac{\sum_{i=1}^N (T_{i\text{ simulated}} - T_{i\text{ measured}})^2}{N}} ; (5.5)$$

$$PRMSE = \sqrt{\frac{1}{N} * \sum_{i=1}^N \left(\frac{T_{i\text{ simulated}} - T_{i\text{ measured}}}{T_{i\text{ measured}}} \right)^2}; (5.6)$$

Where N is the number of hours. Since the measured temperature is an hourly vector and the simulated temperature vector has three values each hour, because the simulation step is twenty minutes, the $T_{\text{simulated}}$ vector contains one value of the simulated temperature vector each three values, one for each hour.

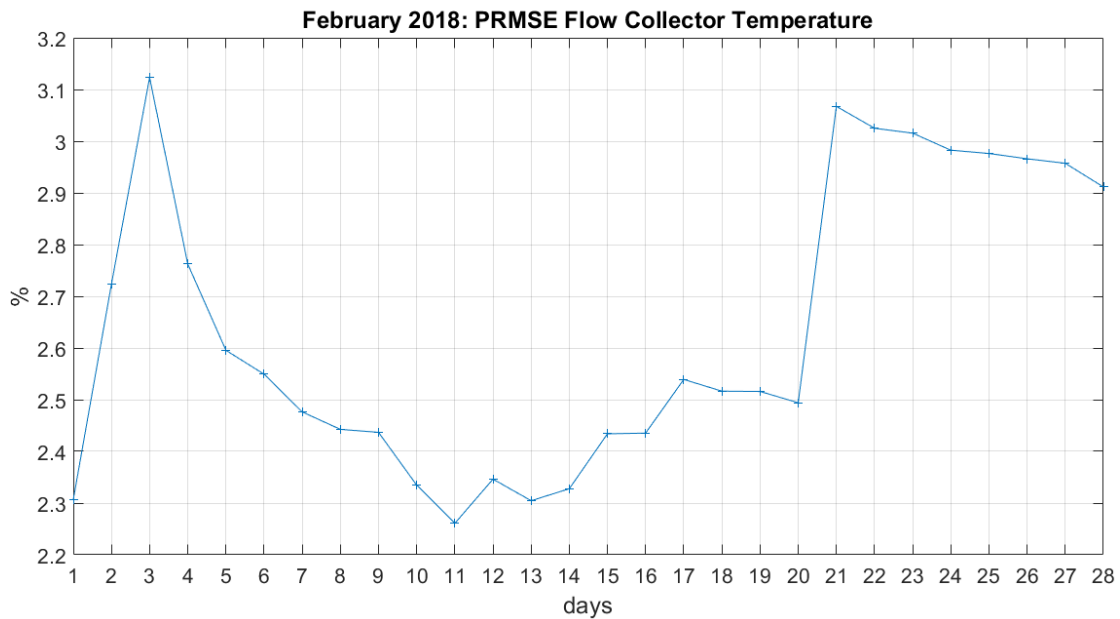


Figure 5. 2: PRMSE of the Flow collector temperature, February 2018, Validation

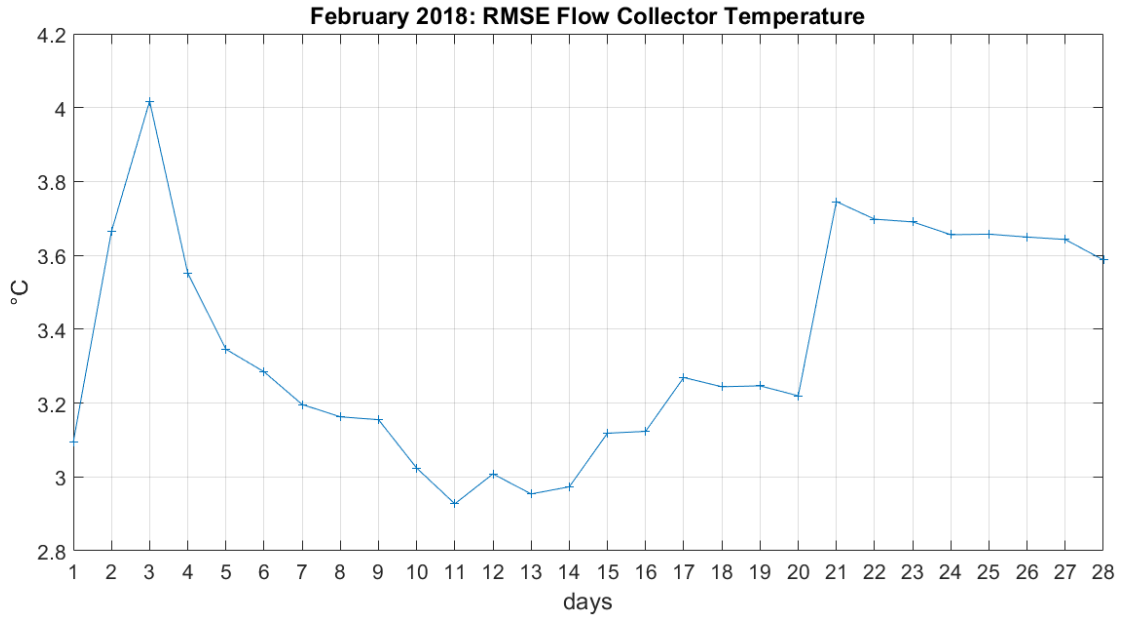


Figure 5. 3: RMES of the Flow collector temperature, February 2018, Validation

The Percentage Root Mean Square Error of the supply temperature is always less than 4 % during February and the Root Mean Square Error never rises above 4°C.

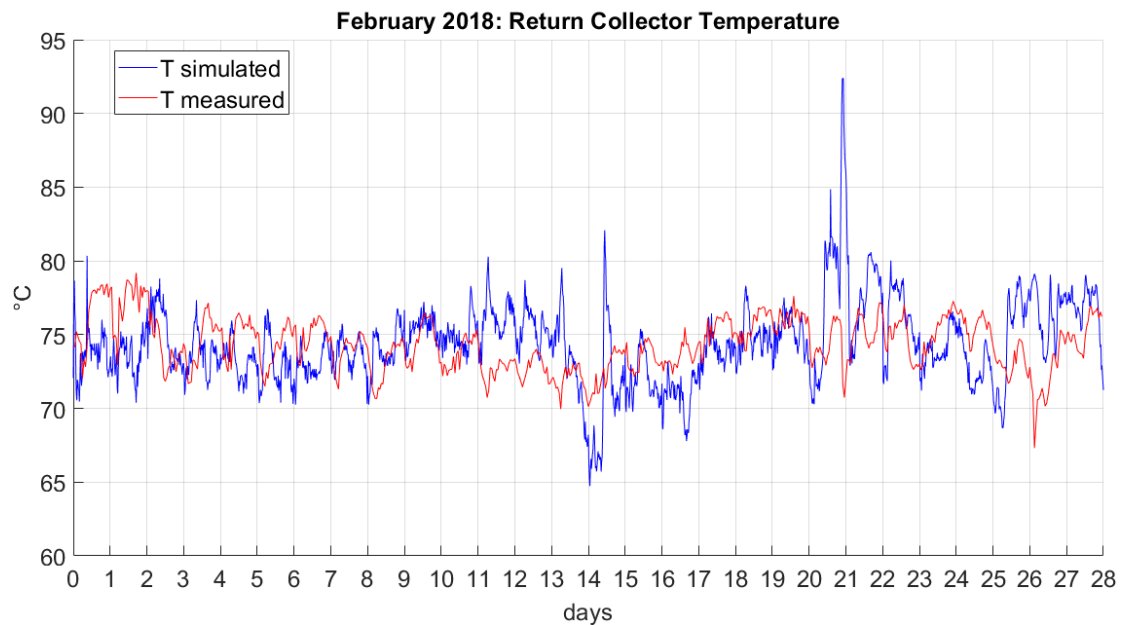


Figure 5. 4: Return collector temperature comparison, February 2018, Validation

Simulated Average Return Temperature	[°C]	74.4
Measured Average Return Temperature	[°C]	74.3

Table 5. 3: Return collector temperature comparison, February 2018, Validation

The simulated return collector temperature is very similar in the average value compared to the measured one, even if its profile is quite different, in particular between the 20th and the 21st day.

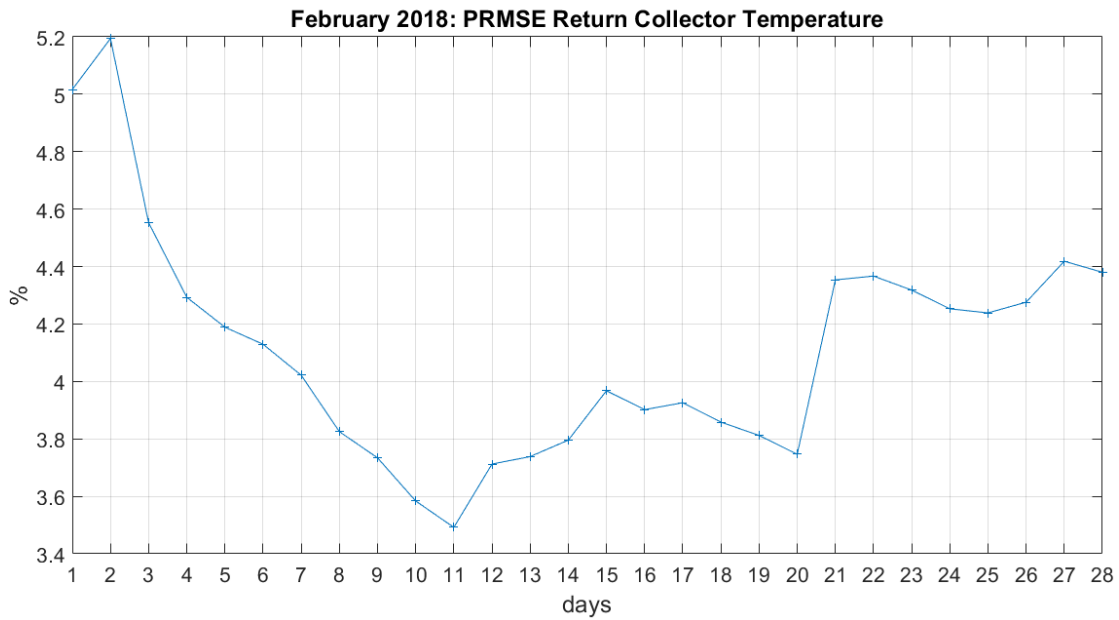


Figure 5. 5: PRMSE of the Return collector temperature, February 2018, Validation

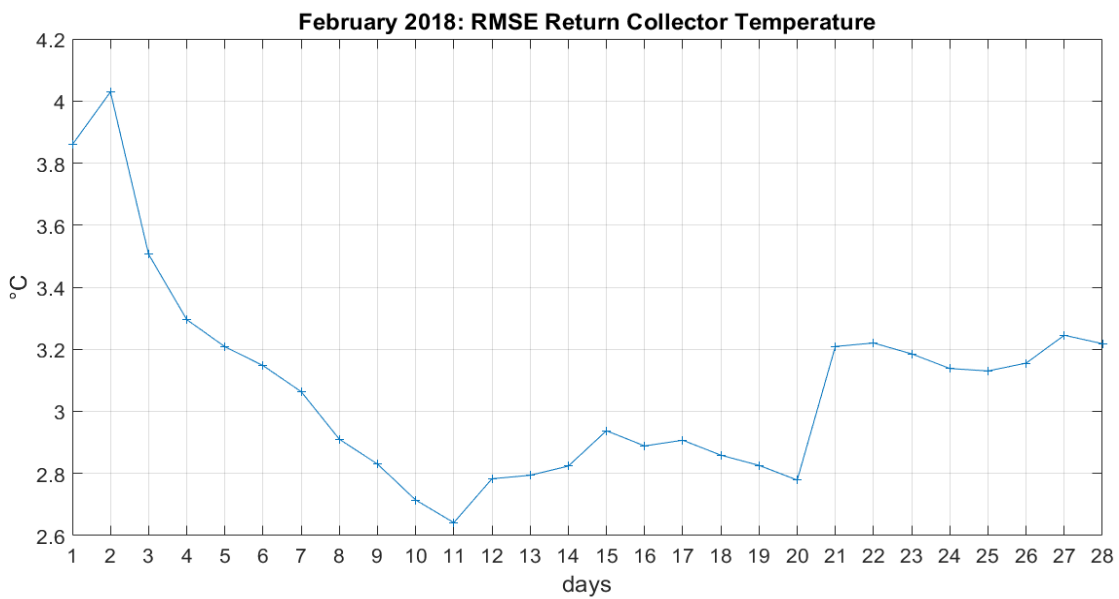


Figure 5. 6: RMSE of the Return collector temperature, February 2018, Validation

The Percentage Root Mean Square Error of the return collector temperature is always less than 5.2 % during February and the Root Mean Square Error never rises above 4°C.

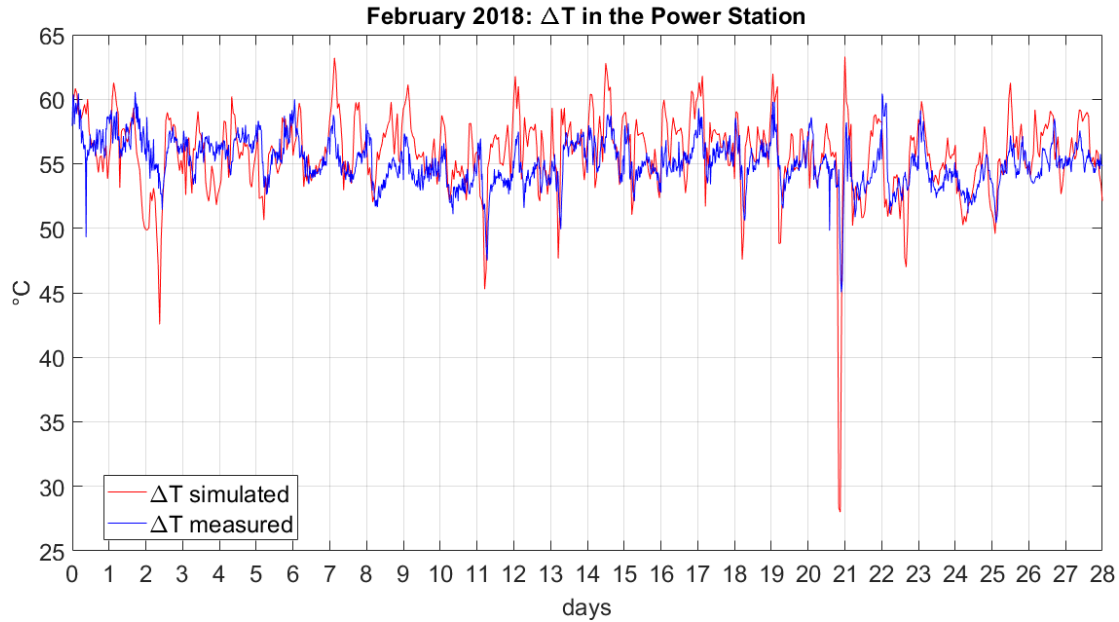


Figure 5. 7: ΔT comparison in the power station, February 2018, Validation

Simulated Average ΔT	[°C]	55.1
Measured Average ΔT	[°C]	55.8

Table 5. 4: ΔT comparison in the power station, February 2018, Validation

Giving the model the temperature drops on the users’ primary circuit as input, we have a high correspondence between the simulated and the measured temperature difference in flow and in return profile inside the power station. The error is due to the users for which we do not have the temperature drops; these are of course the user of Molo E (user 27 chamber 9.1), the absorption chiller of Terminal 1 (user 155, between chamber 14 and chamber 15), the user of PG 33 (user 54, chamber 1) and the user of PG 296 (user 53, chamber 6).

For the users of Molo E, PG 33 and PG 296 we set a fixed temperature drop of 50 °C, whereas for the user of Terminal 1, a double stage absorption chiller machine, we set a temperature drop of 60 °C.

In Figure 5. 8 we will see the mass flow rate comparison. The global mass flow rate flowing inside the network at each time step is:

$$G = \sum_{i=1}^N \frac{Q_{load,i}}{cp \Delta T_i}$$

$Q_{load,i}$: Load of the i user [kW] ;

ΔT_i : ΔT on the primary circuit of the i user [°C];

cp : specific heat of water $\left[\frac{kJ}{kgK} \right]$

N : number of users ;

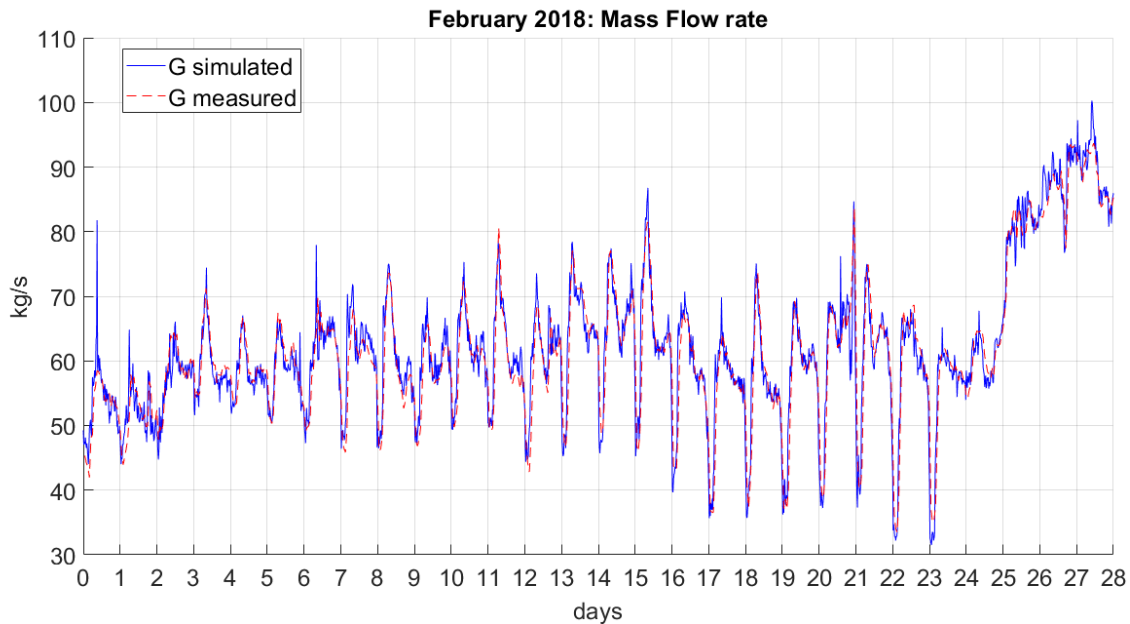


Figure 5. 8: Mass flow rate comparison, February 2018, Validation

In Figure 5. 9 Figure 5. 10, we will see the PRMSE and the RMSE computed for the mass flowrate flowing inside the network. The RMSE and PRMSE of the mass flow rate were computed with the same algorithm we used to compute the RMSE and the PRMSE of the supply temperature.

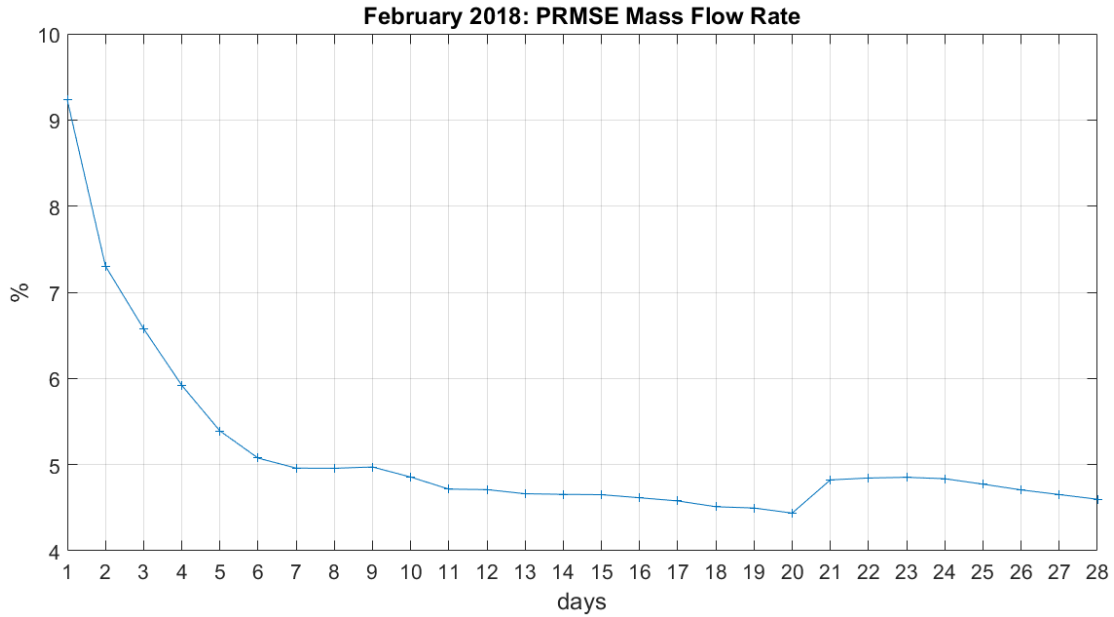


Figure 5. 9: PRMSE of the Mass flow rate, February 2018, Validation

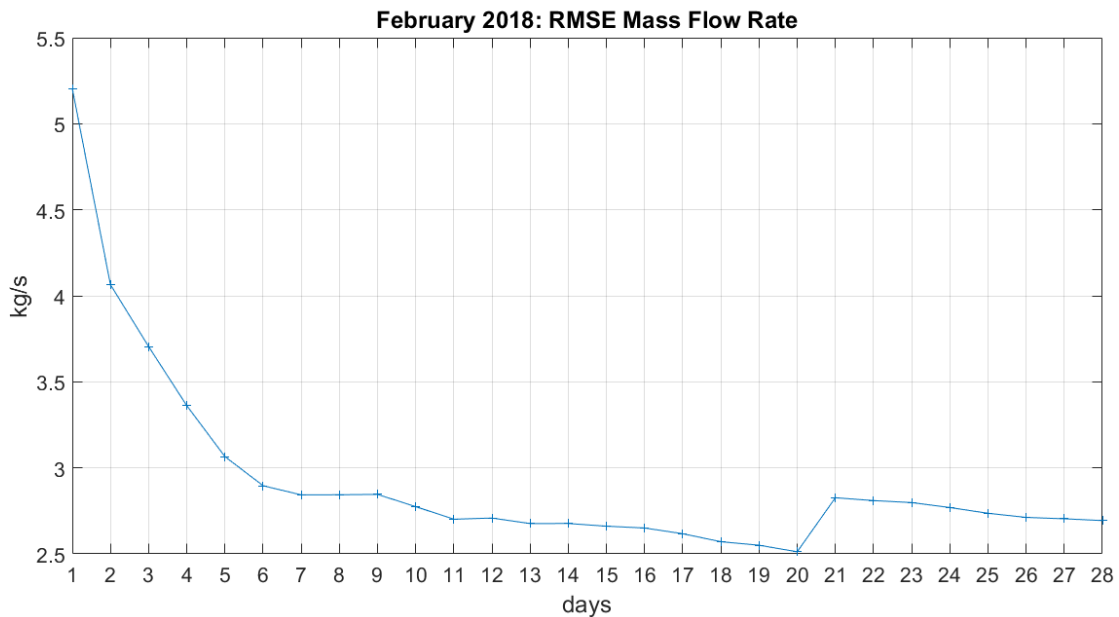


Figure 5. 10: RMSE of the Mass flow rate, February 2018, Validation

As we would expect, the simulated global mass flow rate profile is almost coincident with the measured one because we give the model the measured temperature drops on the users at each time step as input. In particular, for twenty days on twenty-eight the PRMSE of the MFR is lower than 5 %, whereas the RMSE of the MFR is lower than 3 kg/s. During the first time steps the correspondence is not so good because the boundary conditions in terms of temperature drops on the substations are not good, since

we set in the Input Excel File 50 °C on the users characterized by heat exchangers, and 60 °C on the users characterized by absorber cooling machines, values given us by ADR.

In the next figures we will see the hourly average thermal power exchanged by the HST, the hourly average heat distribution losses, the hourly average load required by the load, the hourly average heat produced in the P.S., and the hourly average thermal power produced by the CHP units.

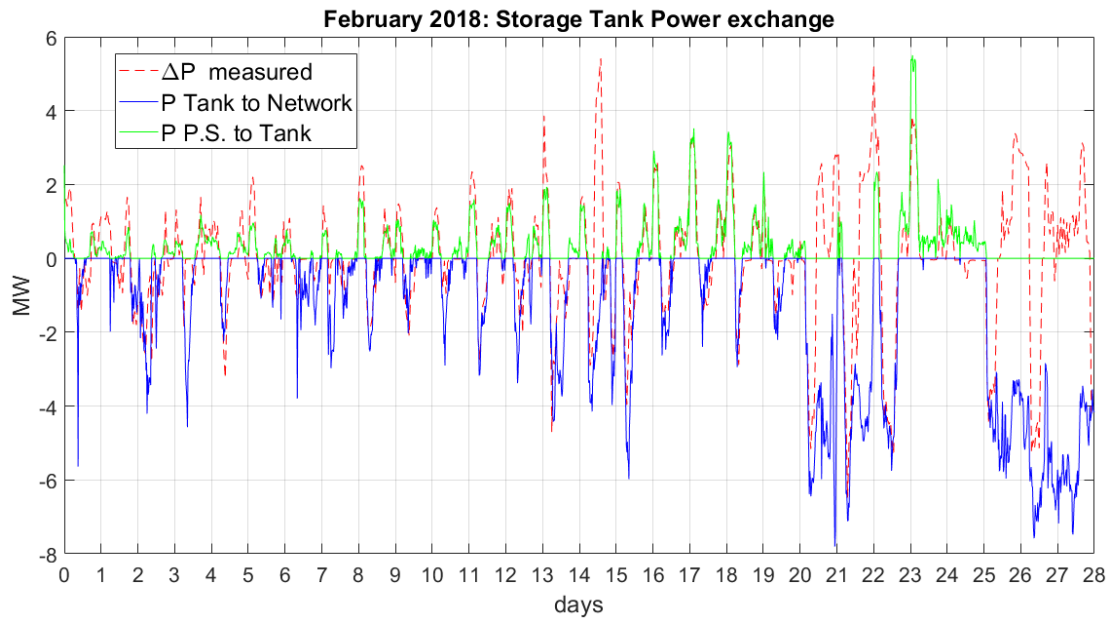


Figure 5. 11: Storage Tank Power Exchange comparison, February 2018, Validation

In Figure 5. 11 we can see the measured and the simulated thermal behaviour of the HST. The red dashed line represents the measured charging and discharging phases. The blue solid line represents the simulated discharging phase, thermal energy from the HST to the network. The green solid line represents the simulated charging phase, thermal energy from the P.S. to the HST. Giving the CHP units the measured mass flow rate as input and giving the model the measured ΔT on the users (from which the model computes the global mass flow rate flowing in the network), the model reproduces the charging and the discharging phases of the HST quite well. Even if the error in the computation of the global MFR is minimum, on the 20th, 21st, 22nd, 25th, 26th, 27th, 28th day, the correspondence between the measured and simulated power exchange with the P.S. and with the network by the HST is not good.

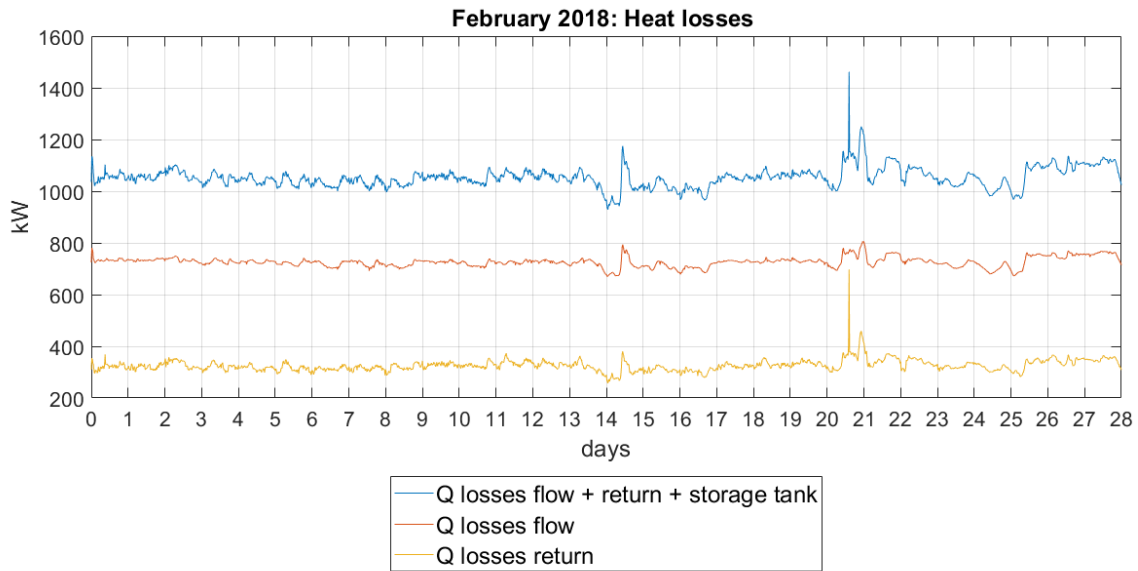


Figure 5. 12: Simulated network heat losses, February 2018, Validation

Global Heat losses (Flow+Return+HST)	<i>MWh</i>	707.5
Heat Distribution Losses (Flow +Return)	<i>MWh</i>	707.0
Heat losses HST	<i>MWh</i>	0.5
Average Global Heat losses	<i>kW</i>	1,100
Specific Heat Distribution losses	<i>W/m</i>	31.8

Table 5. 5: Simulated network heat losses, energy results, February 2018, Validation

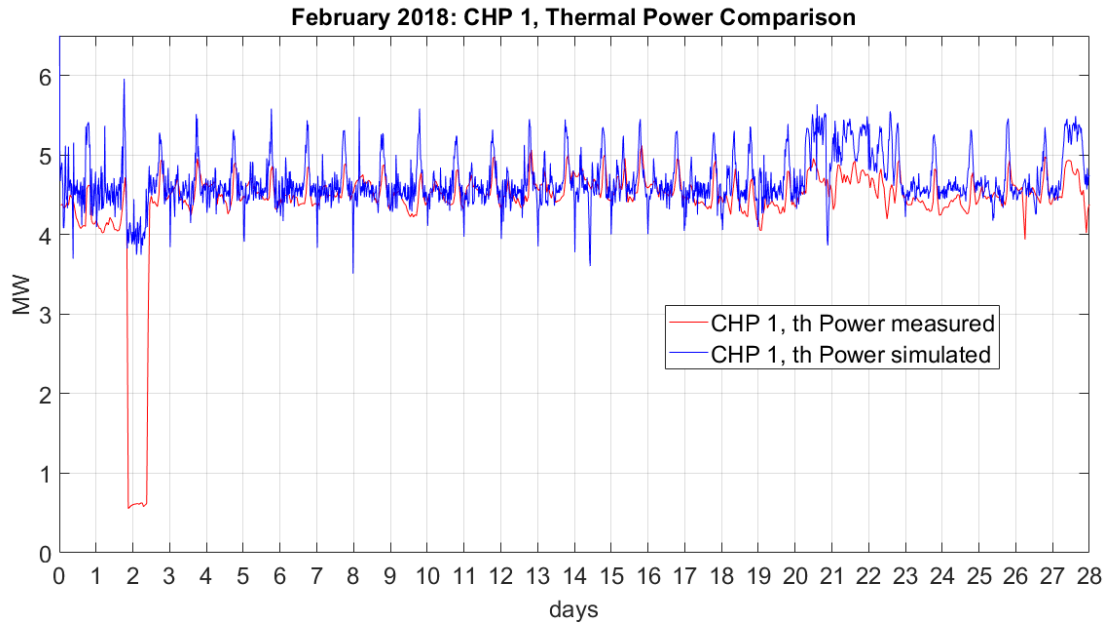


Figure 5. 13: CHP 1, thermal Power comparison, February 2018, Validation

Simulated Energy produced, CHP 1	<i>MWh</i>	3,149
Measured Energy produced, CHP 1	<i>MWh</i>	2,986
Simulated Average th. Power, CHP 1	<i>MW</i>	4.7
Measured Average th. Power, CHP 1	<i>MW</i>	4.4
Energy Difference	<i>MWh</i>	163
Energy Difference	%	5

Table 5. 6: CHP 1, thermal comparison, February 2018, Validation

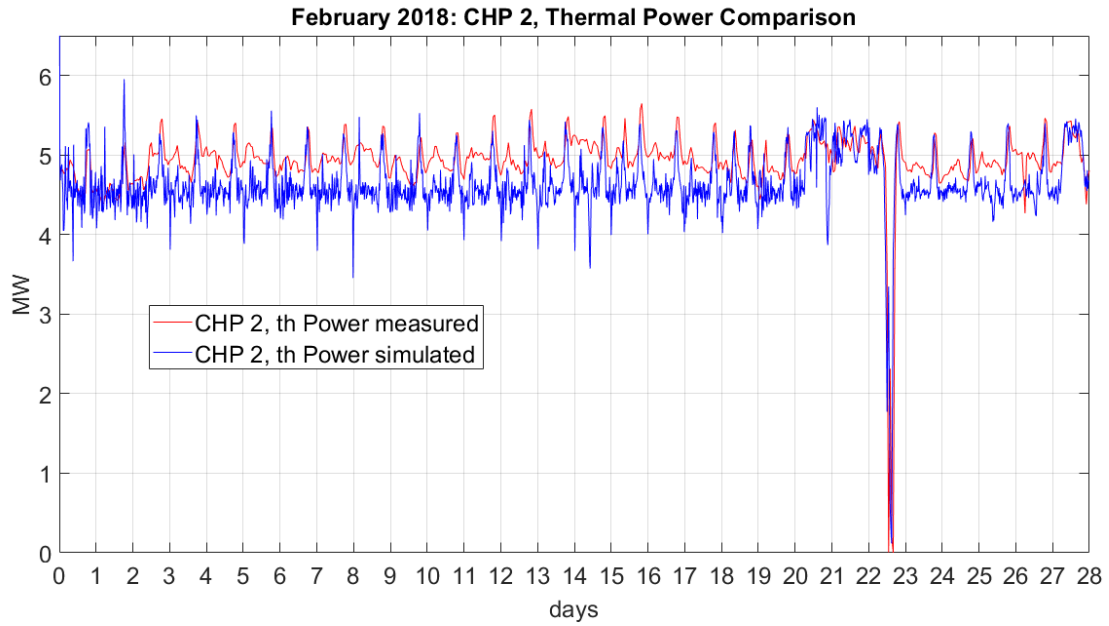


Figure 5. 14: CHP 2, thermal Power comparison, February 2018, Validation

Simulated Energy produced, CHP 2	<i>MWh</i>	3,125
Measured Energy produced, CHP 2	<i>MWh</i>	3,309
Simulated Average th. Power, CHP 2	<i>MW</i>	5.0
Measured Average th. Power, CHP 2	<i>MW</i>	4.9
Energy Difference	<i>MWh</i>	184
Energy Difference	<i>%</i>	6

Table 5. 7: CHP 2, thermal comparison, February 2018, Validation

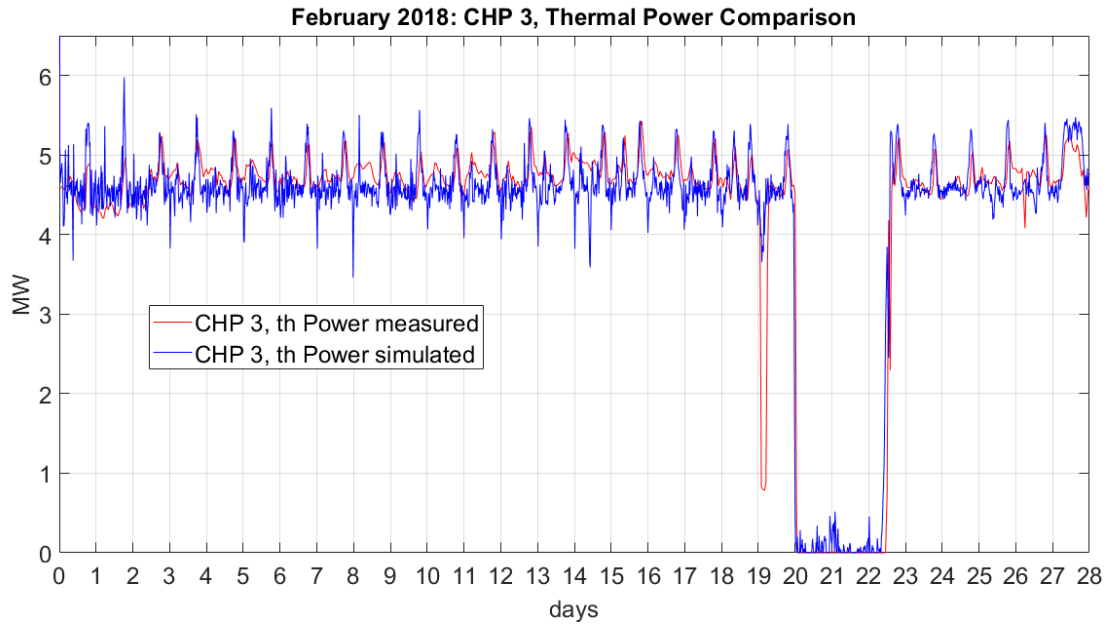


Figure 5. 15: CHP 3, thermal Power comparison, February 2018, Validation

Simulated Energy produced, CHP 3	<i>MWh</i>	2,854
Measured Energy produced, CHP 3	<i>MWh</i>	2,875
Simulated Average th. Power, CHP 3	<i>MW</i>	4.0
Measured Average th. Power, CHP 3	<i>MW</i>	4.3
Energy Difference	<i>MWh</i>	21
Energy Difference	<i>%</i>	0.7

Table 5. 8: CHP 3, thermal comparison, February 2018, Validation

The thermal energy produced by the simulated CHP units is very similar to the measured one; in particular, there is an overestimation of 5% for the first and an underestimation of 6% for the second CHP, whereas for the third simulated CHP unit the thermal energy measured and simulated are more or less the same.

The thermal power generated by CHP units, depending on the electric profile given as input, shows us the behaviour of the power station. The difference in the thermal energy produced, with reference to the measured one, is due to the fact that as input we give the model of the CHP the electric profile that is quite different from the thermal one. In fact, the measured thermal energy produced by the CHP does not consider the heat dissipated by each CHP unit dissipater, of which we do not have information. The existence of the CHP units' dissipaters is proved by the sudden drops in their thermal production, as we can see in Figure 5. 13 on the second day, and in Figure 5. 15 on the nineteenth day. For these reasons, we can say that the model of the CHP unit dissipater, that in our case dissipates the heat of the cooling water of the lubricant oil in order to keep the same cooling water at 43 °C, does not reproduce the management of the real CHP unit dissipater.

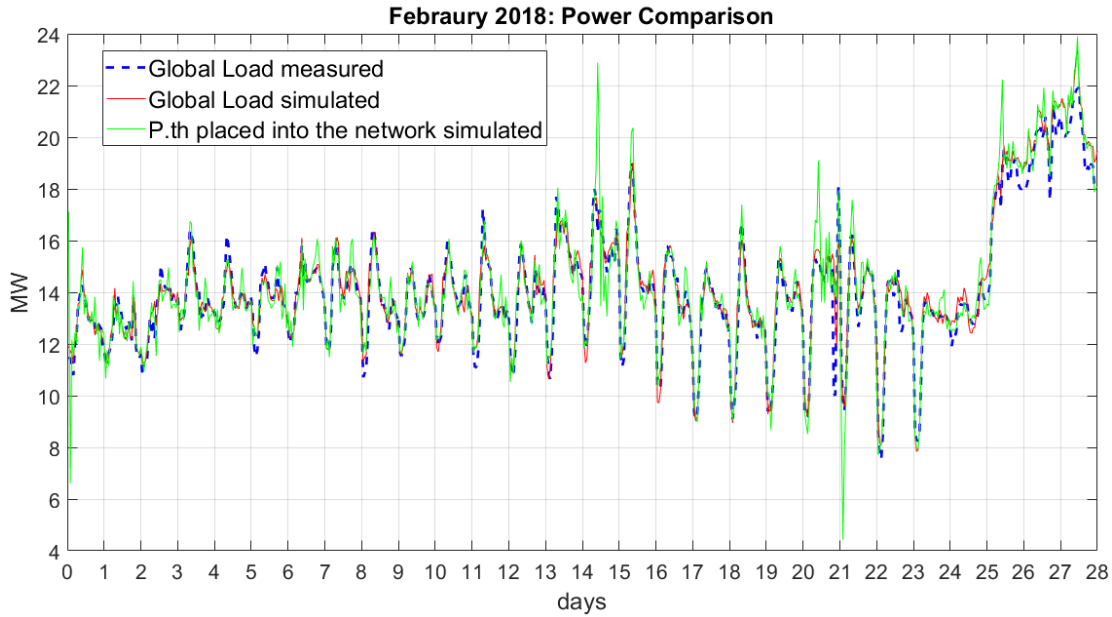


Figure 5. 16: Power Comparison in the Power Station, February 2018, Validation

Measured Energy Produced in PS	<i>MWh</i>	9,827
Simulated Energy Produced in PS	<i>MWh</i>	9,785
Measured Average th. Power Produced in PS	<i>MW</i>	14.6
Simulated Average th. Power Produced in PS	<i>MW</i>	15.0
Measured Global Load	<i>MWh</i>	9,518
Simulated Global Load	<i>MWh</i>	9,611
Measured Average Global Load	<i>MW</i>	14.0
Simulated Average Global Load	<i>MW</i>	14.3
Simulated Energy placed into the Network	<i>MWh</i>	9,604
Average Simulated th. Power placed into the Network	<i>MW</i>	14.3
Measured Sm³ of Methane consumed by CHP	<i>Sm³</i>	3,269,814

Table 5. 9: Comparison in the Power Station, February 2018, Validation

The energy produced in the power station is the sum of the energy produced by the cogenerators and by the boilers. The simulated energy placed into the network is measured at the flow collector and it is the energy feeding the network, at net of the energy dissipated by the network dissipater. The simulated thermal power placed into the network follows the load perfectly because of the proper setting of the network dissipater that dissipates all the heat produced that is not requested by the load.

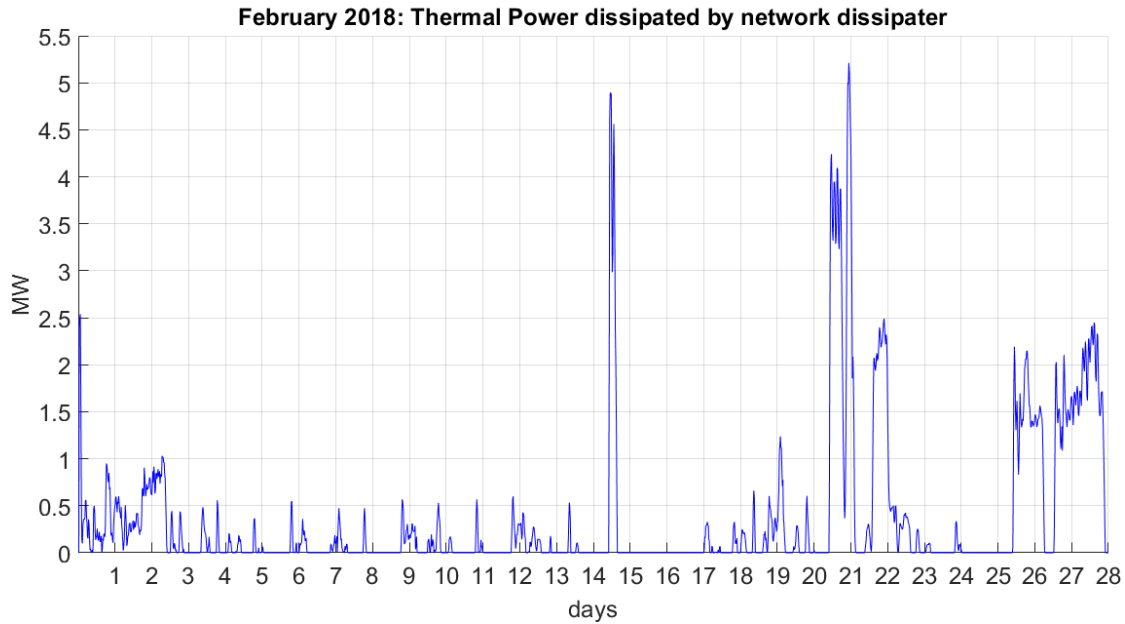


Figure 5. 17: Thermal Power dissipated by the network dissipater, February 2018, Validation

Simulated Energy Dissipated by Network Dissipater	<i>MWh</i>	174
Simulated Average th Power Dissipated by Network Dissipater	<i>MW</i>	0.3

Table 5. 10: Heat dissipated by the network dissipater, February 2018, Validation

As we can see in Table 5. 10, the heat dissipated by the network dissipater is about 2% of the energy produced in the power station. The network dissipater has to work for most of the month otherwise the flow temperature would go above 140 °C.

The simulation results reproduce the measured data of the real district heating network of Roma Fiumicino in the real working conditions in a satisfying way. For this reason, we can say that our model can be used to run efficiency scenarios which results will be useful to evaluate feasible changes of the working condition in order to optimize the network from the energy point of view.

Validation scenario	
	<i>MWh</i>
Users Load	8,903
Global Heat Losses	707.5
Energy Placed into the Network	9,604
Energy Produced by CHP	9,128
Boilers Heat Production	657
Energy Produced in the P.S.	9,785
Energy Dissipated in the HST Dissipater	0.6
Energy Dissipated in the Network Dissipater	174

Table 5. 11: Simulation Energy Results, February 2018, Validation

Chapter 6: Working Network at Time 0

6.1 Brief introduction to the simulation of the Working Network at Time 0

This scenario was thought to compare the working conditions of the network, those that ADR claimed were the real ones, at fixed temperature drops on the users' primary circuit, with the efficiency scenarios. We will call this scenario 'Time 0'. This scenario was obtained running the working network for the month of February with fixed temperature drops on the users, 50 °C on the heat exchangers and 60 °C on the double stage absorption cooling machines. In this simulation we will see that the temperature difference between flow and return in the power station is flatter than in the simulation of validation, where the ΔT on the users changed at each time step. The results of this section were not commented on as they are really similar to those from the previous chapter.

Inside the power station of the model we have three CHP units, a hot storage tank of 1,000 cubic meters, a network dissipater that can dissipate all the thermal power produced inside the P.S. and not required by the load. The real thermal profile of the back-up boilers is directly given to the model as input, because we did not receive enough information to create a model for the boilers.

Power Station			
3 CHP units	<i>Nominal th. Power</i>	<i>[kW]</i>	3x7,987
3xBoilers	<i>Nominal th. Power</i>	<i>[kW]</i>	3x8,000
HST	<i>Volume</i>	<i>[m³]</i>	1,000

Table 6. 1 Power station

The simulation results of this section will be compared with the ones of the efficiency scenarios.

6.2 Simulation Results of the Working Network at Time 0

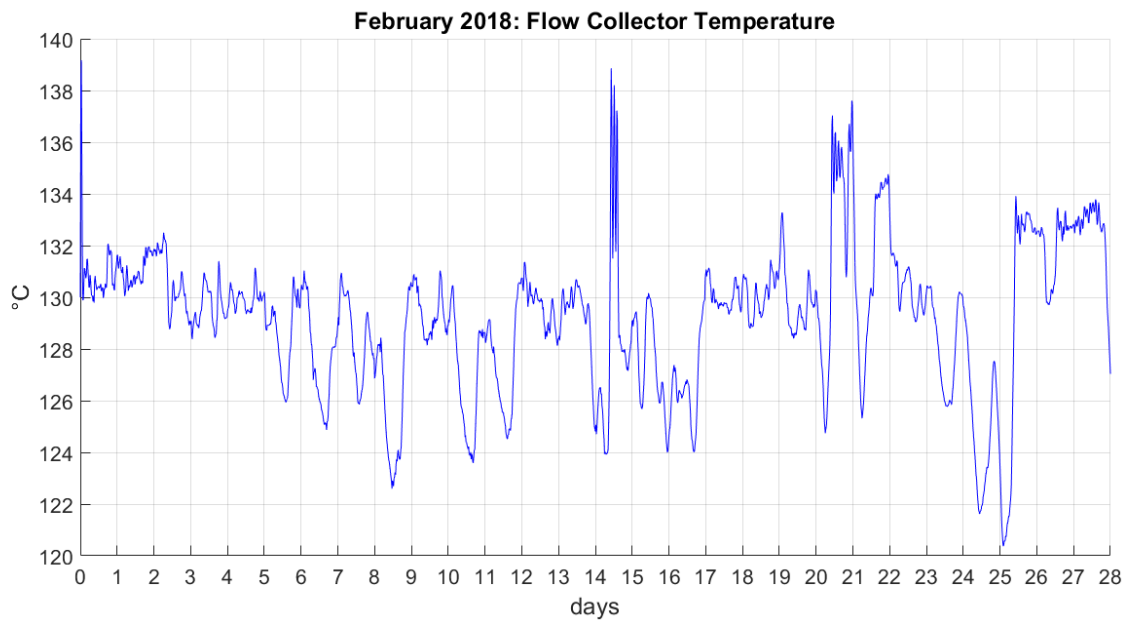


Figure 6. 1: Flow collector temperature, February 2018, Time 0

Simulated Average flow Temperature	[°C]	129.2
---	-------------	--------------

Table 6. 2: Flow collector temperature, February 2018, Time 0

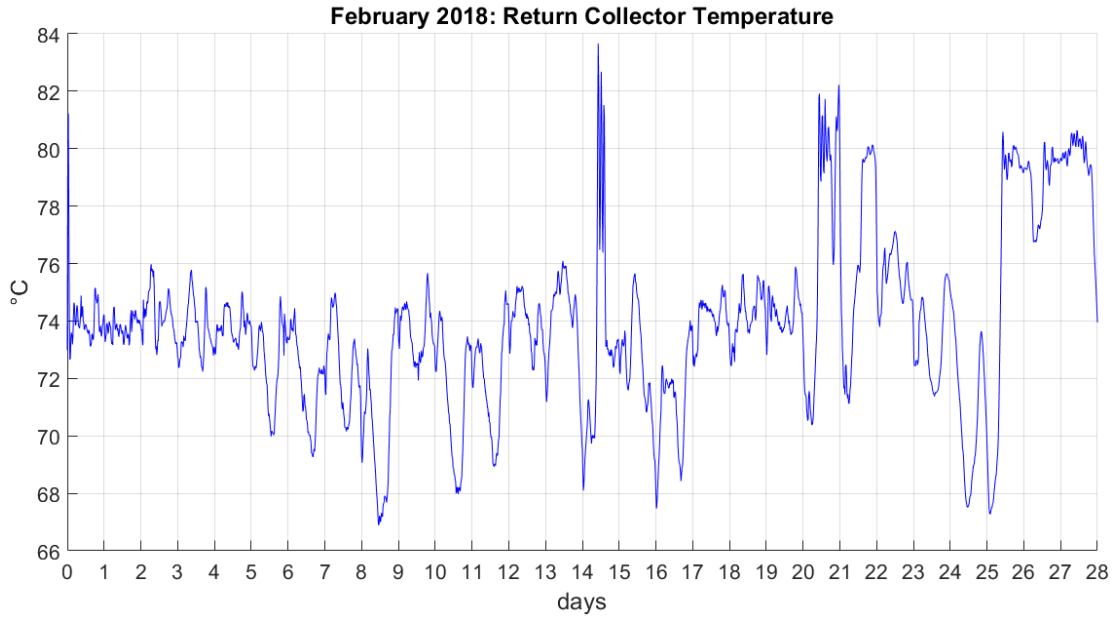


Figure 6. 2: Return collector temperature comparison, February 2018, Time 0

Simulated Average Return Temperature	[°C]	73.8
---	-------------	-------------

Table 6. 3: Return collector temperature comparison, February 2018, Time 0

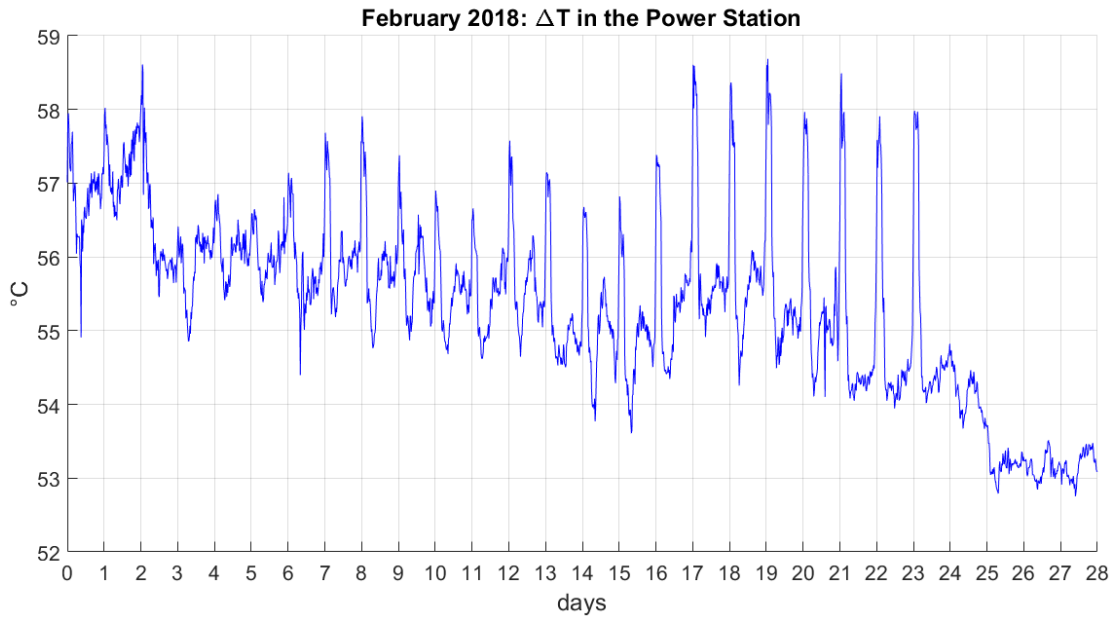


Figure 6. 3: ΔT in the power station, February 2018, Time 0

Simulated Average ΔT	[°C]	55.4
--	-------------	-------------

Table 6. 4: ΔT in the power station, February 2018, Time 0

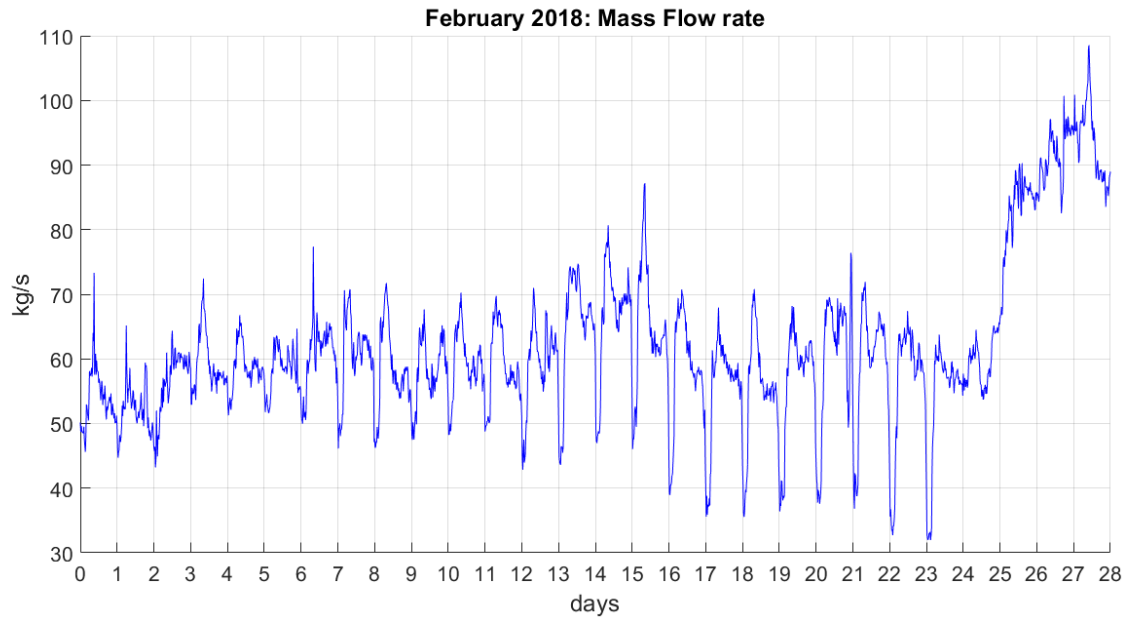


Figure 6. 4: Mass flow rate, February 2018, Time 0

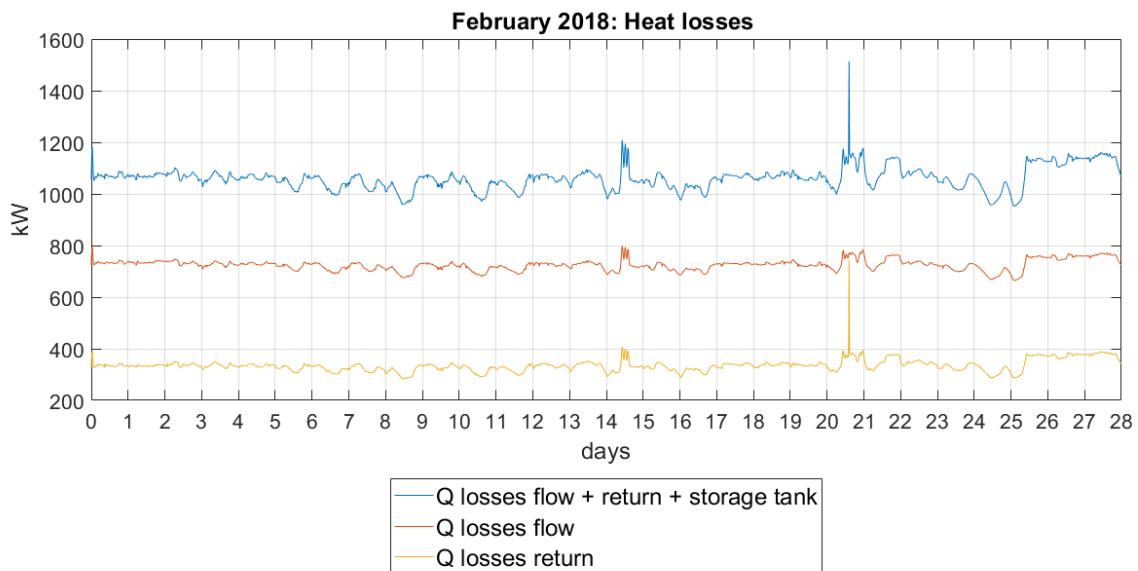


Figure 6. 5: Network heat losses, February 2018, Time 0

Global Heat losses (Flow+Return+HST)	<i>MWh</i>	713
Heat Distribution Losses	<i>MWh</i>	712.4
Heat losses HST	<i>MWh</i>	0.6
Average Global Heat losses	<i>kW</i>	1,100
Specific Network Heat losses	<i>W/m</i>	32.0

Table 6. 5: Network heat losses results, February 2018, Time 0

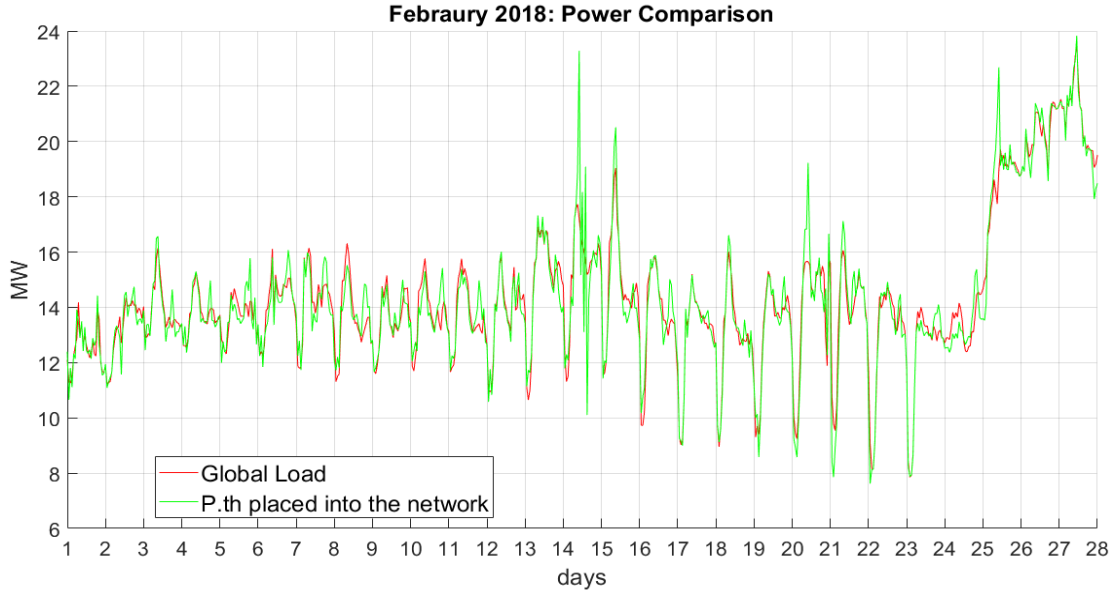


Figure 6. 6: Power Comparison in the Power Station, February 2018, Time 0

Energy Produced in P.S.	<i>MWh</i>	9,786
Global Load	<i>MWh</i>	9,616
Energy placed into the Network	<i>MWh</i>	9,609
Average th. Power Produced in PS	<i>MW</i>	14.6
Average Global Load	<i>MW</i>	14.3
Average th. Power placed into the Network	<i>MW</i>	14.3

Table 6. 6: Energy Comparison in the Power Station, February 2018, Time 0

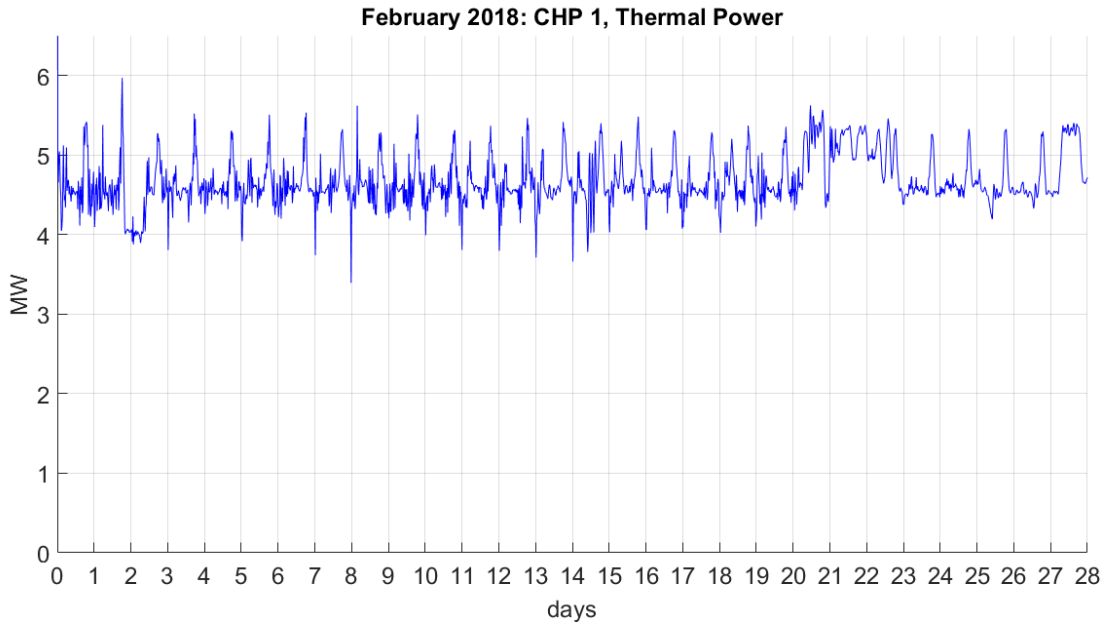


Figure 6. 7: CHP 1, thermal Power, February 2018, Time 0

Energy produced, CHP 1	<i>MWh</i>	3,150
Average th. Power, CHP 1	<i>MW</i>	4.7

Table 6. 7: CHP 1, thermal comparison, February 2018, Time 0

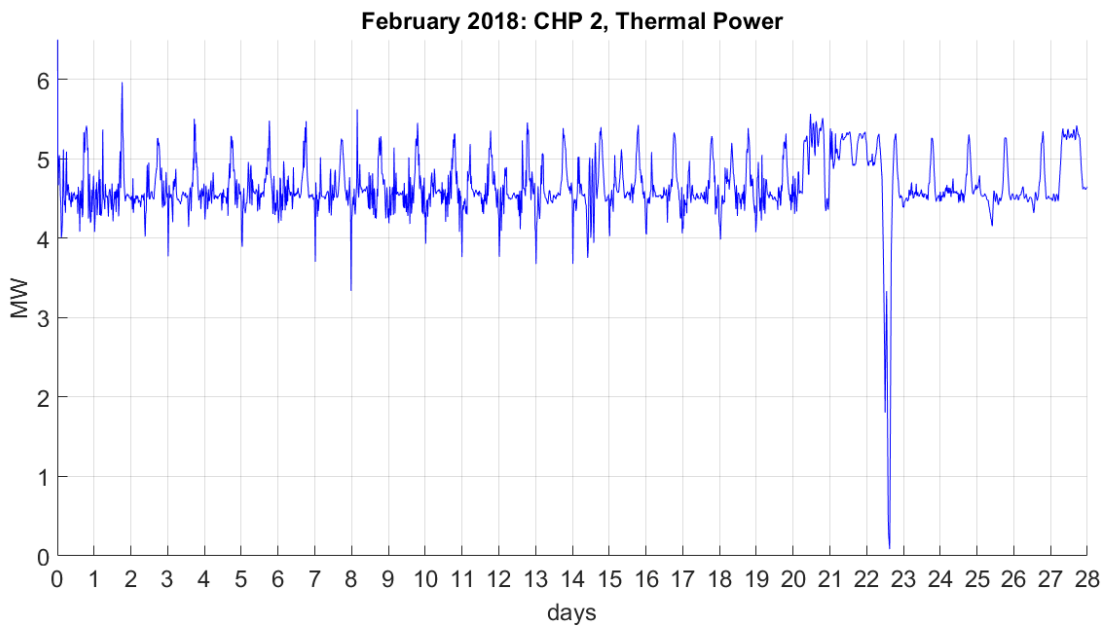


Figure 6. 8: CHP 2, thermal Power, February 2018, Time 0

Energy produced, CHP 2	<i>MWh</i>	3,126
Average th. Power , CHP 2	<i>MW</i>	4.7

Table 6. 8: CHP 2, thermal comparison, February 2018, Time 0

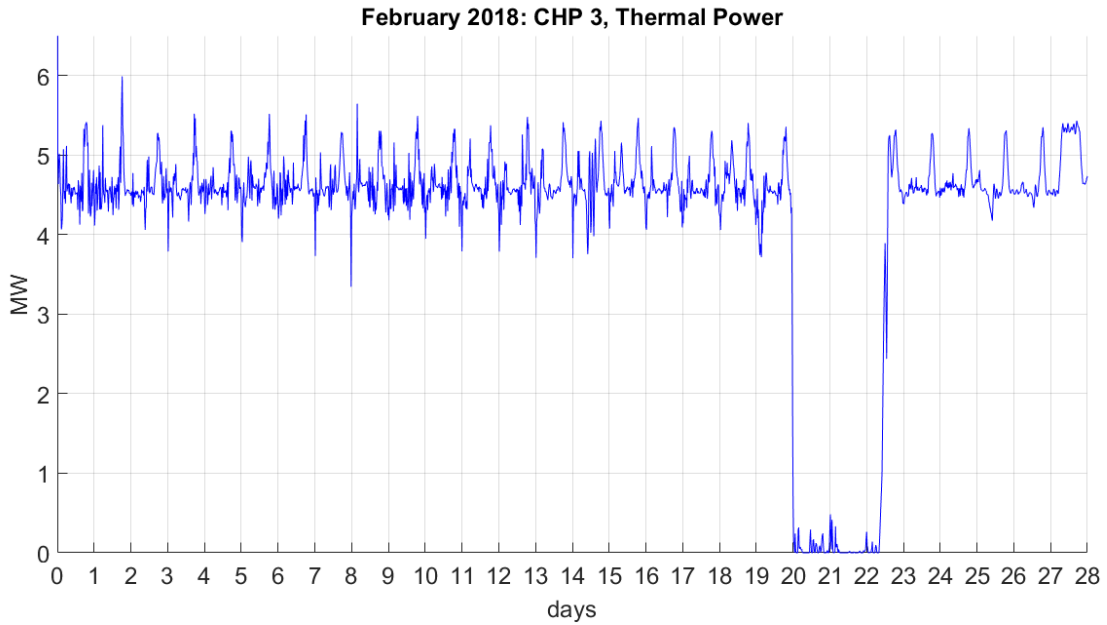


Figure 6. 9: CHP 3, thermal Power, February 2018, Time 0

Energy produced, CHP 3	<i>MWh</i>	2,853
Average th. Power, CHP 3	<i>MW</i>	4.2

Table 6. 9: CHP 3, thermal comparison, February 2018, Time 0

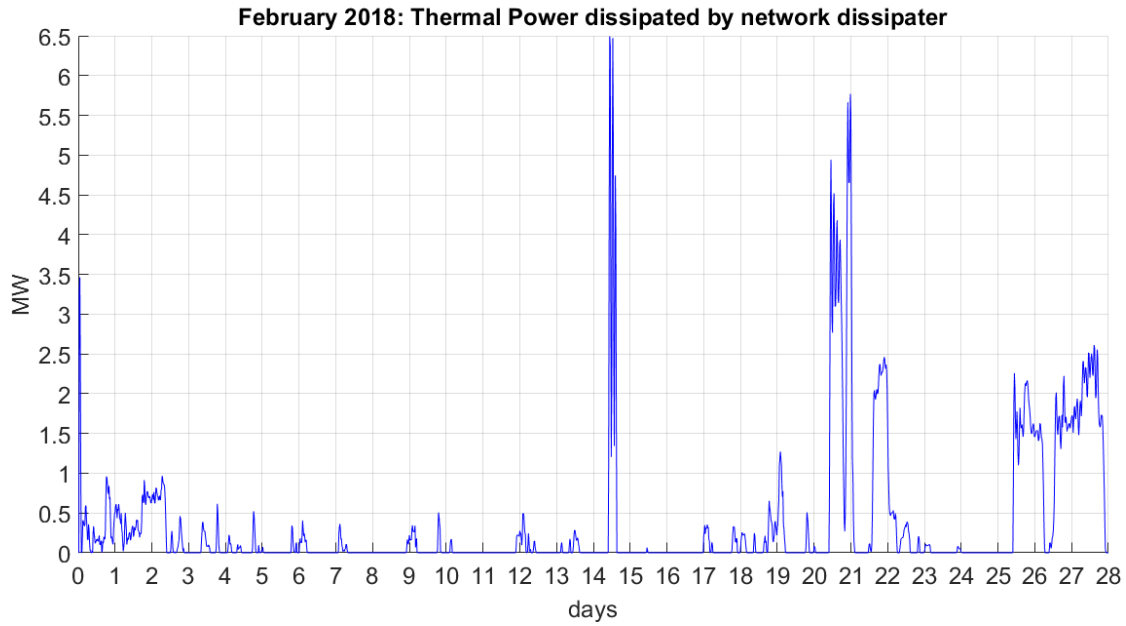


Figure 6. 10: Power dissipated by the network dissipater, February 2018, Time 0

Energy Dissipated by Network Dissipater	<i>MWh</i>	169
Average th Power Dissipated by Network Dissipater	<i>MW</i>	0.3

Table 6. 10: Energy dissipated by the network dissipater, February 2018, Time 0

Scenario Time 0	
	<i>MWh</i>
Users Load	8,903
Global Heat Losses	713
Energy Placed into the Network	9,609
Energy Produced by CHP	9,129
Boilers Heat Production	657
Energy Produced in the P.S.	9,786
Energy Dissipated in the HST Dissipater	0.6
Energy Dissipated in the Network Dissipater	169

Table 6. 11: Simulation Energy Results, Time 0

6.3 Brief Introduction to the energy efficiency scenarios

In the following chapters we will simulate four different energy efficiency scenarios. In these scenarios we will see it is possible to produce more thermal energy using the CHP units, reducing the return temperature in the power station. In the actual working conditions, the dissipater of each CHP unit dissipates the heat of the cooling water of the lubricant oil in order to keep the same cooling water at 43 °C. At each time step of simulation, the cooling water of the lubricant oil has to remove 2,083 kW of heat from the lubricant oil itself, making a temperature drop between 43 °C and 57 °C. When the return mass flow rate in the power station is below 57 °C each CHP unit can recover up to 2,083 MWth of heat from the cooling water of the lubricant oil inside the low temperature heat exchanger.

In the first efficiency scenario we will simulate the Network of Roma Fiumicino setting two different supply temperatures on its two loops, 130 °C on the DN 200 and 90 °C on the DN 350. We will connect all the users characterized by heat exchangers to the loop DN 350, whereas we will connect the two users characterized by double stage absorption machines, user 125 and user 155, to the DN 200. From this efficiency scenario we expect to recover heat from the low temperature heat exchangers of the CHP units connected to the DN 350 managed at lower temperature, and we also expect to reduce the heat distribution losses, in particular on the DN 350.

In the second efficiency scenario we will run the model of the network at two different temperatures but, this time we will also connect two single stage absorption chillers to the loop at lower temperature, DN 350. From this scenario we expect to significantly reduce the heat dissipated by the network dissipater, with reference to the first scenario, and to produce useful cooling energy.

In the third efficiency scenario we will simulate the Network of Roma Fiumicino using only the loop DN 350, setting as flow temperature 90 °C. All the loads will be connected to the DN 350 and the DN 200 will be completely absent, completely OFF. The double stage absorption chillers will be replaced by single stage absorption chillers. From this efficiency scenario we expect to significantly reduce the heat distribution losses and to recover heat from the low temperature heat exchangers of the CHP units.

In the fourth and last efficiency scenario we will run the model of the network using only the DN 350 but this time we will connect two new single stage absorption chillers to the network. From this scenario we expect to reduce the heat dissipated from the network dissipater, compared to scenario 3, and to produce useful cooling energy, as well as reducing the heat distribution losses.

As should be clear, the second efficiency scenario is directly linked to the first one, as the fourth efficiency scenario is directly linked to the third one, since recovering heat from the low temperature heat exchangers of the CHP units is meaningless if we dissipate the same heat inside the network dissipater. All the energy efficiency scenarios will have the CHP units working with the real electric profiles, the same we used in the validation scenario and in scenario Time 0, electric profiles derived from the monitoring data. This assumption brings all the simulations to have the same methane consumption and the same electric energy production inside the CHP units.

Chapter 7: Scenario 1: Two Temperatures Network

7.1 Brief introduction to scenario 'Two Temperatures Network'

In this chapter we will see the simulation results of the Network of Roma Fiumicino managed at two different temperatures for its two loops. One loop, the DN 200, will be run with a dissipater reference flow temperature of 140 °C and a fixed temperature drop on the users' primary circuit of 60 °C, whereas the second loop, the DN 350 will be run with a dissipater reference flow temperature of 103 °C and a fixed temperature drop on the users of 50 °C.

The two loops are completely separated and independent from the hydraulic point of view. To the loop DN 200, the double stage absorption chillers will be connected, placed in PG 107, user 125, and in Terminal 1, user 155.

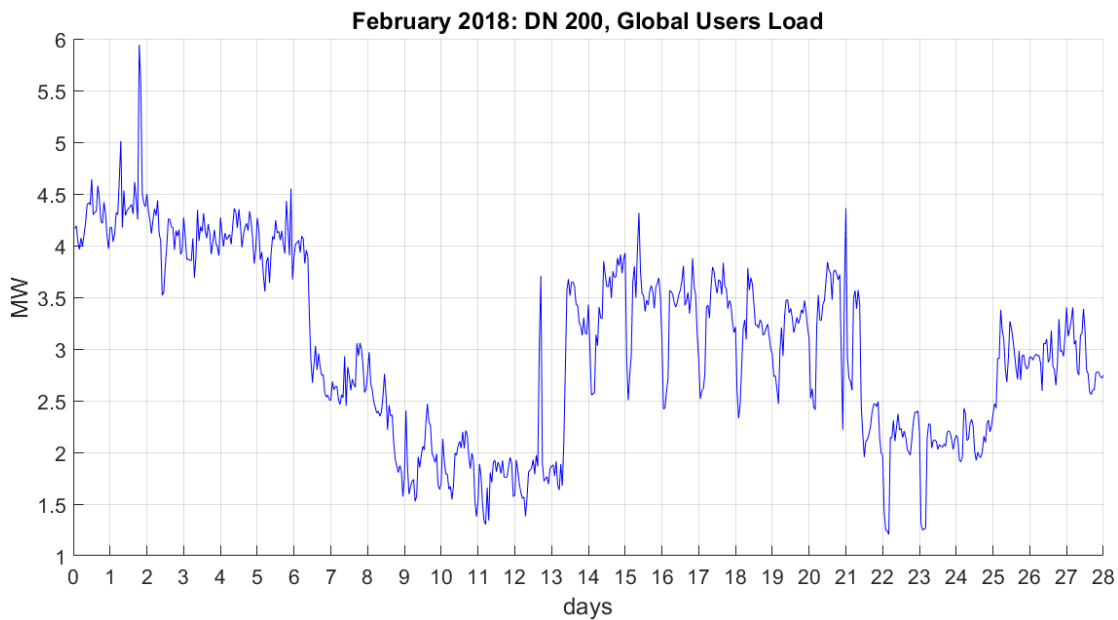


Figure 7. 1: DN 200, Users Load, Scenario 1

All the other loads will be connected to the loop DN 350, loads characterized by heat exchangers.

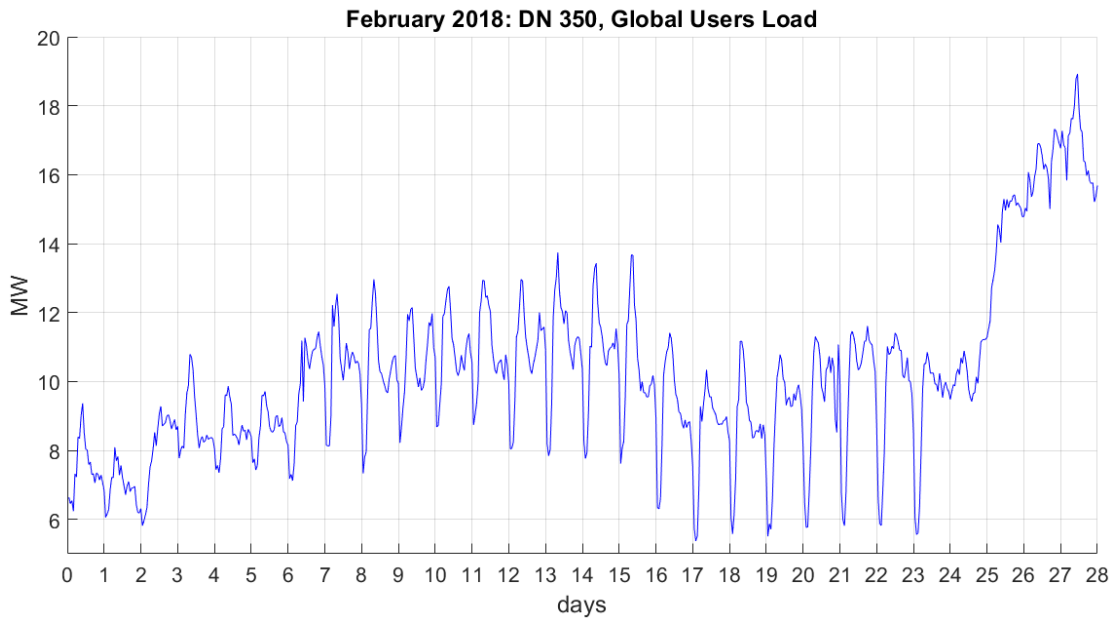


Figure 7. 2: DN 350, Users Load, Scenario 1

This first scenario intends to clarify if it is possible to recover heat on the low temperature heat exchangers of the CHP units connected to the loop managed at lower temperature, heat that today is dissipated. We built a new model where each loop has its own setting parameters and its own power station.

The loop we will call DN 200 has one CHP unit (CHP 1), a hot storage tank of 500 cubic meters, and a backup boiler of 8 MWth inside the power station. The boiler works when the flow temperature goes below 130 °C.

Power Station DN 200			
1 CHP unit	Nominal th. Power	[kW]	7,987
1xBoiler	Nominal th. Power	[kW]	8,000
HST	Volume	[m ³]	500

Table 7. 1: Power Station DN 350, Scenario 1

The loop we will call DN 350 has two CHP units, (CHP 2 and CHP 3) a hot storage tank of 500 cubic meters and a backup boiler of 16 MWth inside the power station. The boiler works when the flow temperature goes below 90 °C.

As we can see in Figure 7. 3 for the substations that previously contained two users fed separately by DN 200 and by DN 350, we have added both the loads to the user of the DN 350.

Substation	Chamber	ID User node	DN
<i>PG 33</i>	1	54	350
<i>PG 360</i>	3	22	350
<i>PG 118</i>	7	23	350
<i>PG 107</i>	9.1	125	200
<i>PG 107</i>	9.1	225	350
<i>PG 327</i>	9.1	228	350
<i>Molo E</i>	9.1	27	350
<i>PG 296</i>	9	1229	350
<i>PG 009</i>	11	233	350
<i>PG 319</i>	11	234	350
<i>PG 359</i>	11	2359	350
<i>PG 010</i>	12	35	350
<i>PG 344</i>	13	237	350
<i>T1</i>	14	155	200
<i>PG 307</i>	E	241	350
<i>PG 309</i>	E	242	350
<i>PG Hilton</i>	17	43	350
<i>PG 21</i>	22	47	350
<i>PG 117</i>	22	49	350
<i>PG 11</i>	24	51	350
<i>PG 298</i>	6	53	350

Table 7. 3: Users identification data, Network Two Temperatures, Scenario 1

The DN 200 is globally 8,792 meters long, considering flow and return, because we closed, and we did not consider, all the branches that previously connected this ring to the users that in this configuration are not fed anymore by the DN 200. The DN 350 is globally 16,670 meters long, considering flow and return.

The DN 350 consists of 2 source nodes, 19 user nodes, 33 mixing nodes, 53 pipes. The DN 200 consists of 2 source nodes, 2 user nodes, 21 mixing nodes, 24 pipes.

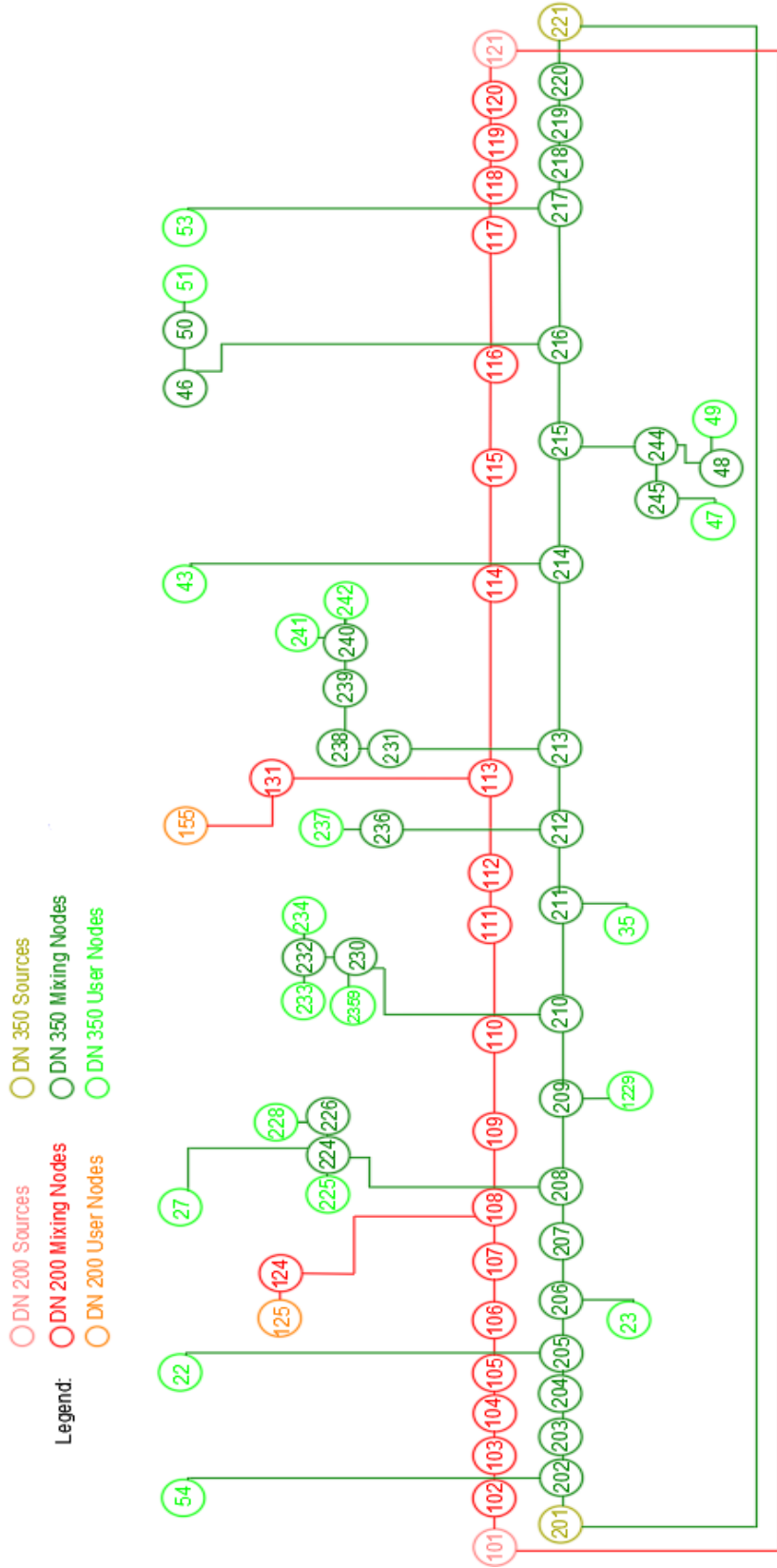


Figure 7. 4: Two Temperatures Network, linearized representation, Scenario 1

As far as the backup boilers, we do not pass their measured heat power to the model any longer but we modelled a simplified traditional gas boiler that is ON only when the flow temperature of the network goes below the reference temperature of the network.

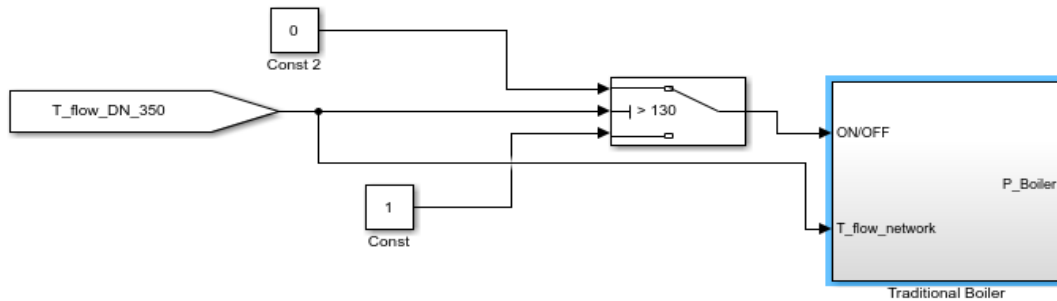


Figure 7. 5: Boiler scheme, Scenario 1

A PI control manages the heat power placed into the network according to the flow temperature of the network at the generic time step.

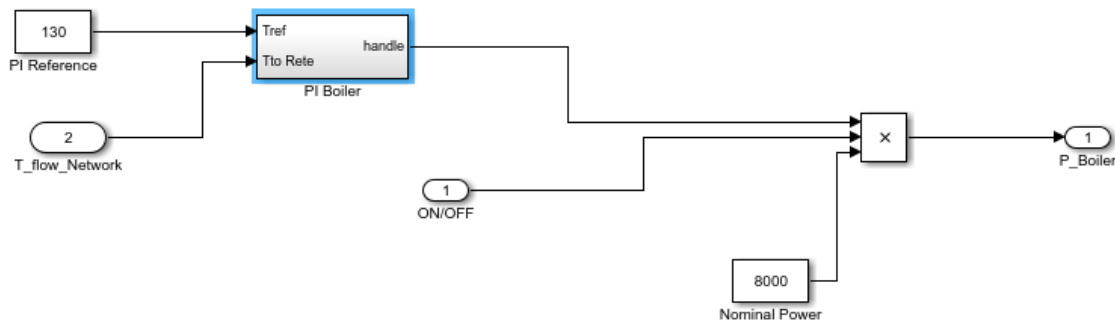


Figure 7. 6: PI of the DN 200 Boiler, Scenario 1

When the boilers are ON, their reference temperature becomes the reference temperature of the network (130 °C-90°C). In this way the flow temperature cannot go below 130 °C and cannot rise above 140 °C in the DN 200, whereas the limits in the DN 350 are 90°C and 103°C. The limits of the DN 350 have been imposed to 90 °C and to 103 °C, since the PI controllers of the network dissipater and of the backup boiler gave a convergence problem when we fixed the limits to 90 °C and 100 °C.

7.2 Simulation Results of scenario ‘Two Temperatures Network’

In this section we are going to see the simulation results of scenario ‘Two Temperatures Network’. As we can see in Figure 7. 7, the flow temperatures are in the ranges we want (140 °C-130 °C and 100 °C-90 °C) and their profiles are quite regular, with brief moments, from the 20th to the 22nd day and from the 25th to the 28th day, in which the flow temperature of the DN 350 goes below the lower limit and the boiler switches ON. As well as for the DN 200, during the first day and from the 3rd to the 6th day, Figure 7. 14. The instability on the 22nd day on the DN 350 is generated by the sudden switching ON of the third CHP, Figure 7. 17

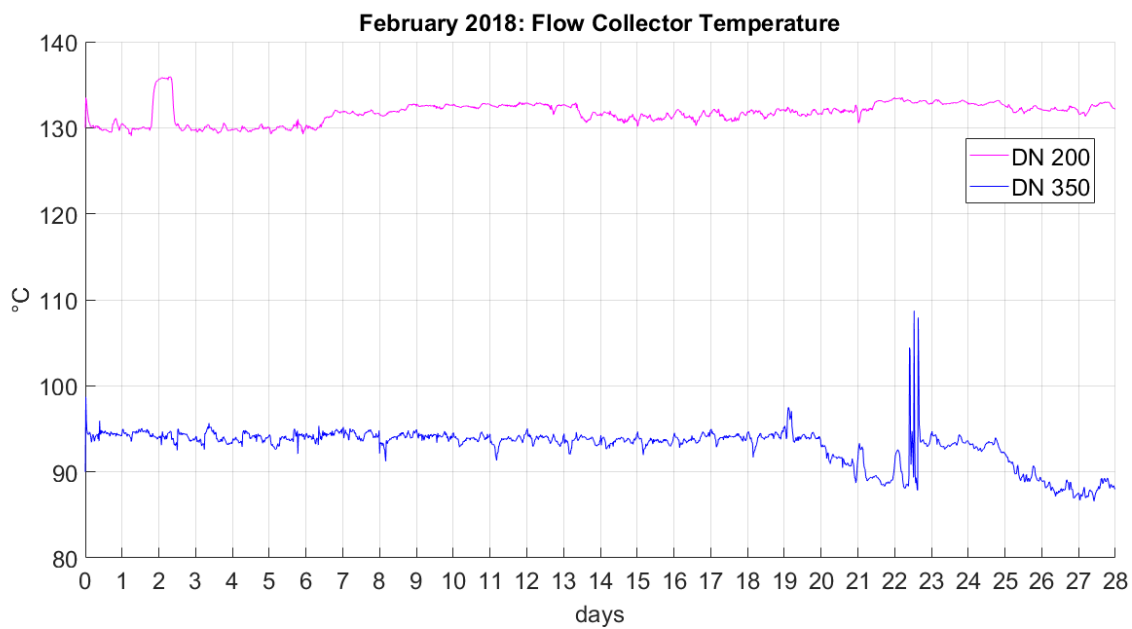


Figure 7. 7: Flow collector temperature, Scenario 1

Average flow Temperature, DN 200	[°C]	131.7
Average flow Temperature, DN 350	[°C]	93.0

Table 7. 4: Flow collector temperature, Scenario 1

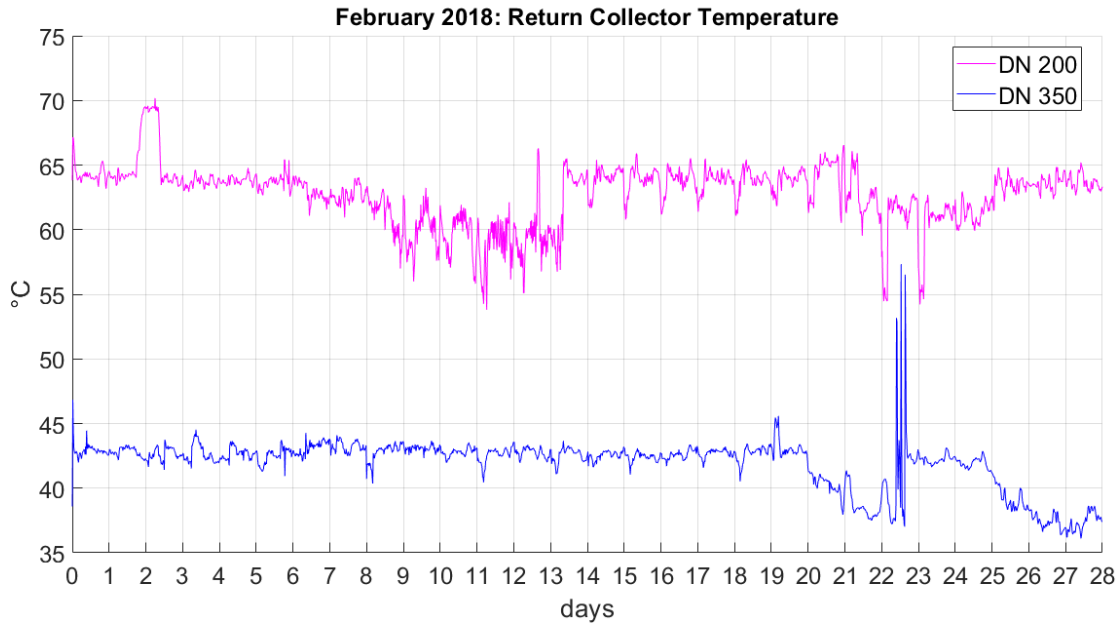


Figure 7. 8: Return collector temperature, Scenario 1

Average Return Temperature, DN 200	[°C]	62.7
Average Return Temperature, DN 350	[°C]	41.9

Table 7. 5: Return collector temperature, Scenario 1

As we would expect, the return temperature of the DN 350 is below 57 °C for most of the month, it means that it is possible to recover heat from the low temperature heat exchangers of the CHP units coupled with the DN 350.

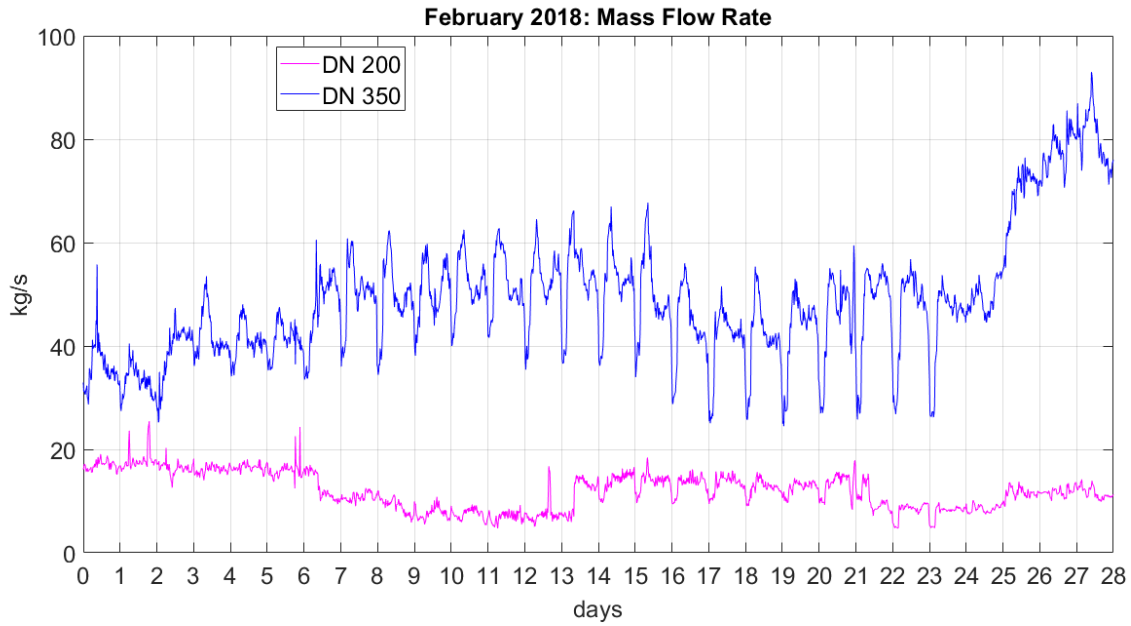


Figure 7. 9: Mass flow rate, Scenario 1

The mass flow rate flowing inside the DN 350 is bigger than inside the DN 200, since the load of the DN 350 is higher.

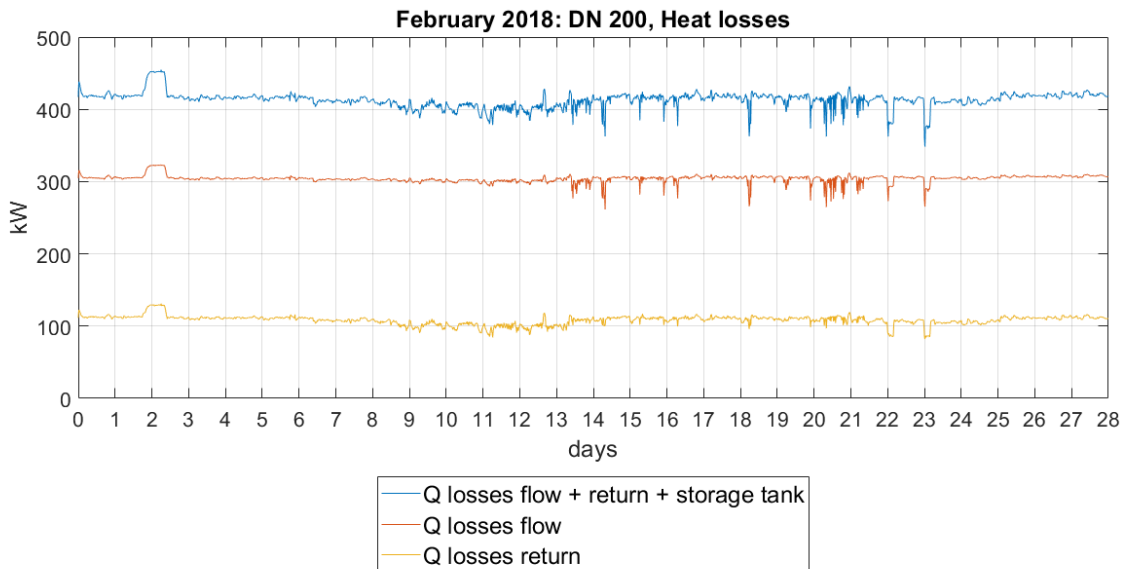


Figure 7. 10: Network heat losses, DN 200, Scenario 1

Global Heat losses (Flow+Return+HST), DN 200	<i>MWh</i>	278
Heat Distribution Losses, DN 200	<i>MWh</i>	277.5
Heat losses HST DN 200	<i>MWh</i>	0.5
Average Global Heat losses, DN 200	<i>kW</i>	410
SpecificNetwork Heat losses DN 200	<i>W/m</i>	47

Table 7. 6: Network heat losses, DN 200, Scenario 1

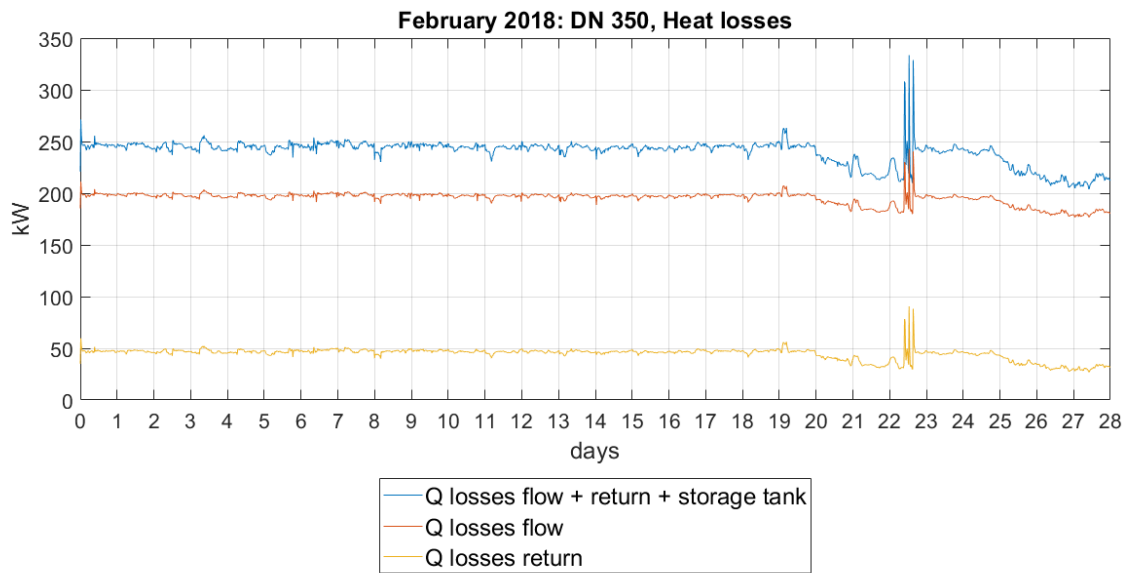


Figure 7. 11: Network heat losses, DN 350, Scenario 1

Global Heat losses (Flow+Return+HST) DN 350	<i>MWh</i>	161
Heat Distribution Losses (Flow+Return), DN 350	<i>MWh</i>	160.9
Heat losses HST DN 350	<i>MWh</i>	0.1
Average Global Heat losses, DN 350	<i>kW</i>	240
Network Heat losses DN 350	<i>W/m</i>	14.4

Table 7. 7: Network heat losses, DN 200, Scenario 1

As we can see in Table 7. 6 and in Table 7. 7 the global heat losses of the DN 350 are smaller than the global heat losses of the DN 200, 42 % less, even if the DN 350 is almost twice as long as the DN 200.

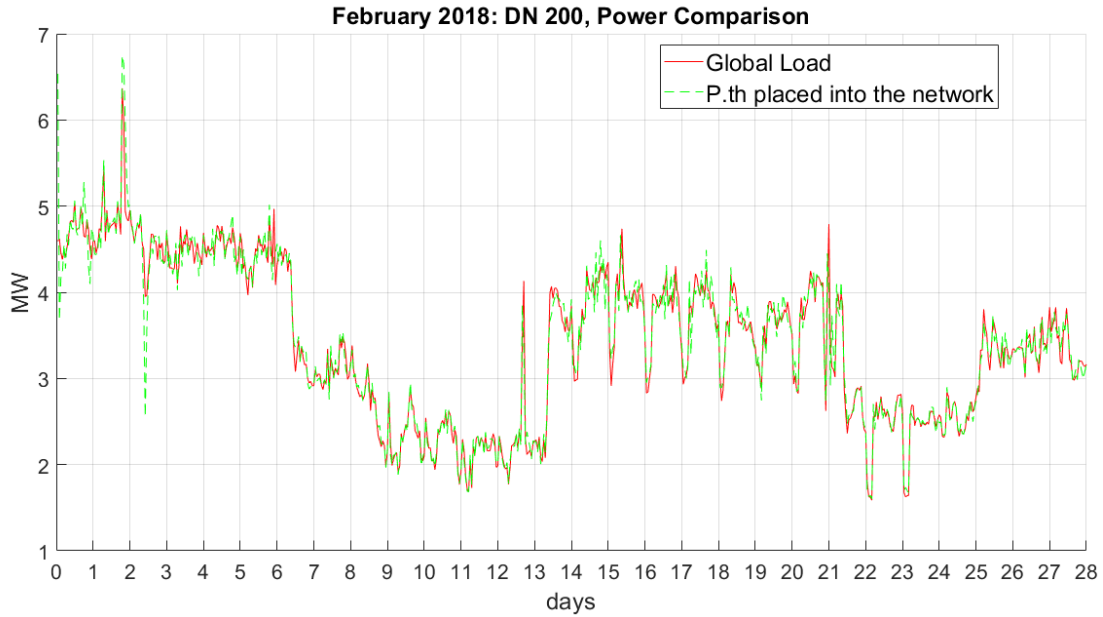


Figure 7. 12: Power Comparison in the Power Station, DN 200, Scenario 1

Energy Produced in PS, DN 200	<i>MWh</i>	3,112
Global Load, DN 200	<i>MWh</i>	2,304
Energy placed into the Network, DN 200	<i>MWh</i>	2,305
Average th. Power Produced in PS, DN 200	<i>MW</i>	4.6
Average Global Load, DN 200	<i>MW</i>	3.4
Average th. Power placed into the Network, DN 200	<i>MW</i>	3.4

Table 7. 8: Comparison in the Power Station, DN 200, Scenario 1

Thanks to the proper setting of the network dissipaters, the thermal Power placed into the network follows the load very well, both in the DN 200 and in the DN 350, as we can see in Figure 7. 12, Figure 7.

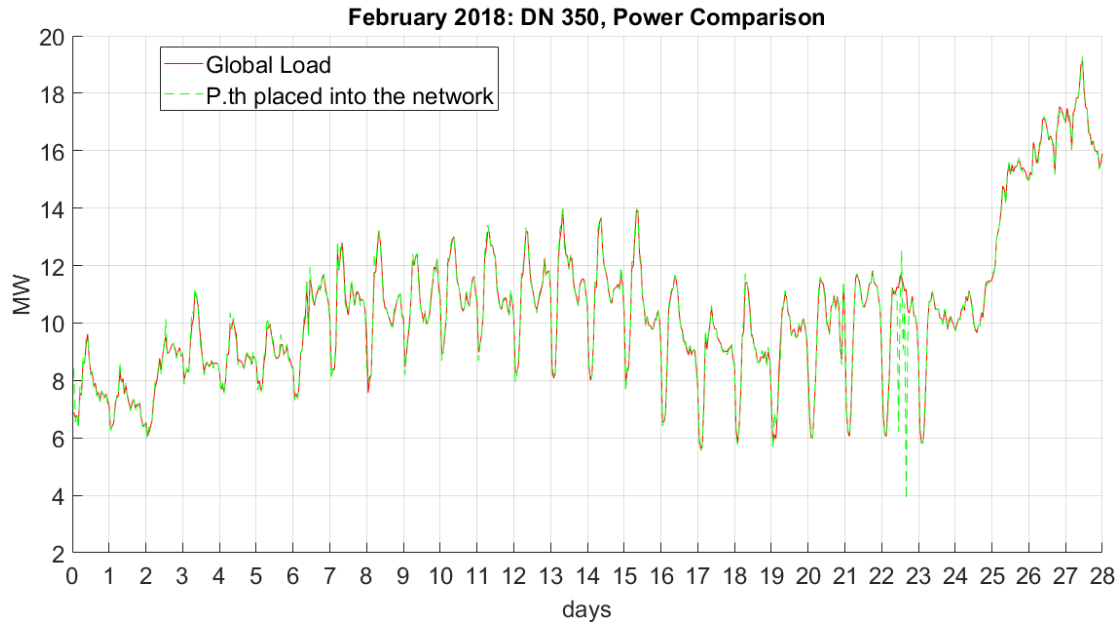


Figure 7. 13: Power Comparison in the Power Station, DN 350, Scenario 1

Energy Produced in PS, DN 350	<i>MWh</i>	8,304
Global Load, DN 350	<i>MWh</i>	7,040
Energy placed into the Network, DN 350	<i>MWh</i>	7,024
Average th. Power Produced in PS, DN 350	<i>MW</i>	12.0
Average Global Load, DN 350	<i>MW</i>	10.5
Average th. Power placed into the Network, DN 350	<i>MW</i>	10.5

Table 7. 9: Energy Comparison in the Power Station, DN 350, Scenario 1

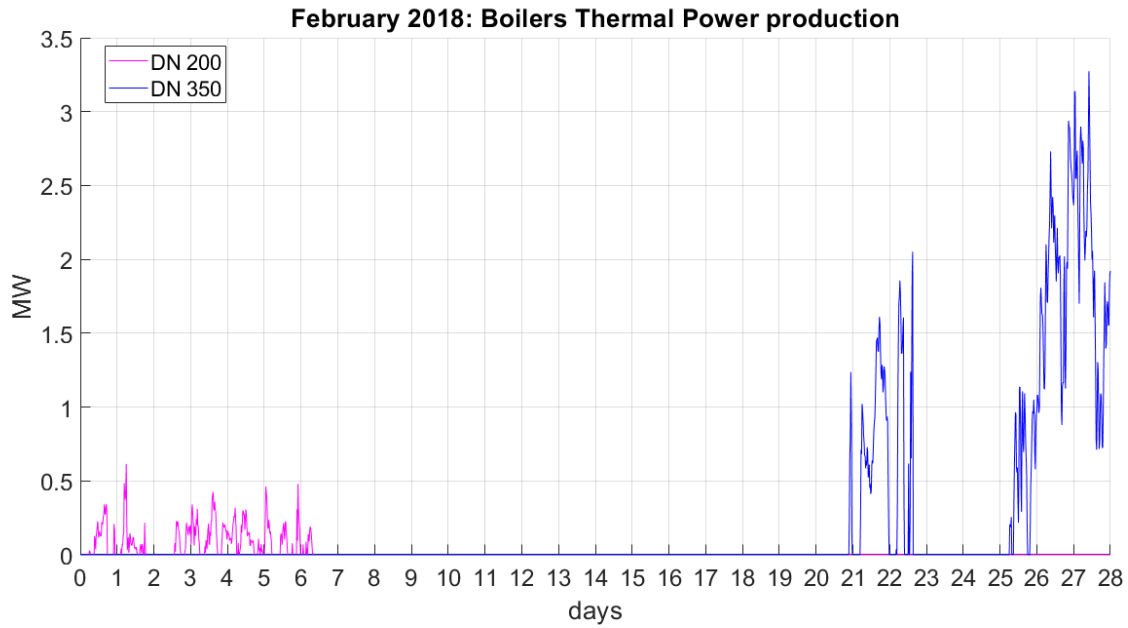


Figure 7. 14: Boilers Thermal Power production, Scenario 1

Energy produced by Boiler DN 200	<i>MWh</i>	13.3
Energy produced by Boiler DN 350	<i>MWh</i>	130

Table 7. 10: Boilers Thermal Energy production, Scenario 1

The boilers work to keep the flow temperatures above the lower limits. In particular, the boiler supplying the DN 200 is ON during the first day and from the 3rd to the 6th day, whereas the boiler supplying the DN 350 is ON from the 21st to the 22nd day, and from the 25th to the 28th day.

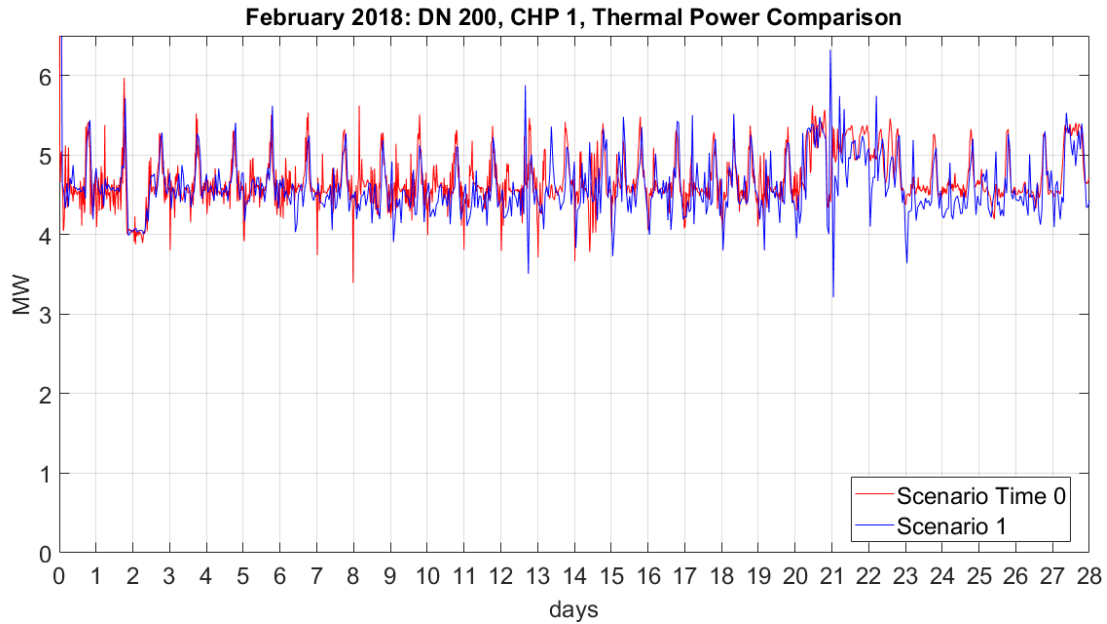


Figure 7. 15: CHP 1, thermal Power comparison, Scenario 1

Average th. Power , CHP 1, Time 0	<i>MW</i>	4.7
Average th. Power , CHP 1	<i>MW</i>	4.6
Energy produced, CHP1, Time 0	<i>MWh</i>	3,150
Energy produced, CHP1	<i>MWh</i>	3,099
Energy Difference	<i>MWh</i>	51
Energy Difference	<i>%</i>	1.6

Table 7. 11: CHP 1, thermal comparison, Scenario 1

As we would expect for CHP 1, being connected to the ring at high temperature (DN 200), it does not have heat recovery from its low temperature heat exchanger and its results are very similar to the ones of scenario Time 0.

In Figure 7. 16 and in Figure 7. 17 we will see that on average the CHP units coupled with DN 350 can recover more than 1 MW from the low temperature heat exchangers, compared to the simulation at Time 0.

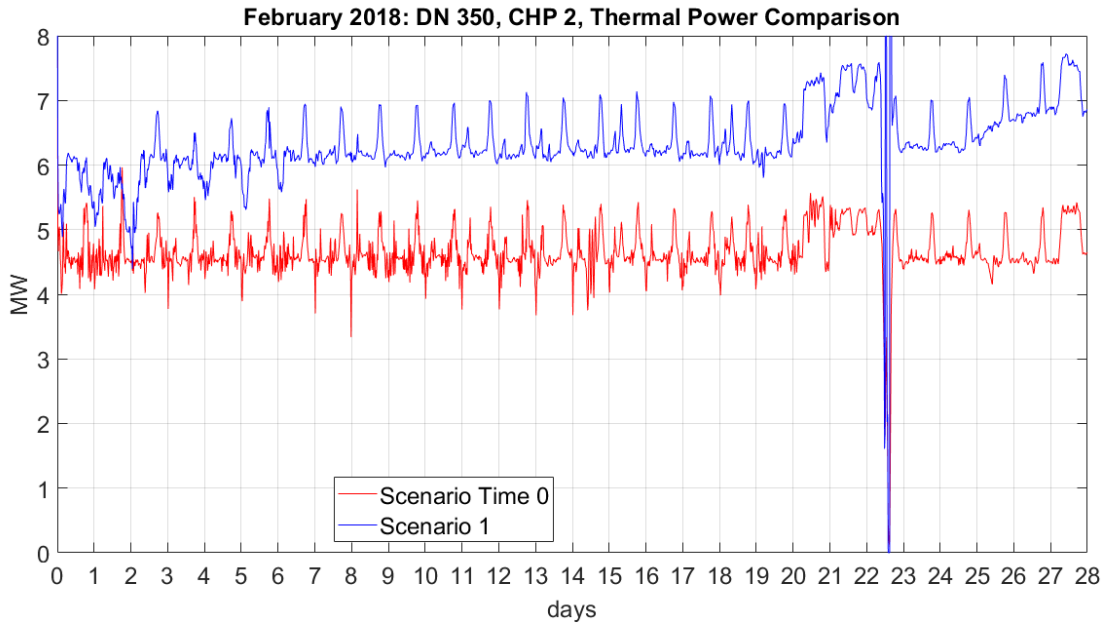


Figure 7. 16: CHP 2, thermal Power comparison, Scenario 1

Average th. Power , CHP 2, Time 0	<i>MW</i>	4.7
Average th. Power , CHP 2	<i>MW</i>	6.4
Energy produced, CHP2, Time 0	<i>MWh</i>	3,126
Energy produced, CHP2	<i>MWh</i>	4,289
Energy difference	<i>MWh</i>	1,163
Energy difference	<i>%</i>	37

Table 7. 12: CHP 2, thermal Energy comparison, Scenario 1

The second CHP unit can produce 37 % more thermal energy than in scenario Time 0.

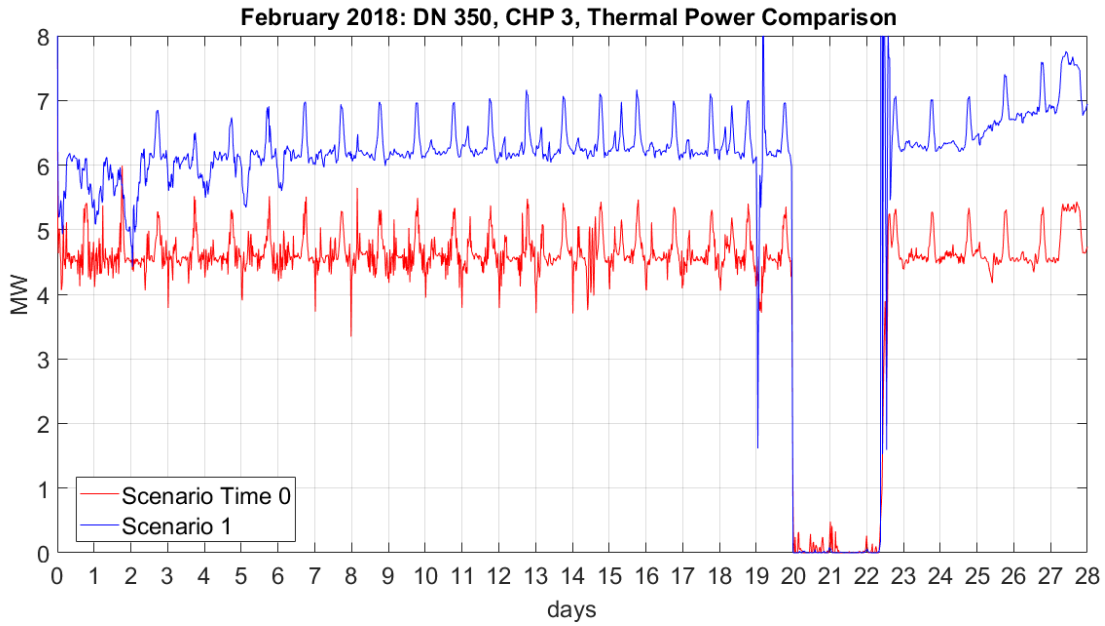


Figure 7. 17: CHP 3, thermal Power comparison, Scenario 1

Average th. Power , CHP 3, Time 0	<i>MW</i>	4.2
Average th. Power , CHP 3	<i>MW</i>	5.8
Energy produced, CHP3, Time 0	<i>MWh</i>	2,853
Energy produced, CHP3	<i>MWh</i>	3,885
Energy difference	<i>MWh</i>	1,032
Energy difference	<i>%</i>	36

Table 7. 13: CHP 3, thermal Energy comparison, Scenario 1

The third CHP unit can produce 36 % more thermal energy than in scenario Time 0. It is not possible to recover all the recoverable heat (about 2 MW) in the low temperature heat exchangers of the CHP units coupled with the DN 350, since the return temperature of the MFR in the power station, the one exchanging thermal power with the LT heat exchangers inside the CHP units, is higher than 43 °C for most of the month, temperature at which the heat recovery would be total, Figure 7. 18.

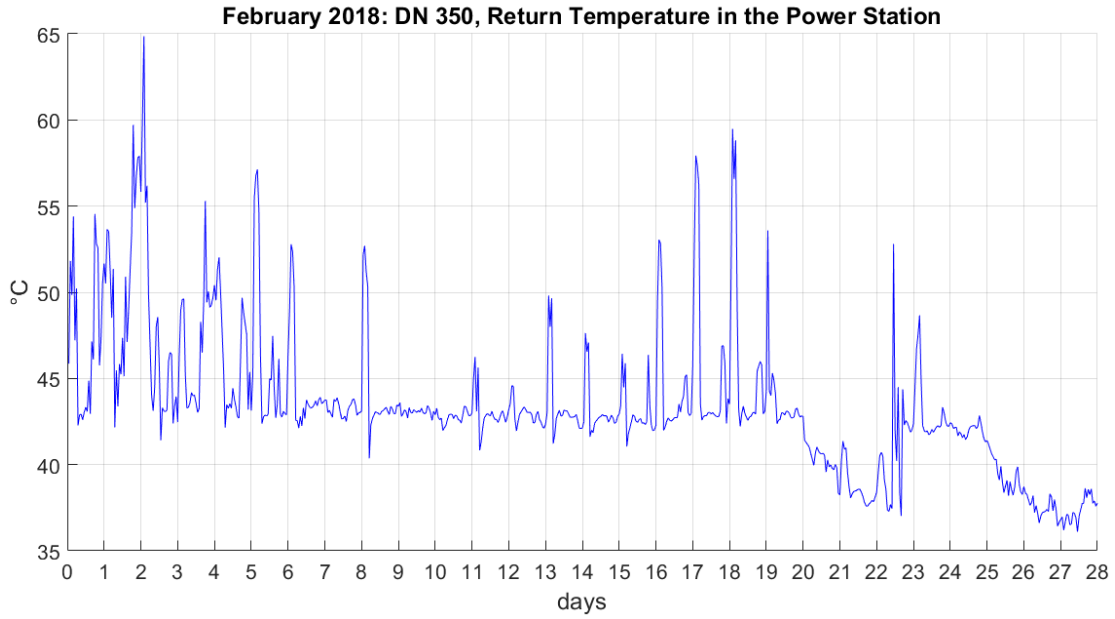


Figure 7. 18: Return temperature in the Power Station, DN 350, Scenario 1

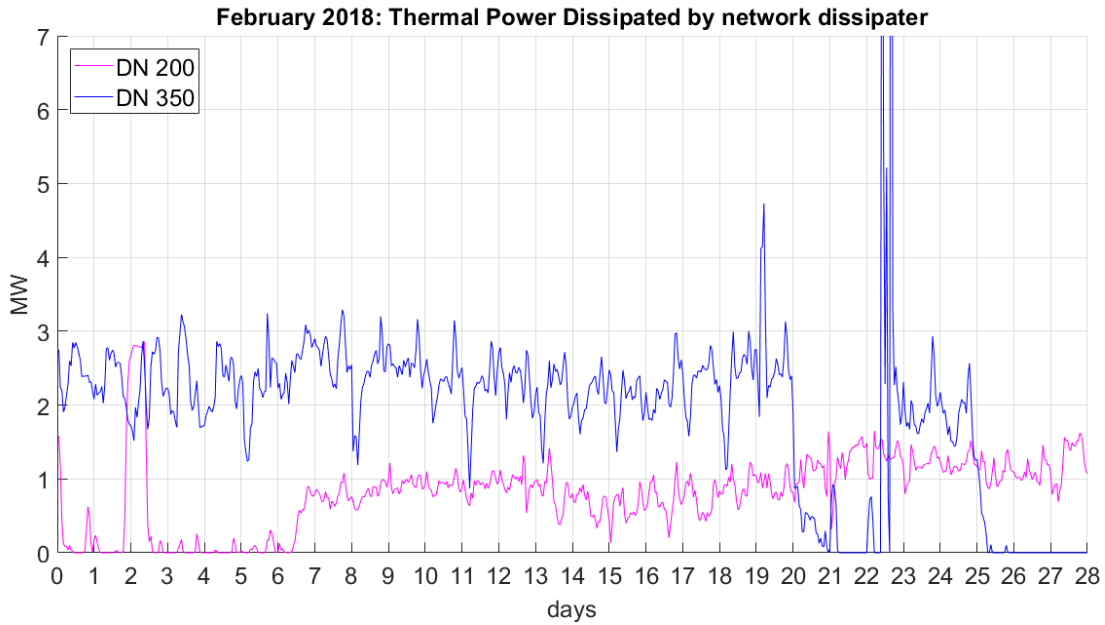


Figure 7. 19: Power dissipated by the network dissipaters, Scenario 1

Energy Dissipated by Network Dissipater, DN 200	<i>MWh</i>	619
Energy Dissipated by Network Dissipater, DN 350	<i>MWh</i>	1,259

Table 7. 14: Energy dissipated by the network dissipaters, Scenario 1

As we can see in Figure 7. 19, the DN 350 network dissipater dissipates a relevant quantity of heat, about 15 % of the thermal energy produced in its power station, because of the excess heat produced with reference to the user load.

In this chapter we have seen that, for the loop at low temperature, DN 350, the most part of the thermal energy recovered from the low temperature heat exchanger of the CHP units is dissipated inside the network dissipater, exactly 58 %. Whereas we have seen that one CHP unit is enough to feed the load of the DN 200.

	Time 0	Scenario 1	
		DN 350	DN 200
	<i>MWh</i>	<i>MWh</i>	<i>MWh</i>
Users Load	8,903	6,878	2,025
Global Heat Losses	713	161	278
Energy Placed into the Network	9,609	7,024	2,305
Energy Produced by CHP	9,129	8,174	3,099
Heat Recoverd by the CHP	/	2,195	0
Boilers Heat Production	657	130	13
Energy Produced in the P.S.	9,786	8,304	3,112
Energy Dissipated in the HST Dissipater	0.6	6.0	190
Energy Dissipated in the Network Dissipater	169	1,259	619

Table 7. 15: Simulation Energy Results, Scenario 1

Chapter 8: Scenario 2: Two Temperatures Network with Dissipated Heat Recovery by the Installation of Absorption Chillers

8.1 Brief Introduction to scenario ‘Two Temperatures Network with Dissipated Heat Recovery’

In this section we will show the results of the simulation of the DH network managed with two separated loops at different temperatures. We added two new users to the DN 350; users representing the single stage absorption chillers ADR would install, with a nominal cooling power of 3 MW each. The Power Stations of the DN 350 and of the DN 200 are the same as scenario 1. The new loads are localized where ADR would install the cooling machines, inside substation PG 327 (chamber 9.1), new user node n.327, and inside substation PG 319 (chamber 11), new user node n.319.

The load profile of the single stage absorption chillers, installed on the loop at low temperature, was obtained dividing the heat dissipated by the network dissipater of the DN 350 of the previous efficiency scenario (Network with two rings at different temperatures, scenario 1) for the nominal thermal power required by the machine itself.

On the Internet we found the data sheet of the single stage absorption chillers we installed in this second scenario: it is a LG Hot fired absorption chiller WC2H Series, Model 083¹¹.

Power Station DN 200			
1 CHP unit	<i>Nominal th. Power</i>	<i>[kW]</i>	7,987
Boiler	<i>Nominal th. Power</i>	<i>[kW]</i>	8,000
HST	<i>Volume</i>	<i>[m³]</i>	500

Table 8. 1: Power Station DN 350, Scenario 1

Power Station DN 350			
2 CHP units	<i>Nominal th. Power</i>	<i>[kW]</i>	2x7,987
Boiler	<i>Nominal th. Power</i>	<i>[kW]</i>	16,000
HST	<i>Volume</i>	<i>[m³]</i>	500

Table 8. 2: Power Station DN 200, Scenario 1

¹¹ LG website ([http:// www.lgeaircon.com](http://www.lgeaircon.com)) Accessed on August 02 2018, [33].

WC2H Series

Model name			047	053	060	068	075	083						
Cooling capacity		USRT	459	470	513	525	586	600	659	675	732	750	806	825
		kW	1,614	1,652	1,803	1,845	2,060	2,109	2,318	2,372	2,573	2,636	2,833	2,900
Chilled water data	Temperature	°C	12-7	13-8	12-7	13-8	12-7	13-8	12-7	13-8	12-7	13-8	12-7	13-8
	Water flow rate	m ³ /h	277.7	284.3	310.2	317.5	354.5	362.9	398.9	408.2	442.7	453.6	487.5	499.0
	Pressure drop	mAq	8.0	8.4	10.1	10.6	6.7	7.0	8.3	8.7	10.8	11.3	6.5	6.8
	Connection size	A(mm)	200	200	200	200	250	250	250	250	250	250	300	300
		B(inch)	8	8	8	8	10	10	10	10	10	10	12	12
Cooling Water Data	Temperature	°C	31.0 → 36.5											
	Water flow rate	m ³ /h	594	608	663	679	758	776	833	873	946	970	1,042	1,067
	Pressure drop	mAq	9.7	10.2	11.4	11.9	7.3	7.6	9.8	10.3	12.9	13.3	7.6	8.0
	Connection size	A(mm)	300	300	300	300	350	350	350	350	350	350	400	400
		B(inch)	12	12	12	12	14	14	14	14	14	14	16	16
Fuel	Temperature	°C	95.0 → 55.0											
	Water Flow rate	ton/h	46.9	48.0	52.4	53.6	59.9	61.3	67.4	69.0	74.8	76.6	82.3	84.3
	Pressure Drop	mAq	3.4	3.6	4.6	4.8	3.1	3.2	4.0	4.2	5.1	5.4	4.1	4.3
	Pressure Drop(Velve)	mAq	1.4	1.5	1.9	2.0	2.4	2.5	3.1	3.2	3.7	3.9	1.7	1.8
	Connection size	A(mm)	100	100	100	100	125	125	125	125	125	125	125	125
		B(inch)	4	4	4	4	5	5	5	5	5	5	5	5
	Connection size of Control valve	A(mm)	100	100	100	100	100	100	100	100	100	100	125	125
		B(inch)	4	4	4	4	4	4	4	4	4	4	5	5
Electrical data	Source	V	3ø 220/380/440V, 50Hz/60Hz											
	Total current	A	28.2	28.2	40.4	40.4	40.4	40.4	46.9	46.9	46.9	46.9	56.1	56.1
	Wire size	mm ²	8.0	8.0	14.0	14.0	14.0	14.0	22.0	22.0	22.0	22.0	22.0	22.0
	Power	kVA	18.5	18.5	26.6	26.6	26.6	26.6	30.8	30.8	30.8	30.8	36.9	36.9
	Absorbent pump no.1	kW(A)	6.7(20.0)	6.7(20.0)	8.7(27.0)	8.7(27.0)	8.7(27.0)	8.7(27.0)	10.5(33.5)	10.5(33.5)	10.5(33.5)	10.5(33.5)	11.5(37.5)	11.5(37.5)
	Absorbent pump no.2	kW(A)	1.2(4.8)	1.2(4.8)	3.0(10.0)	3.0(10.0)	3.0(10.0)	3.0(10.0)	3.0(10.0)	3.0(10.0)	3.0(10.0)	3.0(10.0)	4.0(12.0)	4.0(12.0)
	Refrigerant pump	kW(A)	0.4(1.4)	0.4(1.4)	0.4(1.4)	0.4(1.4)	0.4(1.4)	0.4(1.4)	0.4(1.4)	0.4(1.4)	0.4(1.4)	0.4(1.4)	4.0(12.0)	4.0(12.0)
	Purge pump	kW(A)	0.4(1.45)											
Dimension	Length	mm	5,540	5,540	6,035	6,035	5,680	5,680	6,180	6,180	6,705	6,705	6,340	6,340
	Width	mm	2,745	2,745	2,745	2,745	3,480	3,480	3,480	3,480	3,480	3,480	3,800	3,800
	Height	mm	3,140	3,140	3,140	3,140	3,600	3,600	3,600	3,600	3,600	3,600	3,900	3,900
Rigging	Operating	ton	28.4	28.4	30.2	30.2	37.5	37.5	39.7	39.7	42.6	42.6	47.5	47.5
	Max. shipping	ton	23.7	23.7	25.2	25.2	31.7	31.7	33.8	33.8	36.6	36.6	39.5	39.5
Clearance for tube removal		mm	5,200	5,200	5,700	5,700	5,200	5,200	5,700	5,700	6,200	6,200	5,800	5,800

Figure 8. 1: Data sheet of LG Hot fired absorption chiller WC2H Series, Model 083, [33]

In nominal condition, the absorption chillers work with a flow temperature of 95 °C, and a ΔT equal to 40 °C. This type of machine was chosen since its working conditions are compatible with the working conditions of the DN 350, that works with a flow temperature of 90-93 °C and a users' ΔT equal to 50 °C.

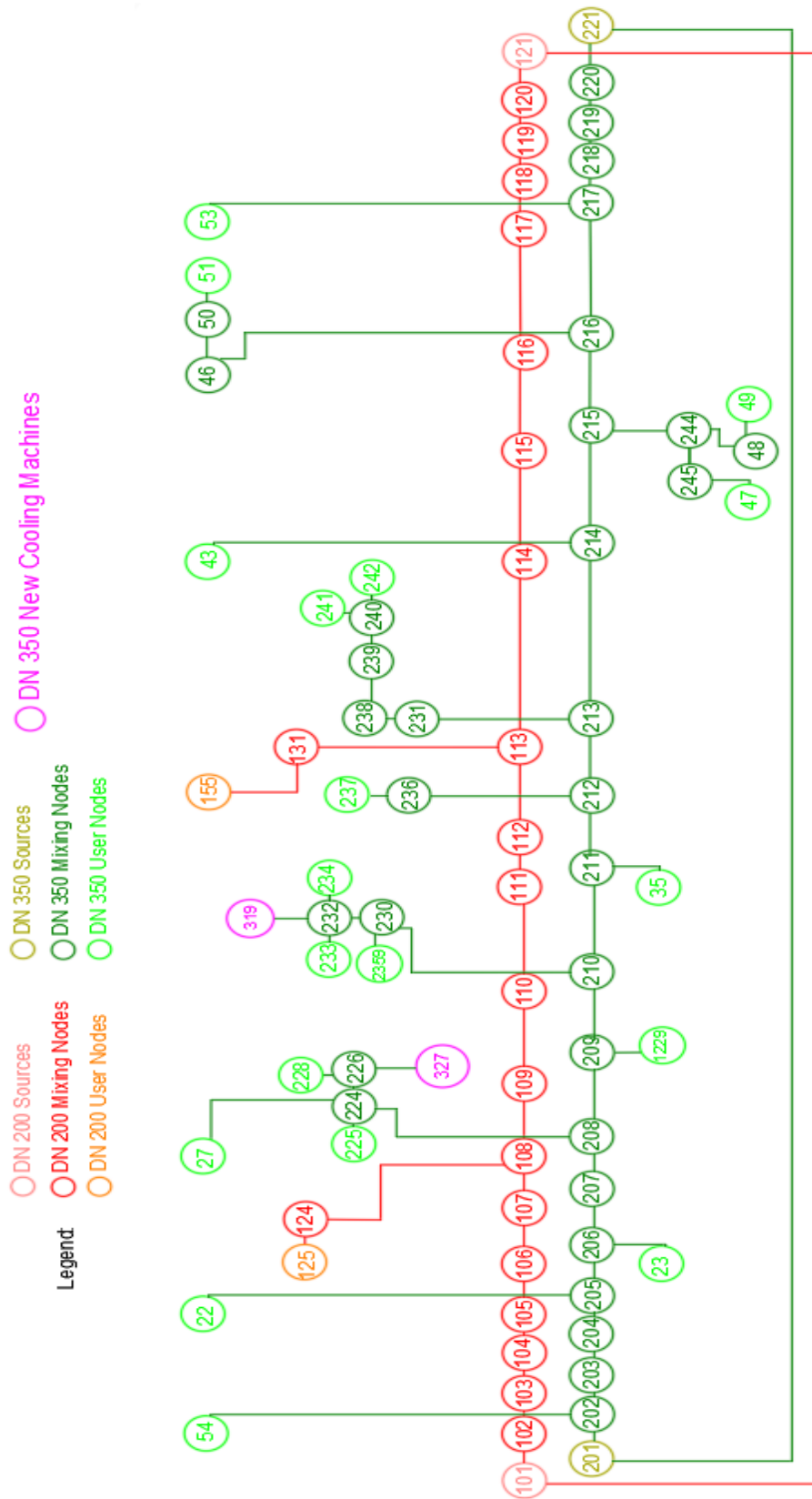


Figure 8. 3: Two Temperatures Network with new absorption Chillers, linearized representation, Scenario 2

8.2 The modelling of the Absorption Chiller

This model was created by ENEA researchers and this is the first time it is applied to the ENSim platform. The model receives the flow temperature at the user node, where the absorption chiller is localized, and the thermal load profile of the machine as input. It gives the cooling power produced as output, computed by a COP map, depending on the flow temperature at the user node, that multiplies the thermal load required. It also gives the heat dissipated by the cooling tower as output, computed as the sum of the thermal load required and the cooling power produced.

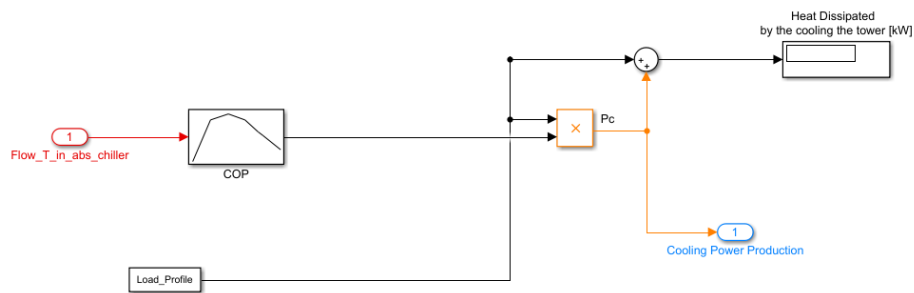


Figure 8. 4: Absorption Chiller model, Scenario 2

8.3 Calibration analysis and simulation results

In this section we will show how we built the load profile of the absorption chillers we gave to the model as input. First of all, we have to say that the load profile is supposed to be equal for the cooling machine in PG 327 and for the one in PG 319. For this reason, we halved the profile of the heat dissipated by the network dissipater in the first efficiency scenario. Then we divided the profile obtained by the nominal thermal power required by the machine (3,921 kWth), value taken from the data sheet showed above. Afterwards we normalized to 1 each value of the profile higher than 1. In the end, we multiplied the profile obtained at the previous step for the nominal thermal power required by the machine. We could not pass this load profile to the model directly, since adding new loads the heat losses along the network would have increased, and this would have caused the increasing energy consumption of the backup boiler to keep the flow temperature of the loop at low temperature at 90 °C. For this reason, we made a calibration analysis, it means that we simulated this second scenario multiplying the load profile of the chillers for a coefficient that decreased the load itself (1, 0.9, 0.8...) till the thermal energy produced by the boiler of the DN 350 was more or less equal to the energy produced by the boiler of the DN 350 of the first efficiency scenario, that we will call scenario 'No Chillers'.

8.3.1 Calibration analysis of the Absorption chillers loads

In this section we are going to see the results of the calibration analysis made to decide which load to give to the model for the absorption chillers as input. This load is equal for the cooling machines we want to install in PG 319 and in PG 317, and it was obtained from the profile of the heat dissipated by the network dissipater of the DN 350 of the first efficiency scenario. As we can see in Figure 8. 5 , the cooling production increases at the increasing of the F coefficient, for which we multiplied the thermal load profile of the chillers.

We show only the cooling power produced in PG 319, because in PG 307 the cooling power production profile is the same.

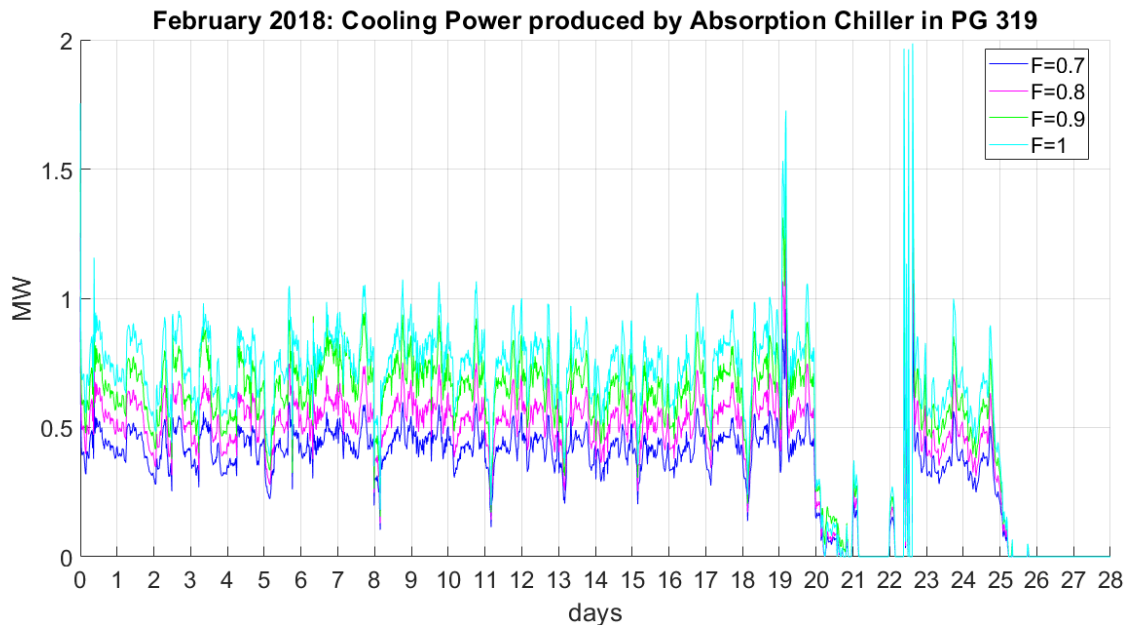


Figure 8. 5: Cooling power produced in PG 319, Scenario 2

	Cooling Energy produced		Thermal Energy required by a single chiller
	MWh	MWh	MWh
	n.319	n.327	/
F=0.7	231	229	352
F=0.8	289	287	440
F=0.9	357	354	541
F=1	408	405	616

Table 8. 3: Cooling energy produced and thermal energy required by absorption chillers, Scenario 2

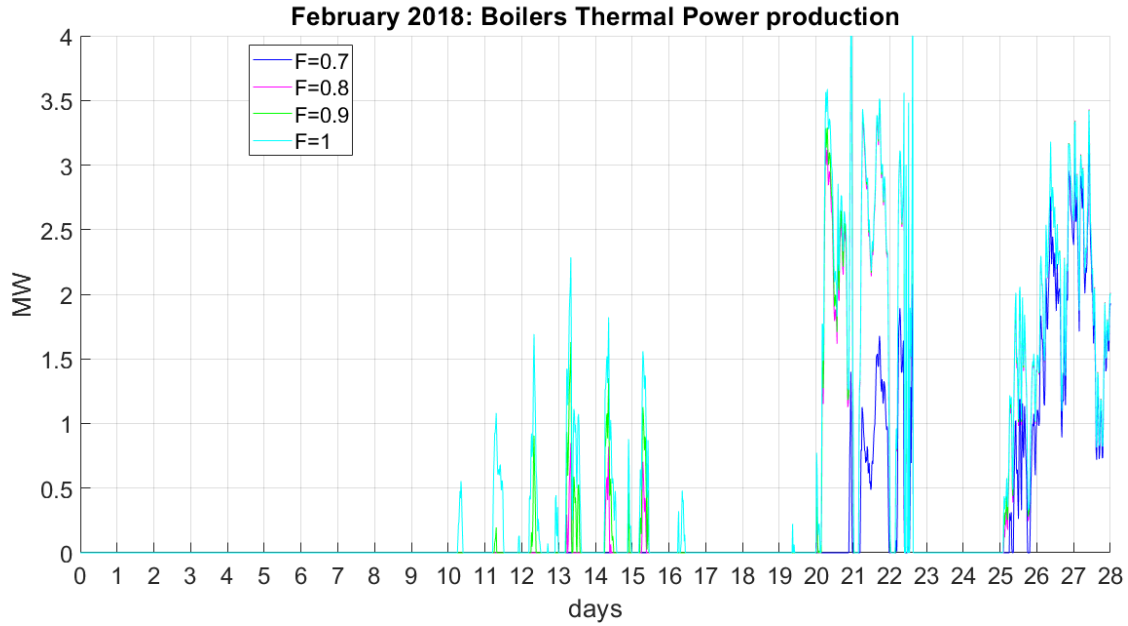


Figure 8. 6: Boilers thermal power produced, DN 350, Scenario 2

Increasing the load of the network, increasing the F coefficient, the boiler of the DN 350 has to place more energy into the network to keep the flow temperature at its set point (90 °C).

	DN 350, Boiler Thermal Energy Production	DN 350 Extra Thermal Energy Produced by Boiler
	<i>MWh</i>	<i>MWh</i>
Scenario No Chillers	130	/
F=0.7	251	121
F=0.8	266	136
F=0.9	293	163
F=1	317	187

Table 8. 4: Boiler energy production, DN 350, Scenario 2

In order to maximize the cooling energy produced by the chillers and to minimize the energy consumed by the boiler we compute the ratio between the extra thermal energy produced by the boiler of the DN 350, and the cooling energy produced, with reference to scenario 1, scenario 'No Chillers'.

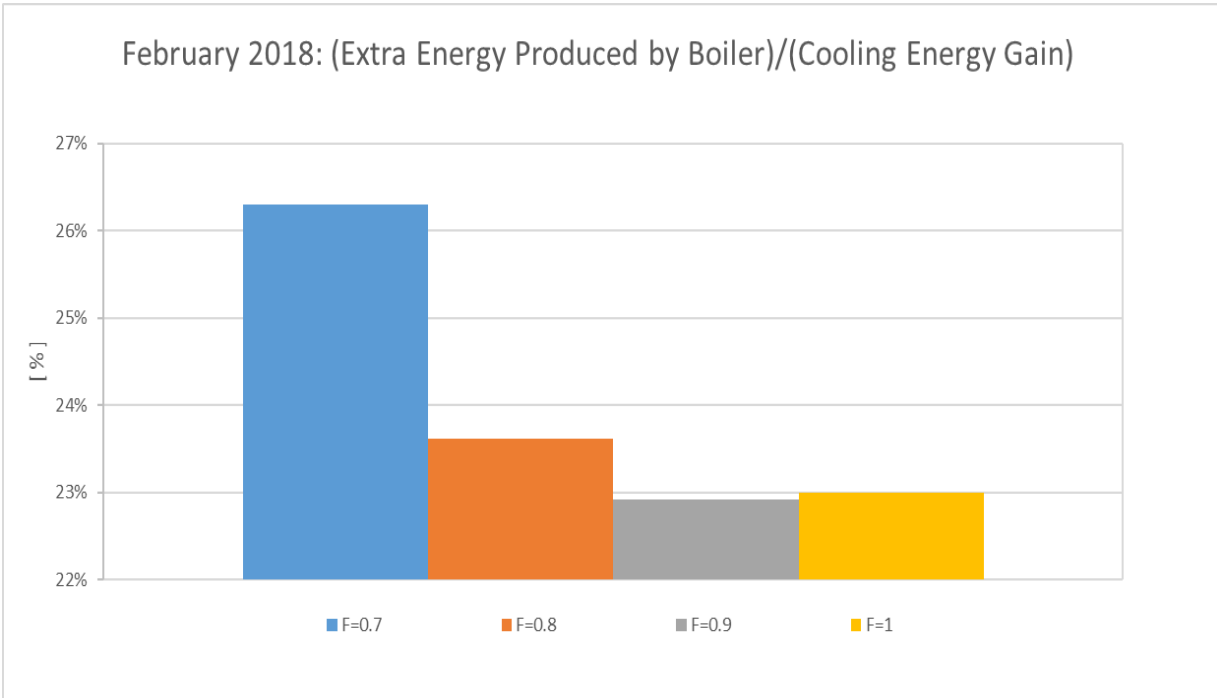


Figure 8. 7: Calibration analysis, DN 350, Scenario 2

	(Extra energy produced by Boiler)/Cooling energy gain
	%
F=0.7	26.30
F=0.8	23.61
F=0.9	22.93
F=1	23.00

Table 8. 5: Calibration analysis results, DN 350, Scenario 2

The function $f = \frac{\text{Extra energy produced by boiler}}{\text{Cooling energy produced}}$ has a minimum for F=0.9. As we can see in Figure 8. 7, multiplying the Chillers load profile by a 0.9 factor we maximize the cooling production and we minimize the utilization of the boiler of the DN 350.

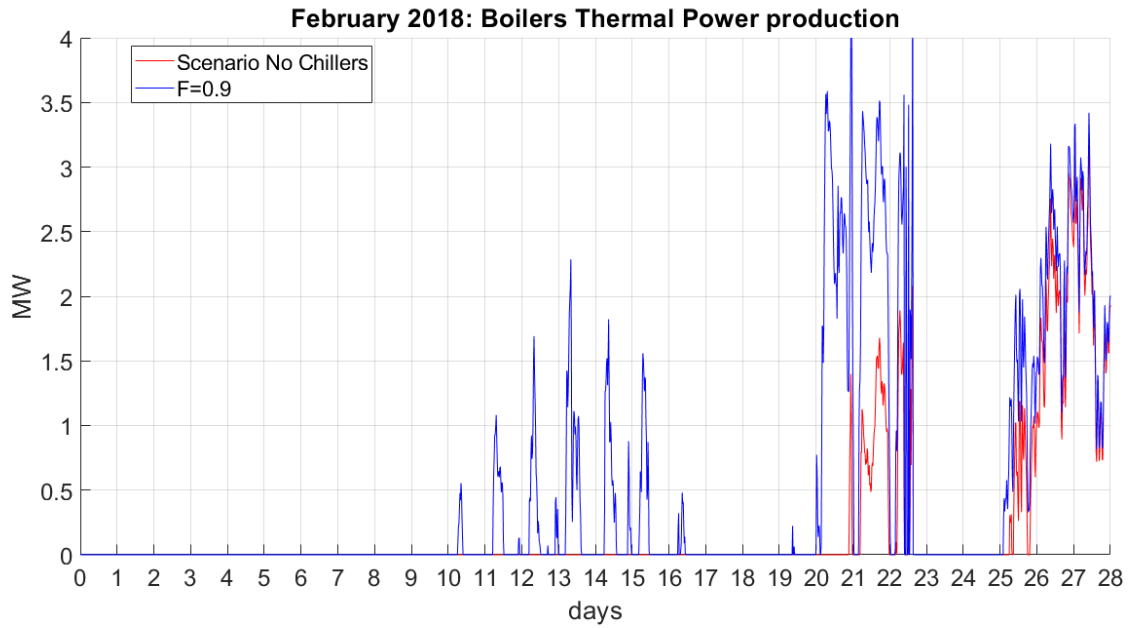


Figure 8. 8: Boilers heat power produced comparison, DN 350, Scenario 2

From the calibration analysis we found that the best coefficient for multiplying the load profile of the new absorption chillers, obtained from the heat dissipated by the network dissipater of the DN 350 of the first efficiency scenario, is equal to 0.9.

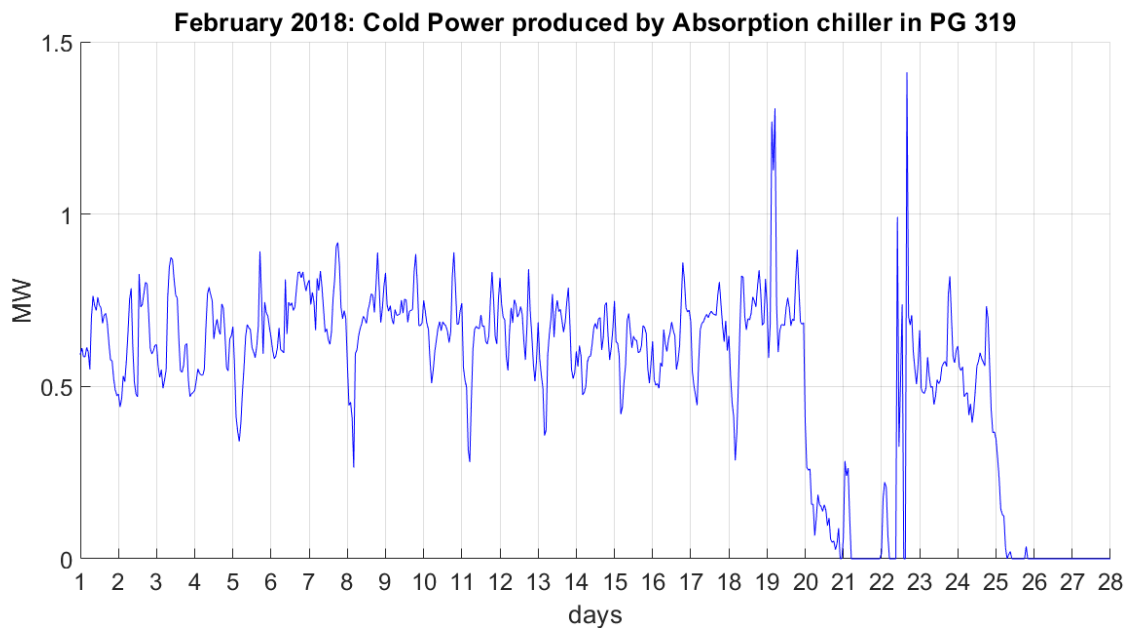


Figure 8. 9: Cooling power produced in PG 319, F=0.9, Scenario 2

8.3.2 Simulation results of scenario ‘Two Temperatures Network with Dissipated Heat Recovery by the Installation of Absorption Chillers’

In this section we are going to see the simulation results for the loop DN 350 of scenario ‘Two Temperatures Network with Dissipated Heat Recovery by the Installation of Absorption Chillers’. The load profiles of the chillers, obtained by the heat dissipated by the network dissipater of scenario 1, have been multiplied by a F coefficient equal to 0.9. We will compare the results of this second scenario with the ones of the previous efficiency scenario, scenario 1, that we will call ‘No Chillers’. We are not going to show the results of the DN 200 since they would be the same of the previous efficiency scenario, because the DN 200 was not modified.

As we would imagine, increasing the load the DN 350 has to feed, its flow temperature decreases, in particular from the 6th day till 25th.

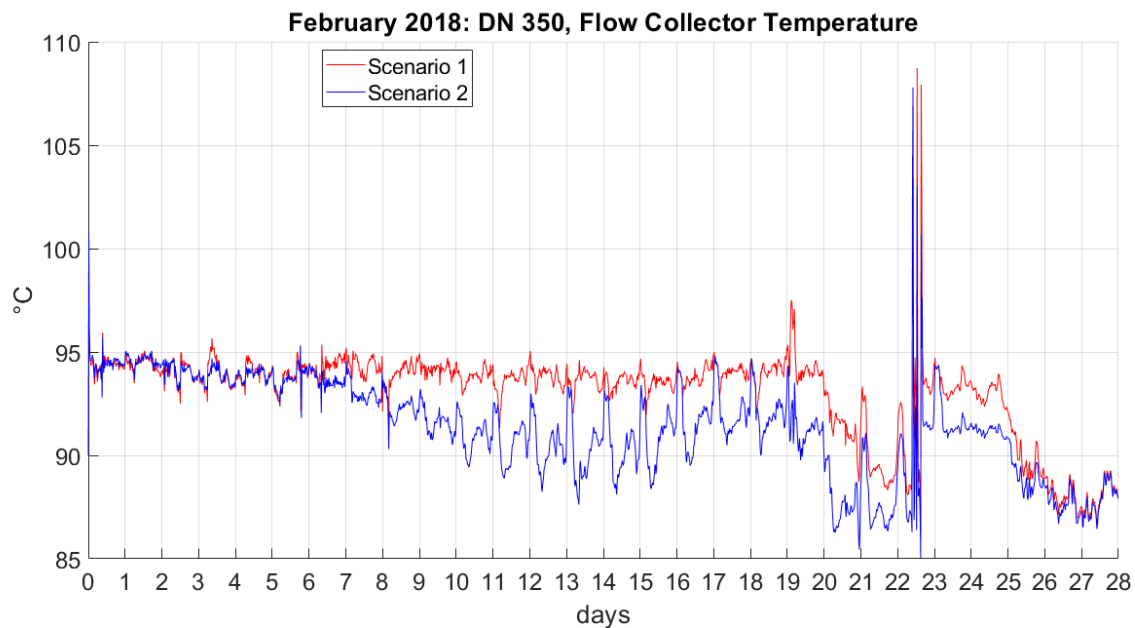


Figure 8. 10: Flow collector temperature comparison, DN 350, Scenario 2

Average flow Temperature, Scenario 2	[°C]	91.4
Average flow Temperature, Scenario 1	[°C]	93.0

Table 8. 6: Flow collector temperature comparison, DN 350, Scenario 2

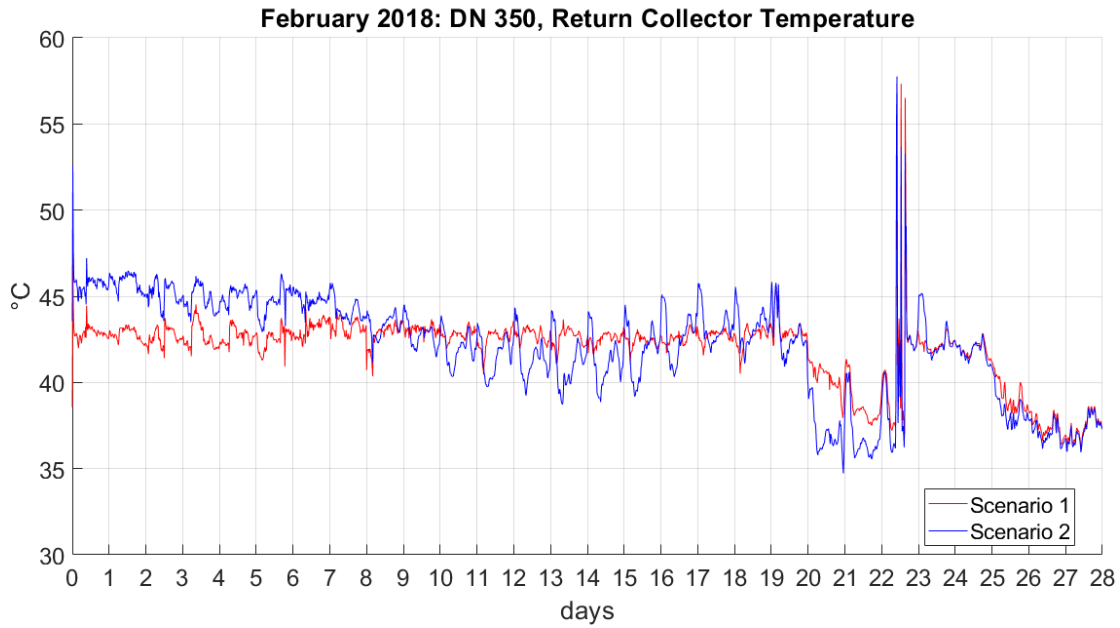


Figure 8. 11: Return collector temperature comparison, DN 350, Scenario 2

Average Return Temperature, Scenario 2	[°C]	42.1
Average Return Temperature, Scenario 1	[°C]	41.9

Table 8. 7: Return collector temperature comparison, DN 350, Scenario 2

On average, the return collector temperature is higher in the scenario with chillers, since the absorption cooling machines, that count for 14 % of the user load of the DN 350, have a lower temperature drop on their substations, 40 °C instead of 50 °C, compared to the other users of the DN 350.

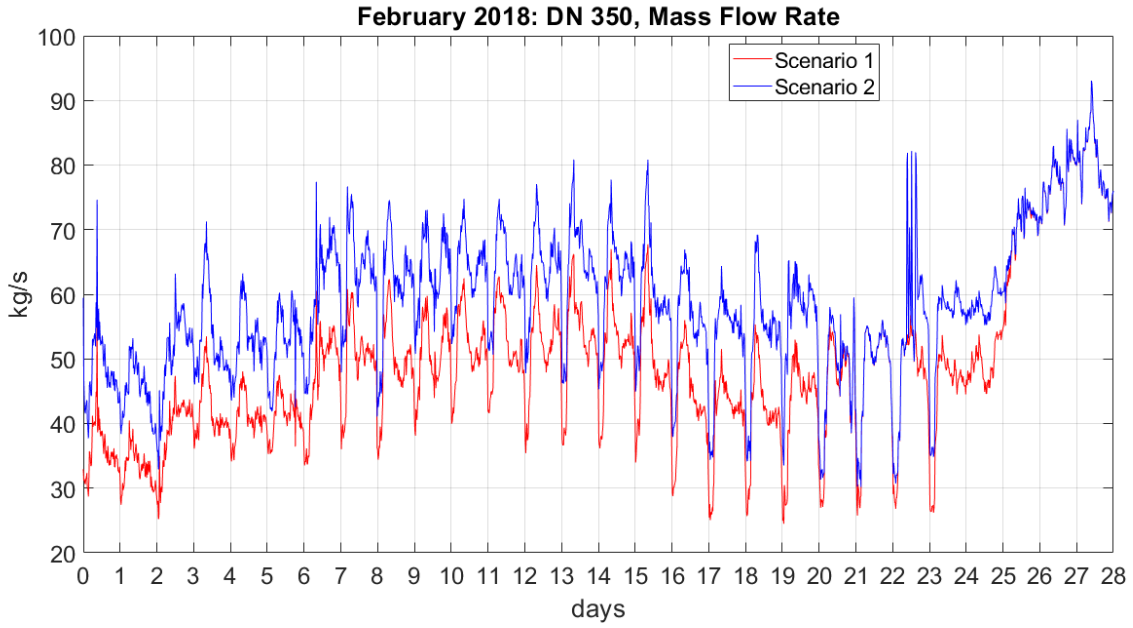


Figure 8. 12: Mass flow rate, DN 350, Scenario 2

Increasing the load of the loop at low temperature, also the mass flow rate flowing inside the DN 350 increases.

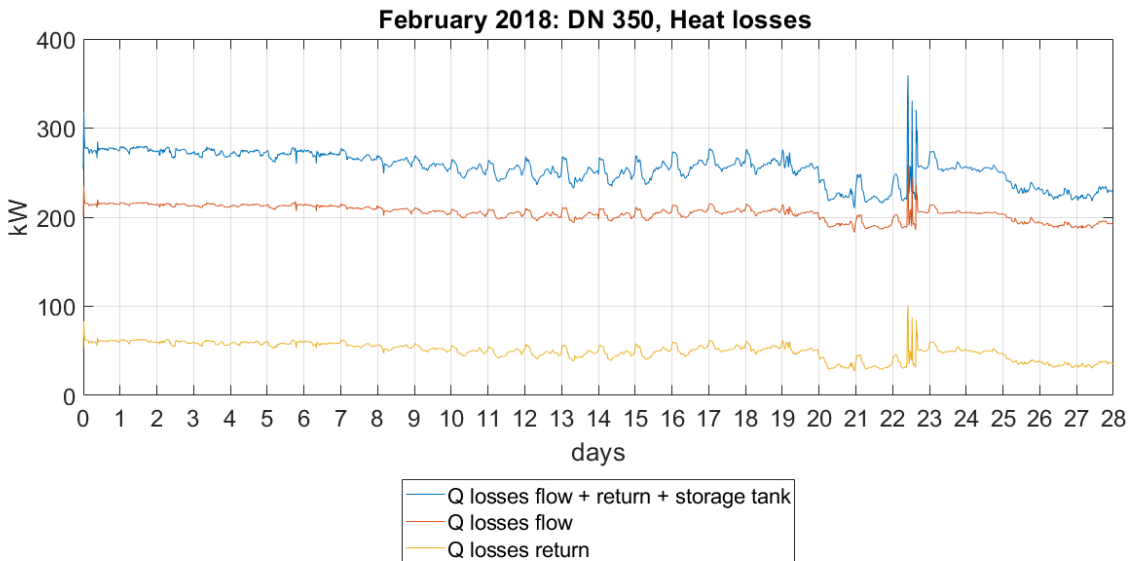


Figure 8. 13: Network heat losses, DN 350, Scenario 2

Global Heat losses (Flow+Return+HST), DN 350	<i>MWh</i>	171
Heat Distribution Losses (Flow+Return), DN 350	<i>MWh</i>	170.9
Heat losses HST, DN 350	<i>MWh</i>	0.1
Average Global Heat losses, DN 350	<i>kW</i>	250
Specific Network Heat losses, DN 350	<i>W/m</i>	14.5

Table 8. 8: Network heat losses, energy results, DN350, Scenario 2

Even adding new loads, moving from scenario 1 to scenario 2, on the DN 350 the global heat losses do not change significantly, from 161 MWh to 171 MWh, about 6%.

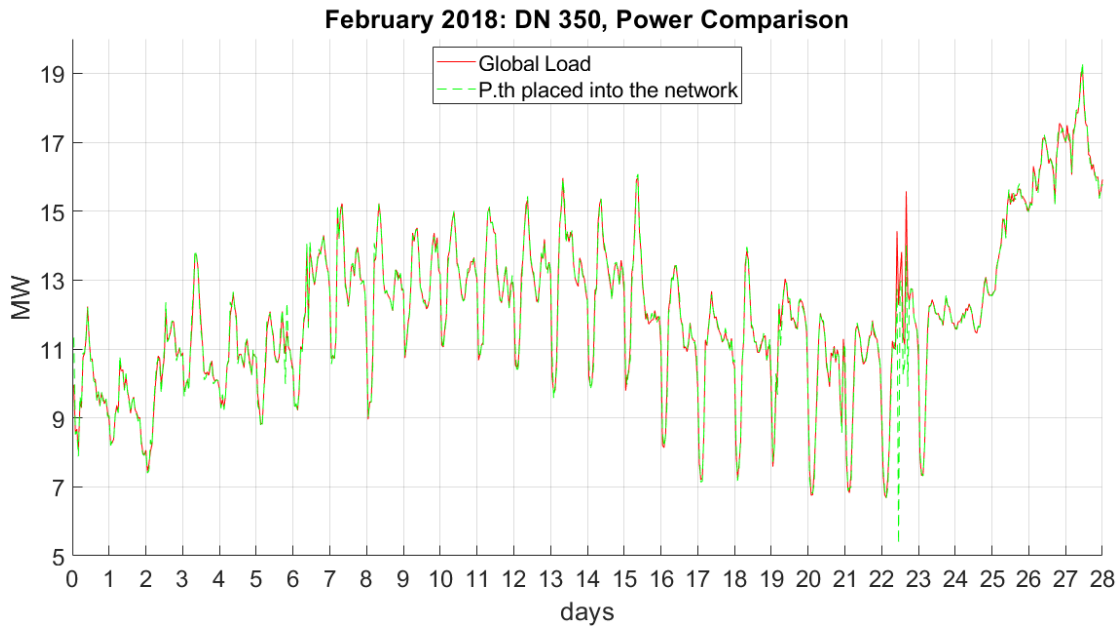


Figure 8. 14: Power Comparison in the Power Station, DN 350, Scenario 2

Average th. Power Produced in PS, DN 350	<i>MW</i>	12.7
Average Global Load, DN 350	<i>MW</i>	12.1
Average th. Power placed into the Network, DN 350	<i>MW</i>	12.1
Energy Produced in PS, DN 350	<i>MWh</i>	8,545
Global Load, DN 350	<i>MWh</i>	8,113
Energy placed into the Network, DN 350	<i>MWh</i>	8,116

Table 8. 9: Comparison in the Power Station, DN 350, Scenario 2

With reference to the first efficiency scenario, the energy produced in the P.S. of DN 350 increases, from 8,304 to 8,545, since it is bigger the thermal energy produced by the boiler, from 130 MWh to 193 MWh, and since it is slightly bigger the thermal energy produced by the CHP units connected to the DN 350. The global load also increases, because we have connected two single stage absorption chillers to

the DN 350, that have an overall load of 1,082 MWh on a global user load of 7,942 MWh, 14% of the load.

In the following figures, we are going to see the thermal power profile of the second and the third CHP unit; we will omit the first CHP, since being connected to the DN 200, its thermal energy production did not change.

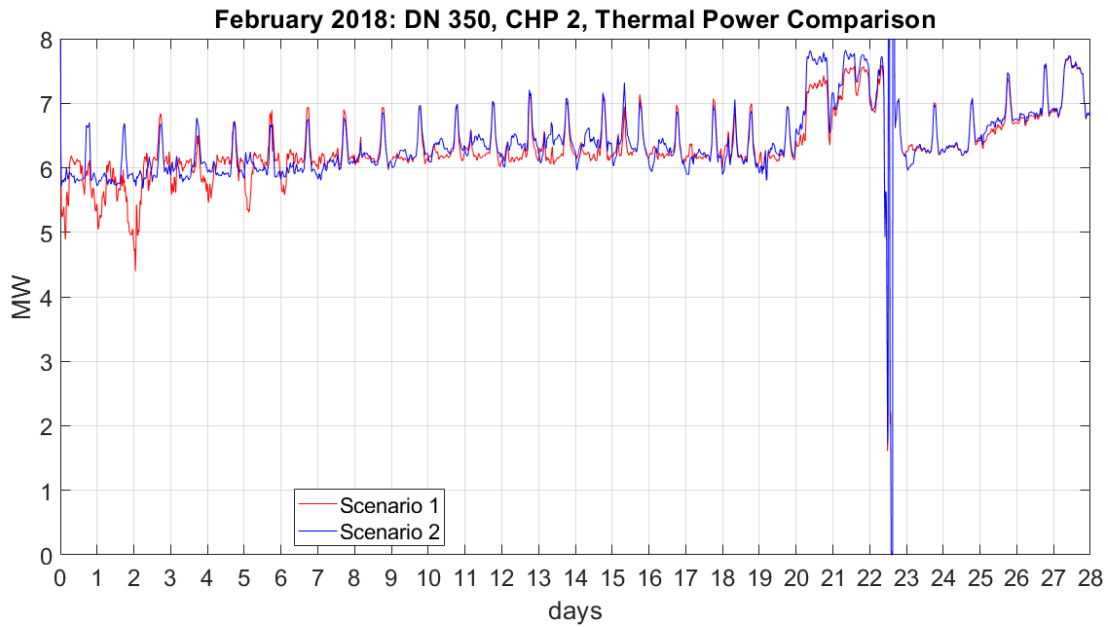


Figure 8. 15: CHP 2, thermal Power comparison, Scenario 2

Energy produced, CHP 2, Scenario 1	<i>MWh</i>	4,289
Energy produced, CHP 2, Scenario 2	<i>MWh</i>	4,332
Energy difference	<i>MWh</i>	43
Average th. Power , CHP 2, Scenario 1	<i>MW</i>	6.4
Average th. Power , CHP 2, Scenario 2	<i>MW</i>	6.4

Table 8. 10: CHP 2, thermal comparison, Scenario 2

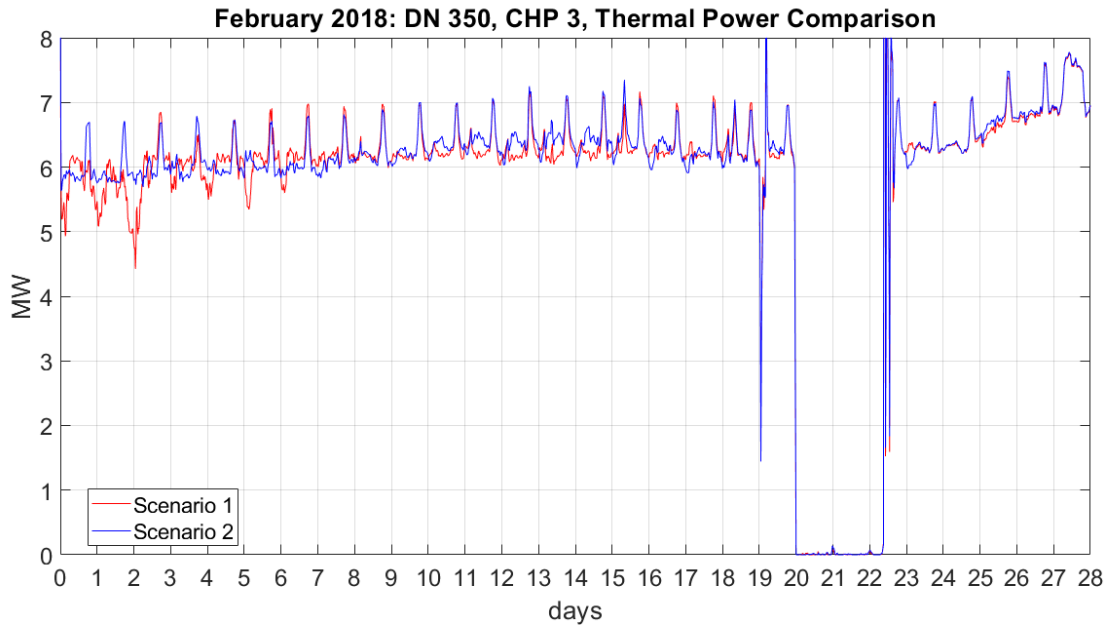


Figure 8. 16: CHP 3, thermal Power comparison, Scenario 2

Energy produced, CHP 3, Scenario 1	<i>MWh</i>	3,885
Energy produced, CHP 3, Scenario 2	<i>MWh</i>	3,918
Energy difference	<i>MWh</i>	33
Average th. Power, CHP 3, Scenario 1	<i>MW</i>	5.8
Average th. Power, CHP 3, Scenario 2	<i>MW</i>	5.8

Table 8. 11: CHP 3, thermal comparison, Scenario 2

The thermal energy produced by the CHP units does not change so much, only 76 MWh, less than 1% compared to the first efficiency scenario.

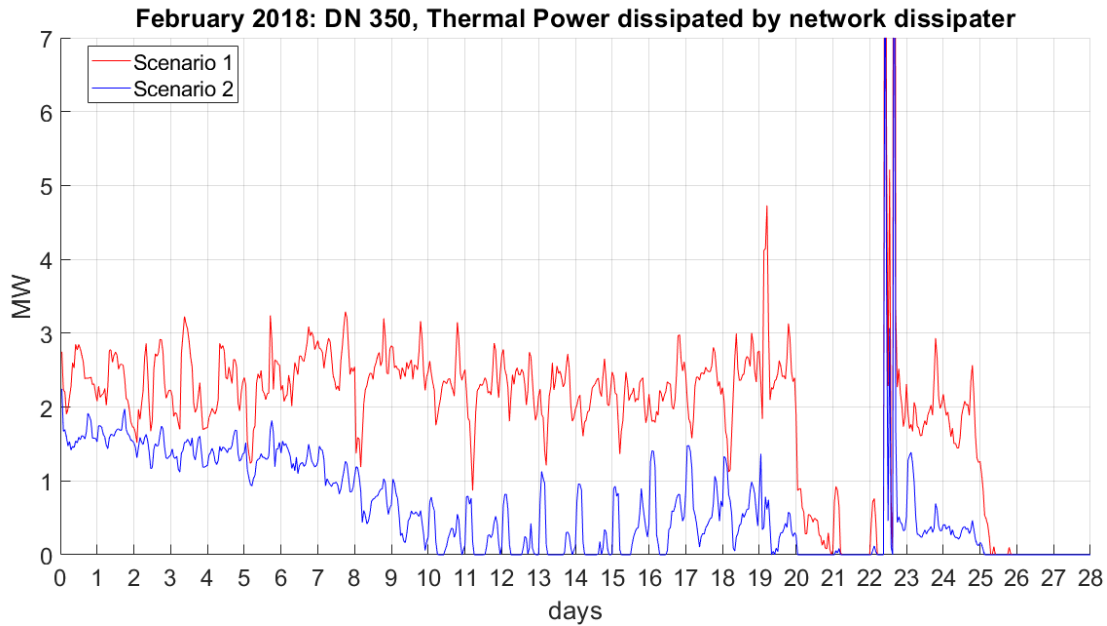


Figure 8. 17: Power dissipated by the network dissipater, DN 350, Scenario 2

Energy Dissipated by Network Dissipater, DN 350, Scenario 1	<i>MWh</i>	1,259
Energy Dissipated by Network Dissipater, DN 350, Scenario 2	<i>MWh</i>	431
Difference	<i>%</i>	66

Table 8. 12: Energy dissipated by the network dissipater, DN 350, Scenario 2

The energy dissipated by the Network dissipater of the DN 350 decreases significantly, about 66%, compared to scenario No chillers. It means that the primary energy was used better, and we recovered heat that would have been wasted otherwise in a positive way, producing 711 MWh of useful cooling energy.

	Time 0	Scenario 2	
		DN 350	DN 200
	<i>MWh</i>	<i>MWh</i>	<i>MWh</i>
Users Load	8,903	7,942	2,025
Global Heat Losses	713	171	278
Energy Placed into the Network	9,609	8,116	2,305
Energy Produced by CHP	9,129	8,250	3,099
Heat Recoverd by the CHP	/	2,271	0.0
Boilers Heat Production	657	293	13
Energy Produced in the P.S.	9,786	8,545	3,112
Energy Dissipated in the HST Dissipater	0.6	0.8	190
Energy Dissipated in the Network Dissipater	169	431	619

Table 8. 13: Simulation Energy Result, Scenario 2s

The active network is 16,899 meters long and it is constituted only by the pipes of the DN 350; the DN 200 is switched OFF completely and it is like it no longer exists. Inside the power station there are all the CHP units and a backup boiler of 16 MWth, a hot storage tank of 1,000 cubic meters of volume and the network dissipater.

Power Station			
3 CHP units	<i>Nominal th. Power</i>	<i>[kW]</i>	3x7,987
Boiler	<i>Nominal th. Power</i>	<i>[kW]</i>	16,000
HST	<i>Volume</i>	<i>[m³]</i>	1,000

Table 9. 1: Power Station, Network DN 350 only, Scenario 3

We do not pass the power produced by the boiler directly to the model any longer, as in the validation scenario, but we modelled a traditional gas boiler. It is ON only when the flow temperature of the network goes below the reference temperature of the network (90°C). A PI control manages the power placed into the network according to the flow temperature of the network at the generic time step. When the boiler is ON, its reference temperature becomes the reference temperature of the network (90°C). The model of the backup boiler is the same we used in the first and in the second efficiency scenario.

The network consists of 2 source nodes, 21 user nodes, 33 mixing nodes, 55 pipes.

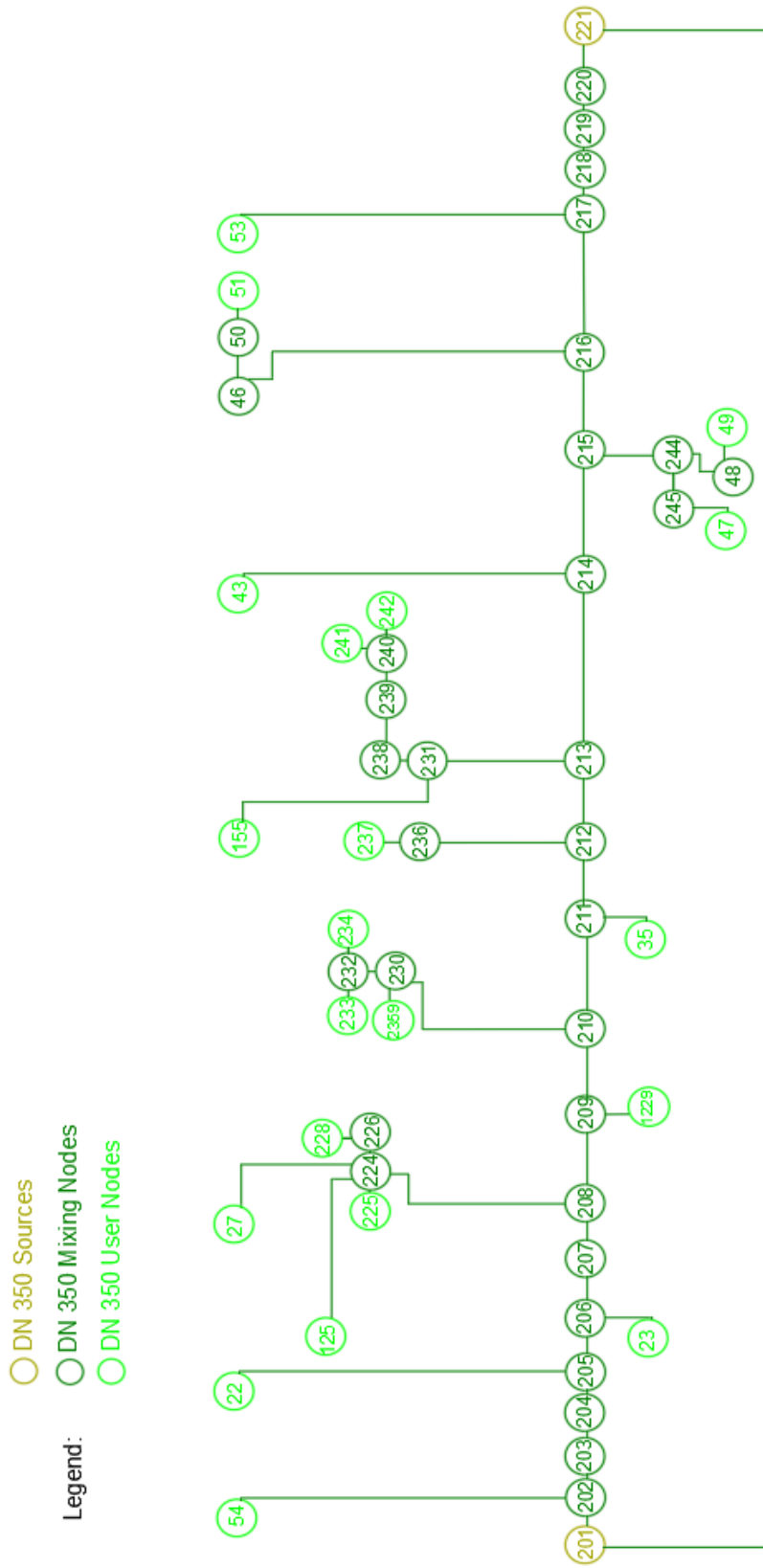


Figure 9. 2: Network DN 350 only, at low Temperature, linearized representation, Scenario 3

9.2 Simulation results of scenario ‘Network DN 350 only, at low temperature’

In this section we are going to see the simulation results of scenario ‘Network DN 350 only, at low temperature’. All the load of the DH network of Roma Fiumicino were shifted to the DN 350, managed at 90°C as reference flow temperature. As we can see in Figure 9. 3, the flow collector temperature has a quite regular profile and it is always between 100 °C and 90 °C, the limits we imposed by the reference temperature of the network dissipater and by the reference temperature of the boiler, except during the 22nd day.

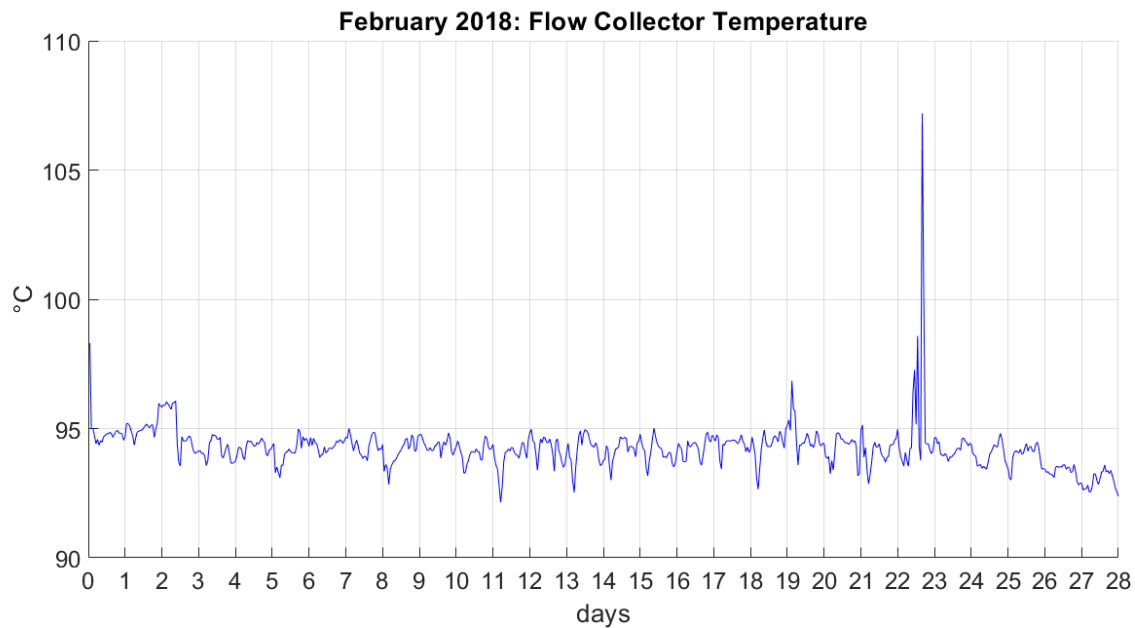


Figure 9. 3: Flow collector temperature, Scenario 3

Average flow Temperature	[°C]	94.2
---------------------------------	-------------	-------------

Table 9. 2: Flow collector temperature, Scenario 3

The sudden ON OFF of the third CHP between the 22nd and 23rd day of February creates instability in the simulation.

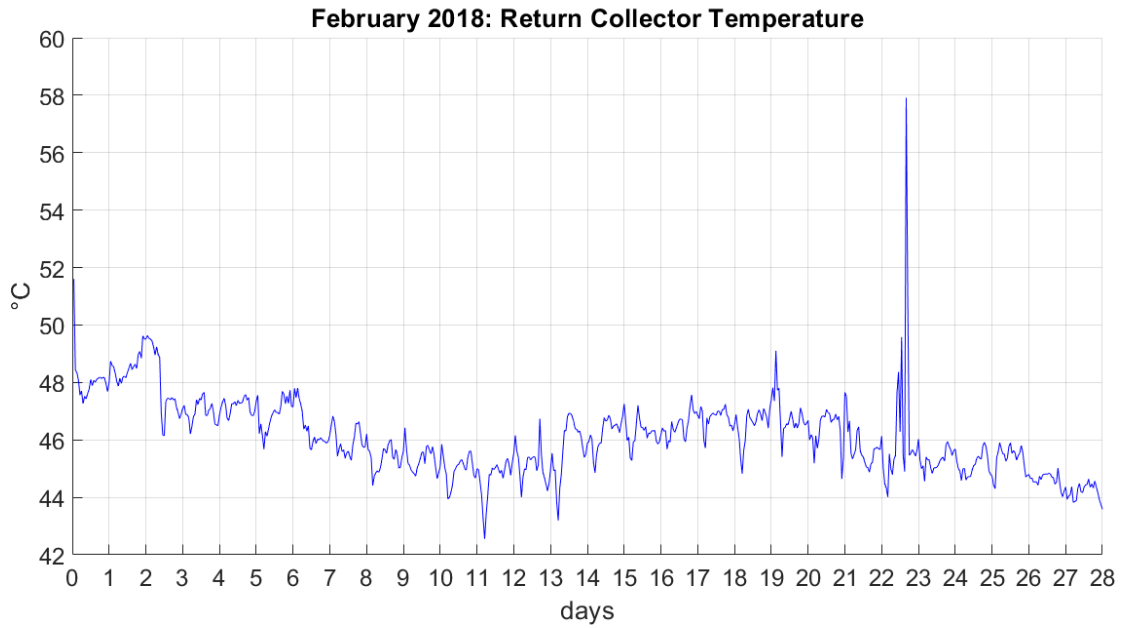


Figure 9. 4: Return collector temperature

Average Return Temperature	[°C]	46.1
-----------------------------------	-------------	-------------

Table 9. 3: Return collector temperature, Scenario 3

The return collector temperature is always below 57 °C and for this reason it is possible to recover heat from the low temperature heat exchanger of the CHP units, except for the 22nd day in which prevails the instability generated by the third CHP.

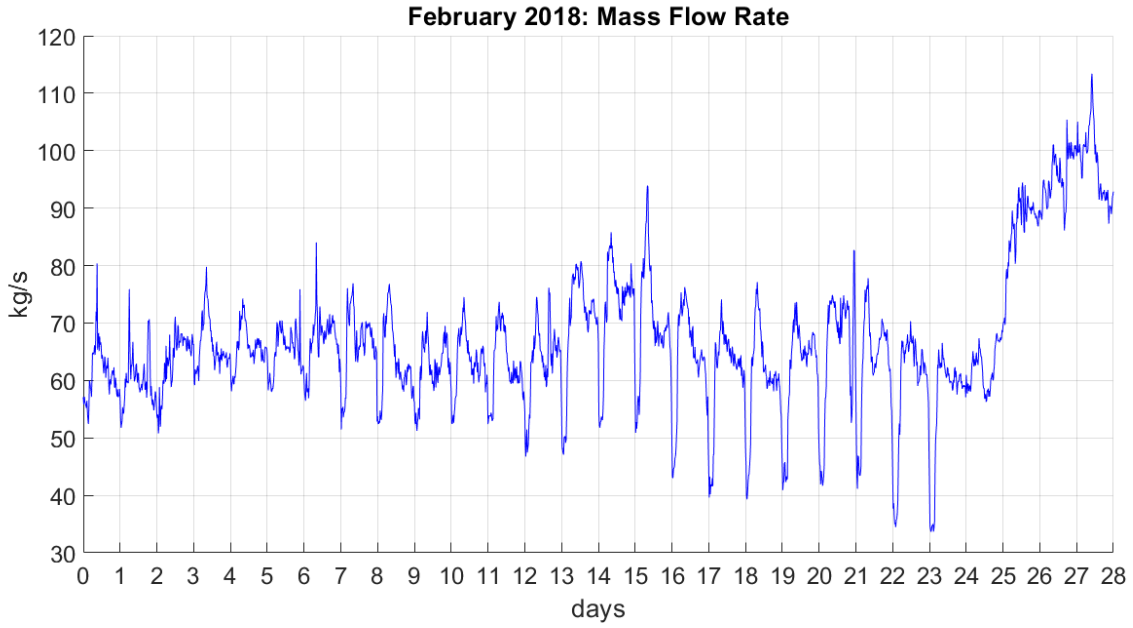


Figure 9. 5: Mass flow rate, Scenario 3

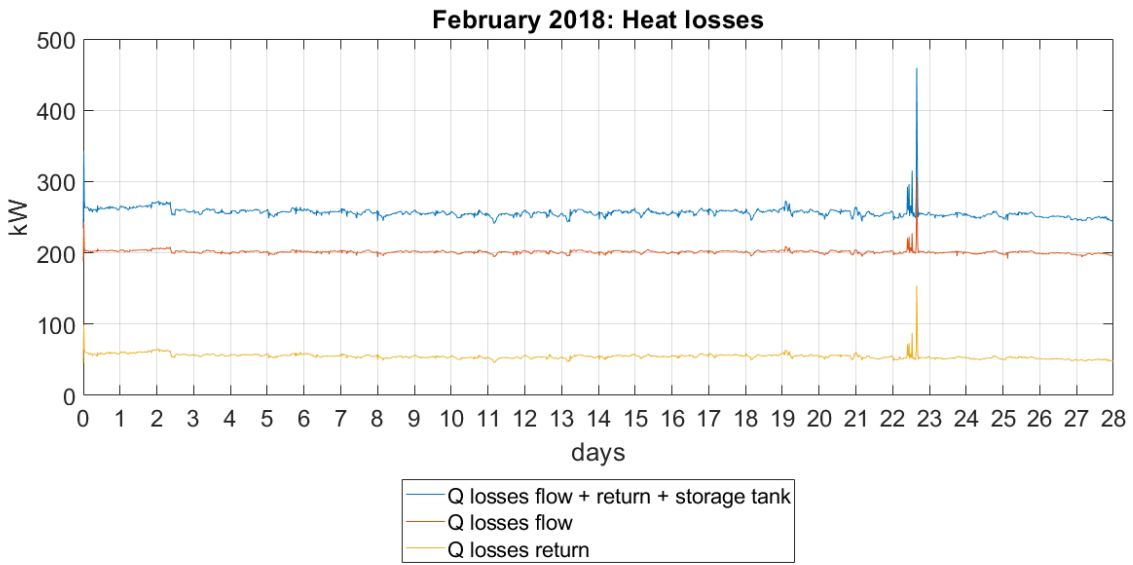


Figure 9. 6: Network heat losses, Scenario 3

Global Heat losses (Flow+Return+HST)	<i>MWh</i>	172
Heat losses HST	<i>MWh</i>	0.2
Average Global Heat losses	<i>kW</i>	256
Specific Network Heat losses	<i>W/m</i>	15.2

Table 9. 4: Network heat losses, energy results, Scenario 3

The heat distribution losses decreased more than three times compared to the simulation at Time 0, from 713 MWh to 172 MWh, because we reduced the overall length of the active network, from almost 33 km to almost 17 km, and because we reduced the reference flow temperature from 130 °C to 90 °C.

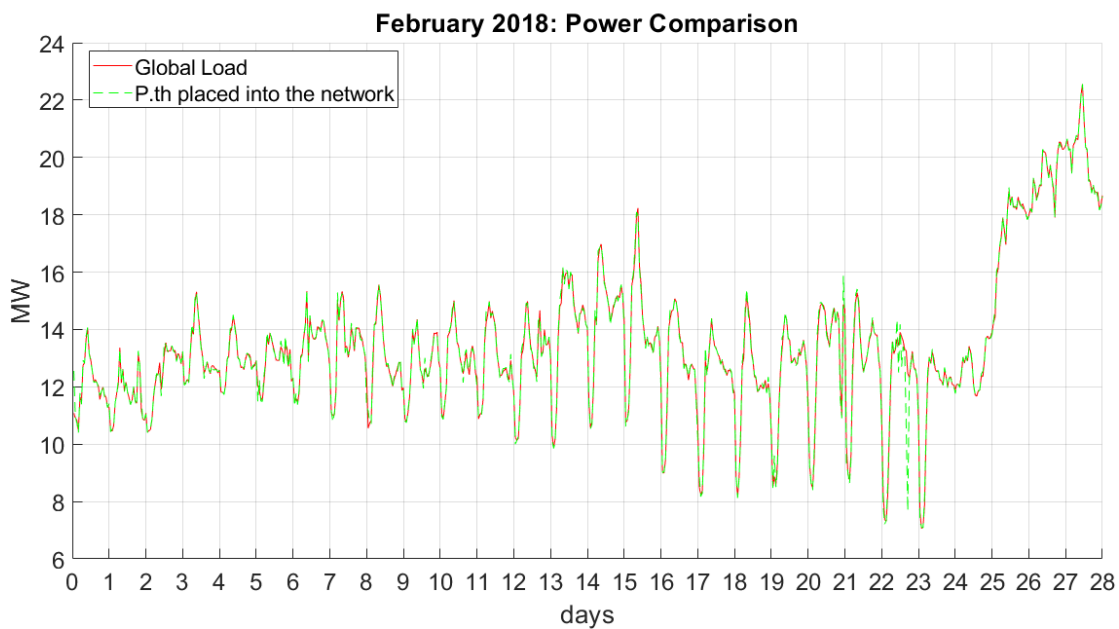


Figure 9. 7: Power Comparison in the Power Station, Scenario 3

Average th. Power Produced in PS	<i>MW</i>	17.4
Average Global Load	<i>MW</i>	13.5
Average th. Power placed into the Network	<i>MW</i>	13.5
Energy Produced in PS	<i>MWh</i>	11,666
Global Load	<i>MWh</i>	9,076
Energy placed into the Network	<i>MWh</i>	9,072

Table 9. 5: Energy Comparison in the Power Station, Scenario 3

The global load, that takes into account the heat distribution losses and the user load, has decreased from 9,619 MWh of the simulation at Time 0, to 9,076 MWh of this third efficiency scenario, almost 6 %, because of the reduction of the heat distribution losses.

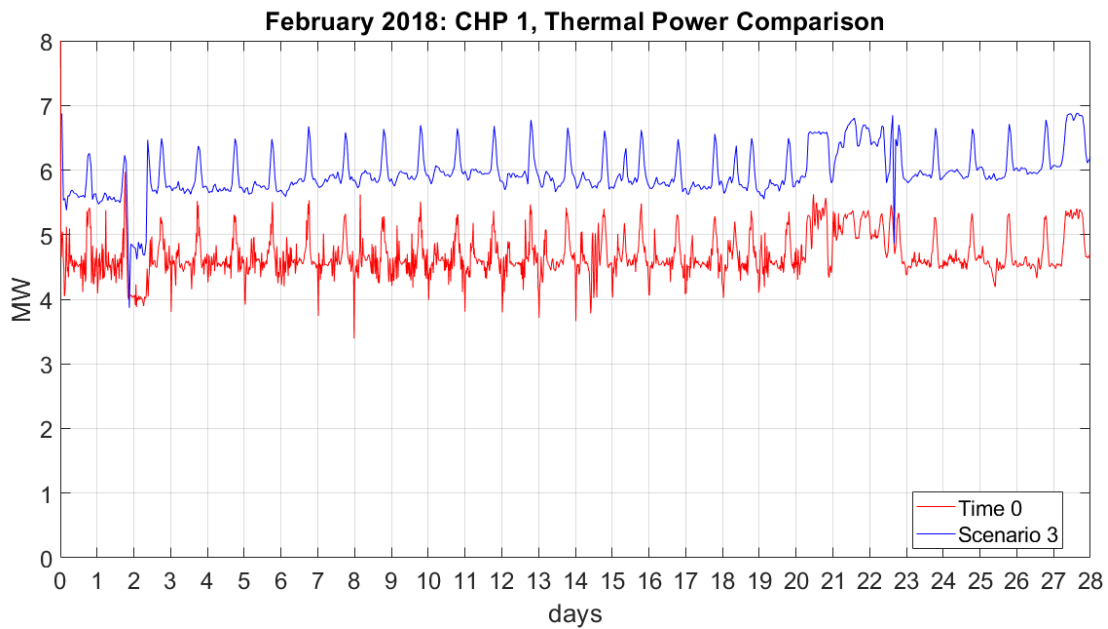


Figure 9. 8: CHP 1, thermal Power, Scenario 3

Average th. Power, CHP 1, Time 0	<i>MW</i>	4.7
Average th. Power, CHP 1, scenario 3	<i>MW</i>	6.0
Energy produced, CHP 1, Time 0	<i>MWh</i>	3,150
Energy produced, CHP 1, scenario 3	<i>MWh</i>	4,004
Energy Difference	<i>MWh</i>	854
Energy Difference	<i>%</i>	27

Table 9. 6: CHP 1, thermal comparison, Scenario 3

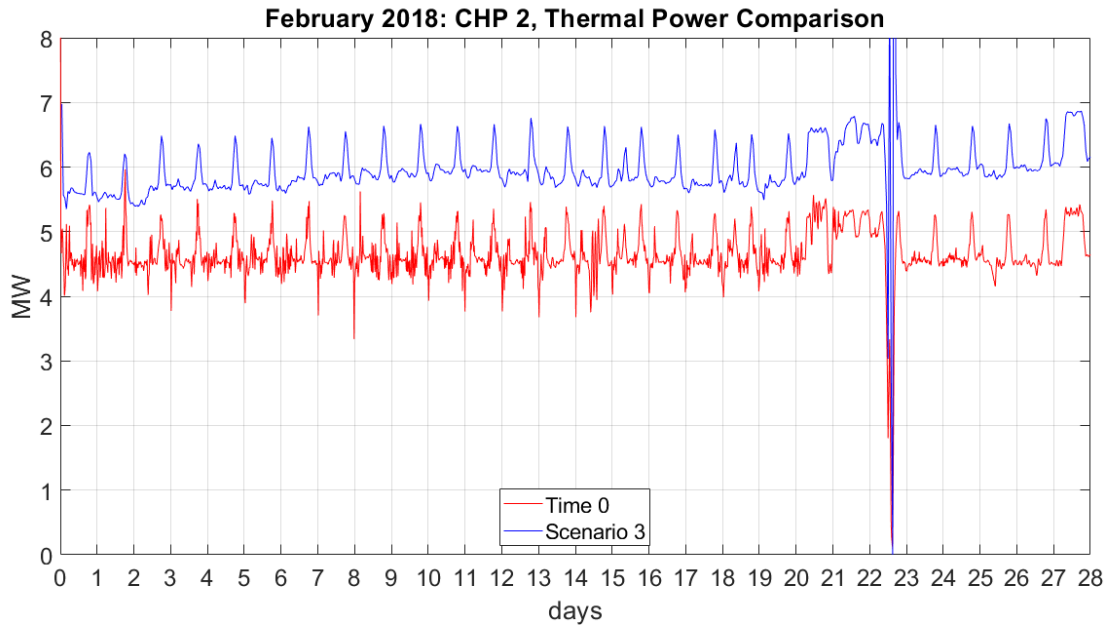


Figure 9. 9: CHP 2, thermal Power, Scenario 3

Average th. Power, CHP 2, Time 0	<i>MW</i>	4,7
Average th. Power, CHP 2, scenario 3	<i>MW</i>	6.0
Energy produced, CHP 2, Time 0	<i>MWh</i>	3,126
Energy produced, CHP 2, scenario 3	<i>MWh</i>	4,011
Energy Difference	<i>MWh</i>	885
Energy Difference	<i>%</i>	28

Table 9. 7: CHP 2, thermal comparison, Scenario 3

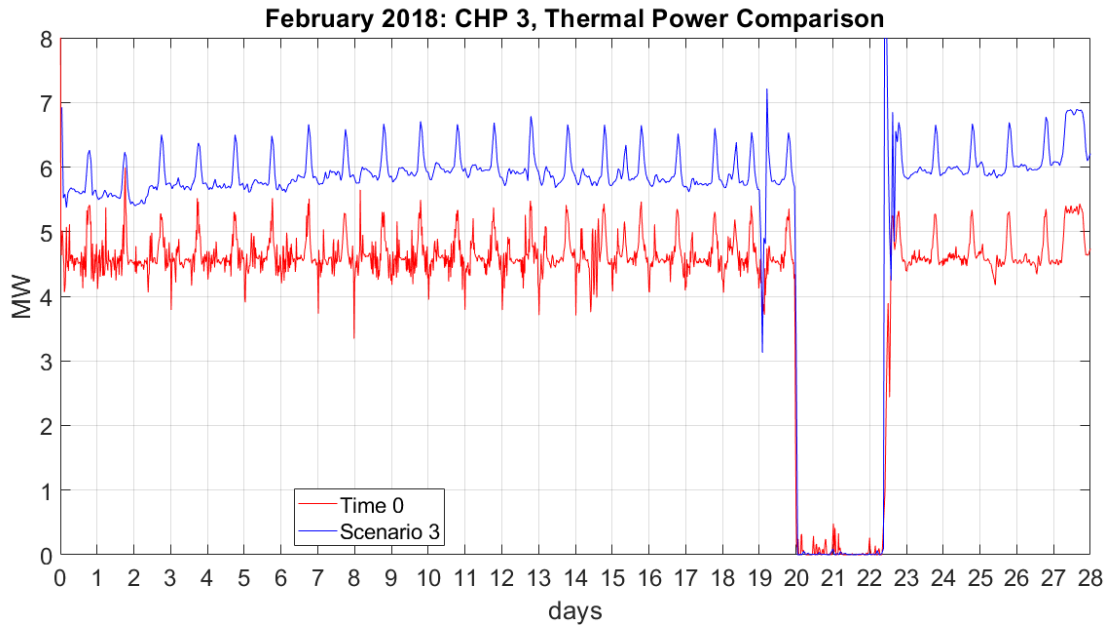


Figure 9. 10: CHP 3, thermal Power, Scenario 3

Average th. Power, CHP 3, Time 0	<i>MW</i>	4.0
Average th. Power, CHP 3, scenario 3	<i>MW</i>	5.4
Energy produced, CHP 3, Time 0	<i>MWh</i>	2,853
Energy produced, CHP 3, scenario 3	<i>MWh</i>	3,651
Energy Difference	<i>MWh</i>	798
Energy Difference	<i>%</i>	28

Table 9. 8: CHP2, thermal comparison, Scenario 3

The sudden ON OFF of the second and the third CHP between the 22nd and 23rd day of February creates instability in the simulation, as we have seen in the results of the flow collector temperature and in the results of the return collector temperature. In this third scenario, 27% more thermal energy was produced recovering heat from the low temperature heat exchanger of each cogenerator, with reference to scenario Time 0.

It is not possible to recover all the recoverable heat (about 2 MW) in the low temperature heat exchangers of the CHP units, since the return temperature of the MFR in the power station, the one exchanging thermal power with the LT heat exchangers inside the CHP units, is higher than 43 °C for most of the month, temperature at which the heat recovery would be total, as we can see in Figure 9. 11.

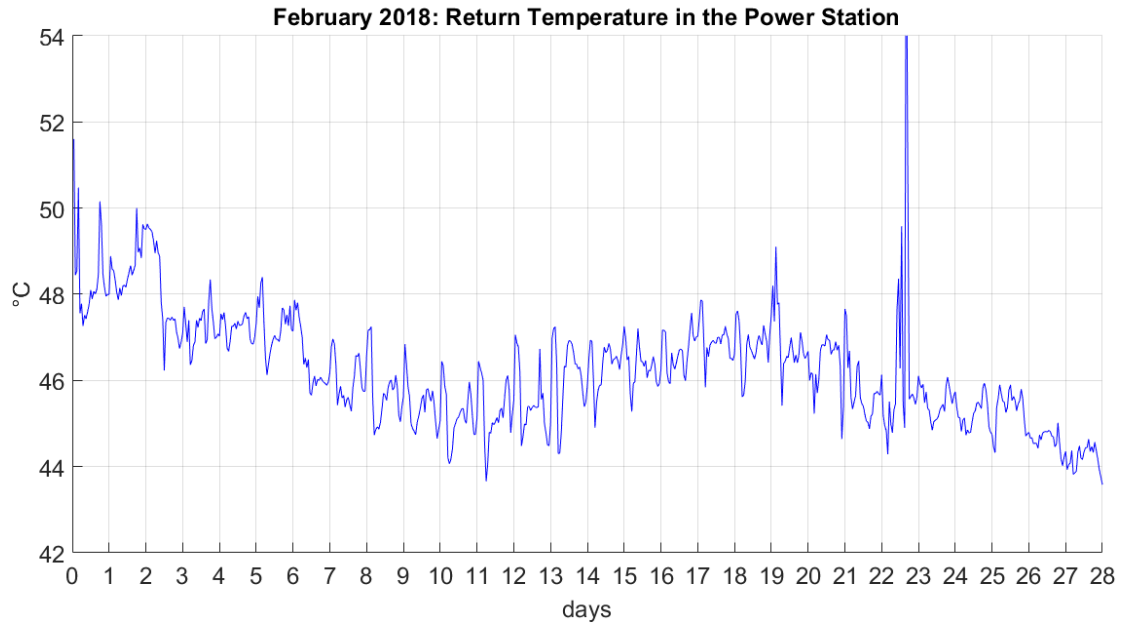


Figure 9. 11: Return temperature in the Power Station, Scenario 3

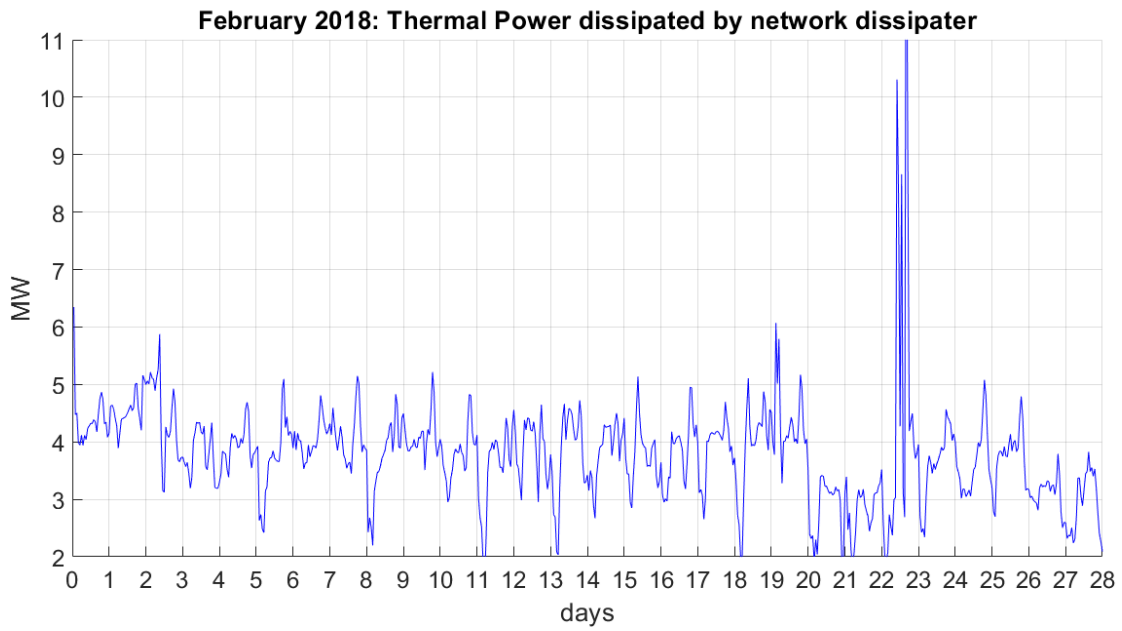


Figure 9. 12: Thermal Power dissipated by the network dissipater, Scenario 3

Energy Dissipated by Network Dissipater	MWh	2,585
--	------------	--------------

Table 9. 9: Energy dissipated by the network dissipater, Scenario 3

More than one third of the thermal energy produced in the power station is dissipated so that the network will not overheat, it corresponds to 100 % of the heat recovered from the low temperature heat exchangers of the CHP units, with reference to scenario Time 0.

We do not show the thermal behaviour of the boiler since it is ON only for short periods, placing into the network 0.4 MWh.

	Time 0	Scenario 3
	<i>MWh</i>	<i>MWh</i>
Users Load	8,903	8,903
Global Heat Losses	713	172
Energy Placed into the Network	9,609	9,076
Energy Produced by CHP	9,129	11,666
Heat Recoverd by the CHP	/	2,537
Boilers Heat Production	657	0.4
Energy Produced in the P.S.	9,786	11,666
Energy Dissipated in the HST Dissipater	0.6	6.2
Energy Dissipated in the Network Dissipater	169	2,585

Table 9. 10: Simulation Energy Results, Scenario 3

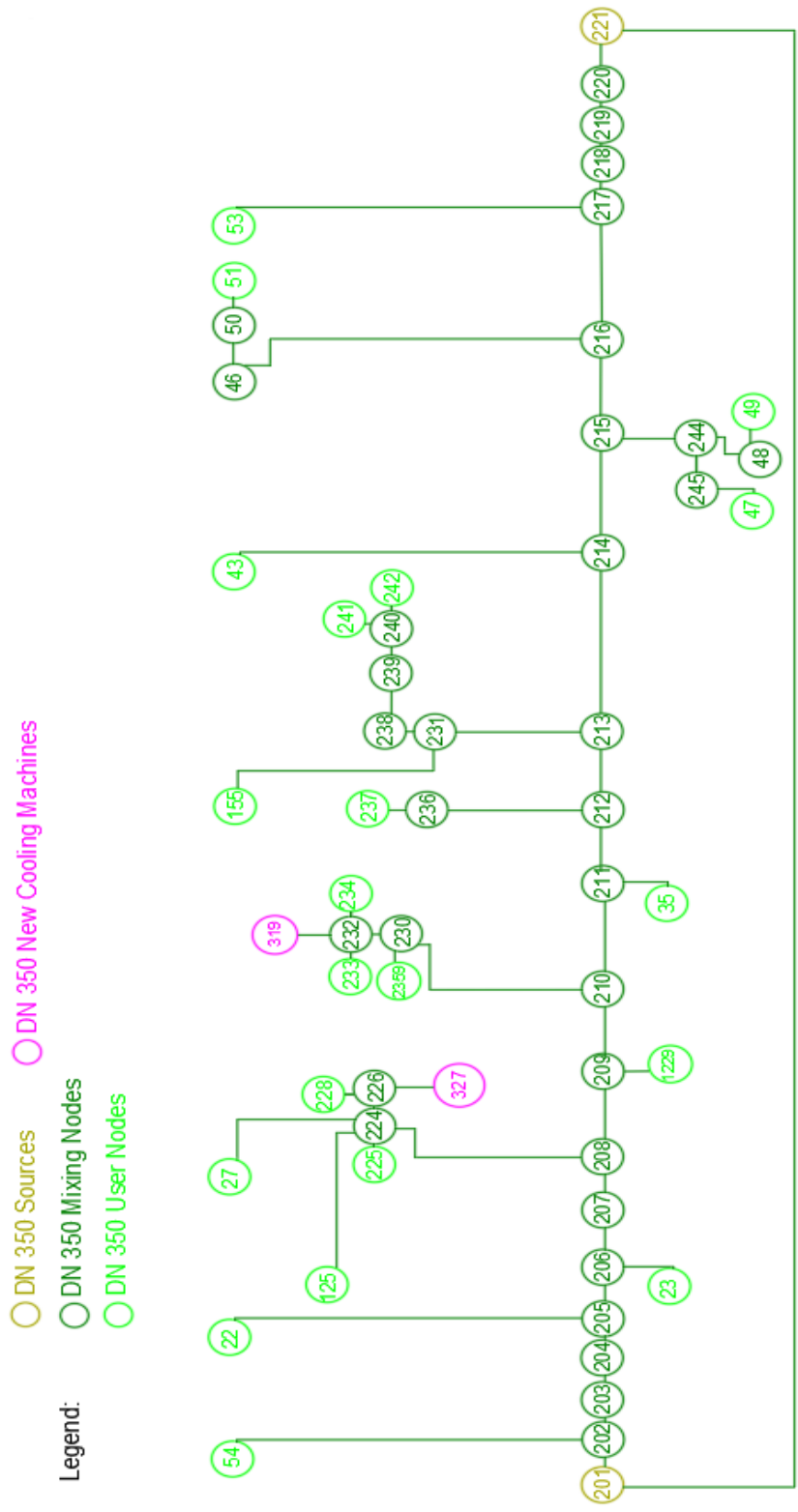


Figure 10. 2: Network DN 350 only, with Dissipated Heat Recovery, linearized representation, Scenario 4

The network consists of 2 source nodes, 23 user nodes, 33 mixing nodes, 57 pipes.

This new version of the network is 17,801 meters long. The load profile of the new absorption chillers has been obtained from the heat dissipated by the network dissipater of the third efficiency scenario, Network DN 350 only at low temperature. This load profile was divided by two because it is supposed to be equal for the cooling machine in PG 327 and for the one in PG 319. Then we divided the load profile by the nominal thermal power required by the absorption chillers (3,921 kWth), value taken from the data sheet of the machine. Afterwards we normalized each value of the profile higher than 1 to 1. In the end we multiplied the profile obtained at the previous step for the nominal thermal power required by the absorption chiller. We could not pass this load profile to the model directly, since adding new loads would cause the heat distribution losses to increase, and this would have caused the increasing energy consumption of the backup boiler to keep the flow temperature at 90 °C. For this reason, we made a calibration analysis, it means that we simulated this fourth scenario multiplying the load profile of the chillers for a coefficient that decreased the load itself (1, 0.9, 0.8...) till, the adding energy required to the boiler of the network, was more or less equal to the energy required to the boiler of the third efficiency scenario (Network DN 350 only at low temperature).

Power Station			
3 CHP units	<i>Nominal th. Power</i>	<i>[kW]</i>	3x7,987
Boiler	<i>Nominal th. Power</i>	<i>[kW]</i>	16,000
HST	<i>Volume</i>	<i>[m³]</i>	1,000

Table 10. 1: Power Station, Network DN 350 only, Scenario 4

10.2 Calibration analysis of the Absorption chillers loads

In this section we are going to see the results of the calibration analysis made to decide which load profile to give to the model for the absorption chillers as input. Load that as we said is equal for the cooling machines we want to install in PG 319 and in PG 317, and that was obtained from the profile of the heat dissipated by the network dissipater of the third efficiency scenario, Network DN 350 only at low temperature, that we will call scenario 'No Chillers'.

As we can see in Figure 10. 3 increasing the F factor, the cooling energy produced by the Absorption chiller would increase.

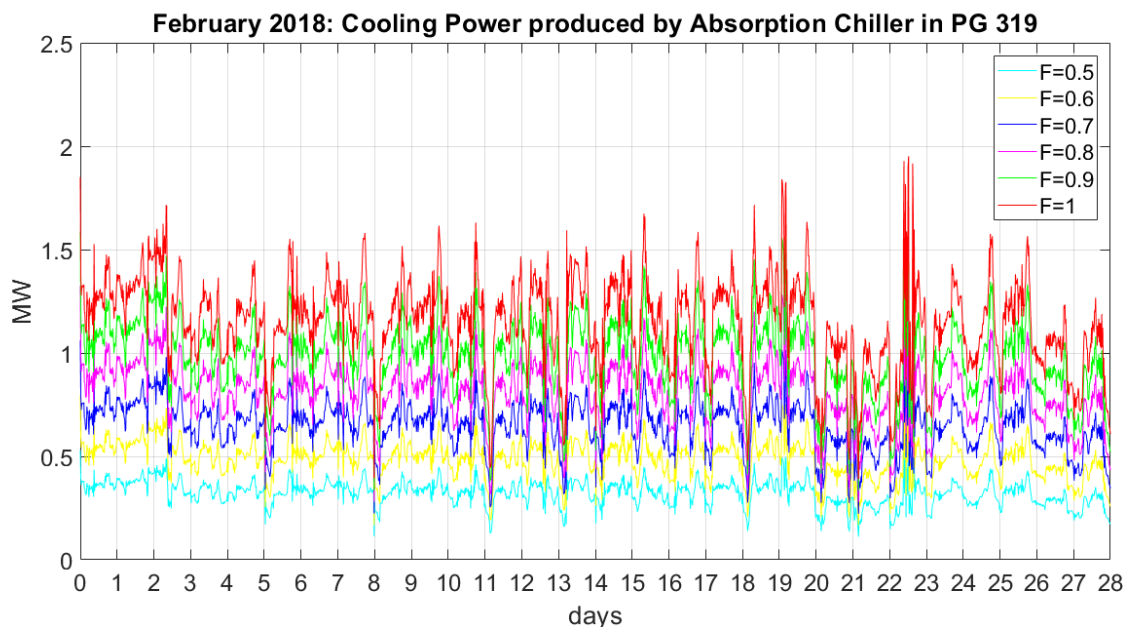


Figure 10. 3: Cooling power produced in PG 319, Scenario 4

We show only the cooling power production in PG 319 because in PG 307 it is more or less the same.

	Cooling Energy produced		Thermal Energy required by a single chiller
	MWh	MWh	MWh
	n.319	n.327	/
F=0.5	217	216	337
F=0.6	326	324	506
F=0.7	437	434	674
F=0.8	548	545	843
F=0.9	661	657	1,012
F=1	775	771	1,180

Table 10. 2: Cooling energy produced and thermal energy required by absorption chillers, Scenario 4

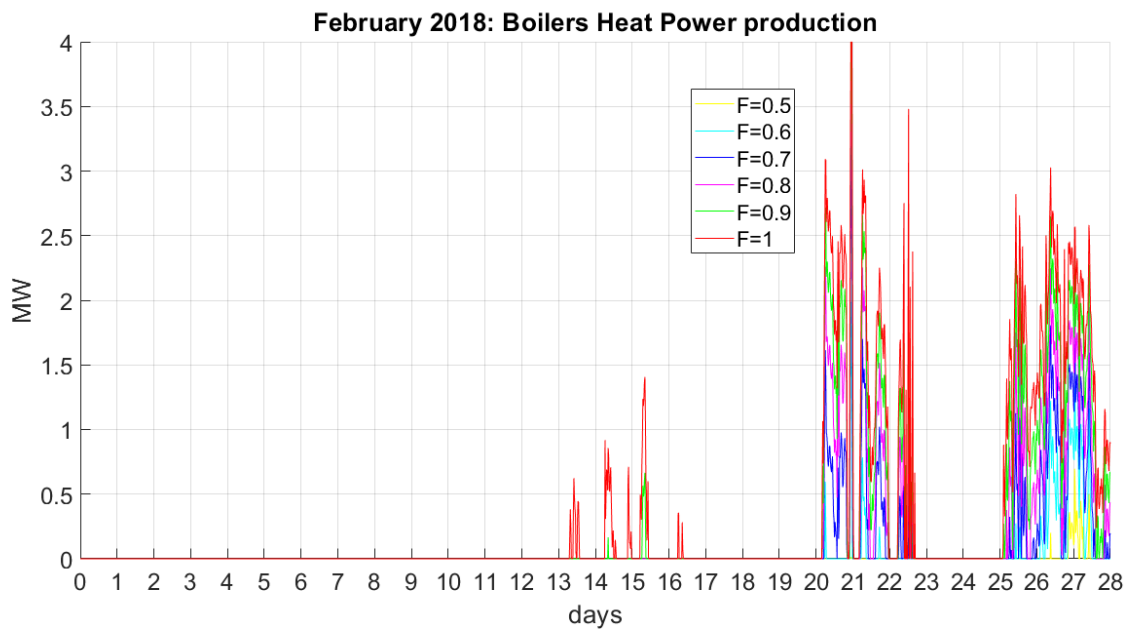


Figure 10. 4: Boiler heat power production, Scenario 4

Increasing the load, also the heat power produced by the boiler would increase to keep the flow collector temperature around 90 °C.

	Boiler Thermal Energy Production	Extra Thermal Energy Produced by Boiler
	<i>MWh</i>	<i>MWh</i>
Scenario No Chillers	0.4	/
F=0.5	3	2.6
F=0.6	22	21.6
F=0.7	63	62.6
F=0.8	108	107.6
F=0.9	154	153.6
F=1	207	206.6

Table 10. 3: Boilers' energy production, Scenario 4

In order to maximize the cooling energy produced and to minimize the energy consumed by the boiler we compute the ratio between the extra thermal energy produced by the boiler and the cooling energy produced, with reference to the third scenario.

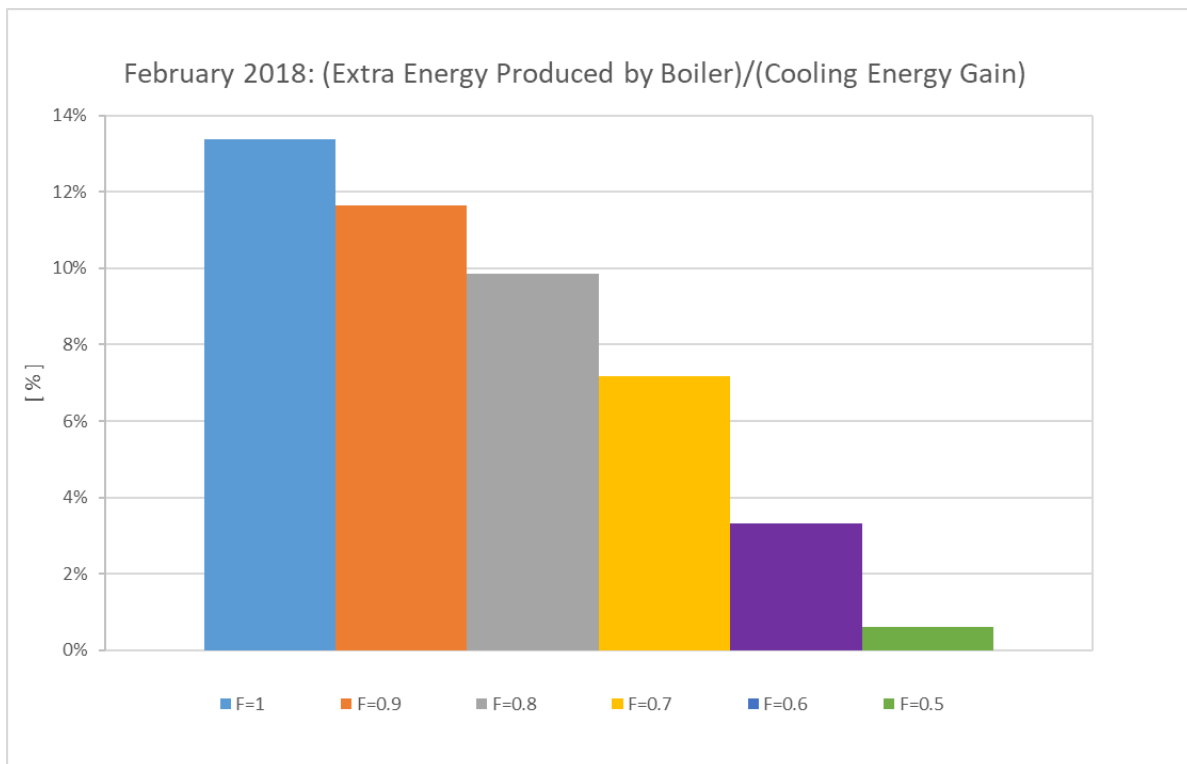


Figure 10. 5: Calibration analysis, Scenario 4

	(Extra thermal energy produced by Boiler)/Cooling energy gain
	%
F=0.5	0.6
F=0.6	3.3
F=0.7	7.2
F=0.8	9.8
F=0.9	11
F=1	13

Table 10. 4: Calibration analysis, Scenario 4

Since the function, $f = \frac{\text{Extra energy produced by boiler}}{\text{Cooling energy produced}}$ has not a minimum, to maximize the cooling production and to minimize the boilers fuel consumption we decided to choose an F factor equal to 0.8, in order to have an extra thermal energy production of the boiler compared to the cooling gain below 10%, thing that seemed us reasonable.

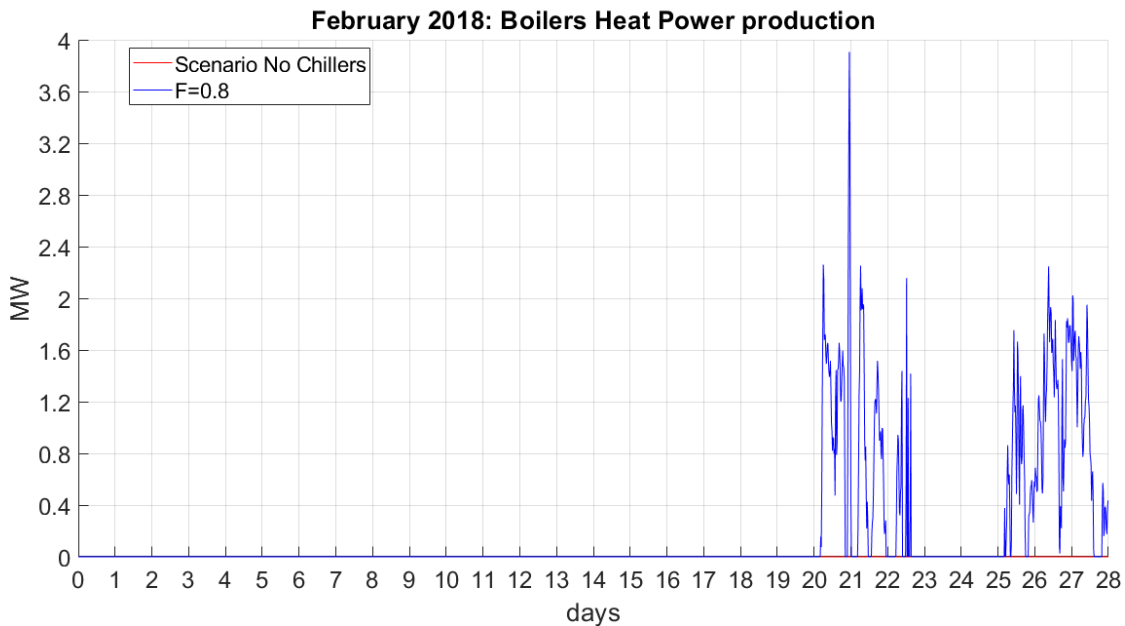


Figure 10. 6: Boilers heat power production comparison, Scenario 4

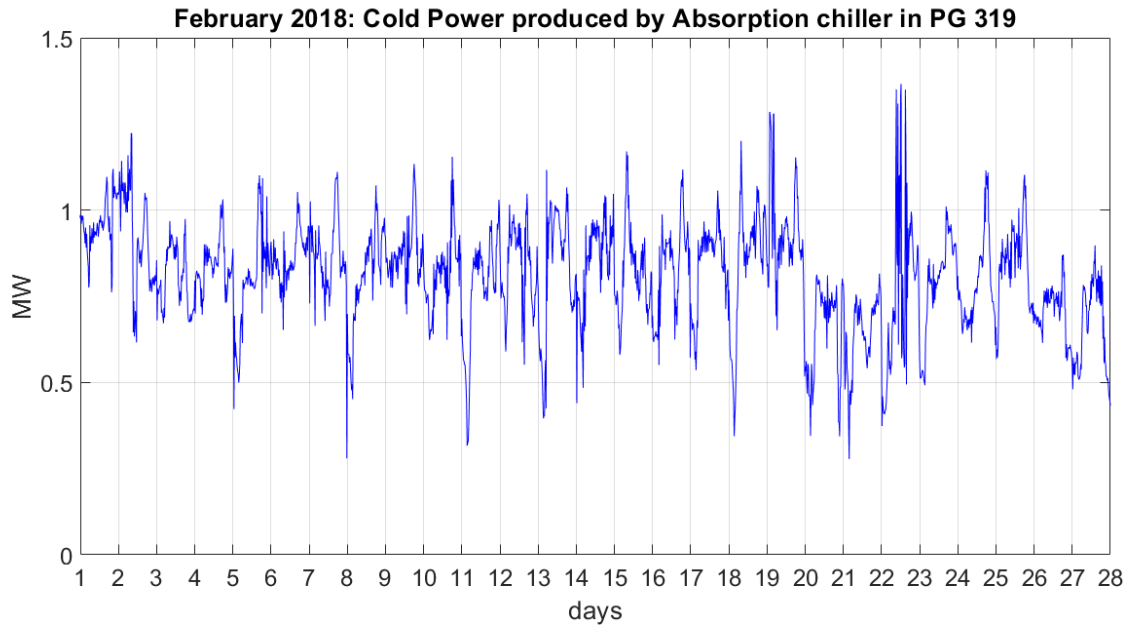


Figure 10. 7: Cooling power produced in PG 319, F=0.8, Scenario 4

10.3 Simulation results of scenario ‘Network DN 350 only, with dissipated heat recovery by the installation of Absorption Chillers’

In this section we are going to see the simulation results of scenario ‘Network DN 350 only with Dissipated Heat Recovery by the Installation of Absorption Chillers’. The load profiles of the chillers, obtained from the heat dissipated by the network dissipater of scenario 3, have been multiplied by a F coefficient equal to 0.8. We will compare the results of this fourth scenario with the ones of the previous efficiency scenario, scenario 3, that we will call ‘No Chillers’.

In scenario 4 the load has increased by 16%, because we installed two new absorption chillers and as we can see in Figure 10. 8 the flow collector temperature decreases with reference to scenario 3, in particular from the 20th to the 23rd day and from the 25th to the 28th day, when it is necessary to switch ON the boiler to keep the flow temperature close to 90 °C.

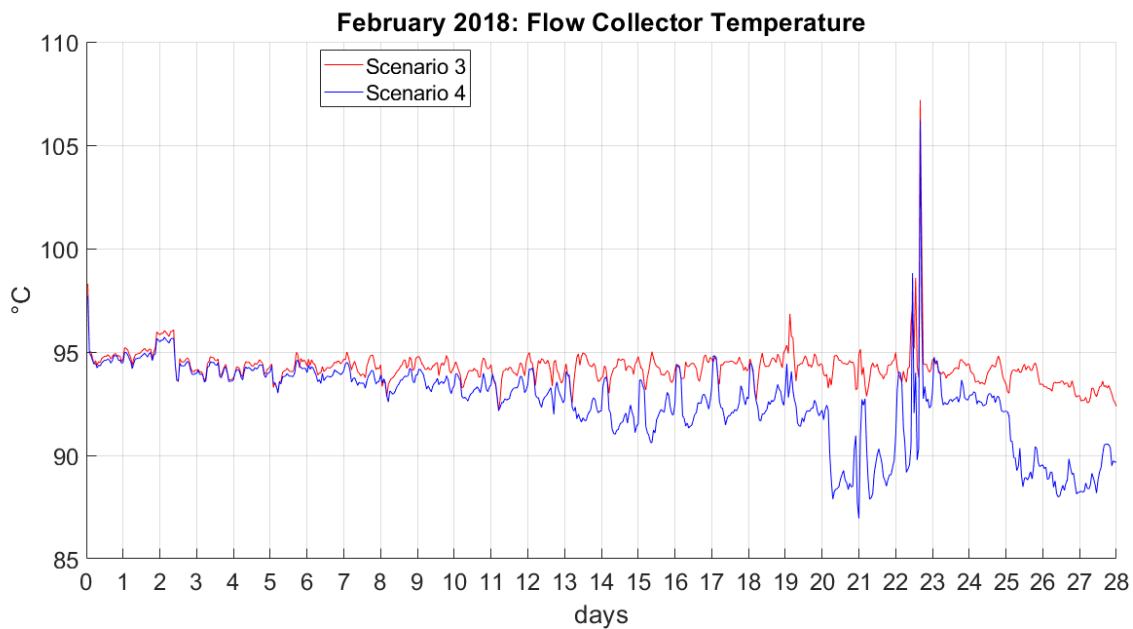


Figure 10. 8: Flow collector temperature comparison, Scenario 4

Average flow Temperature, Scenario 3	[°C]	94.2
Average flow Temperature, Scenario 4	[°C]	92.6

Table 10. 5: Flow collector temperature comparison, Scenario 4

The sudden switching ON of the third CHP, between the 22nd and the 23rd day, creates instability in the results.

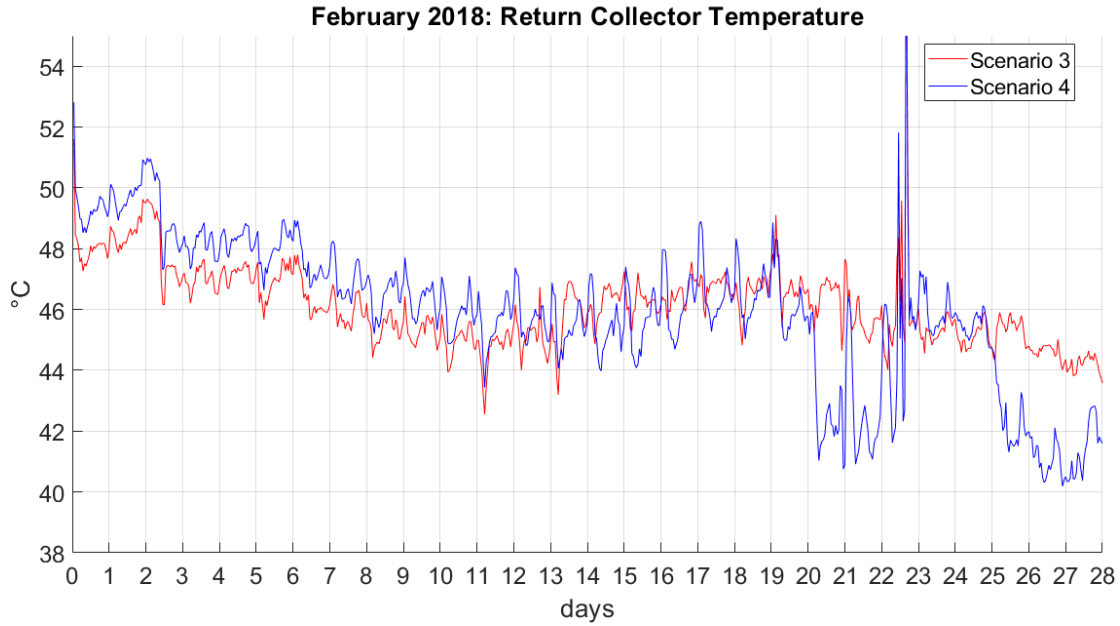


Figure 10. 9: Return collector temperature comparison, Scenario 4

Average Return Collector Temperature, Scenario 3	[°C]	46.1
Average Return Collector Temperature, Scenario 4	[°C]	45.9

Table 10. 6: Return collector temperature comparison, Scenario 4

From the 1st to the 19th day of the month, the return collector temperature of the fourth efficiency scenario is higher than in the third efficiency scenario, because the users characterized by absorption chillers have a lower temperature drop in the substation, 40 °C instead of 50 °C, and they count for almost 27 % of the global user load.

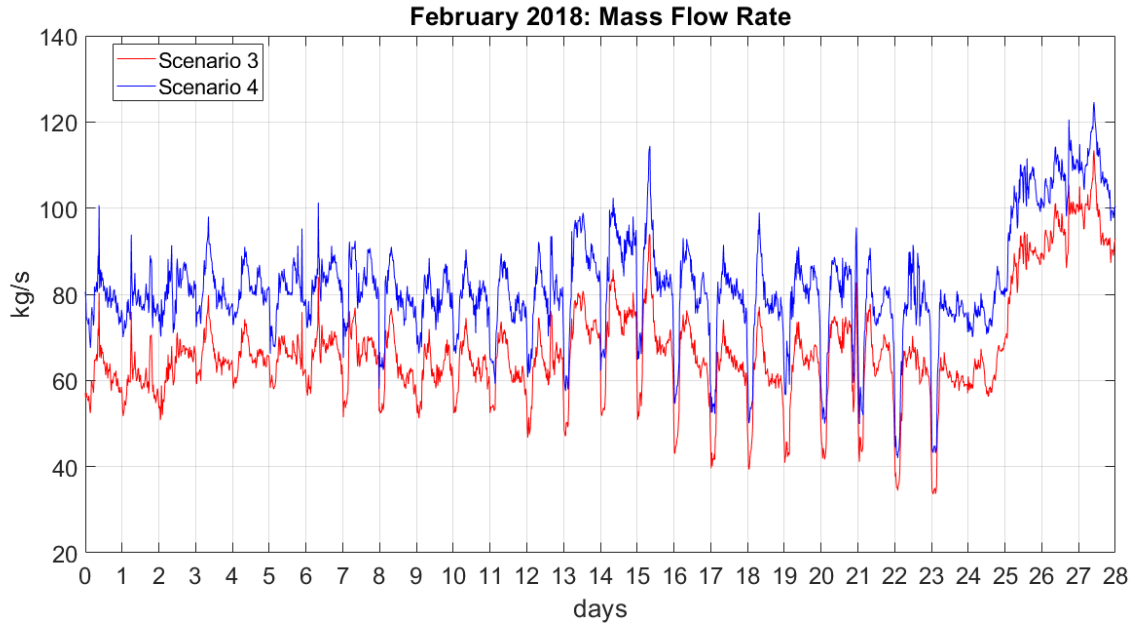


Figure 10. 10: Mass flow rate comparison, Scenario 4

As we could imagine for scenario 4, increasing the load, the mass flow rate also increases, with reference to scenario 3.

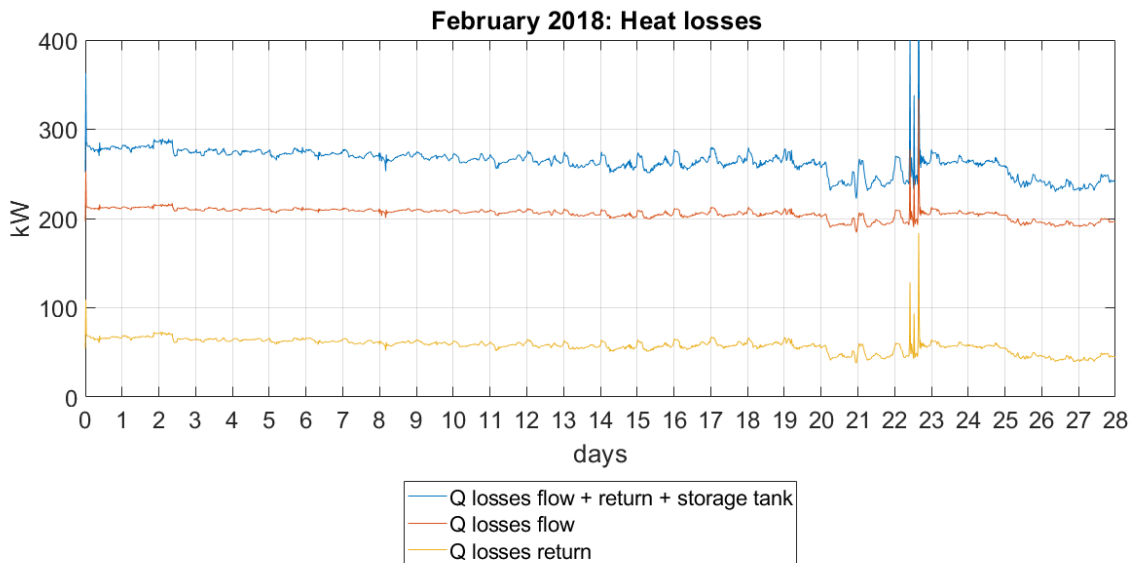


Figure 10. 11: Network heat losses, Scenario 4

Global Heat losses (Flow+Return+HST)	<i>MWh</i>	177
Heat Distribution Losses	<i>MWh</i>	176.9
Heat losses HST	<i>MWh</i>	0.1
Average Global Heat losses	<i>kW</i>	263
Network Heat losses	<i>W/m</i>	14.8

Table 10. 7: Network heat losses, energy results, Scenario 4

The distribution heat losses increase from 172 MWh to 177 MWh, moving from scenario 3 to scenario 4, since the increasing of the load.

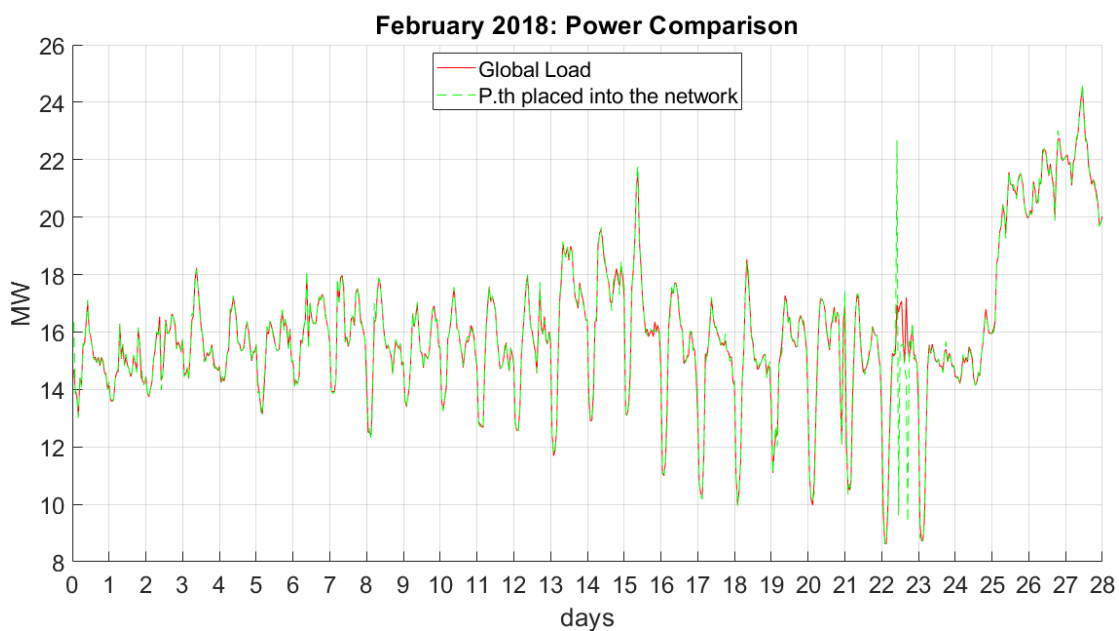


Figure 10. 12: Power Comparison in the Power Station, Scenario 4

Energy Produced in PS	<i>MWh</i>	11,843
Global Load	<i>MWh</i>	10,767
Energy placed into the Network	<i>MWh</i>	10,755
Average th. Power Produced in PS	<i>MW</i>	17.6
Average Global Load	<i>MW</i>	16.0
Average th. Power placed into the Network	<i>MW</i>	16.0

Table 10. 8: Energy Comparison in the Power Station, Scenario 4

The thermal energy produced in the P.S. increases about 180 MWh, 1.5 % more than in the third scenario, because of the operation of the boiler and because of a slight increasing of the thermal energy produced by the CHP units.

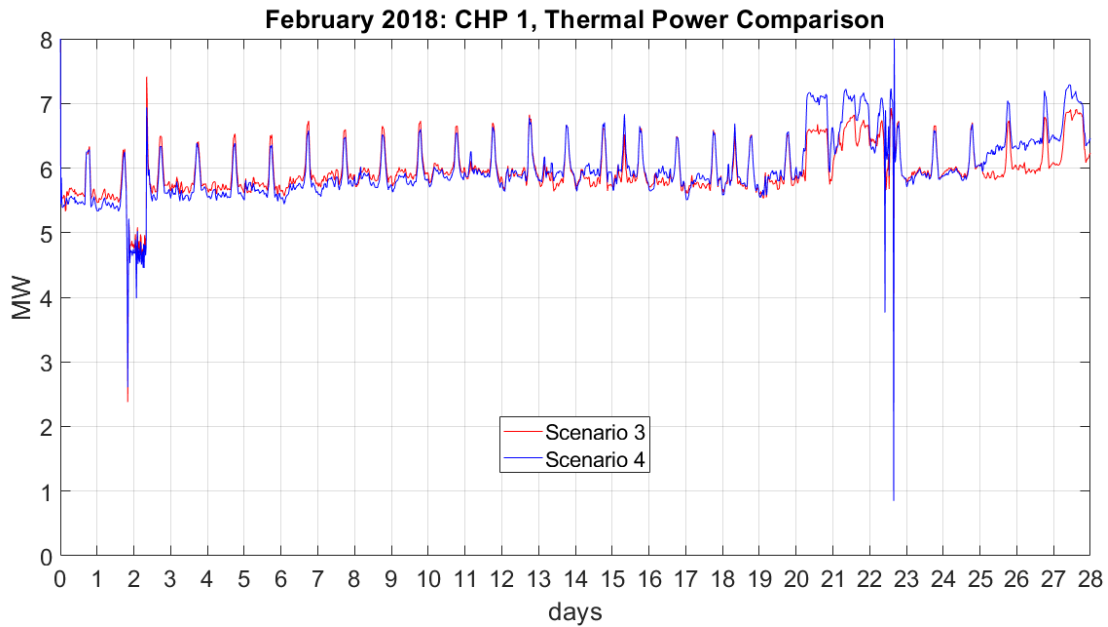


Figure 10. 13: CHP 1, thermal Power comparison, Scenario 4

Energy produced, CHP 1, Scenario 3	<i>MWh</i>	4,004
Energy produced, CHP 1, Scenario 4	<i>MWh</i>	4,030
Energy Difference	<i>MWh</i>	26
Average th. Power, CHP 1, Scenario 3	<i>MW</i>	6.0
Average th. Power, CHP 1, Scenario 4	<i>MW</i>	6.0

Table 10. 9: CHP 1, thermal Energy comparison, Scenario 4

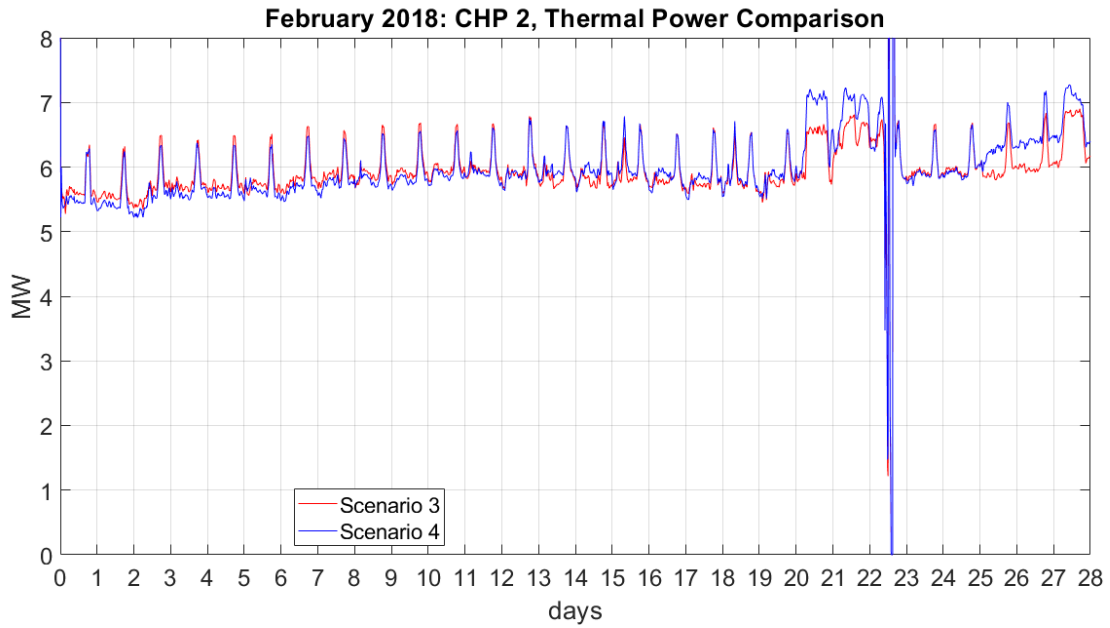


Figure 10. 14: CHP 2, thermal Power comparison, Scenario 4

Energy produced, CHP 2, Scenario 3	<i>MWh</i>	4,011
Energy produced, CHP 2, Scenario 4	<i>MWh</i>	4,042
Energy Difference	<i>MWh</i>	31
Average th. Power, CHP 2, Scenario 3	<i>MW</i>	6.0
Average th. Power, CHP 2 Scenario 4	<i>MW</i>	6.0

Table 10. 10: CHP 2, thermal Energy comparison, Scenario 4

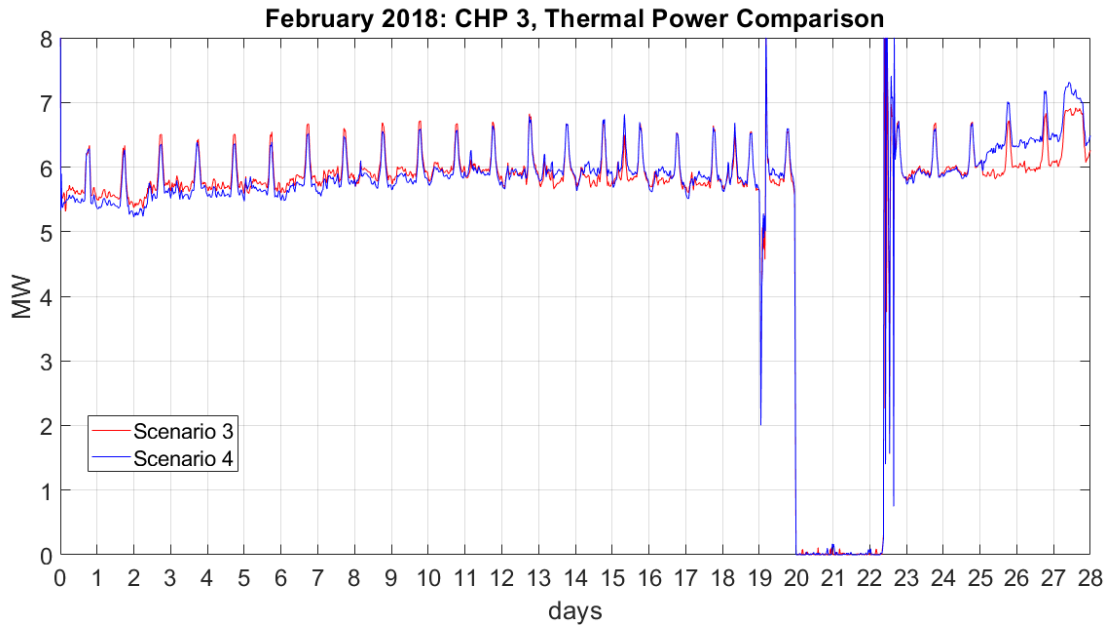


Figure 10. 156: CHP 3, thermal Power comparison, Scenario 4

Energy produced, CHP 3, Scenario 3	<i>MWh</i>	3,651
Energy produced, CHP 3, Scenario 4	<i>MWh</i>	3,663
Energy Difference	<i>MWh</i>	12
Average th. Power, CHP 3, Scenario 3	<i>MW</i>	5.4
Average th. Power, CHP 3 Scenario 4	<i>MW</i>	5.5

Table 10. 11: CHP 3, thermal Energy comparison, Scenario 4

The thermal energy produced by the CHP units stays almost the same, it increases 60 MWh, less than 0.1 %, compared to the third scenario.

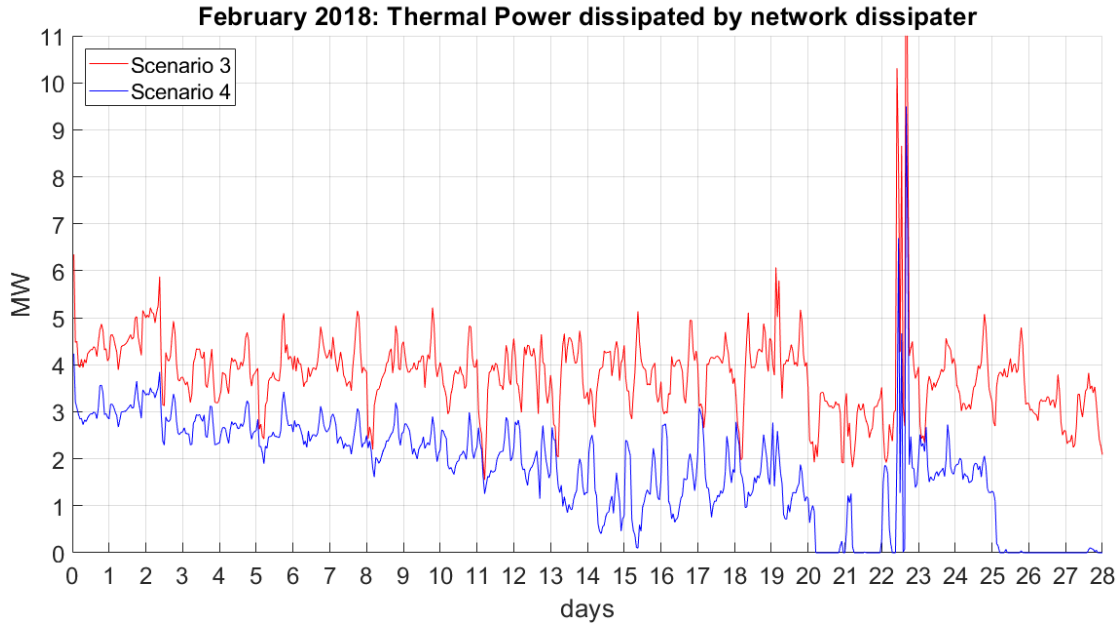


Figure 10. 167: Thermal Power dissipated by the network dissipater comparison, Scenario 4

Energy Dissipated by Network Dissipater, Scenario 3	<i>MWh</i>	2,585
Energy Dissipated by Network Dissipater, Scenario 4	<i>MWh</i>	1,075
Energy Difference	<i>%</i>	58

Table 10. 12: Energy dissipated by the network dissipater comparison, Scenario 4

The reduction of the energy dissipated by the network dissipater is more than 58 %, compared to the third scenario. It means that the primary energy was used better, and we recovered heat that would have been otherwise wasted in a positive way, producing 1,093 MWh of useful cooling energy. It is possible to install the absorption machines reducing the heat dissipated by the network dissipater, without significantly increasing the fuel consumption of the boiler.

	Time 0	Scenario 4
	<i>MWh</i>	<i>MWh</i>
Users Load	8,903	10,590
Global Heat Losses	713	177
Energy Placed into the Network	9,609	10,755
Energy Produced by CHP	9,129	11,735
Heat Recoverd by the CHP	/	2,606
Boilers Heat Production	657	108
Energy Produced in the P.S.	9,786	11,843
Energy Dissipated in the HST Dissipater	0.6	0.8
Energy Dissipated in the Network Dissipater	169	1,075

Table 10. 13: Simulation Energy Results, Scenario 4

Chapter 11: Energy Efficiency Indexes

11.1 Brief overview of European Regulation

The following discussion is based on the Italian and European standard UNI EN 15316-4-5:2007. This regulation describes the methodology to evaluate the energy performance of DH systems by primary energy factors.

Each energy carrier has its total primary energy factor; for fossil energy carriers it is computed as:

$$f_{p,j} = \frac{LHV + E_{p,j}}{LHV}$$

LHV = Low heating Value, energy inside each unit of energy carrier;

E_{p,j} = Primary energy to produce each unit of energy carrier, it depends on the mining, storage and transportation of the energy carrier;

The total primary energy factors are defined in Italy by 'Comitato Termotecnico Italiano (CTI)', 'Raccomandazione CTI 14: 2013':

Energy Carrier	Total Primary Energy Factor fp	Non Renewable Primary Energy Factor fp,NREN
Natural Gas	1	1
GPL	1	1
Fuel Oil	1	1
Biomass	0.3	1
Electricity	2.174	2.174
District Heating	**	*
	* defined in D.Lgs 152 April 3 2006	
	** given by the supplier	

Table 11. 1: Raccomandazione CTI 14: 2013'

The total primary energy factors are defined in Europe by the standard FprEN 15603:2014:

Energy Carrier	Total primary Energy factor fP	Non renewable primary Energy factor fP,NREN
Delivered from distant		
Solid	1,1	1,1
Liquid	1,1	1,1
Gaseous	1,1	1,1
Delivered from nearby		
District heating a)	1,3	1,3
District cooling	1,3	1,3
Grid delivered electricity	2,5	2,3
Grid exported electricity	2,5	2,5
Delivered from on-site		
Solar - PV electricity	1	0
Solar - Thermal	1	0
Geo -, aero -, hydrothermal	1	0
Temporary exported and reimported later		
PV electricity	1	0
a) Default value based on a natural gas boiler. Specific values are calculated according to EN 15316-4-5		

Table 11. 2: European standard FprEN 15603:2014

The standard UNI EN 15316-4-5:2007 evaluates the energy performance of a DH system subdividing it in two sections. The first section includes the heat and power generation system, the pumping system and the heat distribution system. The second section includes all the building connected to the network from the heat exchange subsystems to the terminals of the users.

We are not going to consider the total primary energy factors of renewable sources since the system we study, the DH system of Fiumicino airport, does not use renewable energy.

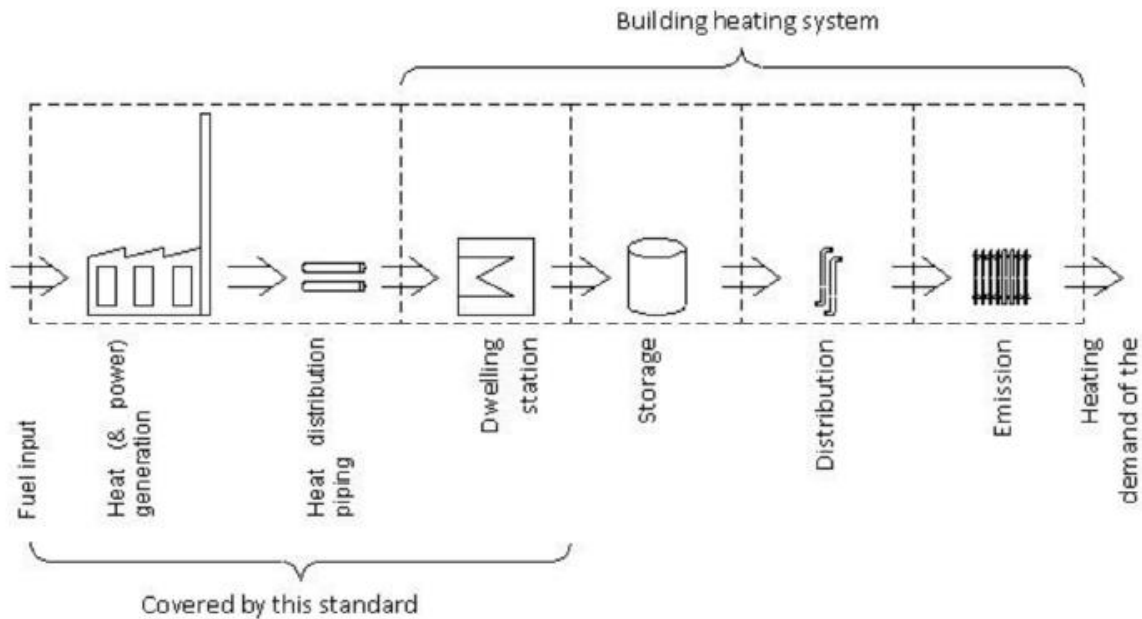


Figure 11 1: District Heating system scheme, readapt from UNI EN 15316-4-5:2007 [26]

Inside the first section the fuel gets inside, whereas the electric and the thermal energy go out.

The net electric energy produced is given by the difference between the electric energy produced and the electric energy needed to feed the auxiliary systems, like the pumping one:

$$E_{el,PS,n} = E_{el,PS} - E_{el,aux}$$

$E_{el,PS,n}$ = net electric energy produced ;

$E_{el,PS}$ = lord electric energy produced ;

$E_{el,aux}$ = electric energy needed to feed the auxiliary systems;

The primary energy getting inside the first section is equal to the product of the fuel getting inside the system and the total primary energy factor of the fuel itself.

$$E_{p,fuel} = E_{fuel} * f_{p,fuel}$$

$E_{p,fuel}$ = Primary energy getting inside the system;

E_{fuel} = fuel getting inside the system;

$f_{p,fuel}$ = total primary energy factor of the fuel;

The primary energy associated with the electric energy produced is:

$$E_{p,el} = E_{el,PS,n} * f_{p,el}$$

$f_{p,el}$ = total primary energy factor of the electricity;

The indexes we are going to use for our discussion will be:

-Primary Energy Factor ($f_{p,DH}$)¹²:

$$f_{p,DH} = \frac{E_{p,fuel} - E_{p,el}}{E_{th,user}}$$

$E_{th,user}$ = Thermal energy needed to feed the users, at the border of the supplied building.

This index ($f_{p,DH}$) defines the amount of primary energy needed to produce one unit of thermal energy consumed by the users.

- Plant Primary Energy Factor (PEF_{plant}):

$$PEF_{plant} = \frac{E_{p,fuel} - E_{p,el}}{E_{th,flow}}$$

We found this index in M. Badami¹³ where it was called PEF. The PEF_{plant} defines the amount of primary energy needed to produce one unit of thermal energy placed into the network, and unlike the $f_{p,DH}$, the denominator also takes into account the heat distribution losses.

$E_{th,flow}$ = Thermal energy placed into the network, it includes the global user load and the heat distribution losses.

¹²UNI, Ente Nazionale Italiano di Unificazione. EN 15316-4-5 (edizione luglio 2007) [27].

¹³ M. Badami, A. Portoraro. *Analisi di performance e monitoraggi energetici di reti termiche distribuite*, Report RdS/2013/056 [26].

-District Heating Global Efficiency (η_{DH}):

$$\eta_{DH} = \frac{E_{th,user}}{E_{th,flow}}$$

We found this index in M. Badami¹¹. The η_{DH} represents the efficiency of the network, from the point of view of the heat distribution losses along the network.

-Primary Energy Efficiency (PEE):

$$PEE = \frac{E_{th,flow} + E_{el,PS,n}}{E_{p,fuel}}$$

We found this index in M. Badami¹¹. The PEE represents the overall efficiency of the DH system.

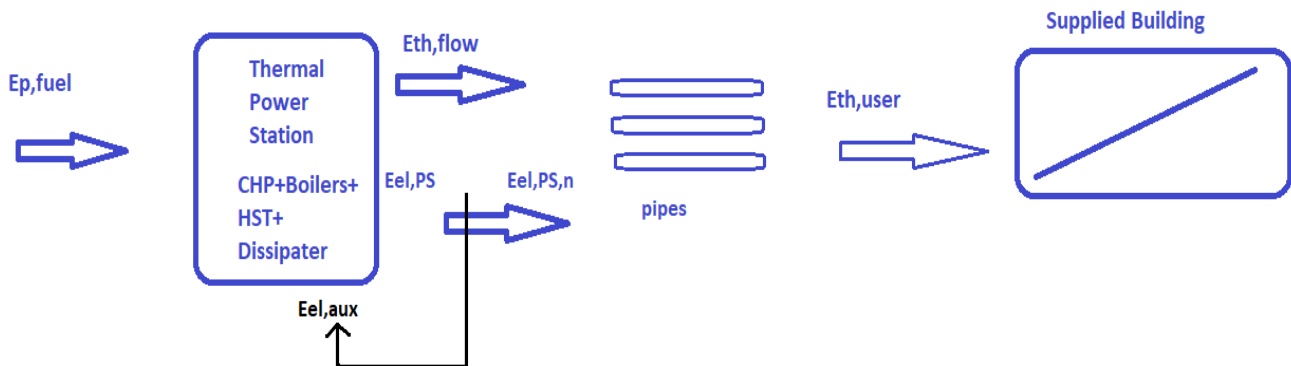


Figure 11 2: Energy fluxes getting inside and outside the Thermal Power Station

11.2 Simulations results analysis

In this section we are going to analyse the energy efficiency indexes obtained from the different efficiency scenarios we simulated. All the energy efficiency scenarios were run with the CHP units working with the real electric profiles we used in the validation scenario and in scenario Time 0, electric profiles derived from the monitoring data. This assumption meant that all the simulations have the same methane consumption and the same electric energy produced by the CHP units.

Legend:

- -Scenario 0: Working Network at Time 0, it is the reference scenario;
- -Scenario 1: first efficiency scenario, Two Temperatures Network;
- - Scenario 2: second efficiency scenario, Two Temperatures Network with Dissipated Heat Recovery by the Installation of Absorption Chillers;
- - Scenario 3: third efficiency scenario, Network DN 350 only, at low Temperature;
- - Scenario 4: fourth efficiency scenario, Network DN 350 only, at low Temperature, with Dissipated Heat Recovery by the Installation of Absorption Chillers.
-

Some tables about methane consumption, electric energy production and reference parameters from the simulated scenarios follow to understand better the results of the efficiency indexes.

CHP, Methane consumed	
<i>Sm³</i>	3,269,814

Table 11. 3: Methane consumed by CHP

Boilers, Methane consumed				
Scenario 0	Scenario 1	Scenario 2	Scenario 3	Scenario 4
<i>Sm³</i>	<i>Sm³</i>	<i>Sm³</i>	<i>Sm³</i>	<i>Sm³</i>
73,711	16,053	34,378	40.4	1,212

Table 11. 4: Methane Consumed by boilers

Parameter	Scenario 0	Scenario 1	Scenario 2	Scenario 3	Scenario 4
$E_{p,fuel}$ [MWh]	33,121	32,549	32,731	32,391	32,510
$E_{l,PS,n}$ [MWh]	14,243	14,243	14,243	14,243	14,243
$E_{th,flow}$ [MWh]	9,609	9,329	10,421	9,072	10,755
$E_{th,user}$ [MWh]	8,903	8,903	9,967	8,903	10,590
Energy dissipated [MWh]	170	2,073	1,241	2,591	1,076

Table 11. 5: Reference parameters of the simulated scenarios

The energy dissipated takes into account both the energy dissipated by the network dissipater and the energy dissipated by the HST dissipater.

The Sm^3 of methane consumed by the boilers has been computed with reference to a low heating value of 9.9 kWh/ Sm^3 of fuel consumed, value given by ADR, and a supposed boiler efficiency of 0.9.

11.2.1 Primary Energy Factor ($f_{p,DH}$):

The primary energy factor gives us information on how much primary energy the district heating system needs to supply a single unit of thermal energy to the user, and it decreases moving from the reference scenario, simulation at Time 0, to the efficiency ones.

	$f_{p,DH}$	$\frac{1}{f_{p,DH}}$
Scenario 0	0.242	4.129
Scenario 1	0.178	5.617
Scenario 2	0.177	5.642
Scenario 3	0.160	6.241
Scenario 4	0.146	6.849

Table 11. 6 $f_{p,DH}$ results

The reference scenario has the highest value of $f_{p,DH}$, 0.242, whereas the fourth scenario has the lowest one, 0.146. With reference to scenario 0, the minimum reduction of $f_{p,DH}$ is 0.064 for scenario 1, with a percentage reduction of 26 %, whereas the maximum reduction is 0.096 for scenario 4, with a percentage reduction of 40 %.

The primary energy factor is very low in all the scenarios, since the most part of the primary energy is consumed to produce the electricity for the auto consumption. The $f_{p,DH}$ mainly depends on the primary energy consumed. Since the primary energy consumed by the CHP units is the same in all the scenarios, the $f_{p,DH}$ shows the influence of the boilers fuel consumption on the overall primary energy

required by the system. The primary energy factor of the second efficiency scenario is very close to the primary energy factor of the first efficiency scenario. Although in the second one we have an increase of the energy supplied to the users, 9 % more than in the first scenario, we have also an increase of the primary energy consumed by the boiler, 47 % more than in the first scenario.

The third scenario is the one that consumes less primary energy since the boiler fuel consumption is less than 0.01 %, compared to the reference scenario. The fourth scenario has the best primary energy factor because it is able to feed the highest load, 16 % more than in scenario Time 0, without altering its primary energy consumption that decreases of 2 % compared to the reference scenario.

We also decided to show the inverse of the primary energy factor since the primary energy used by the system in the simulated scenarios is more or less the same. It mainly depends on the CHP fuel consumption. In fact, the maximum fuel consumed by the boilers is 2 % of the fuel consumed by the CHP; this happens in the reference scenario. From the inverse of the primary energy factor we can see how many units of useful energy we can produce for the users from one unit of primary energy consumed for thermal production. Optimizing the network, using more or less the same primary energy with reference to the simulation at Time 0, it is possible to produce up to 40 % more useful thermal energy for the users, a thing that happens in the last and best efficiency scenario.

11.2.2 Plant primary energy factor PEF_{plant}

The plant primary energy factor gives us information on how much primary energy for thermal production the district heating system needs to place into the network a single unit of thermal energy. It decreases moving from the reference scenario, simulation at Time 0, to the efficiency ones.

	PEF_{plant}	$\frac{1}{PEF_{plant}}$
Scenario 0	0.224	4.456
Scenario 1	0.170	5.885
Scenario 2	0.170	5.899
Scenario 3	0.157	6.360
Scenario 4	0.144	6.956

Table 11. 7: PEF_{plant} results

The reference scenario has the highest value of PEF_{plant} , 0.224, whereas the fourth scenario has the lowest one, 0.144. With reference to scenario Time 0, the minimum reduction of PEF_{plant} is 0.054 for scenario 1, with a percentage reduction of 24 %, whereas the maximum reduction is 0.08, for scenario 4, with a percentage reduction of 36 %.

The results of the plant primary energy factor are very close to the ones of the primary energy factor, since the heat distribution losses along the network represent at maximum 7 % of the user load, in the reference scenario.

From the inverse of the plant primary energy factor we can see how many units of useful energy we can place into the network from the same unit of primary energy consumed for thermal production. Optimizing the network, consuming more or less the same primary energy with reference to scenario Time 0, it is possible to produce up to 36 % more thermal energy to place into the network, something that happens in the last and best efficiency scenario.

11.2.3 District Heating Global Efficiency η_{DH} :

From the District Heating Global efficiency, we can see how much the heat distribution losses decrease when the reference temperature of the network is shifted from 130 °C to almost 90 °C.

	η_{DH}
Scenario 0	0.927
Scenario 1	0.954
Scenario 2	0.956
Scenario 3	0.981
Scenario 4	0.985

Table 11. 8: η_{DH} results

In the first two scenarios, those ones where the loops are managed at two different supply temperatures, the η_{DH} increases on average 2.8 %. In the last two scenarios, those ones where there is only one working loop, the η_{DH} increases on average 5.6 %. The η_{DH} does not depend on the thermal energy dissipated by the network dissipater, because it does not significantly change moving from the first to the second scenario, and moving from the third to the fourth scenario.

As we would expect, the district heating global efficiency increases moving from the reference scenario to the efficiency scenarios. In particular, we have to notice that in the third scenario the distribution losses are about 3.7 times less than in the reference scenario (from 713 MWh to 172 MWh). The latter comparison is important because in the third scenario there is only the ring DN 350 working at low temperature, and it feeds the same user load of the reference scenario.

11.2.4 Primary Energy Efficiency (PEE):

The primary energy efficiency represents the ratio between the global net energy exiting the power station, thermal and electric, and the primary energy getting inside the power station by means of fuel.

	PEE
	%
Scenario 0	72.0
Scenario 1	72.4
Scenario 2	75.4
Scenario 3	72.0
Scenario 4	76.9

Table 11. 9: PEE results

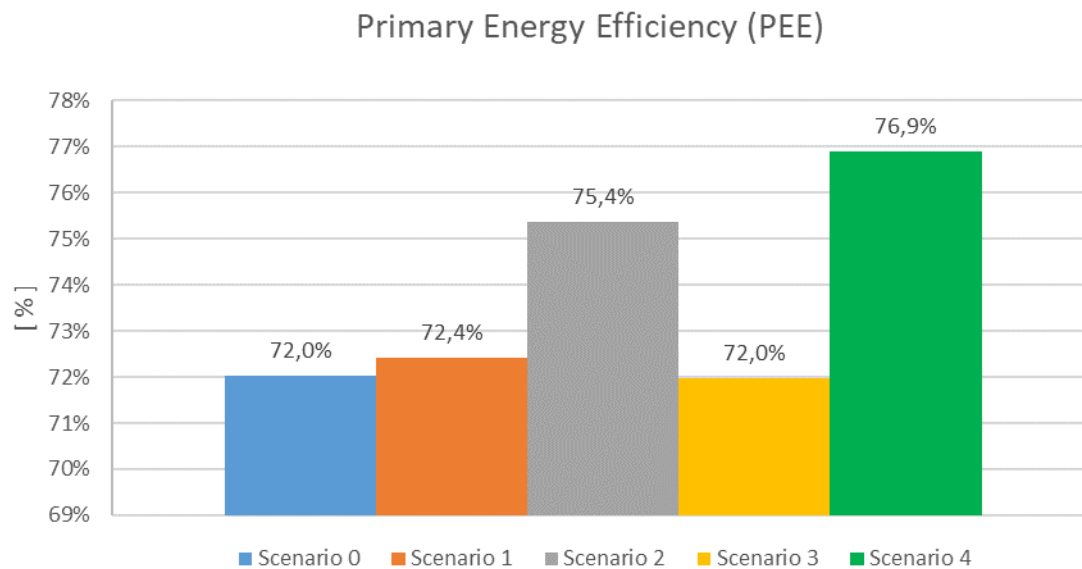


Figure 11 3: PEE results

The fourth scenario has the highest value of *PEE*, 76.9 %, which corresponds to an increase of 4.9 %, compared to the simulation at Time 0. The reference scenario and the third scenario have the worst primary energy efficiency, 72 %. The *PEE* index does not depend on the supply temperature of the network, in fact, the third scenario, which is managed at low temperature, has the worst *PEE*. The *PEE* mainly depends on how much energy is dissipated by the network dissipater. In fact, the second and

the fourth scenarios, the ones with the dissipated heat recovering by the installation of new absorption chillers, have the highest value of PEE, that is on average almost 4 % higher than in the reference scenario, Time 0.

As we would expect, the second and the fourth efficiency scenarios are the ones with the best primary energy efficiency, because consuming more or less the same primary energy than in the other scenarios, they use the heat recovered from the low temperature heat exchanger of the CHP units to feed also new single stage absorption chillers. The first and the third efficiency scenarios have a primary energy efficiency really similar to the reference scenario, since they dissipate in the network dissipater and in the HST dissipater all the heat (100%) they recover from the low temperature heat exchanger of the CHP units.

The energy efficiency indexes analysis has been useful to compare all the scenarios we simulated from the energy point of view. At the end of this work, it is evident that optimizing the existing network, shifting the supply temperature from 130 °C to almost 90 °C, is meaningless if the heat recovered from the CHP units is then dissipated in the network dissipater. For this reason, keeping the same electric management for the CHP units, an efficient optimization of the DH network of Fiumicino Airport would also involve the installation of new loads to use the heat recovered usefully, as it happens in the second and in the fourth efficiency scenario.

Conclusions

In this thesis, we have simulated the district heating network that feeds the thermal users of the airport of Roma Fiumicino. It consists of two loops, the DN 200 and the DN 350, that work at the same flow temperature (130 °C). Inside the power station there are 4 storage tanks of 250 m³, 3 CHP units, 5 back up boilers. Before starting the modelling phase, we analysed the data collected for the month of February 2017. Nowadays, the CHP units, that feed the network, work in nominal condition, for most of the time, to produce as much electric energy as they can for self-consumption, even when the load does not require all the thermal energy produced that, if in excess, is dissipated. In the actual working conditions, the CHP units cannot recover heat from the low temperature heat exchanger because the return mass flow rate in the power station has a temperature that is too high.

The starting point of the modelling was the ENSim platform for the dynamic simulation of district heating systems. The model we implemented is made by different Simulink blocks that reproduce the components of the network: the thermal power station with the CHP units, the network dissipater, the hot storage tank and the distribution pipelines. This new version of ENSim platform does not model each pipe of the network by a Matlab function, but hydraulically and thermally solves the network, at each time step of simulation, by using software IHENA that has been fully integrated in platform ENSim. The real network was linearized to simplify the topology of the network given to the model as input, but we kept the real length between node and node.

After overcoming and implementing the pre-existing model, we validated the model, comparing the measured data for the months of February 2018, with the results of the simulation of the network in the working conditions derived from the monitoring data. We validated the model for the month of February because it is the one in which we have all the temperature drops on the primary circuit of all the users, excluding user 155, 27, 53, 54. Giving the model the temperature drops on the user nodes at each time step as input, it is possible to have high correspondence between the simulated global mass flow rate and the measured one.

In particular, we validated the model comparing the measured data with the simulation results with regards to the supply temperature, the return collector temperature, the mass flow rate, the thermal energy produced in the power station. The simulated supply temperature has a percentage root mean square error (PRMSE) between 2.3 %, which corresponds to a RMSE of 2.9 °C, and 3.1 %, which corresponds to a root mean square error (RMSE) of 4 °C. The simulated return collector temperature has a PRMSE between 3.5 %, which corresponds to a RMSE of 2.6 °C, and 5.2 %, which corresponds to a RMSE of 4 °C. The simulated global mass flow rate flowing inside the network has a PRMSE between 4.5 %, which corresponds to a RMSE of 2.5 kg/s, and 9 %, which corresponds to a RMSE of 5.2 kg/s. The simulated thermal energy produced by the CHP units underestimates the measured value of 0.5 %, which corresponds to 42 MWh.

The simulation results reproduced the measured data of the real district heating network of Roma Fiumicino in the actual working conditions in a satisfying way. For this reason, we thought the

implemented model could have been used to run efficiency scenarios which results would have been useful to evaluate feasible changes of the working condition in order to optimize the network from the energy point of view.

After validating the model, we ran it in the working conditions ADR claimed are the real ones, with fixed temperature drops on the primary circuit of the users. From this simulation we obtained the reference scenario, called Time 0, for the energy efficiency scenarios we ran later.

The next phase of this thesis was to simulate the model according to four different efficiency scenarios, keeping the same electric management for the CHP units, because we did not know the price ADR pays for the electric energy and the fuel (methane). The efficiency scenarios were intended to study how much thermal energy is possible to recover from the low temperature heat exchanger of the CHP units, decreasing the supply temperature of the network, and consequently, decreasing the temperature of the return mass flow rate in the power station.

In the first efficiency scenario we managed the two loops of the network at different flow temperatures, the DN 200 at 130 °C, and the DN 350 at 90 °C. In this scenario we obtained an almost 38% reduction of the heat distribution losses, an almost 24% increase of the heat produced by the CHP units but an increase of almost twelve times that of the dissipated heat by the network dissipater and by the hot storage tank dissipater, with reference to scenario Time 0.

In the second efficiency scenario we managed the two loops at different flow temperature, the DN 200 at 130 °C, and the DN 350 at 90 °C. In this scenario we installed two new users on the low temperature loop, representing two single stage absorption chillers, in order to recover the heat dissipated otherwise. In this scenario we obtained an almost 37 % reduction of the heat distribution losses, an almost 24 % increase of the heat produced by the CHP units, with reference to scenario Time 0. In the second scenario, we also obtained a decrease of almost 40% of the dissipated heat, with reference to the first efficiency scenario, and a cooling production of 711 MWh.

In the third efficiency scenario we managed the DH network of Roma Fiumicino by a single loop at low temperature, DN 350 at 90°C, shifting all the loads to this loop, closing completely the DN 200, and replacing the existing double stage absorption chillers with single stage absorption chillers. In this scenario we obtained a reduction of almost 76 % of the heat distribution losses, an increase of almost 27 % of the heat produced by the CHP units but an increase of almost fifteen times of the dissipated heat, with reference to scenario Time 0.

In the fourth efficiency scenario we managed the network of Roma Fiumicino by a single loop at low temperature, DN 350, shifting all the loads to this loop, closing the DN 200 completely, replacing the existing double stage absorption chillers with single stage absorption chillers. In this fourth scenario we installed two new users on the working loop, representing two single stage absorption chillers, in order to recover the heat otherwise dissipated. In this scenario we obtained a reduction of almost 75 % of the heat distribution losses, an increase of almost 27 % of the heat produced by the CHP units, with reference to scenario Time 0. In the fourth scenario we also obtained a decrease of almost 58% of the dissipated heat, with reference to the third efficiency scenario, and a cooling production of 1,093 MWh.

At the end of this thesis, we compared the results of the efficiency scenarios with the reference scenario Time 0, by means of energy efficiency indexes.

From the Primary Energy Factor ($f_{p,DH}$) comparison we found that the primary energy used just to feed the thermal users is very low, since it is used mainly to produce electricity for self-consumption. In general, the $f_{p,DH}$ decreases in the energy efficiency scenarios and in particular, in those ones with the installation of the absorption chillers, because the user load is higher. The reference scenario has the highest value of $f_{p,DH}$, 0.242, whereas the fourth scenario has the best one, 0.146. With reference to scenario Time 0, the minimum reduction of $f_{p,DH}$ is 0.064 for scenario 1, with a percentage reduction of 26 %, whereas the maximum reduction is 0.096 for scenario 4, with a percentage reduction of 40 %.

From the District Heating Global Efficiency (η_{DH}) comparison we found that the heat distribution losses along the network are small, since the network is well insulated. In particular, the η_{DH} increases most in the scenarios where the network works with a single loop at low temperature. In the first two scenarios, those ones where the loops are managed at two different supply temperatures, the η_{DH} on average increases 2.8 %, compared to the reference scenario. In the last two scenarios, those ones where there is only one working loop, the η_{DH} on average increases 5.6 %, compared to the reference scenario.

From the Primary Energy Efficiency (PEE) comparison we found that the overall efficiency of the system increases when the heat dissipated by the network dissipater and by the hot storage tank dissipater decreases. The fourth scenario has the highest value of PEE , 76.9%, which corresponds to an increase of 4.9 %, compared to scenario Time 0. The reference scenario, and the third scenario have the worst primary energy efficiency, 72%.

We could not make an economic analysis of the benefits of the energy efficiency scenarios, because we did not receive by ADR the purchasing cost of the methane consumed in the power station.

In the end it is our duty to suggest ADR to manage at least one loop of the network at low temperature, since in this way it is possible to recover heat from the low temperature heat exchangers of the CHP units and to feed new loads, for example single stage absorption chillers, in order to replace the electric chillers actually working.

List of Figures

Figure 1.1: Cogeneration Ratio ⁴ , [9].	14
Figure 1.2: DH Network Tree configuration	14
Figure 1.3: DH Network Loop configuration	15
Figure 1.4: DH Mesh Network configuration	15
Figure 1.5: Pipe of a DH network	16
Figure 1.6: Investment and pumping trend for a DH network ⁵ [32]	17
Figure 2 1: Hydraulic network representation, [29]	23
Figure 2 2: Map with the identification number of the load chambers and user substations, [29]	24
Figure 2 3: Operation scheme of CHP units	26
Figure 2 4: Inspection chamber 6	29
Figure 2 5: Temperature drop and Mass flow rate for substation PG 319, February 2018	30
Figure 2 6: Hourly Thermal Energy in Power Station, February 2018	31
Figure 2 7: Accumulated thermal production and Load, February 2018	32
Figure 2 8: Cumulative Users Load, February 2018	33
Figure 2 9: Users Loads, February 2018	33
Figure 2 10: Mass flow rate, February 2018	35
Figure 2 11: Temperature profiles, February 2018	35
Figure 2 12: Electric production of the CHP 1, February 2018	36
Figure 2 13: Electric production of the CHP 2, February 2018	36
Figure 2 14: Electric production of the CHP 3, February 2018	37
Figure 2 15: Cumulative Average Electric Profile respect to the Nominal Power, February 2018	38
Figure 3. 1: Flow Collector Comparison, New model VS Previous model, December 2017	50
Figure 3. 2: Wrong verses in flow, December 2017	51
Figure 3. 3: Detail of the flow network from the previous model	52
Figure 3. 4: Schematic representation of the MFR balance at the user node	53
Figure 3. 5: Scheme of the Power Station	55
Figure 3. 6: Fictitious Storage Tank	58
Figure 3. 7: Particular from the return collectors block	59
Figure 3. 8: CHP scheme	60
Figure 3. 9: Mixing 3 valves block	61
Figure 3. 10: Motor scheme	62
Figure 3. 11: Low temperature heat exchanger model	63
Figure 3. 12: CHP unit reference scheme	65
Figure 3. 13: Network dissipater model	66
Figure 3. 14: Dissipater of the thermal storage tank	67
Figure 3. 15: Thermal storage tank model	68
Figure 3. 16: Real Network: hydraulic scheme	70
Figure 3. 17: Working Network, linearized representation	72

Figure 4. 1: Real Network: hydraulic scheme	73
Figure 4. 2: Equivalent Network: hydraulic scheme	74
Figure 4. 3: Energy comparison	75
Figure 4. 4: Estimated heat distribution losses MWh	76
Figure 4. 5: Estimated heat distribution losses W/m	77
Figure 4. 6: Estimated heat distribution losses MWh/m.....	78
Figure 4. 7: Ratio (heat distribution Losses)/Generation	79
Figure 4. 8: Equivalent Network, hydraulic scheme	82
Figure 4. 9: Equivalent Network, linearized representation	83
Figure 4. 10: Heat losses comparison: December 2017	84
Figure 4. 11: Heat losses comparison: February 2018	85
Figure 4. 12: Heat losses comparison: March 2018	86
Figure 4. 13: Heat losses comparison: April 2018	87
Figure 5. 1: Flow collector temperature comparison, February 2018, Validation	90
Figure 5. 2: PRMSE of the Flow collector temperature, February 2018, Validation	91
Figure 5. 3: RMSE of the Flow collector temperature, February 2018, Validation	92
Figure 5. 4: Return collector temperature comparison, February 2018, Validation.....	92
Figure 5. 5: PRMSE of the Return collector temperature, February 2018, Validation.....	93
Figure 5. 6: RMSE of the Return collector temperature, February 2018, Validation.....	93
Figure 5. 7: ΔT comparison in the power station, February 2018, Validation.....	94
Figure 5. 8: Mass flow rate comparison, February 2018, Validation.....	95
Figure 5. 9: PRMSE of the Mass flow rate, February 2018, Validation.....	96
Figure 5. 10: RMSE of the Mass flow rate, February 2018, Validation.....	96
Figure 5. 11: Storage Tank Power Exchange comparison, February 2018, Validation.....	97
Figure 5. 12: Simulated network heat losses, February 2018, Validation.....	98
Figure 5. 13: CHP 1, thermal Power comparison, February 2018, Validation.....	99
Figure 5. 14: CHP 2, thermal Power comparison, February 2018, Validation.....	100
Figure 5. 15: CHP 3, thermal Power comparison, February 2018, Validation.....	101
Figure 5. 16: Power Comparison in the Power Station, February 2018, Validation.....	102
Figure 5. 17: Thermal Power dissipated by the network dissipater, February 2018, Validation	103
Figure 6. 1: Flow collector temperature, February 2018, Time 0.....	106
Figure 6. 2: Return collector temperature comparison, February 2018, Time 0	107
Figure 6. 3: ΔT in the power station, February 2018, Time 0	107
Figure 6. 4: Mass flow rate, February 2018, Time 0	108
Figure 6. 5: Network heat losses, February 2018, Time 0	108
Figure 6. 6: Power Comparison in the Power Station, February 2018, Time 0	109
Figure 6. 7: CHP 1, thermal Power, February 2018, Time 0	110
Figure 6. 8: CHP 2, thermal Power, February 2018, Time 0	110
Figure 6. 9: CHP 3, thermal Power, February 2018, Time 0	111
Figure 6. 10: Power dissipated by the network dissipater, February 2018, Time 0.....	112

Figure 7. 1: DN 200, Users Load, Scenario 1.....	114
Figure 7. 2: DN 350, Users Load, Scenario 1.....	115
Figure 7. 3: Two Temperatures Network, hydraulic scheme, Scenario 1.....	116
Figure 7. 4: Two Temperatures Network, linearized representation, Scenario 1.....	118
Figure 7. 5: Boiler scheme, Scenario 1.....	119
Figure 7. 6: PI of the DN 200 Boiler, Scenario 1.....	119
Figure 7. 7: Flow collector temperature, Scenario 1.....	120
Figure 7. 8: Return collector temperature, Scenario 1.....	121
Figure 7. 9: Mass flow rate, Scenario 1.....	122
Figure 7. 10: Network heat losses, DN 200, Scenario 1.....	122
Figure 7. 11: Network heat losses, DN 350, Scenario 1.....	123
Figure 7. 12: Power Comparison in the Power Station, DN 200, Scenario 1.....	124
Figure 7. 13: Power Comparison in the Power Station, DN 350, Scenario 1.....	125
Figure 7. 14: Boilers Thermal Power production, Scenario 1.....	126
Figure 7. 15: CHP 1, thermal Power comparison, Scenario 1.....	127
Figure 7. 16: CHP 2, thermal Power comparison, Scenario 1.....	128
Figure 7. 17: CHP 3, thermal Power comparison, Scenario 1.....	129
Figure 7. 18: Return temperature in the Power Station, DN 350, Scenario 1.....	130
Figure 7. 19: Power dissipated by the network dissipaters, Scenario 1.....	130
Figure 8. 1: Data sheet of LG Hot fired absorption chiller WC2H Series, Model 083, [33].....	133
Figure 8. 2: Two Temperatures Network with absorption Chillers, hydraulic scheme, Scenario 2.....	134
Figure 8. 3: Two Temperatures Network with new absorption Chillers, linearized representation, Scenario 2.....	135
Figure 8. 4: Absorption Chiller model, Scenario 2.....	136
Figure 8. 5: Cooling power produced in PG 319, Scenario 2.....	138
Figure 8. 6: Boilers thermal power produced, DN 350, Scenario 2.....	139
Figure 8. 7: Calibration analysis, DN 350, Scenario 2.....	140
Figure 8. 8: Boilers heat power produced comparison, DN 350, Scenario 2.....	141
Figure 8. 9: Cooling power produced in PG 319, F=0.9, Scenario 2.....	141
Figure 8. 10: Flow collector temperature comparison, DN 350, Scenario 2.....	142
Figure 8. 11: Return collector temperature comparison, DN 350, Scenario 2.....	143
Figure 8. 12: Mass flow rate, DN 350, Scenario 2.....	144
Figure 8. 13: Network heat losses, DN 350, Scenario 2.....	144
Figure 8. 14: Power Comparison in the Power Station, DN 350, Scenario 2.....	145
Figure 8. 15: CHP 2, thermal Power comparison, Scenario 2.....	146
Figure 8. 16: CHP 3, thermal Power comparison, Scenario 2.....	147
Figure 8. 17: Power dissipated by the network dissipater, DN 350, Scenario 2.....	148
Figure 9. 1: Network DN 350 only, at low Temperature, hydraulic scheme, Scenario 3.....	149
Figure 9. 2: Network DN 350 only, at low Temperature, linearized representation, Scenario 3.....	151
Figure 9. 3: Flow collector temperature, Scenario 3.....	152
Figure 9. 4: Return collector temperature.....	153
Figure 9. 5: Mass flow rate, Scenario 3.....	154
Figure 9. 6: Network heat losses, Scenario 3.....	154

Figure 9. 7: Power Comparison in the Power Station, Scenario 3.....	155
Figure 9. 8: CHP 1, thermal Power, Scenario 3.....	156
Figure 9. 9: CHP 2, thermal Power, Scenario 3.....	157
Figure 9. 10: CHP 3, thermal Power, Scenario 3.....	158
Figure 9. 11: Return temperature in the Power Station, Scenario 3.....	159
Figure 9. 12: Thermal Power dissipated by the network dissipater, Scenario 3	159
Figure 10. 1: Network DN 350 only, with Dissipated Heat Recovery, hydraulic scheme, Scenario 4	161
Figure 10. 2: Network DN 350 only, with Dissipated Heat Recovery, linearized representation, Scenario 4.....	162
Figure 10. 3: Cooling power produced in PG 319, Scenario 4	164
Figure 10. 4: Boiler heat power production, Scenario 4.....	165
Figure 10. 5: Calibration analysis, Scenario 4	166
Figure 10. 6: Boilers heat power production comparison, Scenario 4	167
Figure 10. 7: Cooling power produced in PG 319, F=0.8, Scenario 4	168
Figure 10. 8: Flow collector temperature comparison, Scenario 4	169
Figure 10. 9: Return collector temperature comparison, Scenario 4.....	170
Figure 10. 10: Mass flow rate comparison, Scenario 4	171
Figure 10. 11: Network heat losses, Scenario 4	171
Figure 10. 12: Power Comparison in the Power Station, Scenario 4.....	172
Figure 10. 13: CHP 1, thermal Power comparison, Scenario 4.....	173
Figure 10. 14: CHP 2, thermal Power comparison, Scenario 4.....	174
Figure 10. 156: CHP 3, thermal Power comparison, Scenario 4.....	175
Figure 10. 167: Thermal Power dissipated by the network dissipater comparison, Scenario 4	176
Figure 11 1: District Heating system scheme, readapt from UNI EN 15316-4-5:2007 [26]	179
Figure 11 2: Energy fluxes getting inside and outside the Thermal Power Station.....	181
Figure 11 3: PEE results	186

List of Tables

Table 2 1: Monitoring chambers	24
Table 2 2: Users identification data.....	28
Table 2 3: Thermal production in Power Station, February 2018	31
Table 2 4: Energy inside the HST	31
Table 2 5: Comparison production and load, February 2018.....	32
Table 2 6: Users Loads, February 2018.....	34
Table 2 7: Temperature comparison in the Power Station, February 2018.....	35
Table 2 8: Electric production CHP1, February 2018.....	36
Table 2 9: Electric production CHP2, February 2018.....	37
Table 2 10: Electric production CHP3, February 2018.....	37
Table 2 11: Cumulative Average Electric Profile, February 2018	38
Table 4. 1: Energy comparison	75
Table 4. 2: Estimated heat distribution losses MWh.....	76
Table 4. 3: Estimated heat distribution losses W/m	77
Table 4. 4: Estimated heat distribution losses MWh/m.....	78
Table 4. 5: Ratio (heat distribution Losses)/Generation	79
Table 4. 6: Layers' thickness	81
Table 4. 7: Layers' conductivity	81
Table 4. 8: Heat losses comparison: December 2017	84
Table 4. 9: Heat losses comparison: February 2018.....	85
Table 4. 10: Heat losses comparison: March 2018.....	86
Table 4. 11: Heat losses comparison: April 2018.....	87
Table 5. 1: Power Station in working conditions.....	89
Table 5. 2: Flow collector temperature comparison, February 2018, Validation	90
Table 5. 3: Return collector temperature comparison, February 2018, Validation	93
Table 5. 4: ΔT comparison in the power station, February 2018, Validation	94
Table 5. 5: Simulated network heat losses, energy results, February 2018, Validation	98
Table 5. 6: CHP 1, thermal comparison, February 2018, Validation	99
Table 5. 7: CHP 2, thermal comparison, February 2018, Validation	100
Table 5. 8: CHP 3, thermal comparison, February 2018, Validation	101
Table 5. 9: Comparison in the Power Station, February 2018, Validation	102
Table 5. 10: Heat dissipated by the network dissipater, February 2018, Validation	103
Table 5. 11: Simulation Energy Results, February 2018, Validation.....	104
Table 6. 1 Power station.....	105
Table 6. 2: Flow collector temperature, February 2018, Time 0.....	106
Table 6. 3: Return collector temperature comparison, February 2018, Time 0.....	107
Table 6. 4: ΔT in the power station, February 2018, Time 0	107

Table 6. 5: Network heat losses results, February 2018, Time 0.....	108
Table 6. 6: Energy Comparison in the Power Station, February 2018, Time 0.....	109
Table 6. 7: CHP 1, thermal comparison, February 2018, Time 0.....	110
Table 6. 8: CHP 2, thermal comparison, February 2018, Time 0.....	111
Table 6. 9: CHP 3, thermal comparison, February 2018, Time 0.....	111
Table 6. 10: Energy dissipated by the network dissipater, February 2018, Time 0.....	112
Table 6. 11: Simulation Energy Results, Time 0.....	112
Table 7. 1: Power Station DN 350, Scenario 1.....	115
Table 7. 2: Power Station DN 200, Scenario 1.....	116
Table 7. 3: Users identification data, Network Two Temperatures, Scenario 1.....	117
Table 7. 4: Flow collector temperature, Scenario 1.....	120
Table 7. 5: Return collector temperature, Scenario 1.....	121
Table 7. 6: Network heat losses, DN 200, Scenario 1.....	123
Table 7. 7: Network heat losses, DN 200, Scenario 1.....	123
Table 7. 8: Comparison in the Power Station, DN 200, Scenario 1.....	124
Table 7. 9: Energy Comparison in the Power Station, DN 350, Scenario 1.....	125
Table 7. 10: Boilers Thermal Energy production, Scenario 1.....	126
Table 7. 11: CHP 1, thermal comparison, Scenario 1.....	127
Table 7. 12: CHP 2, thermal Energy comparison, Scenario 1.....	128
Table 7. 13: CHP 3, thermal Energy comparison, Scenario 1.....	129
Table 7. 14: Energy dissipated by the network dissipaters, Scenario 1.....	130
Table 7. 15: Simulation Energy Results, Scenario 1.....	131
Table 8. 1: Power Station DN 350, Scenario 1.....	132
Table 8. 2: Power Station DN 200, Scenario 1.....	132
Table 8. 3: Cooling energy produced and thermal energy required by absorption chillers, Scenario 2.....	138
Table 8. 4: Boiler energy production, DN 350, Scenario 2.....	139
Table 8. 5: Calibration analysis results, DN 350, Scenario 2.....	140
Table 8. 6: Flow collector temperature comparison, DN 350, Scenario 2.....	142
Table 8. 7: Return collector temperature comparison, DN 350, Scenario 2.....	143
Table 8. 8: Network heat losses, energy results, DN350, Scenario 2.....	145
Table 8. 9: Comparison in the Power Station, DN 350, Scenario 2.....	145
Table 8. 10: CHP 2, thermal comparison, Scenario 2.....	146
Table 8. 11: CHP 3, thermal comparison, Scenario 2.....	147
Table 8. 12: Energy dissipated by the network dissipater, DN 350, Scenario 2.....	148
Table 8. 13: Simulation Energy Result, Scenario 2s.....	148
Table 9. 1: Power Station, Network DN 350 only, Scenario 3.....	150
Table 9. 2: Flow collector temperature, Scenario 3.....	152
Table 9. 3: Return collector temperature, Scenario 3.....	153
Table 9. 4: Network heat losses, energy results, Scenario 3.....	155
Table 9. 5: Energy Comparison in the Power Station, Scenario 3.....	155

Table 9. 6: CHP 1, thermal comparison, Scenario 3	156
Table 9. 7: CHP 2, thermal comparison, Scenario 3	157
Table 9. 8: CHP2, thermal comparison, Scenario 3	158
Table 9. 9: Energy dissipated by the network dissipater, Scenario 3	159
Table 9. 10: Simulation Energy Results, Scenario 3.....	160
Table 10. 1: Power Station, Network DN 350 only, Scenario 4	163
Table 10. 2: Cooling energy produced and thermal energy required by absorption chillers, Scenario 4.....	165
Table 10. 3: Boilers' energy production, Scenario 4.....	166
Table 10. 4: Calibration analysis, Scenario 4	167
Table 10. 5: Flow collector temperature comparison, Scenario 4	169
Table 10. 6: Return collector temperature comparison, Scenario 4.....	170
Table 10. 7: Network heat losses, energy results, Scenario 4.....	172
Table 10. 8: Energy Comparison in the Power Station, Scenario 4	172
Table 10. 9: CHP 1, thermal Energy comparison, Scenario 4	173
Table 10. 10: CHP 2, thermal Energy comparison, Scenario 4	174
Table 10. 11: CHP 3, thermal Energy comparison, Scenario 4	175
Table 10. 12: Energy dissipated by the network dissipater comparison, Scenario 4.....	176
Table 10. 13: Simulation Energy Results, Scenario 4.....	176
Table 11. 1: Raccomandazione CTI 14: 2013'	177
Table 11. 2: European standard FprEN 15603:2014.....	178
Table 11. 3: Methane consumed by CHP	182
Table 11. 4: Methane Consumed by boilers.....	182
Table 11. 5: Reference parameters of the simulated scenarios.....	183
Table 11. 6 f_p, DH results.....	183
Table 11. 7: PEF_{plant} results.....	184
Table 11. 8: η_{DH} results.....	185
Table 11. 9: PEE results.....	186

Bibliography

- [1] B. Di Pietra, J. Canonaco, A. Pannicelli, G. Puglisi, F. Zanghirella, Ottimizzazione della piattaforma ENSim per la simulazione di reti termiche in assetto poligenerativo, Report Rds/PAR2014/013.
- [2] M. A. Ancona, L. Branchini, F. Melino, Analisi di strategie per la gestione ottimizzata di reti complesse di distribuzione dell'energia termica, Report Rds/PAR2015/151.
- [3] Ministero dello Sviluppo Economico, Ministero dell'Ambiente e della Tutela del Territorio e del Mare, Strategia Energetica Nazionale 2017.
- [4] M. A. Ancona, L. Branchini, F. Melino, Analisi di strategie di gestione di reti complesse di distribuzione di energia elettrica e termica, Report Rds/PAR2016.
- [5] M. A. Ancona, L. Branchini, F. Melino, Analisi di strategie per la gestione ottimizzata di reti complesse di distribuzione dell'energia termica, Report Rds/PAR2015/151.
- [6] P. Barucci et al., IC46, Indagine conoscitiva sul settore del teleriscaldamento, AGCM.
- [7] M. Badami, A. Portoraro. Studio e caratterizzazione di reti termiche distribuite, Report RdS/2013/105.
- [8] L. Mongibello, N. Biancob, M. Di Somma, G. Graditia. Experimental validation of a tool for the numerical simulation of a commercial hot water storage tank.
- [9] A. Franco, F. Bellina. Methods for optimized design and management of CHP systems for district heating networks (DHN).
- [10] J. O. Sola, X. Gabarrell, J. Rieradevall. Environmental impacts of the infrastructure for district heating in urban neighbourhoods.
- [11] A. Hast, S. Syri, V. Lekavicius, A. Galinis. District heating in cities as a part of low-carbon energy system.
- [12] S. Werner. International review of district heating and cooling.
- [13] IEA. World Energy Outlook, 2014.
- [14] E. Todini. A gradient method for the analysis of pipe networks.
- [15] F. Zanghirella, J. Canonaco, G. Puglisi, B. Di Pietra. Analisi energetica di un'ipotesi di trasformazione di reti di teleriscaldamento esistenti in reti poligenerative con presenza di scambio attivo. Report Rds/PAR2014/015.
- [16] M. A. Ancona, F. Melino. Analisi di soluzioni tecniche e gestionali che favoriscano l'implementazione di nuovi servizi energetici nelle reti termiche in presenza di sistemi di generazione distribuita. Report RdS/PAR2013/053.
- [17] M. A. Ancona, F. Melino. Analisi di soluzioni progettuali per la trasformazione di reti di teleriscaldamento esistenti in reti poligenerative con presenza di scambio attivo. Report RdS/PAR2014/019.
- [18] Annuario Airu 2015. Il teleriscaldamento urbano.
- [19] Annuario Airu 2017. Il teleriscaldamento urbano.
- [20] Ruscica, Badami, Portoraro. Micro - cogenerazione nel settore residenziale con l'utilizzo di motori a combustione interna: Sviluppo di un modello matematico per la simulazione oraria e analisi di un caso reale.
- [21] F. Zanghirella, J. Canonaco, G. Puglisi, B. Di Pietra. Introducing solar thermal "net metering" in an actual small-scale district heating system: a case-study analysis.

- [22] M. Versace. Analisi dinamica e valutazione delle prestazioni di una rete di teleriscaldamento.
- [23] L. Rignanese. Analisi e ottimizzazione delle prestazioni di una rete di teleriscaldamento mediante modelli di simulazione avanzati. (M. A. Ancona L. F.) (Segnaposto1)
- [24] M. Moretti. Modellazione della rete termica dell'aeroporto di Fiumicino e analisi prestazionale.
- [25] S. Deputato. Ottimizzazione tramite peak shaving della domanda termica di un baricentro della rete di teleriscaldamento.
- [26] M. Badami, A. Portoraro. Analisi di performance e monitoraggi energetici di reti termiche distribuite, Report RdS/2013/056.
- [27] UNI, Ente Nazionale Italiano di Unificazione. EN 15316-4-5 (edizione luglio 2007).
- [28] Trane Commercial Global Product System, (<http://www.trane.com>). Accessed on August 20 2018.
- [29] Service SRL. Aerostazione di Fiumicino, Relazione Tecnica, Analisi Fluidodinamica della rete acqua surriscaldata.
- [30] F. Incropera, D. Dewit, T. Bergman, A. Lavine. Introduction to heat transfer, 6th edition.
- [31] Legambiente, *Report sul Teleriscaldamento Urbano, 2014*.
- [32] A. Sciacovelli, V. Verda, R. Borchiellini. Numerical design of thermal systems, 2nd edition.
- [33] LG website ([http:// www.lgeaircon.com](http://www.lgeaircon.com)) Accessed on August 02 2018